



1971-2021

中华人民共和国恢复联合国合法席位50周年
THE 50TH ANNIVERSARY OF THE RESTORATION OF THE LAWFUL SEAT
OF THE PEOPLE'S REPUBLIC OF CHINA IN THE UNITED NATIONS



Big Earth Data in Support of the Sustainable Development Goals



Chinese Academy of Sciences
September 2021

Big Earth Data in Support of the Sustainable Development Goals



CONTENTS



04 **Foreword**

05 **Preface**

06 **Executive Summary**

08 **Introduction**

12  **SDG 2: Zero Hunger**

14 **Background**

15 **Main Contributions**

16 **Case Study**

2.4 Spatiotemporal variations of cropping intensity over 20 years in China\ 16

2.4 Mapping crop distribution and its changes in China\ 20

2.4 An experiment of efficient ecological agricultural paradigm in the low-medium-yield region along the lower reaches of the Yellow River\ 23

26 **Summary**

28  **SDG 6: Clean Water and Sanitation**

30 **Background**

31 **Main Contributions**

32 **Case Study**

6.3 Monitoring and evaluating the dynamic changes in lake water clarity\ 32

6.4 Assessment of change in global crop water-use efficiency\ 36

6.5 The assessment of China's Integrated Water Resources Management\ 40

6.6 Change in natural and artificial water bodies in China from 2000 to 2020\ 43

6.6 Spatiotemporal changes in China's vegetated wetlands\ 46

49 **Summary**

50  **SDG 11: Sustainable Cities and Communities**

52 **Background**

53 **Main Contributions**

54 **Case Study**

11.2 Proportion of the population with convenient access to public transportation in China\ 54

11.5 Interannual variation of total loss of natural disasters at prefectural level (2010-2020)\ 57

11.7 The patterns and dynamics of urban green space in China\ 60

11.1 11.2 11.3 11.7 Community-scale urban landscapes' temporal change and sustainable development indicators in major Chinese cities\ 64

11.2 11.3 11.5 11.6 11.7 Integrated evaluation of SDG 11 indicators in Chinese cities from 2015 to 2020\ 68

72 **Summary**



74



SDG 13: Climate Action

76 Background

77 Main Contributions

78 Case Study

13.1 Interannual changes of sand and dust weather in China in the past 10 years\ 78

13.2 Spatiotemporal variations of greenhouse gas concentration in China\ 81

13.2 Impacts of climate change on net ecosystem productivity of forest in China\ 84

13.2 Impacts of land cover change on global net ecosystem productivity\ 87

13.3 Global ocean heat content change\ 90

93 Summary

94



SDG 14: Life below Water

96 Background

97 Main Contributions

98 Case Study

14.2 Monitoring and forecasting macroalgal blooms in the Yellow Sea\ 98

14.2 Changes of mangrove forests in China\ 101

14.2 Changes of coastal aquaculture ponds in China\ 105

108 Summary

110



SDG 15: Life on Land

112 Background

113 Main Contributions

114 Case Study

15.1 Changes in ecosystems and their quality in China\ 114

15.1 Current status of and gaps in grassland ecosystem conservation in China\ 117

15.1 15.4 Big data simulation to generate high-resolution distribution of rare and endangered plants\ 119

15.4 High-resolution monitoring of global mountain green cover index\ 122

15.5 Monitoring spatiotemporal variations of wintering Siberian crane habitats\ 126

128 Summary

130 Interactions among SDG indicators

136 Summary and Prospects

139 Acronyms & Abbreviations

141 References

146 Core Team of Authors

Foreword

In 2015, the United Nations adopted the 2030 Agenda for Sustainable Development, which includes 17 Sustainable Development Goals (SDGs) to be achieved by 2030. The SDGs are about achieving economic, social and environmental sustainability on a global scale. Since the launch of the 2030 Agenda, China has worked to promote the SDGs while embracing a new philosophy of innovative, coordinated, green, open and shared development, achieving impressive results in eradicating absolute poverty, addressing climate change, improving ecological environment, promoting public health service and ensuring food security. Steady progress has been made in achieving high-quality development. At the same time, China has actively engaged in and promoted international development cooperation and provided reliable public goods for the realization of SDGs across the world.

Experience of the past six years, however, has shown that there remain a number of major challenges to scientifically evaluating the implementation of the 2030 Agenda, the most serious ones being the lack of data, the incompleteness of the indicator system, and the gap in capacity of having and using data as a result of development disparity. As China's national scientific institute, the Chinese Academy of Sciences (CAS) has long been devoted to promoting SDGs through big data. In recent years, CAS has been working with universities, research institutes and enterprises at home and abroad to explore the application of combined new technologies such as cloud computing, artificial intelligence, space technology and network communication technology to improving the evaluation system for SDGs, developing public data products and informing decision-making.

Chinese President Xi Jinping announced on September 22, 2020 at the 75th session of the UN General Assembly that China will establish an International Research Center of Big Data for Sustainable Development Goals (CBAS), to provide new impetus for the implementation of the 2030 Agenda. Subsequently, CBAS was officially launched in Beijing on September 6, 2021. President Xi Jinping sent a congratulatory letter and UN Secretary-General António Guterres delivered a video message to congratulate on the

establishment of the Center. I believe that CBAS will use big data to give support to the sustainable development of China and the world.

In recent years, CAS has, based on its advantages, done demonstration studies on monitoring and evaluation of indicators for the goals of zero hunger, clean water and sanitation, sustainable cities and communities, climate action, life below water and life on land, and issued annual report on Big Earth Data in Support of the Sustainable Development Goals. The 2021 report continues to focus on the practical scenarios for these SDGs' realization, and presents research results including single indicator progress evaluation and integrated multi-indicator evaluation. These results provide stronger scientific basis for understanding the dynamic trends of SDG indicators and analyzing the problems hindering sustainable development and they can inform decision on SDG realization in different scales and regions.

2021 marks the 50th anniversary of the restoration of the People's Republic of China's lawful seat in the United Nations. This CAS report is part of China's sustained contribution in the form of science and technology to the implementation of the 2030 Agenda. CAS will further strengthen the collaborations with international counterparts to address new challenges to sustainable development through science, technology and innovation.



Hou Jianguo
President, Chinese Academy of Sciences

Preface

The COVID-19 pandemic has brought unprecedented challenges to the implementation of the 2030 Agenda for Sustainable Development across the world, affecting, to a large extent, the existing achievements, and resulting in stagnation or even regression. Recognizing the important role scientific and technological innovation can play in promoting economic and social development, the United Nations established in 2015 the Technology Facilitation Mechanism for SDGs. In *the Sustainable Development Goals Report 2020*, United Nations Secretary-General António Guterres called for a coordinated and comprehensive international response and recovery effort, based on sound data and science and guided by the Sustainable Development Goals.

More effective ways need to be explored to address the data challenge facing SDGs. Thanks to the development of science and technology, the global data volume is growing exponentially. Advances in computing and data technologies have made real-time processing and analysis of big data a reality, while new types of data combined with traditional data, such as statistical and survey data, can create more detailed, timely high-quality information. Big Earth Data technology, through its extensive use and further innovation, can be an effective way to address the data divide and the lack of information and tools for sustainable development.

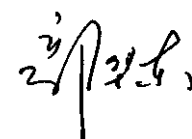
The International Research Center of Big Data for Sustainable Development Goals, built on the strength of the Chinese Academy of Sciences, will use big data to support the SDGs. A full-fledged Center will have functions including building an SDG big data technology service system capable of storage, calculation, analysis and service, conducting scientific research on monitoring and evaluation of SDG indicators, developing and operating SDG science satellites, constructing a think tank on science and technology for sustainable development, and promoting personnel training and capacity building of big data for SDGs.

In recent years, CAS has conducted case studies that use Big Earth Data technology to monitor and evaluate indicators for six SDGs -- zero hunger, clean water and sanitation, sustainable cities and communities, climate action, life below water and life on land. CAS issued the report on *Big Earth Data in Support of the Sustainable Development Goals* for two consecutive years during the 74th and 75th

United Nations General Assembly sessions, highlighting the important value and role of Big Earth Data technology in addressing challenges for sustainable development.

The 2021 report integrates innovations in the past three years in the practice of using Big Earth Data technology to monitor and evaluate SDGs. Focusing on six Goals, the report presents 26 typical cases on four scales -- local, national, regional and global, detailing the results of research, monitoring and evaluation of SDG indicators from the perspectives of data, methods and models, and decision support. Furthermore, the report demonstrates methods for monitoring, evaluating and analyzing the interactions among multiple SDGs, thus laying a good foundation for future coordinated pursuit of multiple SDGs in different scenarios. The findings of the report can provide new analytical tools for better understanding and more accurate identification of issues related to SDGs and they are also of great practical value to promoting SDGs through science, technology and innovation.

This report could not have been completed without the guidance given by the Ministry of Foreign Affairs, and the valuable feedback and suggestions from leaders and experts of the National Development and Reform Commission, the Ministry of Natural Resources, the Ministry of Ecology and Environment, the Ministry of Housing and Urban-Rural Development, the Ministry of Transport, the Ministry of Water Resources, the Ministry of Agriculture and Rural Affairs, the Ministry of Emergency Management, the National Bureau of Statistics and the National Forestry and Grassland Administration. Finally, our utmost appreciation goes to all the scientists on the team for their hard work.



Guo Huadong

Director of the International Research Center of Big Data for Sustainable Development Goals
Member of the UN 10-Member Group to support the TFM for SDGs (2018-2021)

Executive Summary

2021 is the first year in the Decade of Action that the United Nations has launched to accelerate the implementation of Sustainable Development Goals (SDGs). There are still severe challenges in realizing the 2030 agenda for Sustainable Development, and the COVID-19 pandemic has had a further serious impact on the realization of the 2030 Agenda. Science and technology are important levers for meeting these challenges, and advancing and implementing the 2030 Agenda. In his congratulatory letter for the inauguration of the International Research Center of Big Data for Sustainable Development Goals (CBAS) and opening ceremony of the International Forum on Big Data for SDGs on September 6th, 2021, Chinese President Xi Jinping noted, "Scientific and technological innovation and application of big data will help the international community overcome difficulties and implement the UN 2030 Agenda globally." UN Secretary General António Guterres said in a video message for the inauguration of the CBAS, "Building on the momentum that's being generated by the UN Technology Facilitation Mechanism – for innovation, solutions and better results where policy meets science, ... we can mobilize scientific and technological communities to help achieve the Sustainable Development Goals." This report showcases the innovative practice of applying Big Earth Data to the monitoring and evaluation of indicators for six SDGs, i.e., SDG 2 Zero Hunger, SDG 6 Clean Water and Sanitation, SDG 11 Sustainable Cities and Communities, SDG 13 Climate Action, SDG 14 Life Below Water, SDG 15 Life on Land, and the analysis of the interactions among multiple SDG indicators.



With regard to SDG 2 Zero Hunger, focusing on sustainable food production systems (SDG 2.4), Big Earth Data technology was used to develop methods for mapping cropping intensity and crop types—two key elements of cropland use, demonstrating Big Earth Data technology's capability of timely and rapid information acquisition and multi-source data fusion. Case studies found that crop intensity dropped slightly by 6% over the past two decades and the centroid of 14 main crops moved mainly in three directions from 2000 to 2015: northeast, northwest and southwest. Besides, a data-driven efficient ecological agricultural paradigm aiming at transforming the grain production system was proposed; through an experimental farm, it provided technical support and demonstration for farmers and farm operators of different scales to move towards sustainable agriculture.



With regard to SDG 6 Clean Water and Sanitation, the studies focused on four targets: water quality (SDG 6.3), water-use efficiency (SDG 6.4), integrated water resources management (SDG 6.5) and protection and restoration of water-related ecosystems (SDG 6.6). Data sets were generated on China's lake water clarity, global large lake water clarity, global crop water-use efficiency, China's natural and artificial water bodies and vegetated wetlands. China's Integrated Water Resources Management (IWRM), covering water quality, quantity, and water-related ecosystems, was evaluated. Demonstrations were done for the global application of Big Earth Data technology to indicators of lake water clarity and crop water-use efficiency. The key findings include that the world's large lake water bodies have become clearer; crop water-use efficiency in agricultural regions in the world is on an upward trend; China has reached the medium-high level in IWRM; China's natural and artificial water bodies have increased in area; the loss of vegetated wetlands in China has significantly slowed down. These results are a useful supplement to the China's data set in the United Nations Global SDG Database and can be drawn on by other developing countries in their monitoring and evaluation of SDG 6.



With regard to SDG 11 Sustainable Cities and Communities, three targets, i.e., public transportation (SDG 11.2), disaster assessment (SDG 11.5) and public open space (SDG 11.7), were monitored and evaluated with the support of Big Earth Data technology, and an integrated evaluation of multiple SDG 11 indicators was carried out at the municipal levels in China. Data sets were generated on the high-precision population kilometre gridded data by gender and age in China, interannual variation of the total loss of natural disasters at the prefectural level in China, China's Urban Green Space (UGS) fraction data products, community-scale Chinese urban landscape datasets. The key findings include that the proportion of the population with convenient access to public transportation was 90.15% in 2020, up 9.59% from 2018, the impact of natural disasters on China showed an overall downward trend, with notable improvement in comprehensive disaster prevention, reduction and resistance, UGS has increased significantly thanks to effective urban greening efforts since 2000, sustainability improved in 2020 at the municipal level compared with 2015. The above research results provide data and decision support

for the realization of SDG 11 in China, and can also provide demonstration and reference for other countries.



With regard to SDG 13 Climate Action, the studies focused on strengthen capacity to natural disasters (SDG 13.1), climate change measures (SDG 13.2) and climate change adaptation and early warning (SDG 13.3). By integrating

Big Earth Data, a series of data sets including interannual range data of sand and dust, CO₂ and NO₂ concentration spatial data in China, China and global forest net ecosystem productivity products, global ocean heat content data set by integrating sea surface satellite and ARGO buoy observation data. Based on these data sets with clear spatiotemporal information, several important discoveries are made, including that in the past 10 years, the frequency of spring dust weather in northern China has fluctuated and decreased; China's CO₂ concentration is still increasing in recent years, but the increase rate decreases. Affected by the fluctuation of economic activities brought by COVID-19, the average concentration of NO₂ in China reached trough in February 2020, and reached its peak in December 2020 and exceeded the previous year. The analysis of NEP in China and the world shows that the increase of forest area has an important contribution to the increase of carbon sink. In recent ten years, the overall performance of China's forests is carbon sink, with an average rate of 199.54 TgC/a; the warming of the upper 2,000 m of the global ocean is significant and increasing, with a warming rate of 2.25×10^8 J/m² per decade. The above data and analysis can provide scientific basis for coping with disasters and long-term impacts caused by climate change and carbon neutralization strategy.



With regard to SDG 14 Life Below Water, the studies focused on the sustainable management and protection of marine and coastal ecosystems (SDG 14.2). Through

three cases at two spatial scales in China and typical regions, the production of data sets such as dynamic changes of Chinese mangrove forests and dynamic changes of Chinese coastal aquaculture ponds and the verification of the practicality of the monitoring and early warning model of Yellow Sea macroalgal blooms were completed by spatiotemporal data overlay, four-Dimensional Variational (4DVar) data assimilation and deep learning methods. The results showed that the spatial distribution of floating macroalgal could be quickly extracted from remote sensing images on the Big Earth Data cloud platform and that the drift trajectory of the algal bloom could

be predicted in real time through the 4DVar model. From 2015 to 2020, mangrove expanded in China and its total area had a net increase of 16%. In the same period, coastal aquaculture ponds in China demonstrated visible spatiotemporal variations. Overall, driven by the policy of returning ponds to wetlands, the total area of such ponds showed a continuous downward trend. The above research results can provide a model reference for effectively supplementing SDG 14 related basic data sets and improving the capacity of marine ecological disaster prevention and control.



With regard to SDG 15 Life on Land, the studies focused on three targets, conservation, restoration and sustainable use of terrestrial and inland freshwater ecosystems (SDG 15.1), conservation of mountain ecosystems (SDG

15.4), halting the loss of biodiversity (SDG 15.5). Two data sets, mountain green cover index and 1 km × 1 km grid spatial distribution of endangered species, were produced. China's ecosystem quality and dynamic change, important grassland ecosystem protection status and gaps and Siberian crane habitats spatiotemporal change were evaluated by taking Big Earth Data approaches. It was found that from 2000 to 2015 the ecosystem quality in China improved significantly, with the integrated ecosystem quality index up by 21% approximately year-on-year, that grassland ecosystems in China were generally well protected but still with five types of grassland of smaller areas being under-protected, and that Siberian crane habitats in Poyang Lake wetlands had degraded and needed urgent protection. These could serve as references for monitoring and evaluating SDG 15 indicators at the global, national and local levels.

With regard to the interactions among SDG indicators, the report discussed the methods and practices of spatial information digging and integrated evaluation by using Big Earth Data, which includes evaluating the synergy and trade-off relationships among SDG indicators in the context of their correlations; simulating multiple indicators' interactions in future environmental, economic and social scenarios in the context of their temporal variations; making integrated evaluation of regional SDGs in the context of multiple indicators experience and study. Through the interactions study of indicators, we can find potential scientific problems and evaluate the impact of policies and measures, guide the dynamic planning of policies, and speed up the implementation process of regional sustainable development.

Introduction

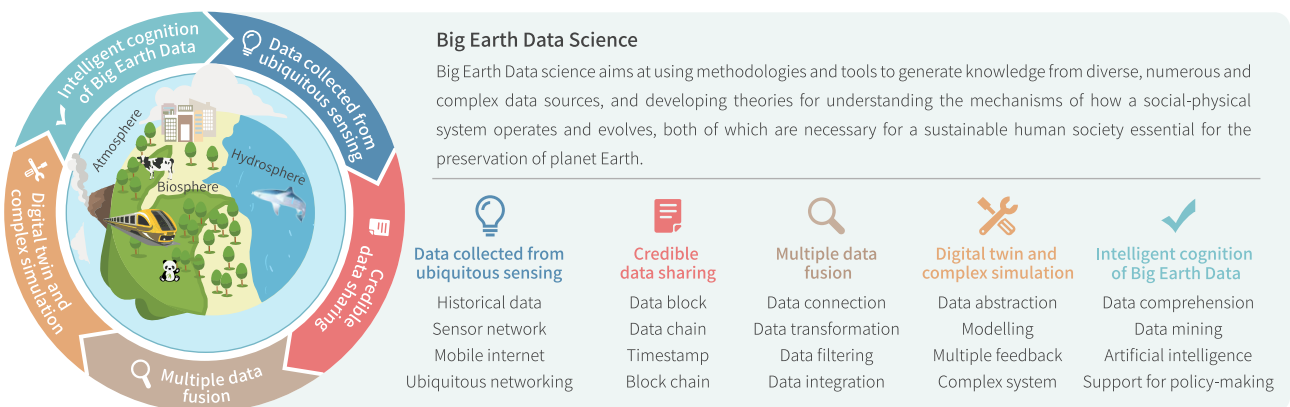
In a bid to push for realization of all the 17 SDGs by 2030, the United Nations formally launched in January 2020 the Decade of Action, calling for accelerating sustainable solutions to all the world's biggest challenges. However, the COVID-19 pandemic has had a serious impact on the global implementation of the 2030 Agenda. It has increased the vulnerability of the global food system, with the number of people facing hunger in 2020 about 118 million, or 18% higher than in 2019, and food security emergencies at the highest level in five years. Over the past century, global water use has grown at more than twice the rate of population growth, and UN estimates suggest that global freshwater resources will decline by 40% by 2030, making a water crisis highly likely. Prior to the pandemic, cities already saw growing numbers of slum-dwellers, more polluted air, minimal public open space and limited public transportation, and the pandemic has further exposed and aggravated such vulnerabilities. The concentration of major greenhouse gases in the atmosphere continues to increase, with 2015-2020 being the warmest six years on record. Climate change has made the achievement of many SDGs less likely. The oceans constantly face threats such as pollution, warming and acidification, which are disrupting the marine ecosystem. Deforestation and forest degradation, the continued loss of biodiversity and degradation of ecosystems are having far-reaching impacts on human well-being and survival. The global target of halting biodiversity loss by 2020 was not met (UN, 2021a, 2021b).

The UN *Sustainable Development Goals Report 2021* points out the need for concerted efforts of the world to support a recovery guided by the 2030 Agenda for Sustainable Development, and

the obtain and the availability of data is one of the key factors in achieving a better recovery.. Data that supports monitoring and evaluation of SDGs has increased significantly over the years, but major gaps remain in terms of geographic coverage and timeliness of data. The Global SDG Indicators Database reveals that only a few SDGs' data cover more than 80% of countries and for most SDGs data timeliness is a serious problem (UN, 2021c). These data gaps hinder the real-time monitoring of progress towards the Goals and the assessment of regional disparities.

Data innovation is the key to closing the gaps and accelerating the realization of SDGs, and an important area of such innovation is the fusion of geospatial information and statistical information. Earth observation data collected by satellites, unmanned aerial vehicles and ground sensors can not only supplement official statistics and survey data, but also be used together with traditional data to create high-quality information that is more timely and spatially representative. Based on earth observation data, Big Earth Data, with spatial attributes, has strong spatiotemporal and physical correlations and good controllability of data generation methods and sources, in addition to the general properties of big data: massive, multi-source, heterogeneous, multi-temporal, multi-scale and non-stationary (Guo *et al.*, 2016; Guo, 2017). Big Earth Data can help us understand the complex interactions and evolutionary processes between the Earth's natural systems and human social systems, thus contributing to the realization of SDGs.

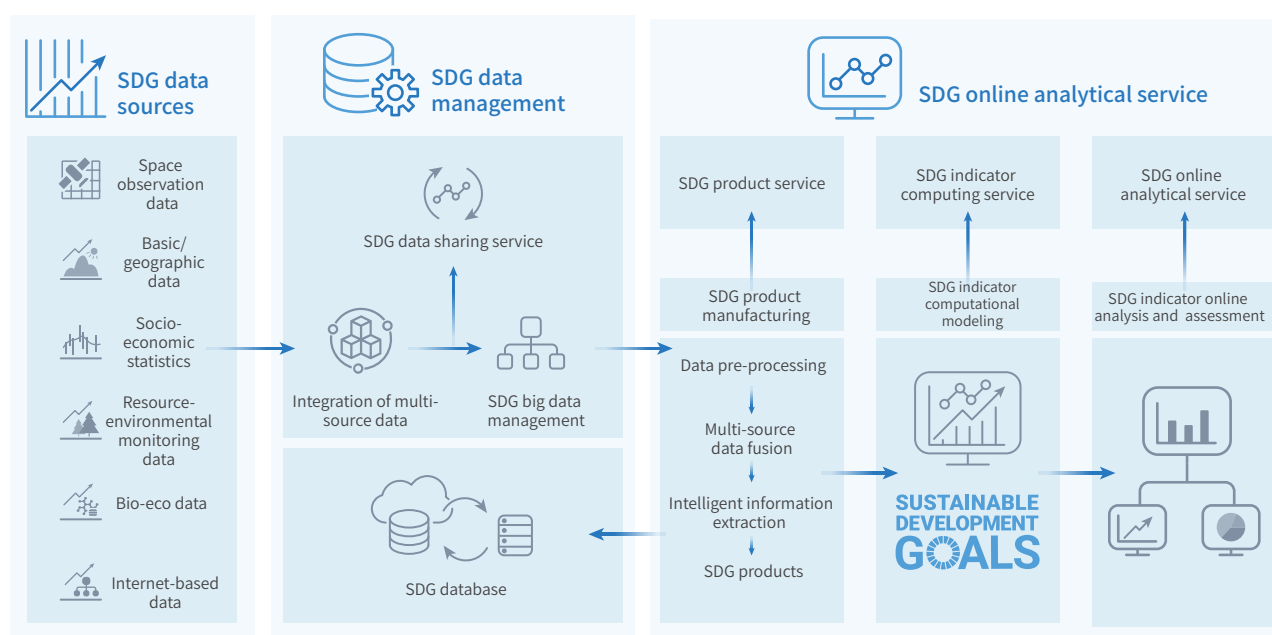
The Big Earth Data science includes these main technological systems: (1) ubiquitous sensing of Big Earth Data, (2) credible



↑ Figure 1-1. The technological systems of the Big Earth Data science

Big Earth Data sharing, (3) multiple Big Earth Data fusion, (4) Big Earth Data digital twin and complex process simulation, and (5) intelligent cognition of Big Earth Data (Fig. 1-1). Using the Big Earth Data to support SDG monitoring and evaluation has the following unique advantages: first, monitoring results are more transparent and repeatable on the strength of data

from diverse sources verifying each other; second, information on spatial difference and dynamic change is linked to SDG indicators, enabling decision-makers to use the former to detect and address the imbalances and weak links in the latter to identify the changing trend and policy effect.



↑ Figure 1-2. Big Earth Data Supporting SDG Roadmap

Since 2018, CAS has been using Big Earth Data to support SDGs. Based on the Big Earth Data Science Engineering Program (CASEarth), the Big Earth Data sharing service platform and the Big Earth Data Cloud service infrastructure have been established to provide data, on-line calculation and visualization for the monitoring and evaluation of SDG indicators (Fig. 1-2). Currently, CASEarth shares a total of about 10 petabytes of data, and updates 3 petabytes of data every year. As of September 2021, there were 360,000 users in 147 countries and territories, with 5797 million data visits.

Of the 17 Goals, SDG 2 Zero Hunger, SDG 6 Clean Water and Sanitation, SDG 11 Sustainable Cities and Communities, SDG 13 Climate Action, SDG 14 Life below Water and SDG 15 Life on Land are closely related to the Earth's environment and resources. The report on *Big Earth Data in Support of the Sustainable Development Goals*, in its current version, presents results of studies carried out on selected indicators under six Goals where Big Earth Data can play an important role in their monitoring and evaluation. In its 2019 and 2020 versions, the

report presented new methods, new products and decision support cases of using Big Earth Data to monitor and evaluate progress on the SDGs.

The 2021 report focuses on the updates and extension, new methodologies and indicators, the tracking and evaluation of several SDGs implementation process of China and the world, and theory and practice of multi-indicator interactive and coordinated development. It presents 26 typical cases on 18 targets, showcasing the results of research, monitoring and evaluation of relevant SDGs and their indicators at four scales, local, national, regional and global, totaling 20 data products, 13 methods and models and 16 decision support. The outcomes include change in cropping intensity and natural and artificial water bodies in China over 20 years, change in urban green space in China, the changes in global terrestrial ecosystem carbon sink and drivers, and the assessment of the effectiveness of ecological protection and restoration in China.

China's sustainable development process between 2010 and 2020 was evaluated centering on 20 indicators of six SDGs, based on

Table 1-1 Evaluation of China's Progress on SDGs Based on Big Earth Data (2010-2020)

	Indicators	Evaluated items	2010-2015	2015-2020
SDG 2	2.2.1 Prevalence of stunting among children under 5 years of age	Under-five stunting	● ↑	● ↑
	2.4.1 Proportion of agricultural area under productive and sustainable agriculture	Land productivity, water resources use, and excess fertilizer application	● ↑	● ↑
SDG 6	6.3.2 Proportion of bodies of water with good ambient water quality	Water clarity in lakes and reservoirs	● ↑	● ↑
	6.4.1 Change in water-use efficiency over time	Water-use efficiency	● ↑	● ↑
	6.5.1 Degree of integrated water resources management	Integrated water resources management	● ↑	● ↑
	6.6.1 Change in the extent of water-related ecosystems over time	Areal extent of wetlands (riverine and lacustrine systems)	● ↑	● ↑
	11.2.1 Proportion of population that has convenient access to public transport, by sex, age and persons with disabilities	Proportion of population that has convenient access to public transport	● ↓	● ↓
SDG 11	11.3.1 Ratio of land consumption rate to population growth rate	Ratio of land consumption rate to population growth rate	● ↓	● ↓
	11.4.1 Total per capita expenditure on the preservation, protection and conservation of all cultural and natural heritage	Unit Input in heritage sites	● ↑	● ↑
	11.5.1 Number of deaths, missing persons and directly affected persons attributed to disasters per 100,000 population	Interannual change in total loss from natural disasters at prefectural level	● ↑	● ↑
	11.6.2 Annual mean levels of fine particulate matter (e.g., PM _{2.5} and PM ₁₀) in cities (population weighted)	Fine particulate matter in cities	● ↓	● ↓
	11.7.1 Average share of the built-up area of cities that is open space for public use for all, by sex, age and persons with disabilities	Area of open space in cities	● ↑	● ↑
	13.1.1 Number of deaths, missing persons and directly affected persons attributed to disasters per 100,000 population	Number of deaths, missing persons and directly affected persons attributed to disasters per 100,000 population	● ↑	● ↑
SDG 13	13.2.2 Total greenhouse gas emissions per year	Concentration of greenhouse gas	● ↑	● ↑
	14.1.1 (a) Index of coastal eutrophication; and (b) plastic debris density	Marine debris and microplastics in coastal waters	● ↑	● ↑
SDG 14	14.2.1 Number of countries using ecosystem-based approaches to managing marine areas	Area of mangrove	● ↑	● ↑
	14.7.1 Sustainable fisheries as a proportion of GDP	Area of raft culture in coastal waters	● ↑	● ↑
SDG 15	15.3.1 Proportion of land that is degraded over total land area	Proportion of degraded land	● ↑	● ↑
	15.4.2 Mountain Green Cover Index	Mountain Green Cover Index	● ↑	● ↑
	15.5.1 Red List Index	Red List Index	● ↓	● ↓

Colored circles indicate state of implementation
 ● Very challenging
 ● Challenging
 ● Close or achieved

Arrows indicate trend
 ↑ Improving
 → Stable
 ↓ worsening

Bright green bars indicate the years covered by the evaluation during the period of 2010-2020. The example below indicates 2010-2018.

the research results from the three editions of Big Earth Data in Support of Sustainable Development Goals (Table 1-1).

So far, of the 20 evaluated indicators, China is close to or has met four, including SDG 2.2.1 prevalence of stunting among children under 5 years of age, SDG 11.2.1 proportion of population that has convenient access to public transport, SDG 15.3.1 proportion of land that is degraded over total land area, and SDG 15.4.2 Mountain Green Cover Index. Attention needs to be given to regional differences in the future. Regarding SDG

6.4.1 change in water-use efficiency over time and SDG 15.5.1 Red List Index, despite improvement in recent years, major challenges remain, and attention should be given to water saving and wildlife protection, two areas where greater efforts are called for. The result shows between 2010 and 2015 two indicators worsened and 11 indicators improved; between 2015 and 2020 no indicator worsened and 16 improved. Overall, China has made significant improvement especially since 2015, and is on track to achieving these six Goals by 2030.



SDG 2



SDG 2

Zero Hunger

Background	14
Main Contributions	15
Case Study	16
Summary	26



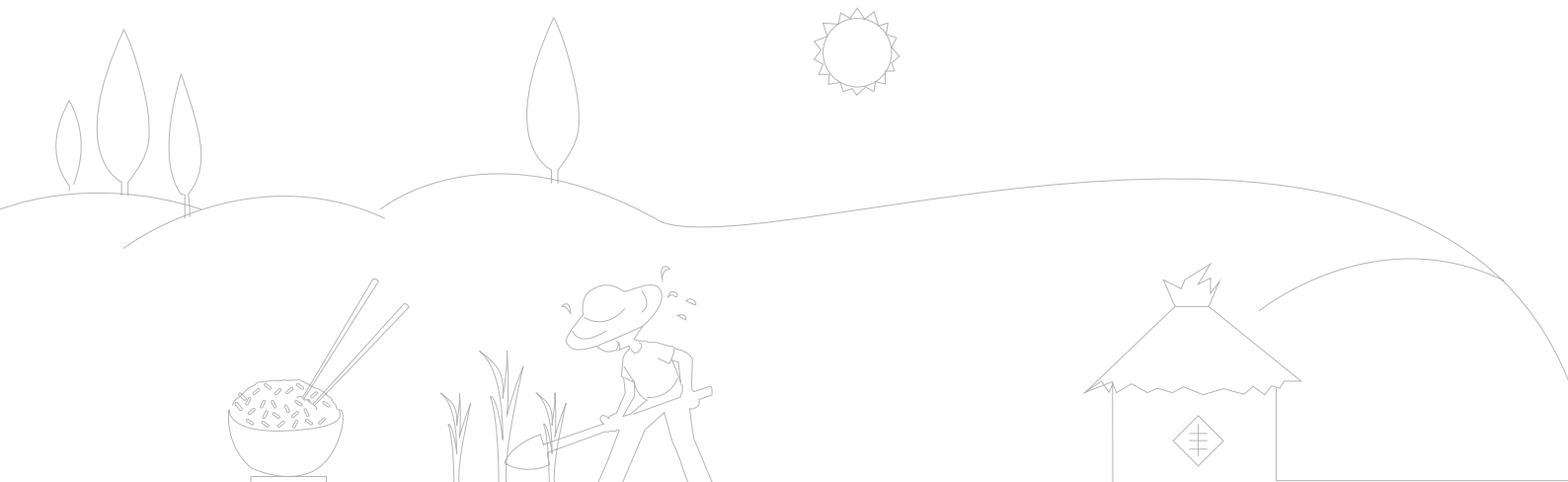
Background

The Goal of zero hunger aims to ensure food security, improve nutrition and promote sustainable agriculture. It is fundamental to global sustainable development. Yet progress toward this Goal has been slow over the past five years since the launch of the 2030 Agenda for Sustainable Development. Hunger and food insecurity at the global level continue to deteriorate due to regional conflicts, climate change, economic recession (as a result of the COVID-19 pandemic recently) and other factors. The prevalence of moderate or severe food insecurity has been slowly increasing for six years in a row, and reaching 30.4% by 2020. The prevalence of undernourishment increased by 1.5 percentage points in 2020 after remaining stable for five consecutive years, making it more challenging to reach the Goal of zero hunger by 2030. The Food and Agriculture Organization of the United Nations (FAO) has outlined six potential pathways for transforming food systems that cover food supply, access, utilization, stability, empowerment and sustainability, while listing technology, data and innovation as one of the two categories of accelerators (FAO *et al.*, 2021).

Tracking, monitoring and evaluating zero hunger, both in terms of degree and process, can clearly identify the breadth and depth of the various food security problems in different regions, and inform decisions on regional food system transformative programs. Currently, the monitoring and evaluation of SDG 2

indicators are mainly accomplished by statistical surveys (FAO, 2020a), result in a problematic timeliness. The COVID-19 pandemic has made the timeliness of data more challenging (FAO *et al.*, 2021). To develop methods of timely access to information is an important prerequisite for immediate feedback and prompt action. At the same time, the integration of geospatial and statistical information is considered an important field of data innovation, instrumental in gaining insight into data linkages and relationships and informing both decision-makers and the general public (UN, 2021a). Especially for SDG 2, a Goal that closely integrates social, economic and environmental dimensions, multi-source data fusion is an important tool for cognitive findings and decision support.

Focusing on SDG 2.4, this chapter will demonstrate the potential of Big Earth Data for timely information acquisition and multi-source data fusion for two fundamental elements closely related to sustainable food production: cropping intensity and crop types. In response to the transformation pathways of food systems proposed by FAO, we developed a data-driven paradigm of efficient ecological agriculture, and built an experimental farm to test the paradigm. It also serves as a demonstration for the transformation of agriculture system to climate-smart and environment-friendly to the benefit of the protection and restoration of the natural environment.





Main Contributions

To promote SDG 2.4 on sustainable food production systems, we have proposed the method of extracting cropping intensity based on real-time Earth observation data, the method of mapping crop spatial distribution by fusing remotely sensed data, statistics and other multi-source data, and the paradigm of data-driven efficient ecological agriculture based on agroecological theory.

Decision-making support for sustainable food production is provided to both government and farmers (Table 2-1). Based on these case studies, more data, technologies and policy tools are made available by Big Earth Data in support of achieving zero hunger.

Table 2-1 Cases and Their Main Contributions

Indicator	Tier	Case	Contributions
2.4.1 Proportion of agricultural area under productive and sustainable agriculture	Tier II	Spatiotemporal variations of cropping intensity over 20 years in China	<p>Method and model: Method for high accuracy remote sensing-based cropping intensity monitoring</p> <p>Decision support: It informs decision on managing cropland multiple cropping system to achieve sustainable food production</p>
		Mapping crop distribution and its changes in China	<p>Data product: Spatial distribution data set of 14 major crops in China in 2000 and 2015</p> <p>Method and model: A crop spatial distribution mapping model integrating remotely sensed time-series data, statistical data, and crop calendars</p>
		An experiment of efficient ecological agricultural paradigm in the low-medium-yield region along the lower reaches of the Yellow River	<p>Method and model: Efficient ecological agricultural paradigm based on agroecological system theory, information technology and modern agricultural technology</p> <p>Decision support: It integrates sensor network technology and big data management platform to inform decisions on developing efficient ecological agriculture.</p>



Case Study

Spatiotemporal variations of cropping intensity over 20 years in China

Target: 2.4 By 2030, ensure sustainable food production systems and implement resilient agricultural practices that increase productivity and production, that help maintain ecosystems, that strengthen capacity for adaptation to climate change, extreme weather, drought, flooding and other disasters and that progressively improve land and soil quality.

Highlights

- *China's cropping intensity data set, with annual updates from 2001 to 2020, was produced based on multi-source remotely sensed data and cloud platform, with an overall accuracy of 93% as verified by ground-based data.*
- *In the past 20 years, China's average cropping intensity has decreased slightly by 6% partly due to impact of agricultural policies to promote cropland sustainability, such as cropland preservation and incentives for fallow and rotation; different regions have seen significant differences, with larger cropping intensity gaps observed in the middle and lower reaches of the Yangtze River Basin, Southwest China and South China.*

Background

Arable land provides food that supports the very existence and development of human beings. Its sustainable use plays an important role in achieving the Goal of zero hunger. China is a large agricultural country with a population of more than 1.4 billion, but it has a low level of per capita arable land and faces pressures on its food production system brought by industrialization and urbanization (Zuo *et al.*, 2018). Cropping intensity is an important indicator to measure arable land use intensity. Tracking the change in cropping intensity can help assess the past development of the food production system and

inform future agro-policies.

Thanks to more advanced remote sensing technology, the popularization of high spatiotemporal resolution data has greatly contributed to the accuracy of cropping intensity mapping. This study focuses on China, where multi-cropping has a long history, and constructs a cropping intensity mapping method, through fusion of multi-source remotely sensed data and cloud computing technology, to map and analyze annually updated cropping intensity at the national scale from 2001 to 2020.

Data used

© Satellite data: Moderate Resolution Imaging Spectroradiometer (MODIS) Normalized Difference Vegetation Index (NDVI) data from 2001 to 2020, Sentinel-2, Landsat-5, Landsat-7 and Landsat-8 data from 2001 to 2020.

© Other data: cropland layer (2000, 2010, and 2015) from ChinaCover 30 m resolution land cover data (Wu, *et al.*, 2017); nine Chinese agro-ecological zones' data (Sun, 1994); and ground-based cropping intensity samples.

Method

Time series NDVI data set was constructed by normalizing multi-source remotely sensed data, upon which a spatiotemporally continuous NDVI data set was generated by data smoothing and gap filling. The phenophase-based approach (Liu *et al.*, 2020) was used to map the annual updates of cropping intensity from 2001 to 2020. The results were validated based on a large

number of ground-based samples obtained nationwide collected using GVG (GPS, Video and GIS) smart phone application.

The average of cropping intensity for the whole country and the 9 agroecological zones were calculated for each year of the studied period. The change rates and linear changing trends were derived, and the spatiotemporal changes analyzed.

Results and analysis

Figure 2-1 shows the cropping intensity maps of China in 2001, 2007, 2013 and 2020. In general, the single cropping pattern is dominant in the country, mostly seen in northern China due to climatic conditions. The double cropping areas mainly concentrate in the North China Plain, where irrigation infrastructures are well developed to compensate for the low rainfall in winter; the double cropping pattern is also commonly observed in the south, the middle and the middle and lower reaches of the Yangtze River, and Taiwan province, where there are abundant rain and heat during the crop growing season. The triple cropping pattern is basically seen in Hainan, Guangdong and Guangxi. The validated results show that the overall accuracy of obtained cropping intensity in China is about 93%, among which the highest accuracy is for the single cropping pattern.

Since 2001, cropping intensity of China has been decreasing in general, and the national average has dropped by 6% in the past 20 years (Fig. 2-2), due to impact of agricultural policies to promote cropland sustainability, such as cropland preservation

and incentives for fallow and rotation. Significant differences on changing patterns in cropping intensity are observed among the nine agroecological zones (Fig. 2-3). In the Huanghuaihai zone, one of the important crop-producing regions, cropping intensity increased by 8% from 2001 to 2020. In the Inner Mongolia and zone, it also showed an upward trend, and the increase was significant. In Gansu, Xinjiang and the Qinghai-Tibet Plateau, there was an upward trend but with fluctuations. In contrast, middle and lower reaches of the Yangtze River has seen a significant decline of 6% in cropping intensity in the past 20 years, making it the only agroecological zone in China with a significant decrease. The prevalent shift from double-cropping rice to single-cropping rice in this region is directly attributable to labor transfer away from agriculture. The cropping intensity in the South and Southwest had a downward trend with fluctuations, while it remained stable without any significant changes in the Northeast and the Loess Plateau. In general, fairly large gaps in cropping intensity were observed in the middle and lower reaches of the Yangtze River, Southwest and South China.

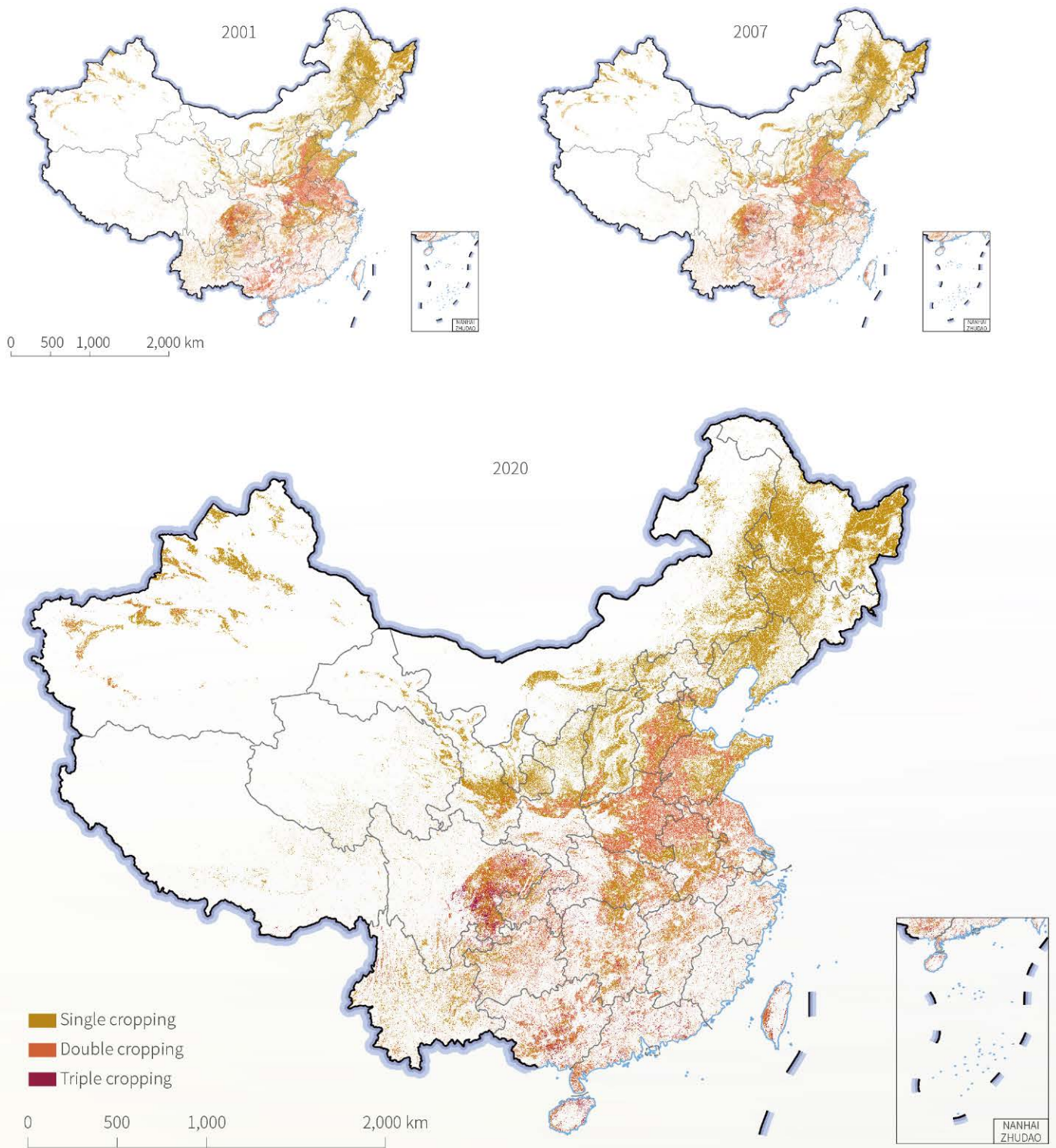


Figure 2-1.

● Cropping intensity in China in 2001, 2007, 2013 and 2020



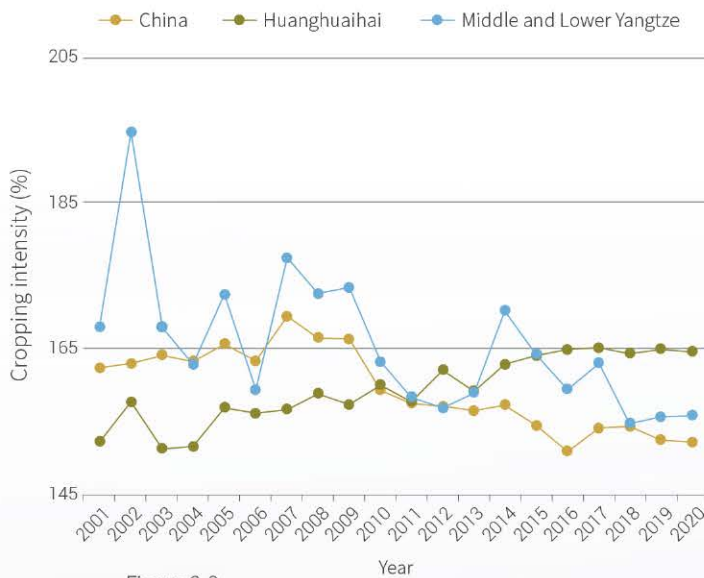
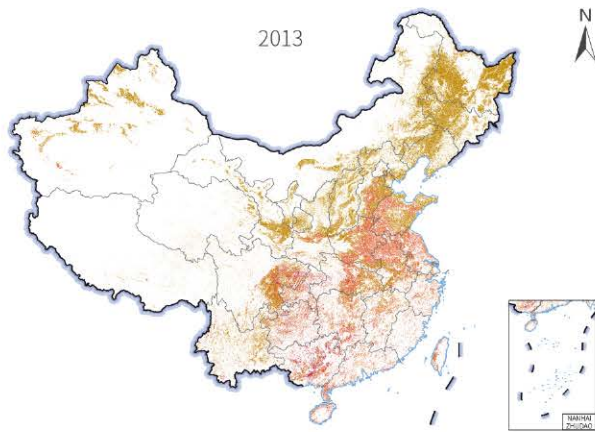


Figure 2-2.

Temporal changes of cropping intensity in China, Huanghuaihai, and Middle and Lower Yangtze

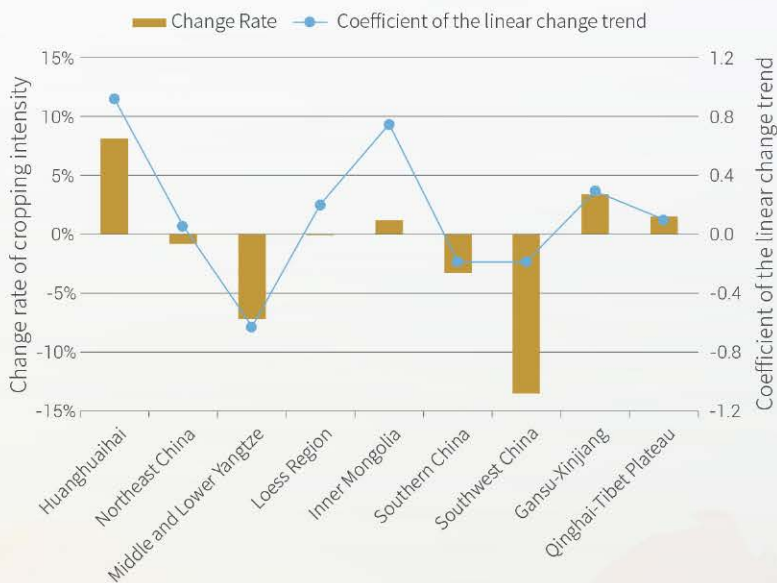


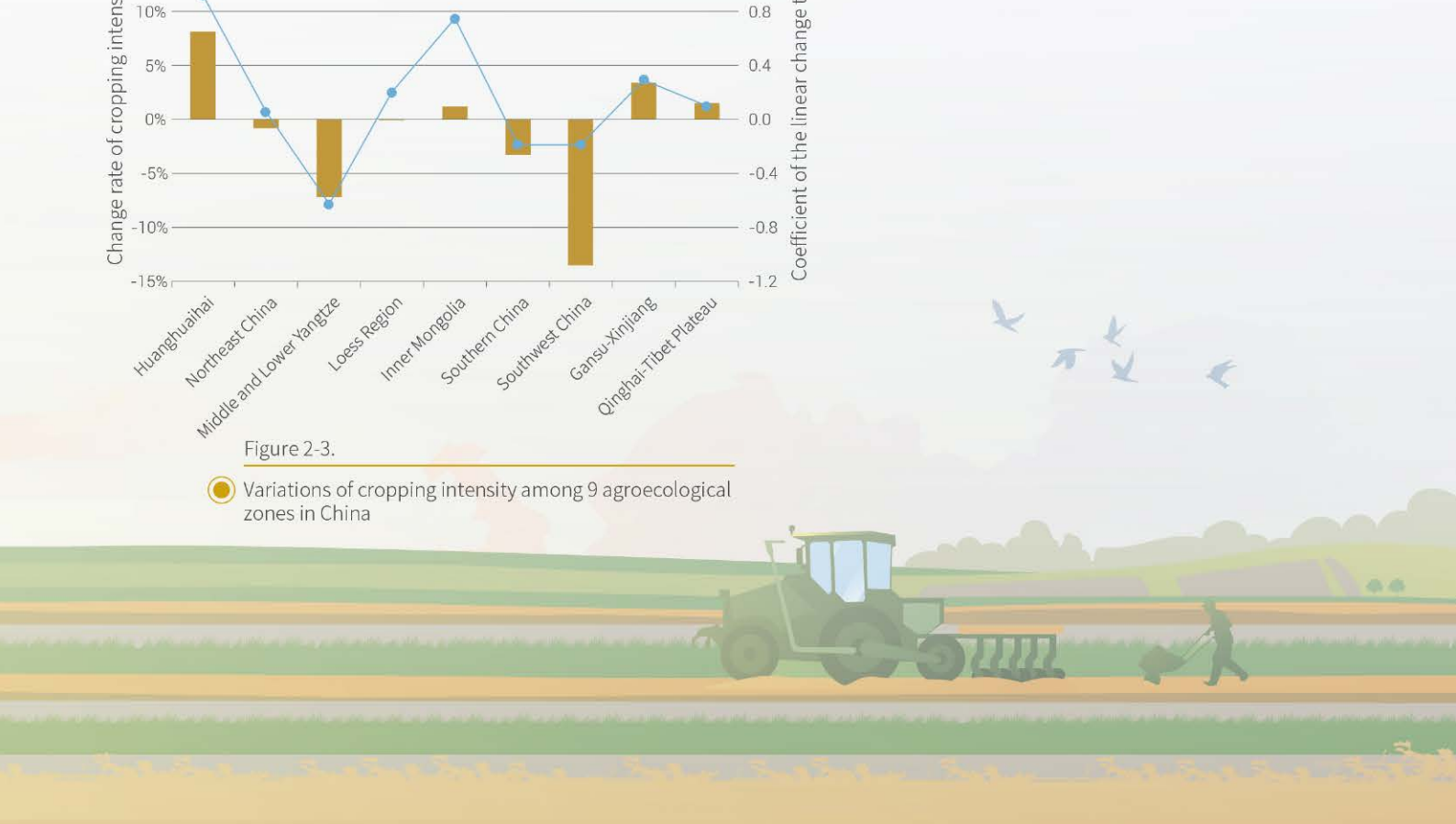
Figure 2-3.

Variations of cropping intensity among 9 agroecological zones in China

Outlook

The cropping intensity mapping can provide scientific data support for quantitative analysis of cropland use intensity and sustainability. The annually updated mapping conducted in this case shows that the cropping intensity in China has overall been on a slightly downward trend. However, remote sensing-based estimates show that the total grain production in China has increased by about 29% in the past 20 years, with year-on-year increase in most years. This increase is closely linked to the increasing crop yield as contributed by the improvement of breeding technology, agricultural management measures (fertilization, irrigation, etc.).

In the future, Synthetic Aperture Radar (SAR) data can be used to tackle the difficulty in obtaining optical images in frequently cloudy and rainy southern regions, and to improve the accuracy and reliability of cropping intensity products in China.



Mapping crop distribution and its changes in China

Target: 2.4 By 2030, ensure sustainable food production systems and implement resilient agricultural practices that increase productivity and production, that help maintain ecosystems, that strengthen capacity for adaptation to climate change, extreme weather, drought, flooding and other disasters and that progressively improve land and soil quality.

Highlights

- *By integrating cropping patterns extracted from time-series remotely sensed data, crop calendars, and statistics on planting area, the spatial distribution maps of 14 major crops in China in 2000 and 2015 with 1 km resolution was generated. The spatial heterogeneity of crop distribution reflected by our results is about 30% higher than the results based on commonly used mapping method.*
- *From 2000 to 2015, the centroids of crops had mainly shifted to the northeast (for corn, peanut, soybean, etc., accounting for 51% of the total crop planting areas), to the northwest (for cotton, millet, etc., accounting for 24% of the total crop planting areas) and to the southwest (for sorghum, sugar beet, etc., accounting for 25% of the total crop planting areas), primarily due to the change in cultivated land distribution, cropping pattern and planting structure.*

Background

Crops grown on cultivated land are the food source for human survival. They provide more than 90% of the calories and about 80% of the protein required by human life and activities (Kastner *et al.*, 2012). Changes in crop spatial distribution and planting structure usually lead to changes in nutrient supply. At the same time, given their different biological characteristics, crops are usually managed differently, which introduces quite different environmental impacts. Mapping crop distribution can provide basic information for the analysis of global food security,

environmental change and climate change in the world.

At present, most researches regarding crop mapping based on remote sensing have focused on a few crops, although earth observation technology have been advanced constantly. Large-scale multi-type crop mapping is still mainly based on the fusion of remotely sensed and statistical data, while the remotely sensed information is yet fully used to better reflect the spatial heterogeneity of crop distribution.

Data used

© Remotely sensed data: China Land Use Data Set with a scale of 1:100,000 and time-series MODIS Enhanced Vegetation Index (EVI) data for 2000 and 2015.

© Statistical and survey data: agricultural statistical data, crop calendar data, and agro-meteorological data for 2000 and 2015.

Method

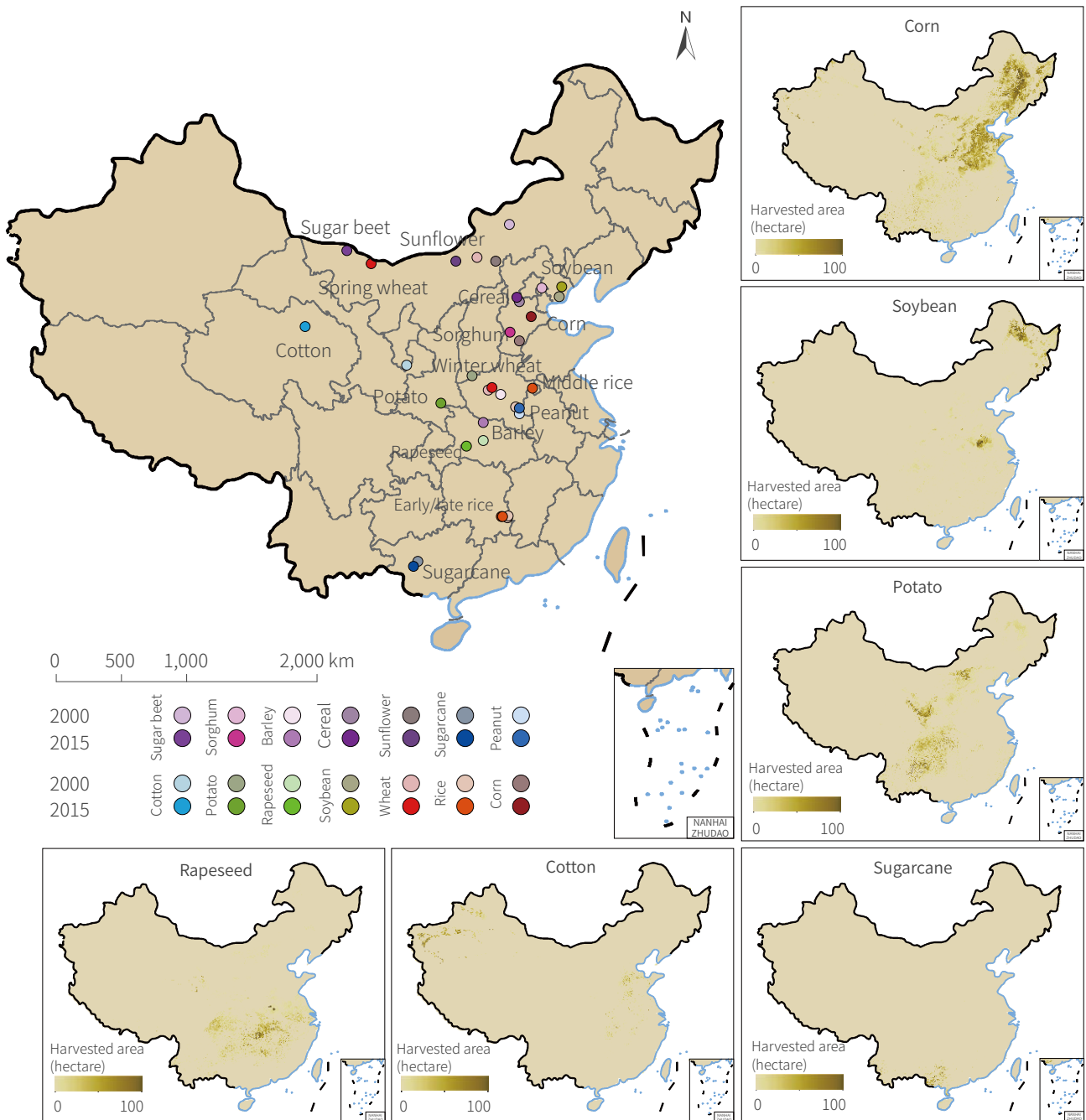
Based on MODIS EVI time series data, Harmonic Analysis of Time Series was used for de-cloud and de-noise process, and then the crop growth process curve at pixel level was constructed.

Through the extraction of peak number and occurrence time of the peaks, the information on cropping pattern of cultivated land was obtained, including single cropping, double cropping (with

or without winter crops), triple cropping (with or without winter crops), etc.

Based on analytical induction of crop calendar survey data, cropping patterns were regionalized; meanwhile, the planting area of each crop by administrative unit was obtained and crops divided into groups according to cropping season, and the planting area was calculated by different cropping season. Based

on the cropping patterns derived from remotely sensed data, their corresponding cropland areas, and planting areas of different crops for each season, the crop area was calculated for each pixel, and then the spatial distribution mapping was generated of 14 major crops in China in 2000 and 2015. We also analyzed the spatial patterns of the crop distribution and change in centroid of each crop from 2000 to 2015.



↑ Figure 2-4. Change in distribution centroid of 14 crop types and distribution maps for some typical crops from 2000 to 2015

Results and analysis

The diversity index was used to measure the richness of spatial information displayed in crop distribution maps, and the mapping results of this study were compared with those generated by the common used method-average allocation mapping. It was found that in eight randomly selected counties, the spatial diversity index of crop planting area under this method was between 6 and 7, while the diversity index under the average allocation mapping method was below 5. At the same time, the linear fitting method was used to compare the spatial distribution of rice on our map with that of paddy fields in the China Land Use Data Set with a scale of 1:100,000. It was found that the fitness was 0.67, indicating that the results obtained by our method can reflect the spatial heterogeneity of crop distribution properly.

Different crops are usually distributed in different areas because of their climatic suitability (Fig. 2-4). As a staple food crop with the largest planting area, corn is mainly distributed in the North China Plain and northeast China. About 32% of the country's cultivated land is sown to corn. Soybean is the largest legume crop, mainly distributed in northeast China and the south of the North China Plain, sown to about 5% of the cultivated land. Potato is the largest of the tuber crop, mainly sown along the Hu Line, using about 3% cultivated land. Among oil crops, rapeseed is most widely sown, mainly in central and southern China,

planted on about 5% of the cultivated land. Sugar crops mainly include sugarcane and sugar beet, distributed in the south and north of China respectively. Sugarcane has a larger sowing area, and mainly concentrated in Guangxi.

The change in crop spatial distribution is in a large part due to human activities, including changes in land use, agricultural policy, food demand, and market supply and demand (Stabile *et al.*, 2020). Analysis of changes in centroids of 14 crops from 2000 to 2015 revealed that the crops mainly moved in three directions: to the northeast (corn, soybean, peanut, etc., accounting for 51% of the total crop planting area), northwest (cotton, millet, etc., accounting for 24% of the total crop planting area), and southwest (sorghum, potato, sugar beet, etc., accounting for 25% of the total crop planting area). The change in spatial distribution of cultivated land, the change in multiple cropping pattern, and the adjustment of planting structure are the main reasons behind these changes. Urbanization has led to the loss of cultivated land in southeast China, while the cultivated land areas in northeast and northwest China have increased due to the influence of the grain market and policies (Zuo *et al.*, 2018). Most area of northeast and northwest China belong to the single cropping region, and the shift of crop area to this region has an impact on crop yield gap.

Outlook

The crop mapping provides information such as crop spatial distribution and planting structure, which can effectively support the evaluation of nutritional security and nutrient stability, thus facilitating the monitoring of SDG 2. In this case, the cropping pattern reflected by MODIS EVI time series data was combined with the regional crop calendar to provide more detailed spatial information for the downscaling of statistical crop planting area,

formulating a crop mapping method suitable for various crops. In the future, more crop growth information will be mined from Earth observation data, such as the length of growing period and the peak of vegetation index during growing period, to improve the accuracy of crop mapping. This method will also be applied to crop mapping on a global level, providing a basis for assessing global nutritional security.

An experiment of efficient ecological agricultural paradigm in the low-medium-yield region along the lower reaches of the Yellow River

Target: 2.4 By 2030, ensure sustainable food production systems and implement resilient agricultural practices that increase productivity and production, that help maintain ecosystems, that strengthen capacity for adaptation to climate change, extreme weather, drought, flooding and other disasters and that progressively improve land and soil quality.

Highlights

- *Based on agroecosystem theory, information technology and modern agricultural technologies, an experimental farm with an efficient ecological agricultural paradigm (EEAP) has been built in the low-medium-yield region along the lower reaches of the Yellow River. The paradigm has significantly improved the economic returns and the sustainability of resources and the environment of the farm. EEAP is a promising paradigm for agricultural production transformation.*
- *Through the EEAP experiment, soil organic matter rose 23.08%, consumption of fertilizer, pesticide and irrigation water dropped by over 10.00%, 70.00%, and 33.33% respectively; compared with the traditional paradigm (TP), the economic returns of the farm increased 61.99% and sustainability based on the emergy theory increased by 172.50%.*

Background

Since the 1950s, the world has made remarkable achievements in food production. Grain output has more than doubled, reducing the proportion of undernourished people from 36% in 1969 to 11% in 2018 (UN, 2019). But this high-unit-yield agricultural production paradigm relies heavily on the use of chemical fertilizers, pesticides, irrigation water, and machinery and has given rise to emerging issues: water consumption for agricultural production accounts for more than 70% of total water consumption (FAO, 2020b), the nitrogen use efficiency is less than 50% (FAO, 2018), about 75% of crop diversity has been lost on cropland, and more than one third of global greenhouse gas emissions are produced by food system (Crippa *et al.*, 2021). Therefore, a transformation in agricultural production paradigm

is urgently called for.

To achieve the social, economic, and environmental benefits sustainable agriculture is to produce, our study proposed the Efficient Ecological Agricultural Paradigm (EEAP), which integrates modern agricultural technologies, to be tested out in a demonstration farm with a medium-scale (15.33 ha) in the low-medium-yield region along the lower reaches of the Yellow River. The experiment was expected to improve the economic return of agricultural production and the sustainability of resources and the environment, and lead to a comprehensive solution of sustainable agriculture, contributing to long-term food security and achieving zero hunger.

Data used

© Observational and experimental data based on a sensor network and an information platform in the Beiqiu Experimental Farm, Yucheng, Shandong province, China: meteorological data, the growing status, soil attributes and productivity of crops and livestock, and the farm input/output data (such as chemical fertilizers, machinery, feed, labor, yield, and economic return)

and field test data (such as soil organic matter, fertilizer use efficiency, and water use efficiency).

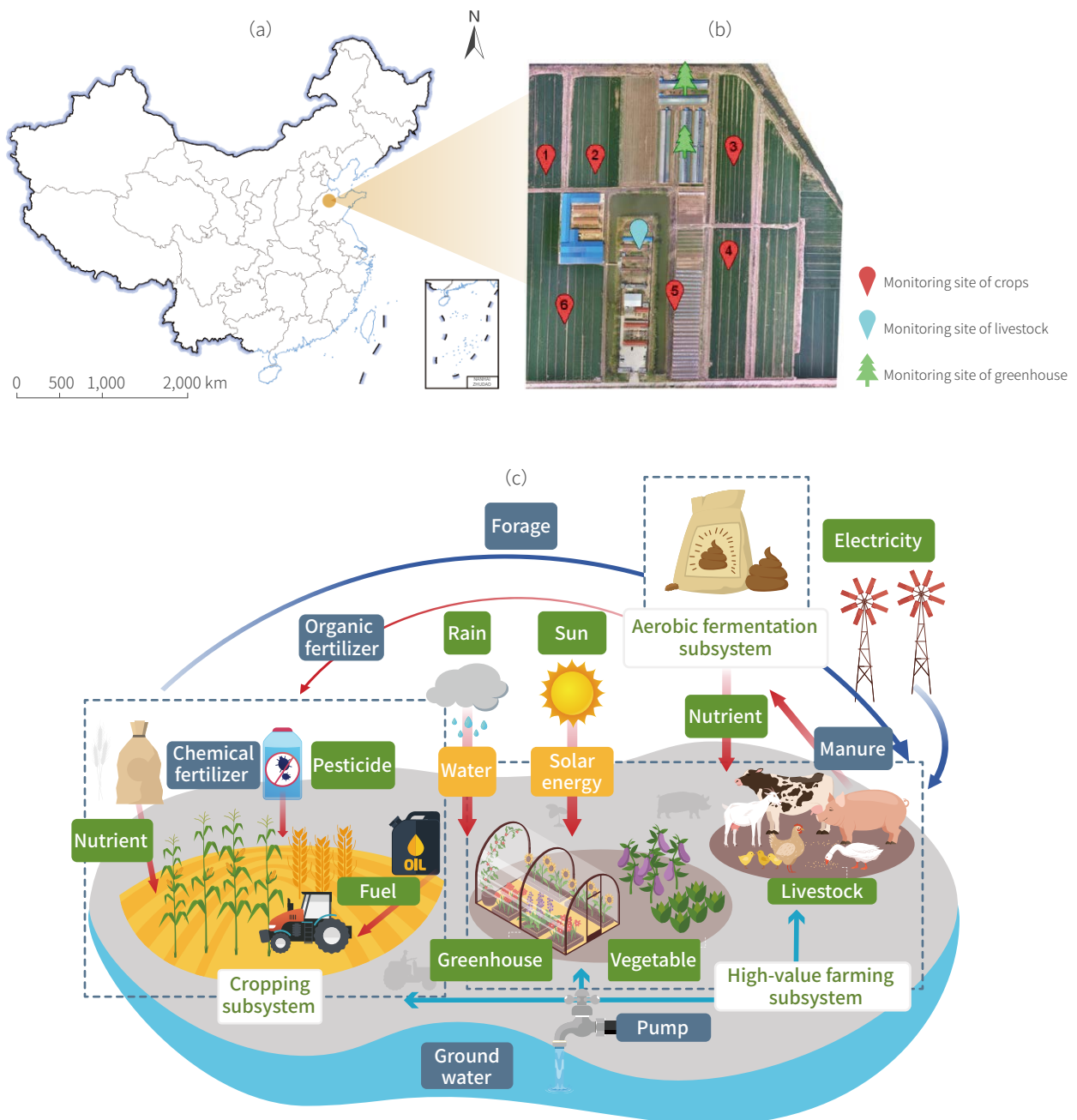
© Survey data on input/output of 271 farming households in Jinan, Dezhou and Weifang, Shandong province, China, including seeds, pesticides, chemical fertilizers, machinery, labor, and productivity.

Method

The EEAP, an efficient circular agricultural system involving crops, livestock and microbe, was developed based on the theories of agroecosystem and food-energy-water nexus, aimed at achieving sustainability in multiple ways, such as improving economic benefits, recycling resources efficiently, and reducing environmental pressures. A 15.33 ha experimental farm was built to test and validate this sustainable agricultural production

paradigm (Fig. 2-5a) in the low-medium-yield region along the lower reaches of the Yellow River. The EEAP consists of a crop subsystem, a high-value subsystem, and a fermentation subsystem, tested out on a 15.33 ha farm (Fig. 2-5b).

(1) The crop subsystem produces grain and provides feed for livestock. The application of organic fertilizer improves soil sustainability.



↑ Figure 2-5. The location (a), layout (b), and structure (c) of the EEAP farm

(2) The high-value subsystem provides nutrient-rich and high-value cash crops and livestock products; meanwhile, it provides the sources of organic fertilizer for crops.

(3) The fermentation subsystem improves the production efficiency of organic manure fertilizer and the use efficiency of livestock feed using microbial fermentation technologies and equipment.

Integrated sensor network and big-data management platform connects all the subsystems and collects data to realize the quantitative optimization of structure. The data technology along with a set of modern ecological agronomic technologies creates a new replicable, efficient, circular agricultural production paradigm. In addition, the data collected by the sensor network

and information platform provides strong support for the EEAP farm's operation, management, and evaluation.

Following the energy theory (Odum, 1996) and considering the renewability of input resources and the output of agricultural systems, a set of comprehensive indexes was created to evaluate the EEAP farm from all the three perspectives of economic benefits, environmental pressure, and sustainability, specifically including Land Profit Output (LPO), Environmental Loading Ratio (ELR), and Energy Sustainability Index (ESI). Additionally, the performance of the Traditional Paradigm (TP) was used as a comparison to measure sustainability improvement on the EEAP farm.

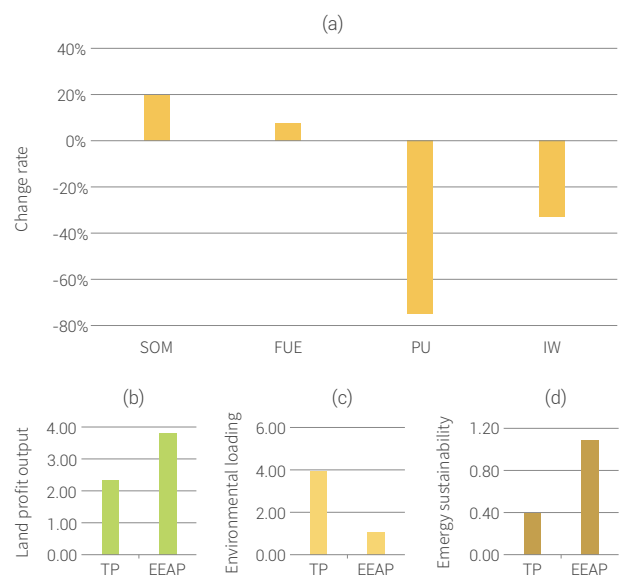
Results and analysis

Through experimental operation on the EEAP farm over two years, the soil organic matter increased by 23.08% from 13 $\text{g}\cdot\text{kg}^{-1}$ to over 16 $\text{g}\cdot\text{kg}^{-1}$; fertilizer consumption dropped more than 10.00% and fertilizer utilization efficiency increased by more than 8.00%; pesticide application decreased by more than 70.00%, farmland biodiversity increased, with a remarkable rise in the number of beneficial insects; irrigation water use decreased approximately by 33.33% from 5400 to 3600 $\text{m}^3\cdot\text{ha}^{-1}$ (Fig. 2-6a).

The LPOs of the EEAP and TP were 3789.94 $\text{\$}\cdot\text{ha}^{-1}\cdot\text{a}^{-1}$ and 2339.61 $\text{\$}\cdot\text{ha}^{-1}\cdot\text{a}^{-1}$, respectively, indicating that the economic benefits of the EEAP increased by 61.99% compared with the TP (Fig. 2-6b). The ELRs of the EEAP and TP were 1.04 and 3.96, respectively, showing that the production pressure on the environment of the EEAP went down by 73.74% (Fig. 2-6c). Meanwhile, the ESIs of the EEAP and TP were 1.09 and 0.40, respectively, indicating that the sustainability of the EEAP increased by 172.50%.

Outlook

For a comprehensive solution for sustainable agriculture, this study proposed an agricultural production paradigm based on the agroecosystem theory and modern agricultural technologies, which improves economic, ecological, and social benefits. A 15 ha experimental farm, suitable for household operation, was built to validate the performance of the new paradigm. The EEAP, which involves optimized subsystems and integrated technologies, can be applied to countries and regions that face pressing resource or environmental issues or poverty. So far, demonstration EEAP farms of different scales have been built in the main regions of China (Tsitsihar, Heilongjiang; Songyuan, Jilin; Hua county, Henan; Zhenjiang, Jiangsu; Heng county, Guangxi).



↑ Figure 2-6. The changes of the experimental farm's performance in Soil Organic Matter (SOM), Fertilizer Use Efficiency (FUE), Pesticide Use (PU), and Irrigation Water (IW) after implementing EEAP (a). The comparisons of EEAP and TP in Land Profit Output (LPO) (b). Environmental Loading Ratio (ELR) (c). and Energy Sustainability Index (ESI)



Summary

Sustainable food production is the foundation for achieving the Goal of zero hunger and an effective way to address global challenges such as climate change and land and ecological degradation. Food production is one of activities with the most intense interactions between nature and human beings. The improvement of its sustainability and security can be achieved by fully applying science, technology and innovation to governance as well as individual and collective actions. Focusing on sustainable food production systems under SDG 2.4, this chapter has presented national-scale spatial mapping methods for cropping intensity and crop distribution based on Big Earth Data technology, and provided spatial and temporal pattern change analysis of these two key elements of cropland use. The results can inform decision-makers on national sustainable agriculture. Moreover, the data-driven Efficient Ecological Agricultural Paradigm, tested out on experimental farms, is proposed to provide decision support as well as a paradigm of sustainable agriculture for farm operators of varying scales. The findings are as follows:

(1) Capacity for timely and rapid information acquisition

Annual updates of cropping intensity index of China from 2001 to 2020 was obtained through fusion of multi-source Earth observation data with a cloud computing platform, and it was found that the index had dropped slightly by 6% over the past 20 years. Areas where improvement was possible in cropping intensity were identified, as a third element that can increase

grain yield.

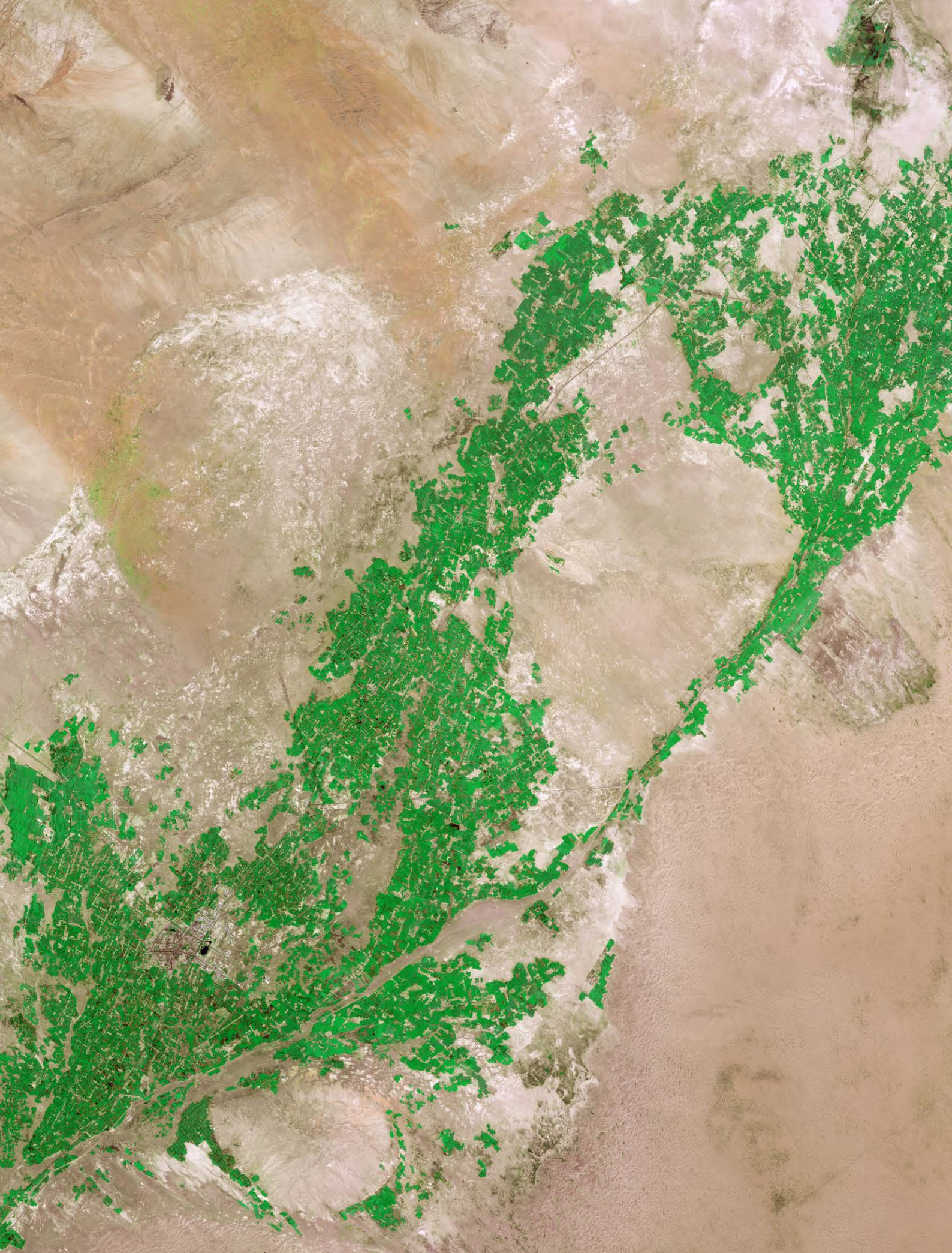
(2) Capacity for information extraction based on multi-source data fusion

Targeting at multi-crop system that underpins the supply of multi-dimensional nutrients, the spatial distribution of 14 major crops in China for 2000 and 2015 was mapped, based on cropping pattern derived from time-series remotely sensed data, crop calendar, and planting area statistics. It was found that the centroids of crop distribution had mainly moved in three directions to the northeast, northwest and southwest.

(3) Transformation of food production system

An efficient ecological agriculture paradigm has been established, based on agroecosystem theory, information technology and modern agricultural technologies, and tested out on experimental farms to be instrumental in enhancing economic benefits, reducing resource consumption, and mitigating environmental impact. The EEAP is an exemplar for sustainable agriculture.

The report demonstrates, through case studies, the capabilities and potential of Big Earth Data for timely information acquisition and multi-source data fusion for detecting and analyzing food production systems, and provides a paradigm in favor of the transformation of food production system toward sustainable development.



Satellite image of Minqin oasis (Gaofen-6 wide swath August 18, 2019)





SDG 6

Clean Water and Sanitation

Background	30
Main Contributions	31
Case Study	32
Summary	49



Background

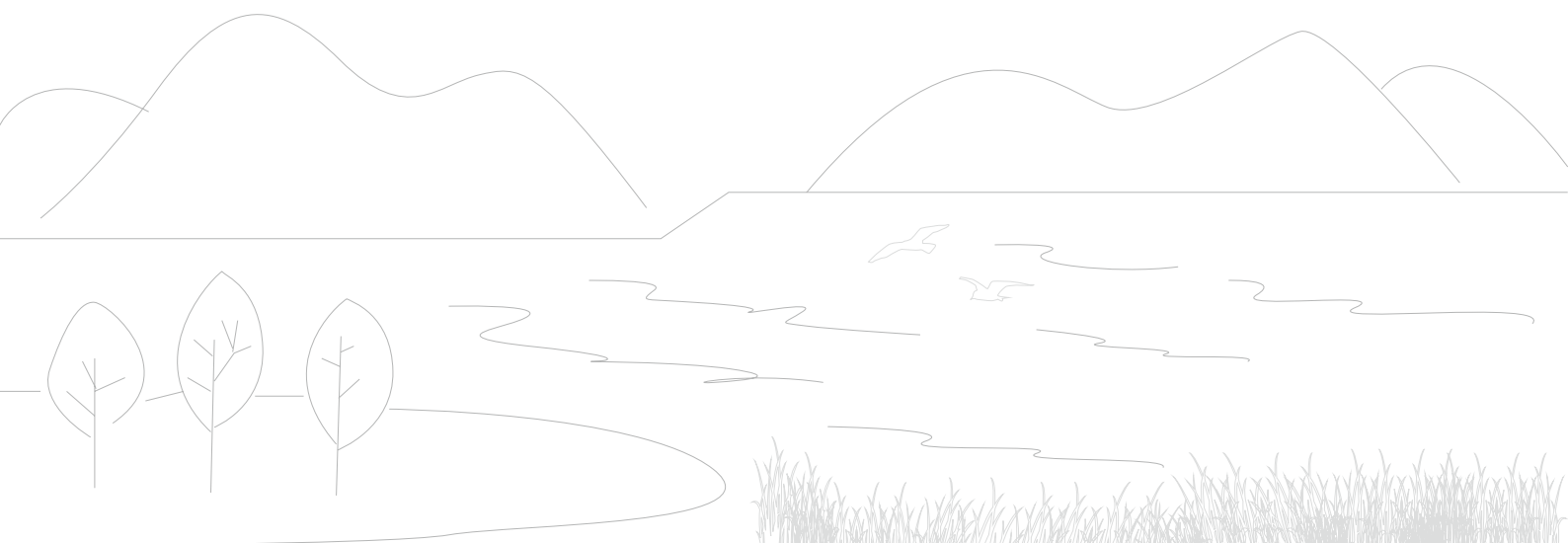
SDG 6 is to provide clean water and sanitation for all and manage them sustainably. According to the latest progress update issued by the UN Water, the world was off track to SDG 6 even before the outbreak of COVID-19 (UN-Water, 2021). At present, billions of people around the world still live without safely managed drinking water and sanitation. Many drinking water sources are drying up; water pollution is increasing; water-intensive industries, agriculture and the energy sector are still growing to meet the needs of an expanding population.

In order to solve the problems hindering the realization of SDG 6 and bring the world back on track, the United Nations has launched a Global Acceleration Framework including financing, data and information, capacity development, innovation, and governance (UN-Water, 2020a). Among them, data and information are meant to improve water-related monitoring and assessment through data generation, validation, standardization and information exchange, including drawing on coherent data, innovative approaches, and tools.

The capacity to monitor and evaluate SDG 6 has already increased greatly in recent years, benefit from the rapid development of Big Earth Data technology. The characteristics of these technical, such as remote sensing, regular revisit, and rapid information extraction, make the high spatiotemporal resolution monitoring of SDG 6 indicators not only possible, but more accurate and comprehensive and less costly and time-consuming. However, despite their availability, up to now,

UN Member States on average only have data on two-thirds of indicators for SDG 6, and 38 member states have data on fewer than half of all indicators (UN-Water, 2021). There is an urgent need to improve the national-level monitoring of SDG 6 indicators through the development of technical and institutional capacity and infrastructure.

Case studies in the past two years involving the use of Big Earth Data have led to technological accumulation and demonstration for application regarding nationwide evaluation of SDG 6.3 and SDG 6.6, and also major progress in the monitoring and evaluation of SDG 6 indicators in China. This chapter evaluates the effectiveness of China's integrated management of water quality, water quantity and water ecosystems, covering SDG 6.3 on improving water quality, SDG 6.4 on increasing water-use efficiency, SDG 6.5 on integrated water resources management, and SDG 6.6 on protecting and restoring water-related ecosystems, and it also demonstrates the use of Big Earth Data in the global monitoring of certain indicators, while being consistent with the methods and regional and national assessment and demonstration used in the 2019 and 2020 reports. The case study results presented in this chapter are a useful supplement to the Chinese data set in the United Nations SDG database system. The use of Big Earth Data for accurate and objective evaluation of SDG 6, as done in China, can also be an exemplar for other developing countries.





Main Contributions

The five cases in this chapter mainly produced data products and decision-making support. The data products include China's lake water clarity data set, the global large lake water clarity data set, China's natural and artificial water bodies data set, China's vegetated wetlands data set, and long-term time series of global crop water-use efficiency data set. In terms of decision support, the assessment results of China's integrated water resources

management will directly inform policy measures to improve the existing system for water resources management, while the assessment conclusions on lake water clarity, distribution of natural and artificial water bodies, dynamic changes in vegetated wetlands can inform water-related environmental governance and ecological protection in different administrative divisions (Table 3-1).

Table 3-1 Cases and Their Main Contributions

Indicator	Tier	Case	Contributions
6.3.2 Proportion of bodies of water with good ambient water quality	Tier II	Monitoring and evaluating the dynamic changes in lake water clarity	<p>Data product: China's lake water clarity remotely sensed data set (1985-2020, every 3 years, 30 m); Global large lake clarity remotely sensed data set (2010, 2015, and 2020, 500 m)</p> <p>Decision support: It provides basic data and scientific evaluation results that can inform efforts of lake water-related ecological restoration and protection</p>
6.4.1 Change in water-use efficiency over time	Tier I	Assessment of change in global crop water-use efficiency	<p>Method and model: Evaluation of crop water-use efficiency based on multi-source remotely sensed data and crop growth processes on a global scale</p> <p>Data product: Global crop water-use efficiency data set from 2001 to 2019 (annual, 1 km)</p>
6.5.1 Degree of integrated water resources management	Tier I	The assessment of China's Integrated Water Resources Management	<p>Decision support: It informs efforts to improve and upgrade the water conservancy governance system and capacity.</p>
6.6.1 Change in the extent of water-related ecosystems over time	Tier I	Change in natural and artificial water bodies in China from 2000 to 2020	<p>Data product: China's natural and artificial water bodies data set (2000, 2005, 2010, 2015, and 2020, 30 m)</p> <p>Decision support: It provides basic data and scientific evaluation results for the investigation and evaluation of surface water resources.</p>
		Spatiotemporal changes in China's vegetated wetlands	<p>Data product: Spatial distribution of China's vegetated wetlands data set (2010, 2015, and 2020, 30 m)</p> <p>Decision support: It provides basic data and scientific results for wetland protection and restoration</p>



Case Study

Monitoring and evaluating the dynamic changes in lake water clarity

Target: 6.3 By 2030, improve water quality by reducing pollution, eliminating dumping and minimizing release of hazardous chemicals and materials, halving the proportion of untreated wastewater and substantially increasing recycling and safe reuse globally.

Highlights

- *This study developed and validated a lake water clarity inversion model based on satellite remotely sensed data and calculated the proportions of clear lakes in China.*
- *Spatial distribution data sets of water clarity were created for China's lakes from 1985 to 2020 and for large lakes in the world in 2010, 2015, and 2020.*
- *During 2001 and 2020, the clarity of China's lake waters increased overall, and so did the clarity of large lakes in the world.*

Background

Under the Goal of water and sanitation for all proposed by the United Nations in 2015, SDG 6.3.2 is defined as the proportion of surface water bodies with good ambient water quality in each country to the total number of surface water bodies. However, conventional field sampling cannot meet the need of large-scale surface water quality monitoring, and satellite remotely sensed data has become an important and low-cost source of data for this purpose. Water clarity, an important lake water quality parameter that can be monitored by satellite remote sensing, is a

significant indicator that reflects the comprehensive conditions of water.

This study proposed a satellite remote sensing method, employing the Big Earth Data technology, to analyze the spatiotemporal changes from 1985 to 2020 in the water clarity of China's lakes larger than 1 km². This method was then applied to monitoring the clarity of large lakes bigger than 25 km² in the world in 2010, 2015, and 2020, producing data sets in support of the global evaluation of SDG 6.3.2.

Data used

© Remotely sensed data: Landsat TM/ETM+/OLI data of China from 1985 to 2020 at a spatial resolution of 30 m. MODIS/Terra global data at a spatial resolution of 500 m in 2010, 2015, and 2020.

© In situ data: field data of water clarity of surface water bodies in China, and data sets from the National Earth System

Science Data Center and China Lake Scientific Database; shared measured data sets of Secchi disk depth acquired from the European Multi Lake Survey (EMLS) and United States AquaSat.

© Preliminary geographic information: global coastal zone vector data and 30 m Global Surface Water (GSW) data set.

Method

This study used Landsat and MODIS surface reflectance products as the main data sources. First, a calculation model was constructed based on the Forel-Ule Index and hue angle α , which was normalized based on the spectral response function of Landsat and MODIS blue, green, and red bands. Then a water clarity retrieval model (Wang *et al.*, 2020) was developed based on the above information and validated by the acquired global data sets of typical surface water bodies. Subsequently, water

clarity data sets were produced for China's lakes larger than 1 km², based on Landsat data from 1985 to 2020, and for large lakes in the world bigger than 25 km² for 2010, 2015, and 2020, based on MODIS data. Finally, the spatiotemporal changes in lake clarity in China and the world were analyzed based on the time-series data sets. Water bodies with Secchi disk depth greater than 0.5 m are generally defined as clear water bodies (Stephens *et al.*, 2015).

Results and analysis

Figure 3-1 shows the long-term trends of average water clarity (also known as Secchi Depth, or SD) of lakes and the proportion of clear lakes in China from 1985 to 2020. An evident inflection point can be observed in 2001, with a significant downward trend in SD before 2001 and a significant upward trend after. Overall, the proportion of clear lake area exhibited a significant increase from 1985 to 2020.

Figure 3-2 shows the spatiotemporal trends of SD of lakes in the five limnetic regions (East Plain Region, Mengxin Plateau Region, Qinghai-Tibet Plateau Region, Northeast Mountain-Plain Region, and Yungui Plateau Region) from 1985 to 2020. Since 1985, the SD of most lakes in China increased, and the number of lakes with increased SD accounted for more than 77.0% in each limnetic region. The proportion of lakes with better clarity was the highest in the East Plain Region (84.3%)

and the lowest in the Mengxin Plateau Region (77.0%).

Figure 3-3 shows the average water clarity distribution of large lakes in the world in the summer of 2020. Compared with 2010, water clarity increased significantly in central Asia, northern Europe, southeastern Africa, northern North America, and central South America in 2015. Compared with 2015, an overall increasing trend in the clarity of large lakes in the world was observed in 2020, with eastern and western Asia, northern Europe, central and eastern Africa, central North America, and southeastern South America showing significant increases. The water clarity of large lakes showed an upward trend with fluctuations from 2010 to 2020, among which the water clarity of 51.1% of the 1,257 large lakes in the world increased, most remarkably in Africa.

Outlook

This study developed a lake water clarity inversion model, using remotely sensed data, at national and global scales. Further, the spatial distribution trends and interannual changes in water clarity of China's and the world's lakes were analyzed, providing baseline data for monitoring and evaluating SDG 6.3 of improving global water quality.

Although there are satellite remote sensing capabilities for monitoring and assessing lake water clarity in China and the

world as demonstrated in this study, water clarity can reflect only the turbidity of lake water, but not the overall water quality. Future efforts are needed to explore means to monitor more parameters for surface water quality to facilitate Indicator 6.3.2 and provide multi-scale water quality information to inform environmental monitoring and management departments at different levels.

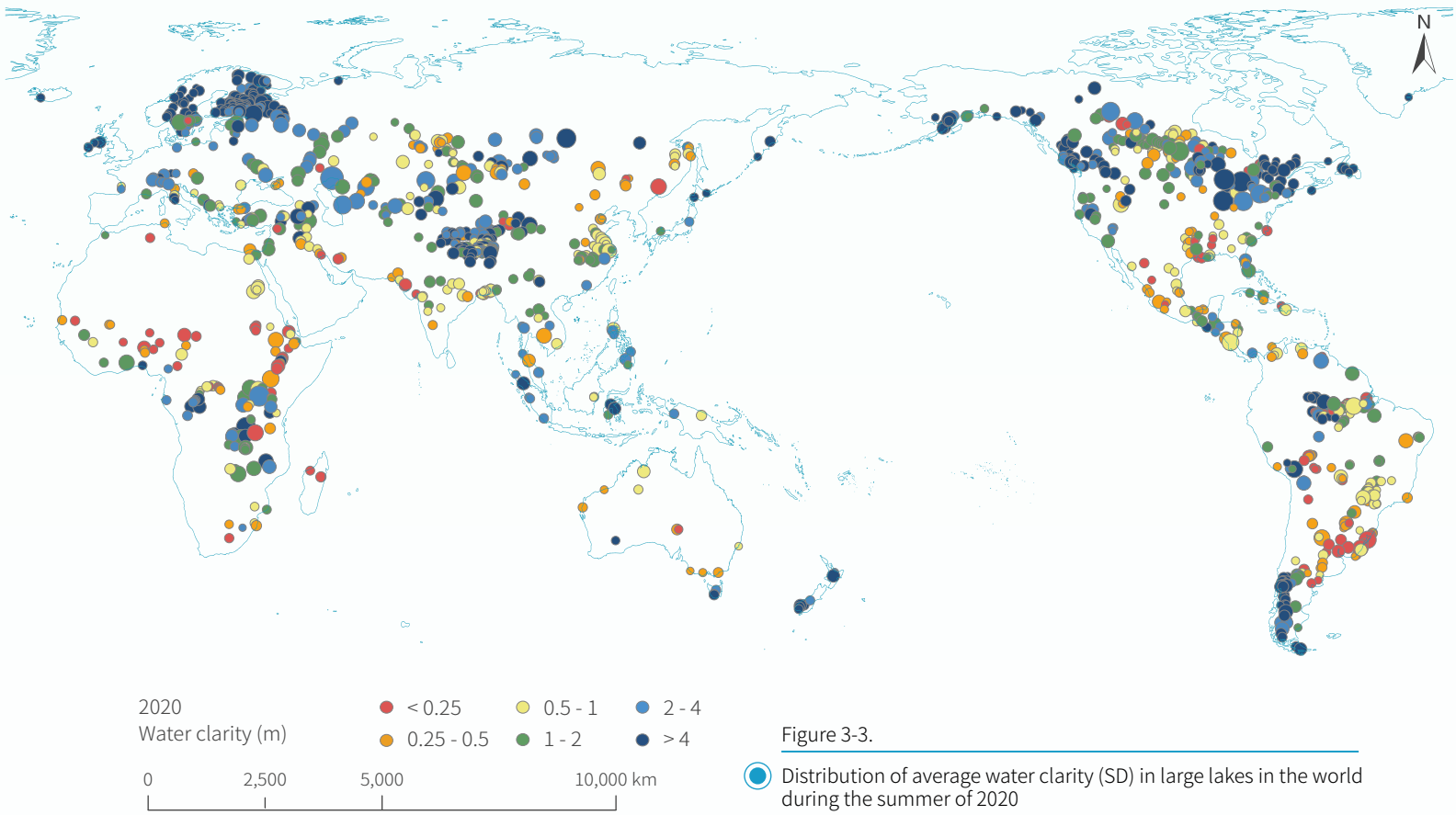


Figure 3-3.

● Distribution of average water clarity (SD) in large lakes in the world during the summer of 2020

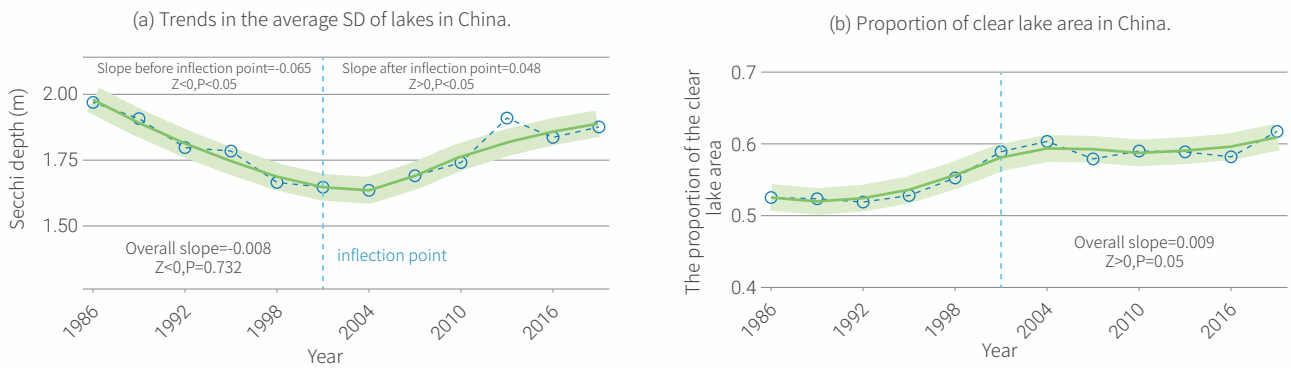
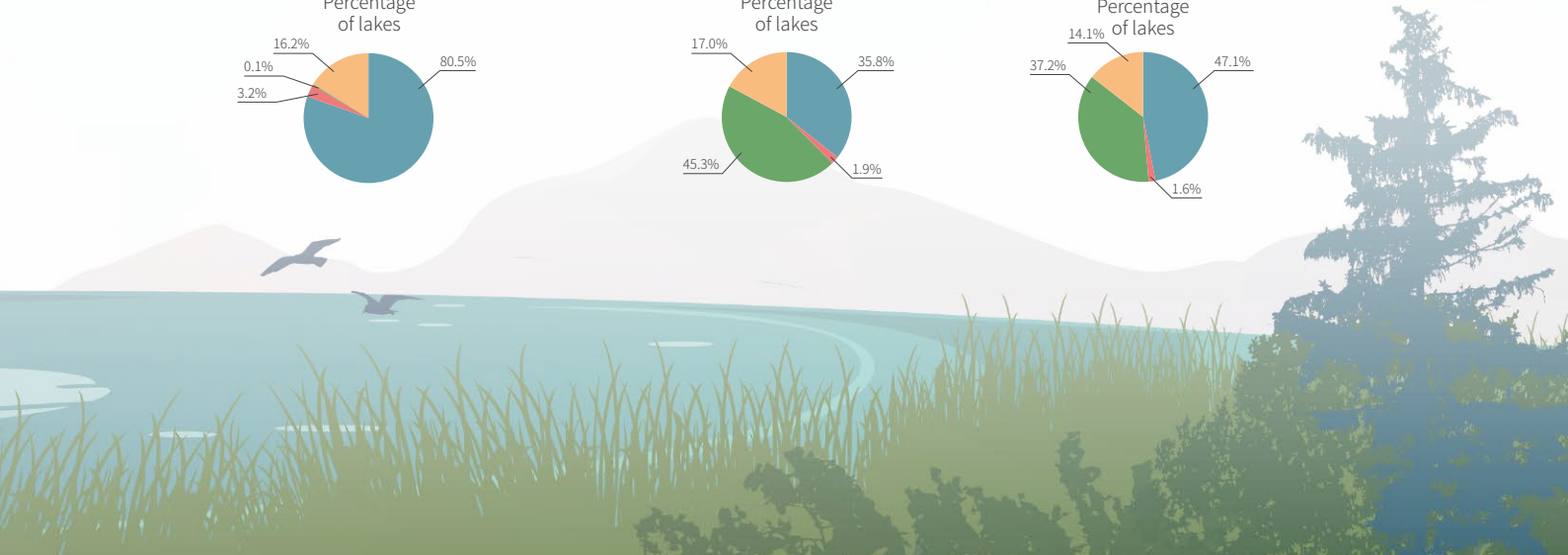
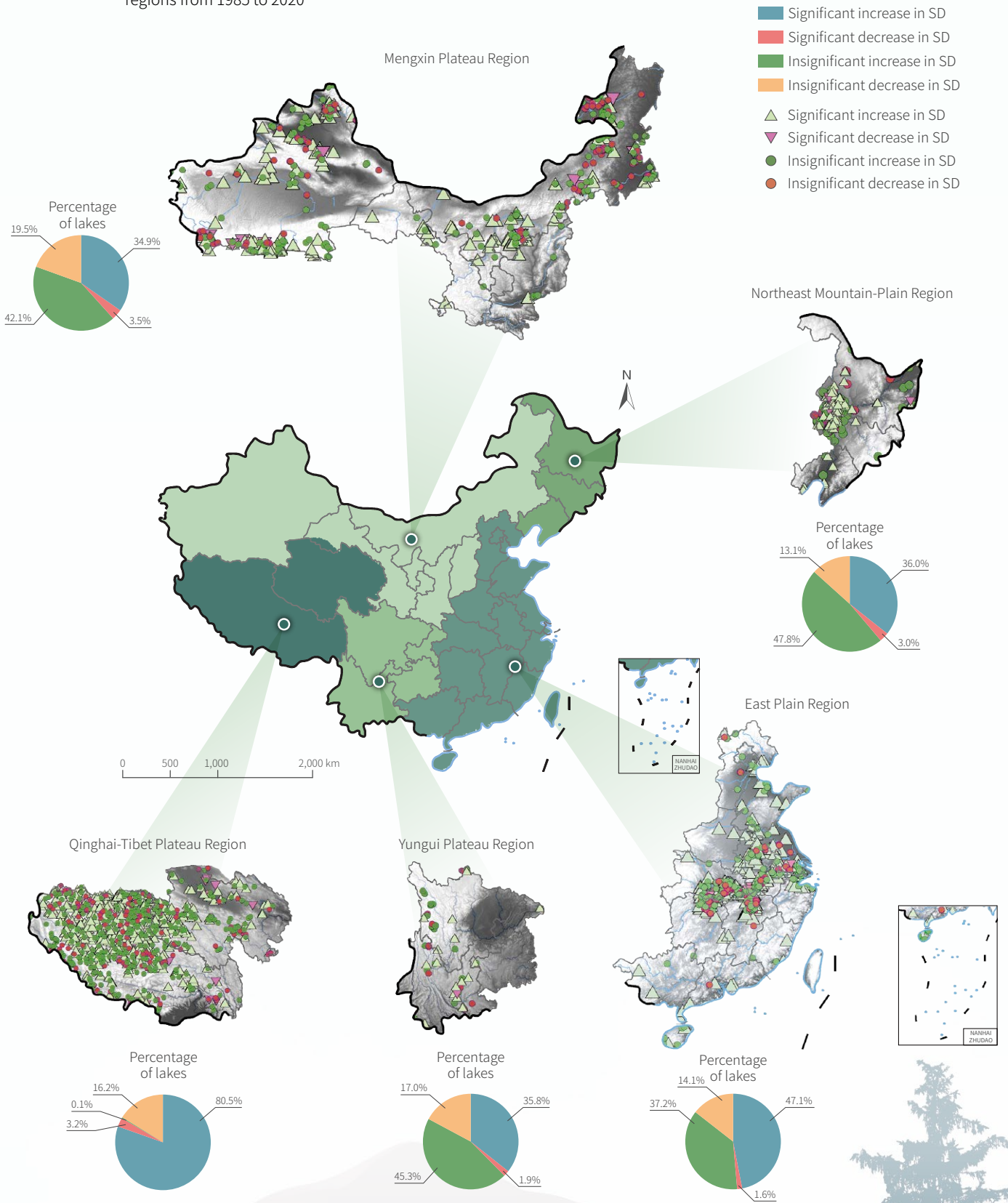


Figure 3-1.

● Trends in the average SD of lakes (a) and the proportion of clear lake area (b) in China from 1985 to 2020

Figure 3-2.

● Spatiotemporal trends of SD of lakes in the five limnetic regions from 1985 to 2020



Assessment of change in global crop water-use efficiency

Target: 6.4 By 2030, substantially increase water-use efficiency across all sectors and ensure sustainable withdrawals and supply of freshwater to address water scarcity and substantially reduce the number of people suffering from water scarcity.

Highlights

- A method was developed for the evaluation of global crop water-use efficiency based on multi-source remotely sensed data and crop growth processes, and a global data set between 2001-2019 was generated, providing an innovative method and data for monitoring and assessing SDG 6.4.1 in spatially comparable agricultural areas in the world.
- In recent 20 years, crop water-use efficiency in agricultural areas in the world has increased, mainly attributable to the increase in crop biomass thanks to technological progress, economic and social development and a certain degree of climate change.

Background

SDG 6.4.1 "change in water-use efficiency over time" is about measuring national water-use in order to help address issues that must be overcome before SDG 6.4 can be met. It involves water-use efficiency in sectors ranging from agriculture to industry to services. Among them, agriculture has high water use and consumption (through evapotranspiration). Improving agricultural water-use efficiency is important to promoting the sustainable use and development of water resources.

A commonly used evaluation indicator of agricultural water-use efficiency is crop Water Use Efficiency (WUE), which refers to the biomass yield per unit of water and can reflect water-use

efficiency from output. Crop water-use efficiency time series estimated from Big Earth Data combined with models can provide scientific support to the assessment of agricultural water-use efficiency and its temporal changes. The spatiotemporal coverage, timeliness and update frequency of such methods and data sets are significantly better than evaluation methods based on statistical data. Targeting the inadequacy of data for evaluating agricultural water-use efficiency, this study developed alternative indicators to evaluate the interannual change in crop water-use efficiency in different regions of the world.

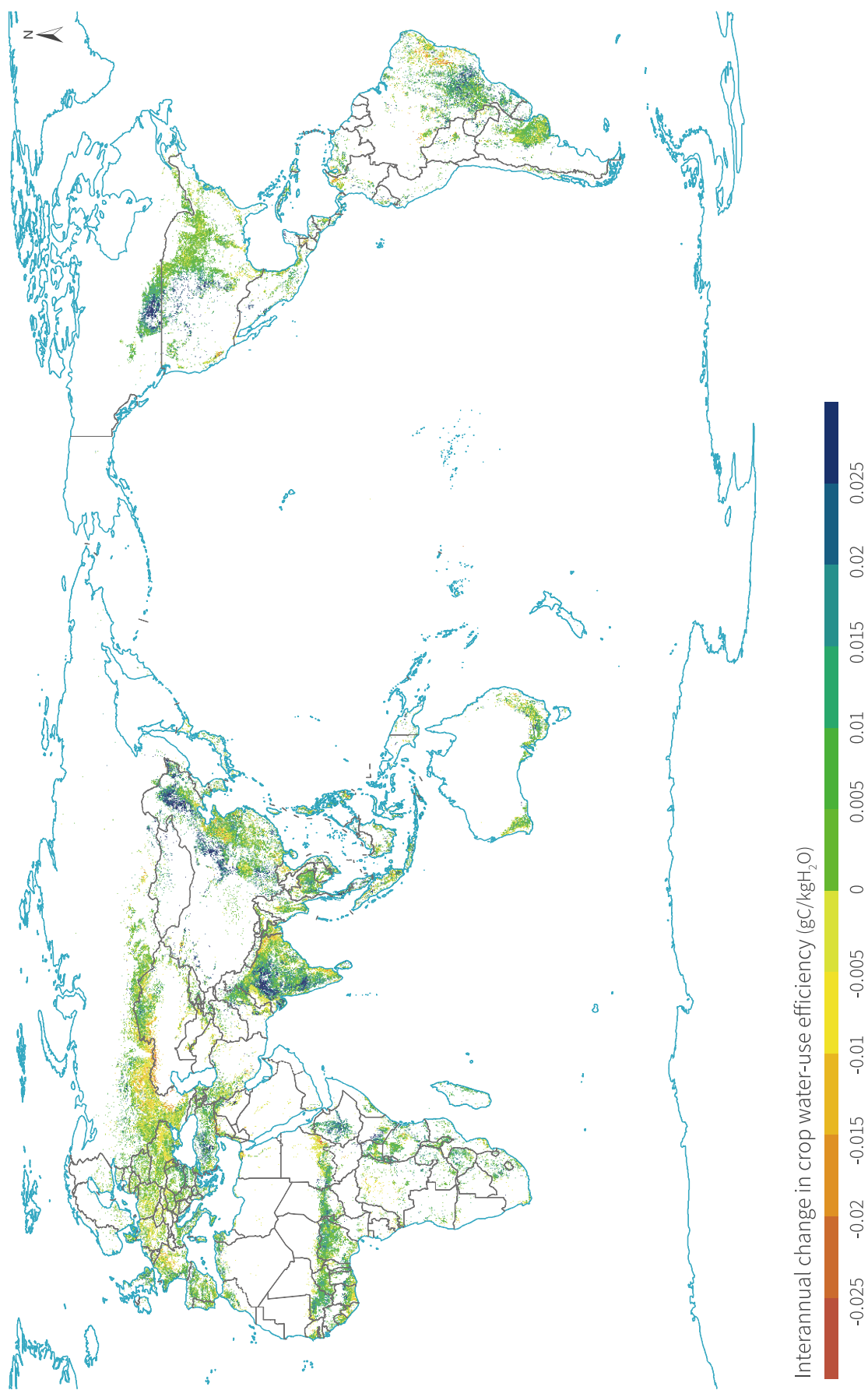
Data used

© Remotely sensed data: global data sets derived from different satellite observations with various spatiotemporal scales in 2001-2019 include albedo, NDVI, Leaf Area Index (LAI), fractional vegetation cover, snow cover and Land Use and Land Cover (LULC) from MODIS and Global Land Surface Satellite (GLASS); dynamic water surface area from Aerospace Information Research Institute, Chinese Academy of Sciences; Global Precipitation Measurement (GPM) precipitation; European Space Agency-Climate Change Initiative (ESA-CCI) soil moisture and LULC; Fraction of

Absorbed Photosynthetically Active Radiation (FAPAR) from Copernicus Global Land Service (CGLS); Shuttle Radar Topography Mission (SRTM) DEM (2000).

© Meteorological forcing and other spatial data: ECMWF ERA5 forcing data in 2001-2019; soil texture data.

© Ground measurements of latent heat flux and CO₂ flux from global flux tower network or Gross Primary Productivity (GPP) observation data, used for calibration and validation.



↑ Figure 3-4. Spatial distribution of interannual trend of global crop water-use efficiency from 2001 to 2019

Method

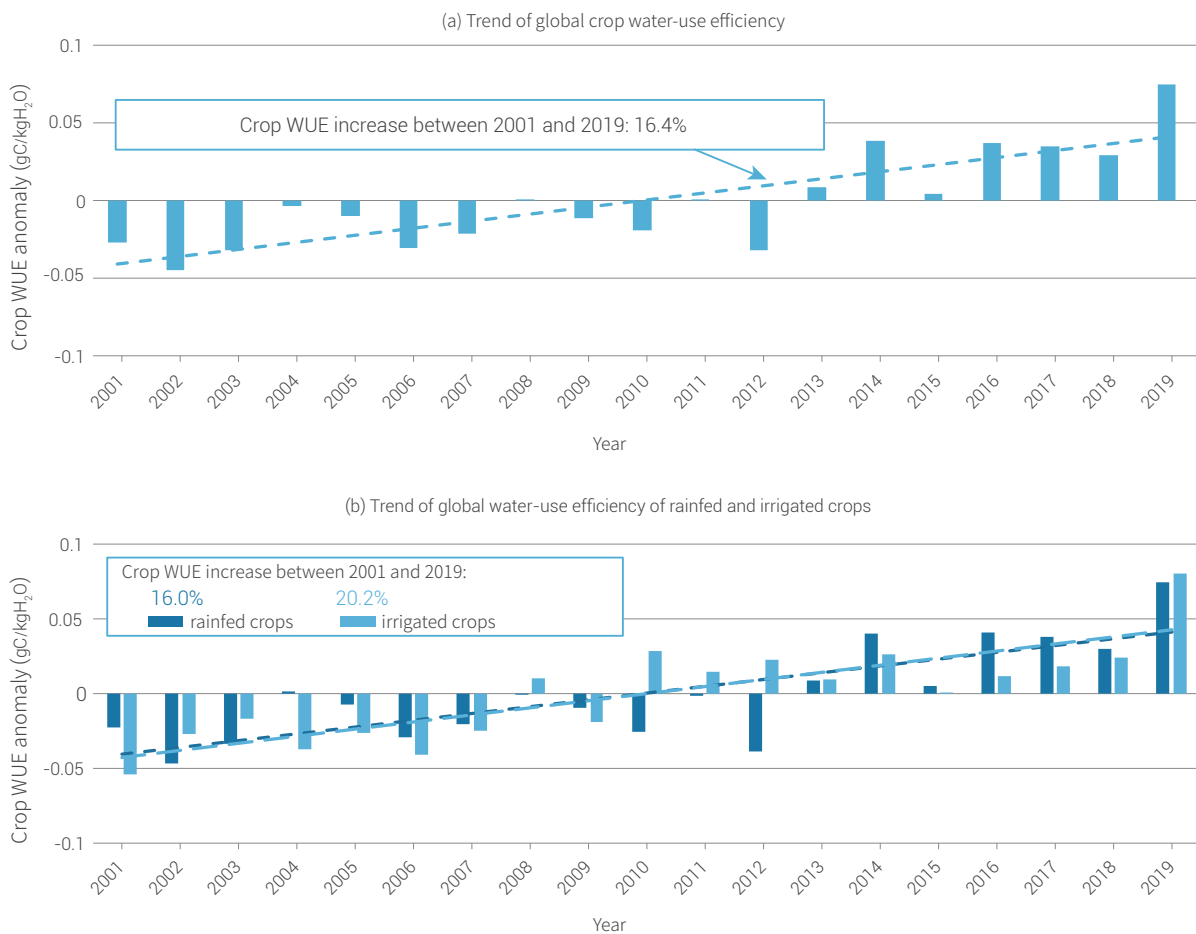
Crop WUE is calculated as the ratio between crop Net Primary Productivity (NPP) and crop water consumption (i.e. evapotranspiration, ET). Method to estimate crop WUE using the aforementioned data is summarized as follows: Firstly, the ET was calculated by applying the ETMonitor model (Hu and Jia, 2015; Zheng *et al.*, 2019) to the corresponding multi-source remotely sensed data and atmospheric reanalysis data ERA5. ETMonitor distinguishes the energy partitioning and water fluxes between soil evaporation and vegetation transpiration upon theories of energy balance, water balance and plant physiology of a soil-vegetation canopy system. Secondly, NPP was estimated by the difference between GPP and respiration. A model for the crop GPP based on light use efficiency (Field

et al., 1995; Zwart *et al.*, 2010) was modified in two aspects: (1) soil water stress factors were introduced to improve the estimation accuracy of GPP under drought conditions; (2) model parameters were calibrated and optimized by using the GPP obtained from the carbon flux data observed from the global eddy-covariance flux tower stations. By comparing the GPP observed by flux tower stations, it was found that the improved light-use efficiency model significantly improved the estimation accuracy of GPP. Thirdly, the estimated daily ET and annual GPP of global crops were validated by comparing with ground measurements. Finally, the time series of global NPP and ET between 2001-2019 with 1 km resolution were generated for the assessment of long-term change in crop water-use efficiency.

Results and analysis

There were some spatial variations in the global trend of crop water-use efficiency from 2001 to 2019. In Asia, America and Oceania, crop water-use efficiency showed a consistent increase. In Europe and Africa, the trend generally was upward, except

in a few countries and regions. China and Canada had the most significant increases in crop water-use efficiency (Fig. 3-4). Crop water-use efficiency has increased by 16.4% on average in the past nearly 20 years. Among them, the water-use efficiency



↑ Figure 3-5. Statistical analysis of interannual variations of global crop WUE from 2001 to 2019

of rainfed and irrigated crops increased by about 16.0% and 20.2% respectively, with the latter remarkably higher than the former (Fig. 3-5). The recent rate of improvement in crop water-use efficiency was higher than the earlier period during 2001-2019, and the turning point came earlier for irrigated crops than for rainfed ones (as shown in Fig. 3-5b where positive anomaly for the former comes before that of the latter). This is due to the joint effect of the increase in crop biomass and the decrease in water consumption caused by technological progress, economic and social development and a certain degree of climate change.

Outlook

In this study, an evaluation method of crop water-use efficiency was developed based on multi-source remotely sensed data combined with crop growth process information. Based on globally consistent and spatially comparable remotely sensed ET and NPP data, the global crop water-use efficiency was estimated and its interannual changes from 2001 to 2019 was extracted and analyzed, instrumental in the accurate understanding of the historical evolution and current state of global crop water-use efficiency.

It should be noted that high NPP of crops does not mean high grain yield. Agrometeorological disasters can result in inconsistencies between the spatiotemporal dynamic changes

of crop water-use efficiency calculated on crop NPP and ET and the crop water productivity calculated on grain yield and ET. The factors affecting the transformation from crop NPP to grain yield are complex, especially because the sensitivity to agrometeorological disasters is different in various crop growth stages. Given the present severe impact of agrometeorological disasters, farmland management needs to be further improved so as to raise the conversion rate from crop NPP or biomass to grain yield (harvest index), which is necessary for the achievement of a higher level of food security and water resource security in 2030.

During the overall increase in crop water-use efficiency, there was a clear decline in 2015, probably caused by the global super El Niño event (occurring between October 2014 and April 2016). The event, the strongest since the 20th century, had three important attributes: long life cycle, high cumulative magnitude, and high peak intensity. The regional droughts caused by it led to a significant decrease in crop biomass (Li and Shi, 2016), which then pushed down crop water-use efficiency through its strong linkage with the interannual dynamic change in crop water-use efficiency.

The assessment of China's Integrated Water Resources Management

Target: 6.5 By 2030, implement integrated water resources management at all levels, including through transboundary cooperation as appropriate.

Highlights

- *The method of assessment of the Integrated Water Resources Management (IWRM) was improved, based on the questionnaire methodology recommended by the United Nations, and supported by big data and spatial analytical technology. China's IWRM during 2015-2017 and 2018-2020 was assessed and analyzed, using China National Water Resources Monitoring Capacity Building statistics and data from Water Resources Bulletin.*
- *China has made progress in improving the level of IWRM. In the 2020 United Nations Survey on IWRM Implementation, China's final score rose to 79 points from 75 points in 2017, reaching the global medium-high level.*

Background

Since the 1990s, Integrated Water Resources Management (IWRM) has been globally accepted as an effective and important method to realize sustainable development, utilization and protection of water resources, and it has been included in the United Nations Sustainable Development Goals (Global Water Partnership Technical Advisory Committee, 2016). SDG 6.5.1 (Degree of Integrated Water Resources Management) measures management policies, laws and regulations, measures, tools, benefits, etc., based on data collected from questionnaire statistics and results reported by the water resources management departments of Member States. In the 2020 survey, 185 out of the 193 UN Member States reported data on their implementation of IWRM (UNEP, 2020a).

In recent years, China has drawn on advanced concepts and experience in the world in deepening IWRM, and gradually put

in place a fairly sound water resources management system and a corresponding administrative management mechanism with China's characteristics. Supported by water conservancy science and technology and growing fiscal input, China has successfully improved its national water resources monitoring capacity. Water security has been enhanced and water-use efficiency improved, with growing water-saving awareness in society.

Following UNEP's *Integrated Monitoring Guide for SDG 6 -- Step-by-Step Monitoring Methodology for Indicator 6.5.1* (UNEP, 2020b), this research used big data and spatial analysis techniques to improve the assessment method for IWRM and applied it to the evaluation and analysis of China's IWRM degree from 2015-2017 and 2018-2020, arriving at an accurate understanding of China's IWRM capacity.

Data used

© Survey data, from 2015-2017 and 2018-2020 China Integrated Water Resources Management Assessment Questionnaire.

© Data on Chinese provincial boundary cross-section water volume and quality, data on water intake, drinking water and water function zone, from 2015 to 2020, from *China Statistical Yearbook*, and data from China National Water Resources Monitoring Capacity Building and Water-use Statistics Direct

Reporting System.

© Provincial-level statistical data from 2015 to 2020 on water supply, water use, precipitation, sea entry, water quality (2015-2018), reservoir and lake water storage, etc., from *China Water Resources Bulletin*.

Method

Using the questionnaire survey methodology recommended by the UNDP (UNEP, 2020a) and big data and spatial analysis technology, a semi-quantitative assessment of the IWRM level in China was made. The specific steps are as follows:

(1) Drawing reference from the IWRM indicators system, a questionnaire was designed, including 33 questions organized into eight groups under four sections – enabling environment, institutions and participation, management instrument, and financing; respondents were selected based on their representation of sectors, regions, professions and levels, age, gender, etc.; survey results were collected and comparatively analyzed, and on-site meetings were organized for respondents to discuss the results and the scoring criteria were further harmonized and errors corrected.

(2) Data from *China Water Resources Bulletin*, Water-use Statistics Direct Reporting System, and China National Water Resources Monitoring Capacity Building were analyzed for the change over time and in spatial distribution, and decomposition of experts' scoring of water resources management instruments into the provincial, basin and national levels, thus achieving multi-leveled semi-quantitative results.

(3) Using the results of both the questionnaire survey and the spatial analysis and review of management instruments, and drawing reference from the UNEP classification standards, the degree of IWRM was categorized into six levels, including very high, high, medium-high, medium-low, low, and very low (UNEP, 2020b). The scoring results were compared with the assessment results of the reference period (2015-2017) to obtain China's degree of IWRM implementation.

Results and analysis

1. Improvement in China's IWRM capacity from 2015 to 2020

From 2015 to 2020, China's IWRM capacity had improved significantly. During this period, the number of survey stations reporting cross-section hydrological data at provincial boundaries increased from 22 to 540; the number of monitored water users increased from 6,569 to 18,383, a growth rate of 179.8%. In 2020, 348.3 billion m³ of water intake and use was monitored online, accounting for about 59% of total water use in China.

2. The degree of China's IWRM from 2018 to 2020

Benefit from IWRM improvement efforts since 2015 that optimized the water resources management system and administrative management mechanism and increased technical and financial input, China's scores under "enabling environment" and "institutions and participation" rose from both at 75 in 2017 to 82 points and 76 points respectively, and the scores under "management instruments" and "financing" increased from 76 points and 72 points in 2017 to 79 points and 80 points respectively, and the final score increased from 75 points in 2017 to 79 in 2020 (Table 3-2).

Table 3-2. Comparison of China's IWRM Assessment Scores in 2020 and 2017

SDG 6.5.1 score = Degree of IWRM implementation (0-100)	2015-2017	2018-2020
1 Enabling environment	75.0	82.0
1.1 What is the status of policies, laws and plans to support IWRM at the national level?	80.0	83.7
1.2 What is the status of policies, laws and plans to support IWRM at other levels?	70.0	81.3
2 Institutions and participation	75.0	76.0
2.1 What is the status of institutions for IWRM implementation at the national level?	76.0	74.0
2.2 What is the status of institutions for IWRM implementation at other levels?	73.3	77.3
3 Management instruments	76.0	79.0
3.1 What is the status of management instruments to support IWRM implementation at the national level?	78.0	81.2
3.2 What is the status of management instruments to support IWRM implementation at other levels?	72.5	75.8

4 Financing	72.0	80.0
4.1 What is the status of financing for water resources development and management at the national level?	80.0	82.0
4.2 What is the status of financing for water resources development and management at other levels?	66.7	79.5
SDG 6.5.1 score	75.0	79.0

The evaluation results show that China's all-encompassing water resources management system has been effectively improved, with constant efforts for digitalization and intelligent technology. The system exercises real-time online monitoring of water

volume, level, flow and other factors, makes forecast or gives early warning on maximum water use or ecological flow, and inform decisions on risks avoidance and contingency plans.

Outlook

By introducing big data and spatial analysis technology, this research has improved the assessment method for "management instruments" in the IWRM evaluation, and addressed the differences in questionnaire respondents' understanding of the standards due to their susceptibility to subjective perceptions and experiences, making the assessment conclusions more objective, accurate and consistent.

The assessment results put China at the global medium-high level, but there is still a gap compared with some developed

countries. To close the gap, it is particularly necessary to synchronize multiple measures to meaningfully engage a wider range of stakeholders in IWRM. IWRM can be made part of the 14th Five-year Plan and Vision 2035 for Water Conservancy Work. By drawing on the international evaluation system and successful experiences, China can improve and upgrade its standards, and modernize its water conservancy management system and capacity.

Change in natural and artificial water bodies in China from 2000 to 2020

Target: 6.6 By 2020, protect and restore water-related ecosystems, including mountains, forests, wetlands, rivers, aquifers and lakes.

Highlights

- Based on the self-developed data set of monthly surface water in China from 2000 to 2020 with a spatial resolution of 30 m, drawing reference from the manually labeled 45,591 samples of artificial water bodies in China, the natural and artificial water bodies data sets in China in 2000, 2005, 2010, 2015, and 2020 were developed through the post-classification of surface water.
- From 2000 to 2020, there was an upward trend for the total area of natural and artificial water bodies in China; among the 34 provincial-level administrative divisions in China, 44% saw increase in natural water bodies, while 65% saw increase in artificial water bodies, and 56% saw decrease in natural water bodies, while 35% saw increase in artificial water bodies.

Background

In recent years, the rapid development of Big Earth Data analysis technology has greatly promoted the measurement and evaluation capacity of SDG 6.6.1. The Global Surface Water data set (GSW) (Pekel *et al.*, 2016) developed by the European Commission's Joint Research Centre (JRC) has become an important reference data set for the evaluation of national-scale water surface changes (including rivers, lakes, reservoirs, ponds, etc.) by the United Nations Statistics Division (UN-Water, 2018). This data set, however, due to the inadequacy of artificial water body sample data, cannot effectively distinguish natural water bodies such as deltas and lakes from artificial water bodies such as reservoirs and ponds, and therefore cannot fully reflect the changes in the proportion of natural and artificial water bodies (UN-Water, 2020b), thus limiting the

degree and capacity of surface water resources management at the national scale, and negatively influencing the objective evaluation and understanding of the impact of the distribution and area change of artificial water bodies on the health status of surface water ecosystem.

Drawing reference from SDG 6.6.1 definition and change assessment methods of natural and artificial water bodies, this study classified natural and artificial water bodies in China from 2000 to 2020 and developed data sets based on the self-developed data set of surface water in China with a spatial resolution of 30 m and evaluated the spatial distribution and area changes of natural and artificial water bodies in China from 2015 to 2020 against the benchmark of 2000 to 2005.

Data used

- © China's monthly surface water data set with 30 m spatial resolution from 2000 to 2020 derived from Landsat TM/ETM+/OLI images.
- © The 45,591 artificial water sample data labeled by the visual interpretation based on GF-1/6, Sentinel-2 and Landsat TM/

ETM+/OLI images in 2019 and 2020.

- © Dam location data of 4,662 large-and-medium-sized reservoirs provided by China Institute of Water Resources and Hydropower Research.

Method

Firstly, based on the self-developed China's monthly surface water data set with 30 m spatial resolution from 2000 to 2020, through the synthesis of monthly maximum, the national surface water distribution data sets in 2000, 2005, 2010, 2015, and 2020 were generated. The calculation formula is as follows:

$$ASW = \text{MAX} \{msw_1, msw_2, \dots, msw_i\} \quad (i = 1, 2, \dots, 12)$$

ASW is the annual surface water data; msw_i is the monthly surface water data of the i^{th} month.

Secondly, the 45,591 artificial water body sample data labeled by visual interpretation were used as input, and the spatial overlay analysis was made with the surface water distribution data of each year. The artificial water body sample points were used to select the artificial water body regions, so as to obtain the preliminary classification of artificial and natural water bodies. On this basis,

the artificial water bodies (including cascade power stations and reservoirs) were manually divided from the natural river channels to obtain the final artificial and natural water bodies data set.

Drawing reference from SDG 6.6.1 calculation method and taking the mean value of natural and artificial water bodies data in 2000 and 2005 as the reference period data, the changes in natural and artificial water bodies from 2015 to 2020 were evaluated. The calculation formula is as follows:

$$P = (\gamma - \beta) / \beta$$

P is the change percentage of natural or artificial water body area in different regions; β is the average area of natural or artificial water bodies in different regions in the period of 2000-2005; γ is the average area of natural or artificial water bodies in the period of 2015-2020.

Results and analysis

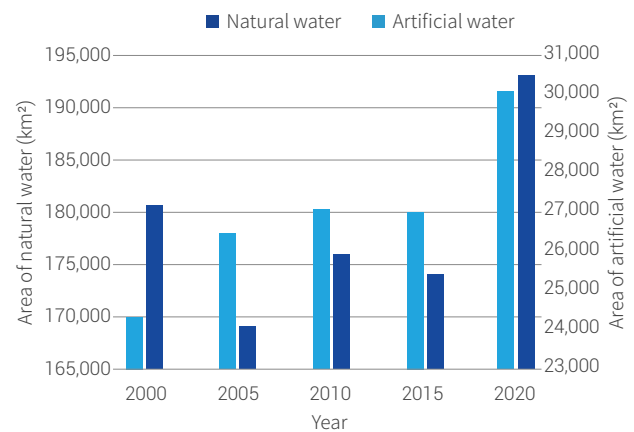
1. Accuracy verification of natural and artificial water bodies data

Six $5^\circ \times 5^\circ$ verification regions were selected nationwide (located in Northeast, North, West, Northwest, South and East of China). The accuracy of remote sensing extraction results of surface water in the 12 months of 2019 was verified, using a total of 144,000 sample points (2,000 verification sample points were randomly collected in each verification region every month, including 1,000 water samples and 1,000 non-water samples). The average Producer's Accuracy (PA) and User's Accuracy (UA) of surface water extraction in the six verification regions in 12 months were 0.950 and 0.998, and the average Overall Accuracy (OA) and Kappa coefficient were 0.975 and 0.949. The verification results indicated that the surface water data set used in the study had very high accuracy and met the classification requirements of natural and artificial water bodies.

Based on the location data of 4,662 reservoir dams in China, the dam buffer zones were generated (by extending outward by 200 meters from the dam location points). The interchapter of the buffer zone data and the national artificial water body data set in 2020 shows that 4,200 artificial water body polygons match the reservoir dam buffer zones, accounting for 90.1% of all reservoir dam sample points. It indicates that the artificial water body data set can accurately reflect the actual distribution of artificial water bodies throughout the country.

2. Changes in China's natural and artificial water bodies

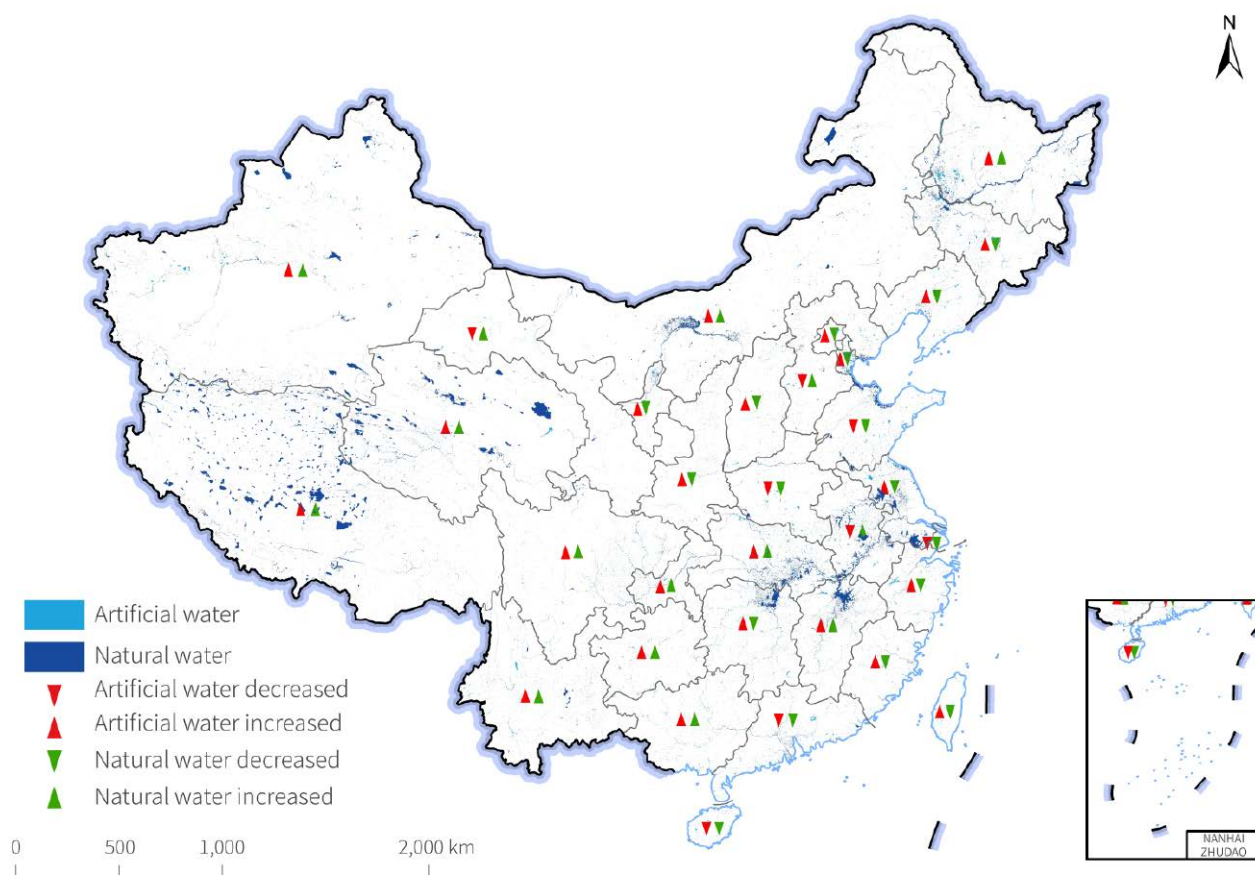
From 2000 to 2020, the area of natural water bodies in China had major fluctuations, but the trend was upward overall. The area of artificial water bodies continued to increase, with the only



↑ Figure 3-6. Changes in China's natural and artificial water bodies from 2000 to 2020

exception of a minor decline occurring in 2015 from 2010 due to the drought in Northeast China (Fig. 3-6). In terms of spatial distribution, natural water bodies were mainly located in the Qinghai-Tibet Plateau, the Eastern Plain, and the Northeast Plain, while artificial water bodies were mainly distributed in the middle and lower reaches of the Yangtze River and coastal provinces (Fig. 3-7).

At the provincial level, compared with the data of the benchmark period from 2000 to 2005, among the 34 provincial-level administrative divisions in China, the area of natural water bodies increased in 15, such as Guizhou, Anhui and Sichuan, and decreased in 19, such as Macao, Beijing and Tianjin, accounting for 44% and 56% of the total administrative divisions



↑ Figure 3-7. Spatial distribution of natural and artificial water bodies in China in 2020 and the changing trend of natural and artificial water bodies in provincial administrative divisions from 2015 to 2020 compared with 2000 to 2005

respectively. The area of artificial water bodies increased in 22, such as Yunnan, Guizhou and Hubei, and decreased in 12 such as

Hebei, Shanghai and Anhui, accounting for 65% and 35% of the total administrative divisions respectively (Fig. 3-7).

Outlook

This study statistically analyzed the spatiotemporal changes in natural and artificial water bodies in China in recent 20 years, based on natural and artificial water bodies data sets in 2000, 2005, 2010, 2015 and 2020. In general, both natural and artificial water bodies exhibited an upward trend, and the increase in the area of artificial water bodies was more significant.

The research results provide scientific data sets and analytical

conclusions for the monitoring and evaluation of SDG 6.6 of protecting and restoring water-related ecosystems in China and can inform decision-making on China's IWRM. Future research will adopt similar technical methods to develop natural and artificial water bodies data sets and to evaluate their changes in China's neighboring countries and also at the global scale.

Spatiotemporal changes in China's vegetated wetlands

Target: 6.6 By 2020, protect and restore water-related ecosystems, including mountains, forests, wetlands, rivers, aquifers and lakes.

Highlights

- Based on the Hybrid Object-based and Hierarchical Classification (HOHC) approach, spatial distributions of China's vegetated wetlands in 2010, 2015 and 2020 were generated.
- A quantitative analysis was made on the effectiveness of China's wetland protection and restoration policy, and found that from 2010 to 2020, there was a net decrease of 4.8% in the area of vegetated wetlands in China and the rate of wetland loss during 2015 to 2020 was significantly lower than in the period of 2010-2015.

Background

Vegetated wetland, as in SDG 6.6.1, is a major type of wetland, making up 83.5% of total natural wetland in the world. It plays an important role in maintaining biodiversity, easing global warming and preserving water sources. Since the 1950s, vegetated wetlands in China have shrunk drastically in terms of both area and spatial distribution under the dual pressure of climate change and human activities. Analysis of change in vegetated wetlands over time is an important basis for the evaluation of national implementation of Target 6.6, and can provide key data in support of China's implementation of the *Ramsar Convention on Wetlands*.

Based on Big Earth Data, including remotely sensed images, ground survey samples and statistics, this study (1) proposed a hybrid object-oriented and hierarchical classification (HOHC) approach; (2) generated data sets of China's vegetated wetland distributions in 2010, 2015 and 2020; (3) analyzed the spatial and temporal changes in China's vegetated wetlands from 2010 to 2020. The results can provide a reliable research methodology for Target 6.6, and offer data products that can be used in direct support of Target 6.6 evaluation or as reference for the evaluation of SDGs 13, 14 and 15. They can also inform Chinese policies on wetland protection and restoration.

Data used

- © Landsat TM/ETM+/OLI images in 2010, 2015, and 2020 and some ZY-3 images
- © DEM, vector data of administrative divisions, 1:1,000,000 vegetation type map, climatic zones map, and global water

distribution maps

- © Ground survey samples, governmental statistics, and monitoring data

Method

Vegetated wetlands are transitional zones between terrestrial and aquatic ecosystems. They have unique spectral and texture characteristics on remotely sensed images. This study classified vegetated wetlands at the national level through remote sensing with a Hybrid Object-oriented and Hierarchical Classification (HOHC) approach. The workflow included: first, collecting

satellite images which covered various climatic zones with different vegetated wetland types in different seasons; second, segmenting remotely sensed images at multi-scale and classifying with hierarchical decision tree method; third, validating classification results against massive field survey samples (Jia *et al.*, 2018; Mao *et al.*, 2019, 2020). When building image

collections, we selected (1) cloudless images from flood season (generally July to September) for inland vegetated wetlands, and (2) cloudless images from dry season and low tide period (November to February in the southeast coast and July to September in the north coast) for coastal vegetated wetlands.

Finally, data sets of China's vegetated wetlands in 2010, 2015, and 2020 were obtained. The overall accuracy of classification, as validated against over 5,000 ground survey samples, is above 92%.

Results and analysis

1. Areal extents and spatial distributions of China's vegetated wetlands

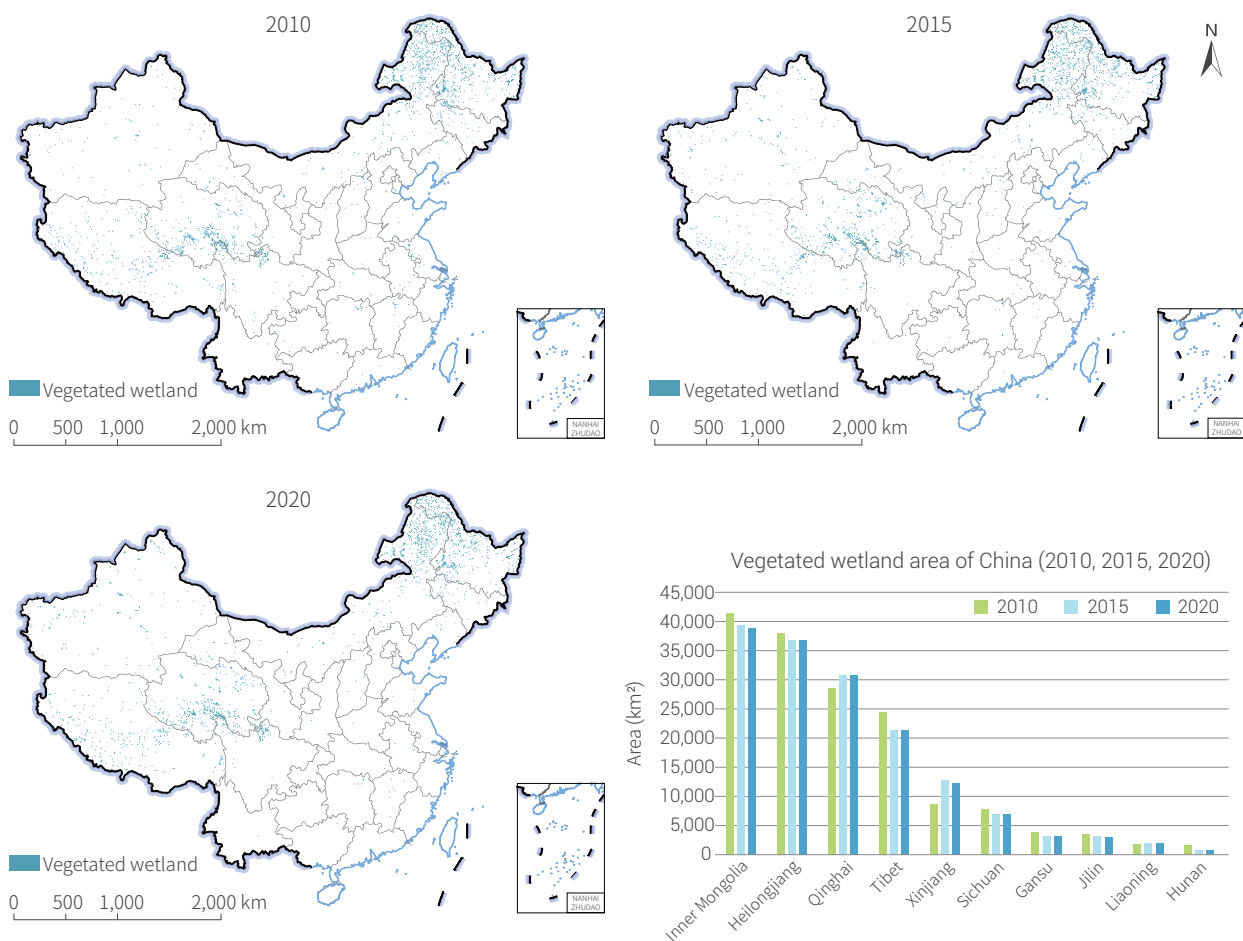
Figure 3-8 shows the areal extents and spatial distributions of China's vegetated wetlands in 2010, 2015, and 2020. The areal extent was estimated to be $1.71 \times 10^5 \text{ km}^2$, $1.64 \times 10^5 \text{ km}^2$, and $1.63 \times 10^5 \text{ km}^2$ in these three years. China's vegetated wetlands were observed mainly in Heilongjiang, eastern Inner Mongolia, Qinghai, Tibet, and Xinjiang, where they accounted for more than 80% of the nation's total.

2. Spatiotemporal change in vegetated wetlands in China from 2010 to 2020

Figure 3-9 shows changes in areal extent and spatial distribution

of vegetated wetlands in China from 2010 to 2020. During this period, China's vegetated wetlands exhibited a downward trend, decreasing by 7,000 km^2 , or by 4.1% between 2010 and 2015, and declining by 1,300 km^2 , or by 0.8% between 2015 and 2020. Compared with the previous five years, the rate of vegetated wetland loss significantly slowed down during 2015 and 2020.

There was a clear spatial heterogeneity in the changes of vegetated wetlands in China from 2010 to 2015. In terms of provincial spatial changes (Fig. 3-8), Tibet lost 3,000 km^2 of vegetated wetlands, more than any other provinces which also saw a decrease. In contrast, Xinjiang's vegetated wetlands increased by 4,000 km^2 , and a few other provinces also saw net gains.

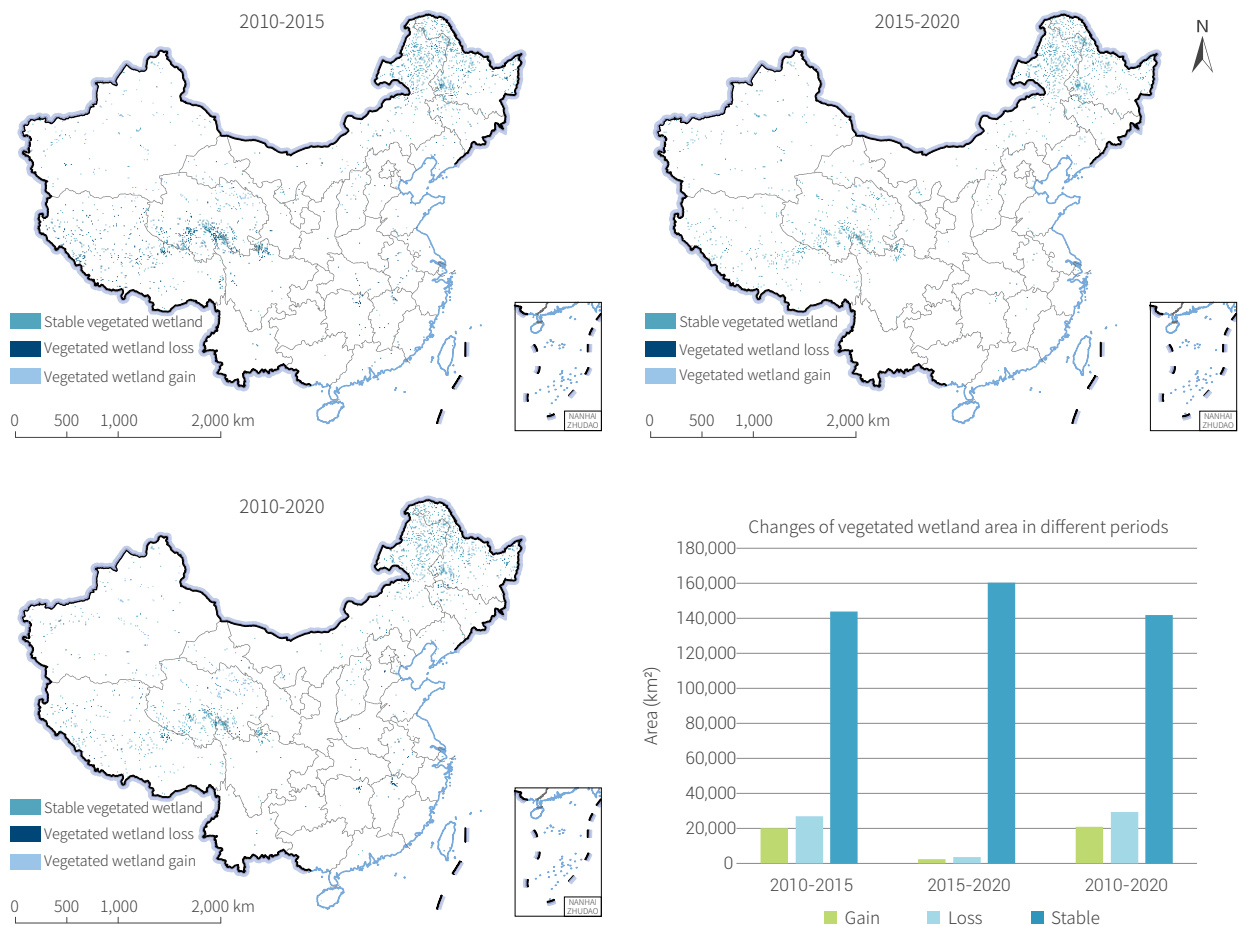


↑ Figure 3-8. Spatial distributions of China's vegetated wetlands and changes among provinces in 2010, 2015 and 2020

From 2015 to 2020, Inner Mongolia lost about 500 km² of vegetated wetlands, more than any other provinces which also saw a decrease. Zhejiang saw the largest net gain in vegetated wetlands of 50 km² among provinces with net gains.

From its accession to the Ramsar Convention in 1992 to the submission of its first draft legislation on wetlands protection to the Standing Committee of the National People's Congress in 2021, China has been exploring ways of protecting and restoring

wetlands. By September 2020, China had 64 Ramsar sites and put 50% of its wetlands under protection. A combination of policies to reverse farmland and ponds to vegetated wetlands and encourage natural rehabilitation has effectively increased the areal extent of wetlands. This study revealed that the downward trend for vegetated wetlands was clearly curbed between 2015 and 2020, compared to the period of 2010-2015.



↑ Figure 3-9. Changes in areal extent and spatial distribution of vegetated wetlands in China for periods 2010-2015 and 2015-2020

Outlook

This study developed a Big Earth Data-based, object-oriented and HOHC approach to map vegetated wetlands in China. The established data sets of China's vegetated wetlands in 2010, 2015 and 2020 are of high mapping accuracy and can provide important scientific data for evaluating SDG 6.6 at the national scale, or be used as reference data for the evaluation of SDG 13, 14 and 15.

This study found that from 2010 to 2020, there was a trend of net decrease in the area of vegetated wetlands in China, but it had significantly slowed down since 2015, indicating the effectiveness of wetland protection and restoration. The findings can be used to support SDG 6 evaluation and inform decisions on wetland conservation and management.



Summary

This chapter presents case study results on the monitoring and evaluation of SDG 6.3, 6.4, 6.5, and 6.6 at national and global scales based on Big Earth Data technology, including China's lake water clarity data set, China's natural and artificial water bodies data sets and China's vegetated wetland data sets, degree of IWRM in China, state of water-related ecosystems and environment in China and the world, and change in crop water-use efficiency in the world. The main conclusions are as follows:

- (1) Between 2010 and 2020, China's lakes larger than 1 km² and the world's lakes larger than 25 km² became clearer.
- (2) Global crop water-use efficiency exhibited an upward trend from 2001 to 2019 due to technological progress and economic and social development.
- (3) China has made progress in the degree of IWRM, reaching the global medium-high level by 2020.
- (4) From 2000 to 2020, the area of natural and artificial water bodies in China increased while the loss of vegetated wetlands

in China slowed down significantly between 2010 and 2020, indicating effectiveness of China's wetland protection and restoration policies.

The five cases in this chapter illustrate the potential of Big Earth Data in monitoring and evaluating SDG 6 indicators such as SDG 6.3.2 (proportion of bodies of water with good ambient water quality), SDG 6.4.1 (change in water-use efficiency over time), SDG 6.5.1 (degree of integrated water resources management) and SDG 6.6.1 (change in the extent of water-related ecosystems over time) at the national and global scales. In the future, satellite remote sensing, model simulation, statistical data, questionnaire survey and other data and tools will be used together to monitor and evaluate more the SDG 6 indicators at the global, national, and provincial scales, with a view to providing continued technological and information support for SDG 6 implementation in China and around the world.



SLU



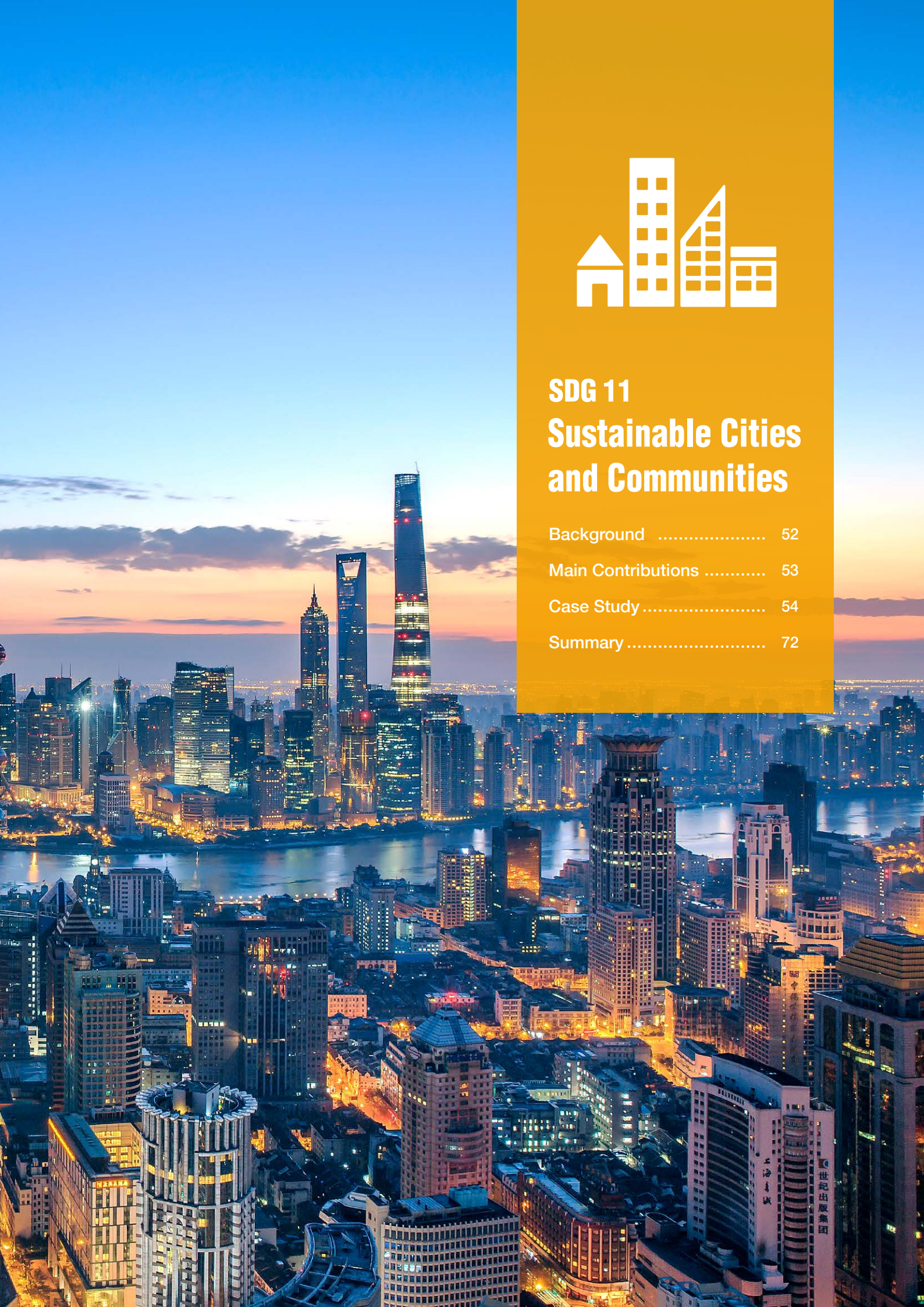
SDG 11 Sustainable Cities and Communities

Background 52

Main Contributions 53

Case Study 54

Summary 72





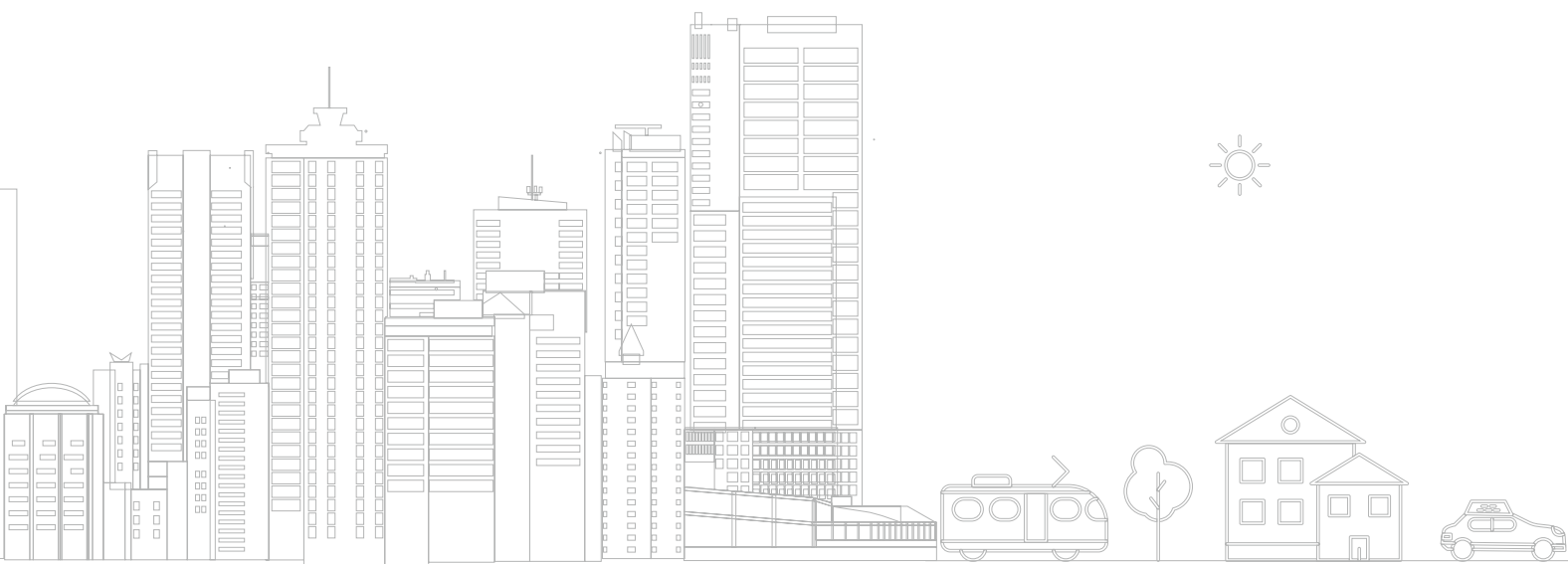
Background

Over the past few decades, the world has been in rapid urbanization. The urban areas, though covering less than 1% of the world's land, contribute 75% of the world's Gross Domestic Product (GDP), consume 60-80% of energy and generate 75% of global waste and carbon emissions (Elmqvist *et al.*, 2019; Jiang *et al.*, 2021). Rapid urbanization has resulted in the world's 4 billion urban population facing increasing air pollution, insufficient infrastructure and public services, and disorderly urban expansion (UN, 2020a). In particular, the COVID-19 pandemic outbreak in early 2020 exposed many urban vulnerabilities due to the lack of adequate and affordable housing, inadequate public health systems, and poor infrastructures (UN, 2021c). More than 90% COVID-19 cases have occurred in city areas, exacerbating the plight of the world's 1 billion population living in informal densely populated settlements and slums (UN, 2020a).

To address these challenges, the United Nations proposed SDG 11 "make cities and human settlements inclusive, safe, resilient and sustainable" (UN, 2015a), a goal crucial to achieving all the other Sustainable Development Goals (Acuto *et al.*, 2018). However, as of March 29, 2021, 10 out of the 15 SDG 11 indicators faced the lack of data for monitoring and evaluation (IAEG-SDGS, 2021). To meet the challenges brought by urbanization and the problems hindering the monitoring and evaluation of SDG 11, 150 countries have developed national

urban plans, nearly half of which are being implemented, helping cities to develop in a more sustainable and inclusive manner. China's success in curbing the rapid spread of COVID-19 pandemic shows that Chinese urban communities have extraordinary flexibility and adaptability in adjusting to new norms (Cheng *et al.*, 2021). Only through data-driven urban inclusiveness and sustainable urban development can cities recover from the pandemic and respond better to future urban disasters and urban public health events.

In the past two years, Big Earth Data was harnessed to support the monitoring and evaluation of SDG 11, showcasing China's achievements and contributions in three aspects: data products, methods and models and decision support (Guo *et al.*, 2021). Consistent with the demonstration of methods and models and regional and national evaluation in the 2019 and 2020 reports, this chapter presents Big Earth Data-enabled monitoring and evaluation of convenient access to public transport (SDG 11.2.1), urban disasters (SDG 11.5.1/11.5.2) and open public space (SDG 11.7.1), and integrated SDG 11 indicators' evaluation at the provincial and municipal levels in China. The case study results in this chapter are a useful supplement to the Chinese dataset in the Global SDG Indicators Database system for the objective evaluation of China's implementation of SDG 11.





Main Contributions

Cases in this chapter address such enormous challenges as housing shortages, traffic congestion, the lack of basic urban services and inadequate infrastructure that some cities face, and offer Big Earth Data-enabled monitoring and evaluation

experience to China and the world. Focusing on eight SDG 11 indicators, this chapter offers China's data products, methods and models and decision support (Table 4-1).

Table 4-1 Cases and Their Main Contributions

Indicator	Tier	Case	Contributions
11.2.1 Proportion of population that has convenient access to public transport, by sex, age and persons with disabilities	Tier II	Proportion of the population with convenient access to public transportation in China	Data product: Data sets of population with convenient access to public transport, by age and gender, with 1 km resolution (2015, 2018 and 2020) Method: Extraction method of Chinese kilometer grid population data by age and gender
11.5.1 Number of deaths, missing persons and directly affected persons attributed to disasters per 100,000 population 11.5.2 Direct economic loss in relation to global GDP, damage to critical infrastructure and number of disruptions to basic services, attributed to disasters	Tier I/ Tier II	Interannual variation of total loss of natural disasters at prefectural level (2010-2020)	Data product: Indicator data set of disaster-affected people per 100,000 population, death and missing persons per 100,000 population and direct economic loss in relation to GRP at prefectural-level by year (2010 - 2020) Method: Standardized data set for Target 11.5, which increases the spatiotemporal monitoring granularity of indicators
11.7.1 Average share of the built-up area of cities that is open space for public use for all, by sex, age and persons with disabilities	Tier II	The patterns and dynamics of urban green space in China	Data product: Vector boundary of China's urban built-up area and spatial component data product of urban green space with 30 m spatial resolution (2000, 2010 and 2020) Method: Extraction method of spatial components of urban green space
11.1.1, 11.2.1, 11.3.1, 11.7.1	Tier I/ Tier II	Community-scale urban landscapes' temporal change and sustainable development indicators in major Chinese cities	Data product: Community-scale landscape data and landscape sample data of major cities in China (2015 and 2020) Method: Scene modeling and extraction method of urban landscape; Heuristic learning method for urban landscape samples
Integrated evaluation of SDG 11	Tier I/ Tier II	Integrated evaluation of SDG 11 indicators in Chinese cities from 2015 to 2020	Data product: Integrated multi-indicator evaluation data set of China for SDG 11.2.1, 11.3.1, 11.5.1, 11.5.2, 11.6.1, 11.6.2 and 11.7.1 Decision support: Provide support for the sustainability evaluation of Chinese cities at prefectural level and inform integrated evaluation of other SDGs in China



Case Study

Proportion of the population with convenient access to public transportation in China

Target: 11.2 By 2030, provide access to safe, affordable, accessible and sustainable transport systems for all, improving road safety, notably by expanding public transport, with special attention to the needs of those in vulnerable situations, women, children, persons with disabilities and older persons.

Highlights

- *High-resolution gridded population distribution data by gender and age group for 2015, 2018 and 2020 were produced to address the lack of such data for SDG 11.2.1.*
- *In 2020, the proportion of the population with convenient access to public transportation in urban built-up areas was 90.15% in China, up by 9.59% over 2018. 96.90% of Chinese cities saw higher proportions to varying degrees, while about 3% experienced slight declines.*

Background

Public transportation, an indispensable part of urban transportation, is a key factor in promoting the development of various industries, cultural prosperity, and connections between urban and rural areas. Fair access to public transportation is significant to cities' sustainable development. An immature, unbalanced public transportation system would reduce the accessibility of public facilities, or force residents to turn to non-public means of transportation, thus hindering people's mobility and standing in the way of a city's fair, sustainable, and economically robust development. To address this issue, the United Nations adopted *the New Urban Agenda*, calling on cities around the world to develop sustainable and efficient transportation infrastructure and services, focusing on the transportation need of all, especially the poor and residents of informal settlements.

In response, China has implemented the strategy of prioritizing the development of public transportation in recent years, making a lot of progress in urban public transportation system. By the end of 2020, 43 cities had built urban rail transit systems, with a total length of 7,354.7 km. Meanwhile, the ground public transit networks have been improving, extending to rural and other remote areas. However, conventional approaches cannot dynamically evaluate the fast-developing public transportation networks or quantify if they meet residents' general needs. This is an area where Big Earth Data can be applied. This study constructed high-resolution gridded population distribution data, combined with public transportation network data, to provide a quantitative assessment by gender and age group of whether urban residents have convenient access to public transportation.

Data used

- Public transportation network (e.g., bus and metro networks) data in China, 2015, 2018 and 2020.
- Land use data with 100 m resolution in China, 2015, 2018 and 2020.
- 1% national population sample survey data, 2015 and census

data, 2010 and 2020.

- Auxiliary data including Visible Infrared Imaging Radiometer Suite Day/Night Band (VIIRS/DNB) night-light remote sensing data, mobile positioning data from Tencent, and Digital Elevation Models (DEMs), 2015, 2018 and 2020.

Method

For each county/district, we extracted the resident population from the population sample survey data (2015, 2018 and 2020), and then the gender ratio and the proportion of each age group from census data (2010). We first redistributed the resident population from an administrative division by the 1 km grid using a random forest spatial downscaling model. Then we rasterized the gender ratio and the proportion of each age group with the same raster template to produce a set of layers containing gender ratio and age group ratio. Finally, we obtained the population distribution by gender and age group by multiplying the ratio layers with gridded population distribution data.

Next, we extracted the public transportation stations (e.g., bus

and metro stations) with spatial attributes from China's public transportation network data, and a 500 m buffer zone was created for each of the stations. We superimposed this buffer layer on the above-mentioned gridded population data to calculate the population within the buffers by gender and age group, which was taken as the people with convenient access to that station.

Finally, we superimposed those layers of the population with convenient access to public transportation on the spatial data of urban areas extracted from land-use data, and then aggregated from the grid level to the prefectural and provincial levels to calculate the proportion of the population with convenient access to public transportation within the built-up area.

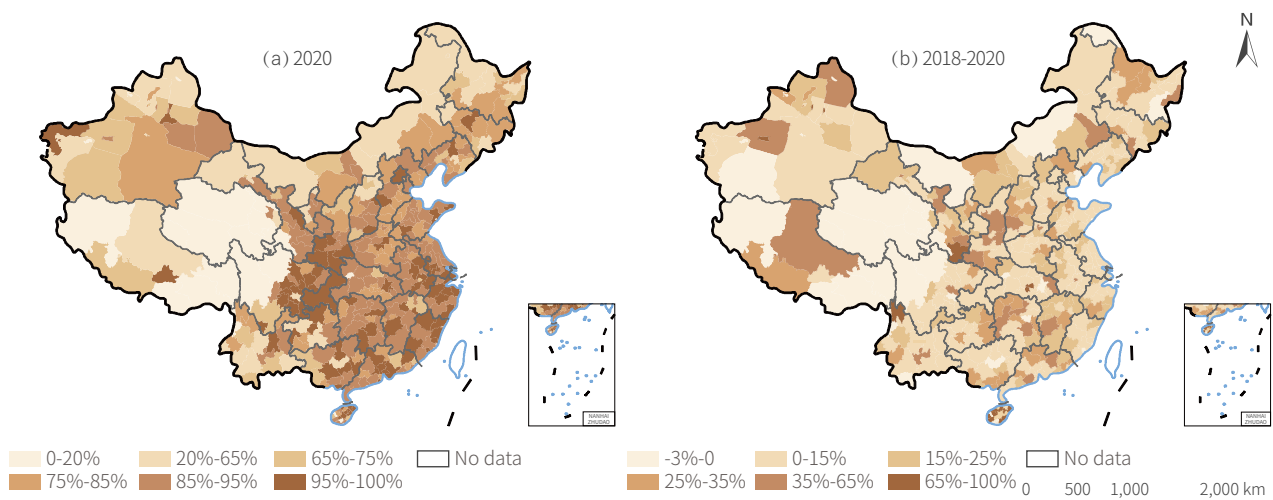
Results and analysis

The distribution of the population with convenient access to public transportation in China in 2020 is shown in Figure 4-1. On average, 90.15% of people in urban built-up areas had convenient access to public transportation in 2020, 25.87% higher than 2015 (64.28%) and 9.59% higher than 2018 (80.56%). The 2018 increase was contributed by 96.90% of cities, whereas 11 cities (about 3%) experienced overall declines of less than 2% (Fig. 4-1). Cities in developed coastal regions such as the Yangtze River Delta and the Pearl River Delta and Sichuan and Chongqing mostly had the highest proportions in China of over 95%. The proportions were above 75% in most other central and eastern cities, but lower in southwest, northwest, and northeast regions such as Yunnan, western

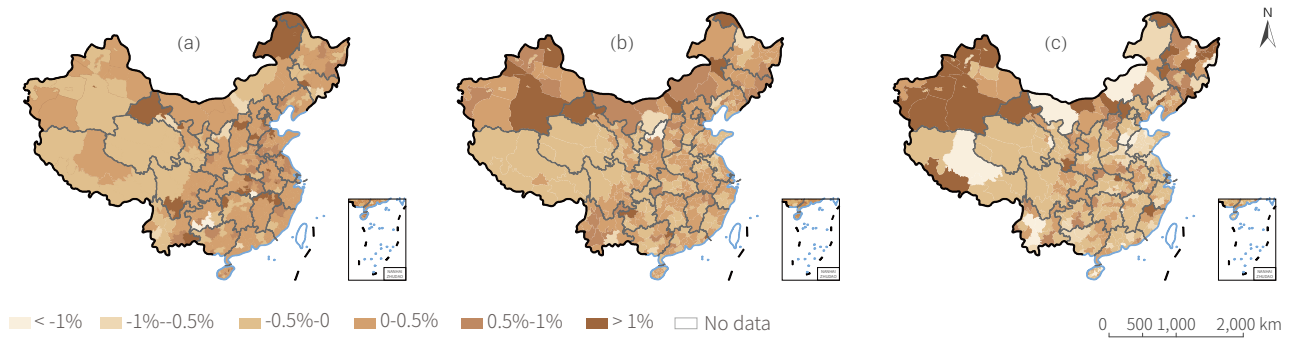
Sichuan, Xinjiang, Inner Mongolia, Heilongjiang and Jilin, and the lowest in the Qinghai-Tibet Plateau region.

In terms of gender, there was little difference across age groups, mostly within 1% (Fig. 4-2). In the 0-14 and 15-64 age groups, the proportion for women was slightly higher than men (< 0.5%) in most eastern and northern cities. In the age group at or above 65, the proportion for women was slightly lower than men (< 0.5%) in most parts of China, except parts of northeast and northwest cities where it was more than 1% higher than men.

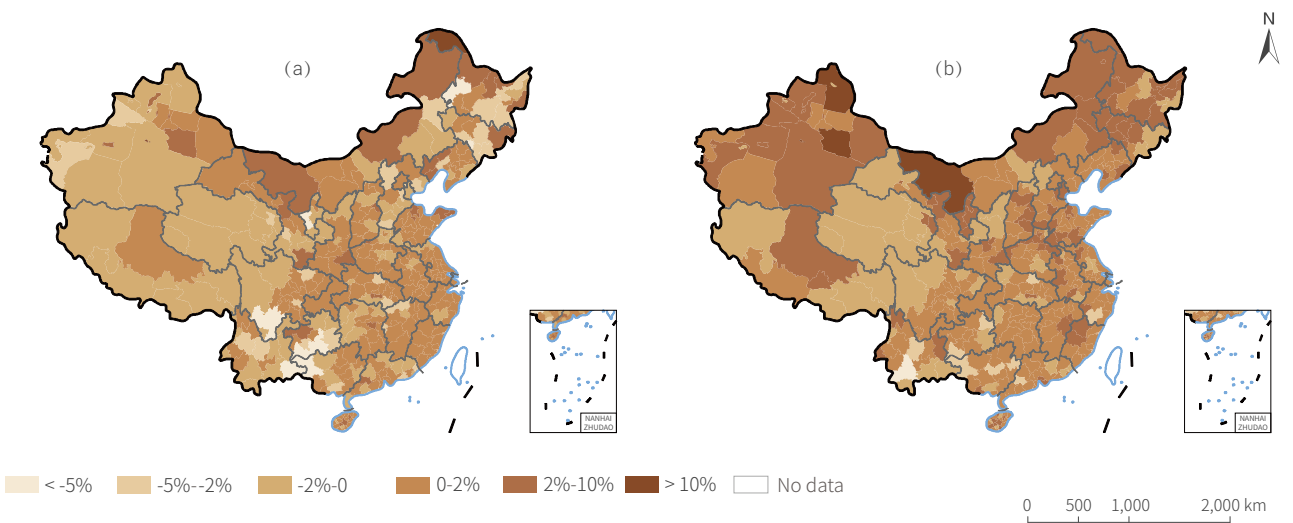
In terms of age groups, in 2020 the 0-14 age group did worse than the 15-64 age group in only 35.5% of Chinese cities, most of which were in western provinces like Qinghai, Tibet and Xinjiang (-5% to 0%), and some were in the boundary area



↑ Figure 4-1. (a) Proportion of the population with convenient access to public transportation in China, 2020; (b) variations in distribution of the proportion of the population with convenient access to public transportation in China in 2018-2020



↑ Figure 4-2. Proportion of the population with convenient access to public transportation by gender in 2020
 (a) 0-14 age group; (b) 15-64 age group; (c) ≥ 65 age group



↑ Figure 4-3. Proportion of the population with convenient access to public transportation by age group in 2020
 (a) differences between 0-14 age group and 15-64 age group; (b) differences between ≥ 65 age group and 15-64 age group

between southeast Yunnan and southwest Guangxi or in the northeast, where the 0-14 age group did significantly worse than the 15-64 age group. The ≥ 65 age group did better than the 15-64 age group in 82.6% of cities with a similar spatial distribution pattern as the 0-14 age group (Fig. 4-3). Compared with the

2018 results where the 15-64 age group did much better than other age groups in most provinces, the 2020 results show that there had been a general improvement in the accessibility of public transportation for children and the elderly.

Outlook

This case study used multi-source Big Earth Data that included public transportation network data, high-resolution gridded population data, and land cover data to measure SDG 11.2.1. It produced estimates of the distribution of the population with convenient access to public transportation on the grid level by gender and age group, and calculated their proportions and made multidimensional comparisons at the prefectural level.

Compared with the calculation of SDG 11.2.1 in 2015 and 2018, this study updated public transportation network vector data and population distribution data. It also realized dynamical evaluation of 2015, 2018, and 2020 data, which can inform the urbanization process and public infrastructure development. The methodology used is easy to apply and data convenient to collect and update. It offers a new approach to national evaluation and international comparison of SDG 11.2.1.

Interannual variation of total loss of natural disasters at prefectural level (2010-2020)

Target: 11.5 By 2030, significantly reduce the number of deaths and the number of people affected and substantially decrease the direct economic losses relative to global gross domestic product caused by disasters, including water-related disasters, with a focus on protecting the poor and people in vulnerable situations.

Highlights

- *Loss from natural disasters in China exhibits a downward trend, with much stronger capacities for comprehensive disaster prevention, reduction and resistance in cities. In 2020, the number of affected persons per 100,000 population, number of deaths and missing persons per 100,000 population, and direct disaster economic losses in relation to GDP decreased by 60.7%, 78.2%, and 60.9%, respectively, compared with their annual means from 2000 to 2019.*

Background

SDG 11.5 consists of two indicators, namely, SDG 11.5.1 -- number of affected persons per 100,000 population and number of deaths and missing persons per 100,000 population, and SDG 11.5.2 -- direct disaster economic losses in relation to Gross Domestic Product (GDP) and damage to critical infrastructure and number of disruptions to basic services, attributed to disasters. These two indicators are important quantitative descriptions of disaster impact on people, economics, and societies, and they are also the only quantitative indicators in the seven global targets proposed in the Sendai Framework (UN,

2015b; UN, 2020b). But currently, the temporal and spatial resolution for dynamic monitoring of SDG 11.5 was limited and incapable of supporting in-depth integrated evaluation at the regional, especially municipal level. Based on disaster losses and social-economic statistics data of cities, this study extended the temporal scale of SDG 11.5 to all years since 2010 and the spatial resolution to the prefectural level, which can improve temporal and spatial resolutions for monitoring and provide clear data to inform policy-making on disaster prevention and reduction.

Data used

© Annual statistics on disaster losses since 2010, including affected population, death toll, and direct economic losses, at prefectural level.

© Annual statistics on total population and Gross Regional Product (GRP) since 2010, at prefectural level.

Method

This study used both statistical data and spatial data to present multi-dimensional monitoring results of SDG 11.5.1 and 11.5.2. Statistics were used to calculate indicators, and GIS thematic

maps were used for regional distribution analysis. The formulas used in this study are as follows:

$$\text{affected persons per 100,000 population} = \frac{\text{number of affected people}}{\text{total population by year end (10,000 population)}} \times 10$$

$$\text{deaths and missing persons per 100,000 population} = \frac{\text{deaths and missing persons}}{\text{total population by year end (10,000 population)}} \times 10$$

$$\text{direct economic loss in relation to GDP} = \frac{\text{direct economic loss (100 million yuan)}}{\text{GDP (100 million yuan)}} \times 100\%$$

$$\text{direct economic loss in relation to GRP} = \frac{\text{direct economic loss (100 million yuan)}}{\text{GRP (100 million yuan)}} \times 100\%$$

Results and analysis

1. Dynamic monitoring of impact of natural disasters on China

For both SDG 11.5.1 and 11.5.2, clearly declining trends have been observed at overall national level since 2000 (Fig. 4-4). Specifically,

① number of affected persons per 100,000 population in 2020 was 9,845, the third lowest since 2000 (after 2018 and 2019), 60.7% lower than the annual mean from 2000 to 2019 (25,026, excluding the year 2008);

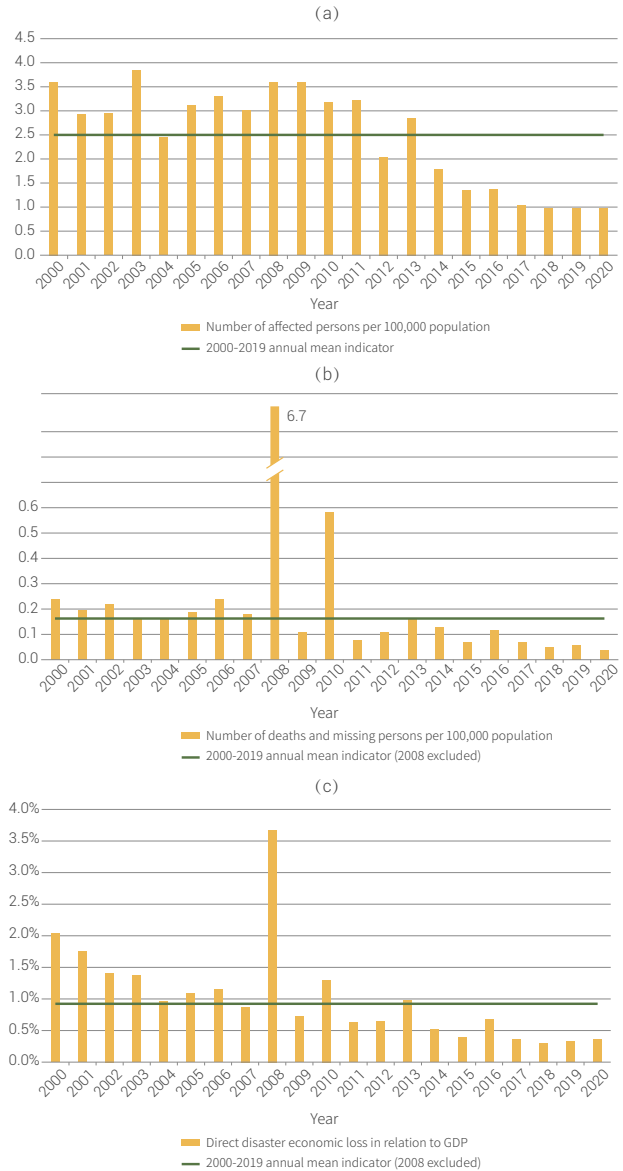
② number of deaths and missing persons per 100,000 population in 2020 was 0.037, the lowest since 2000, 78.2% lower than the annual mean from 2000 to 2019 (0.17, excluding the year 2008);

③ direct disaster economic losses in relation to GDP in 2020 were 0.36%, the fourth lowest since 2000 (after 2017, 2018, 2019), 60.9% lower than the annual mean from 2000 to 2019 (0.92%, excluding the year 2008).

2. Overall analysis of natural disaster impact at prefectural level

Fig. 4-5 shows temporal and spatial trends in China for SDG 11.5.1 – number of deaths, missing persons and directly affected persons attributed to disasters per 100,000 population. Since 2010, with increasing input in disaster prevention, disaster reduction and relief capacity has been greatly improved. Due to rapid social-economic development and urbanization, cities have become better prepared to resist disasters. Progress in these two aspects has resulted in significant decrease for this indicator at the prefectural level. Especially, in the Yan-Tai Mountain Area, Qin-Ba Mountain Area, Wumeng Mountain Area, and Liupan Mountain Area, that are with high disaster risk, a clear downward overall trend has been observed. However, Sichuan, Yunnan, Guizhou, Shaanxi, Gansu and the mid-reach of the Yangtze River are still highly prone to disasters, due to the monsoon climate and location in the seismic fault zone.

The temporal and spatial trend at the prefectural level for SDG 11.5.1, number of deaths and missing persons per 100,000 population, is shown in Fig. 4-5. Over 60% of disaster-affected prefectures and cities at the same level saw a decline in this indicator during the 13th Five-year Plan period (2016-2020) from the 12th Five-year Plan period (2011-2015). According to the *National Program for Comprehensive Disaster Reduction (2016-2020)*, number of deaths per 100,000 population related to natural disasters should not exceed 0.13. Between 2016 and 2020, prefectures and cities that failed to stay below that level decreased by 18.8% than in the previous five years. Along with rapid economic development and comprehensive poverty alleviation, capacities of disaster reaction, rescue, reduction,



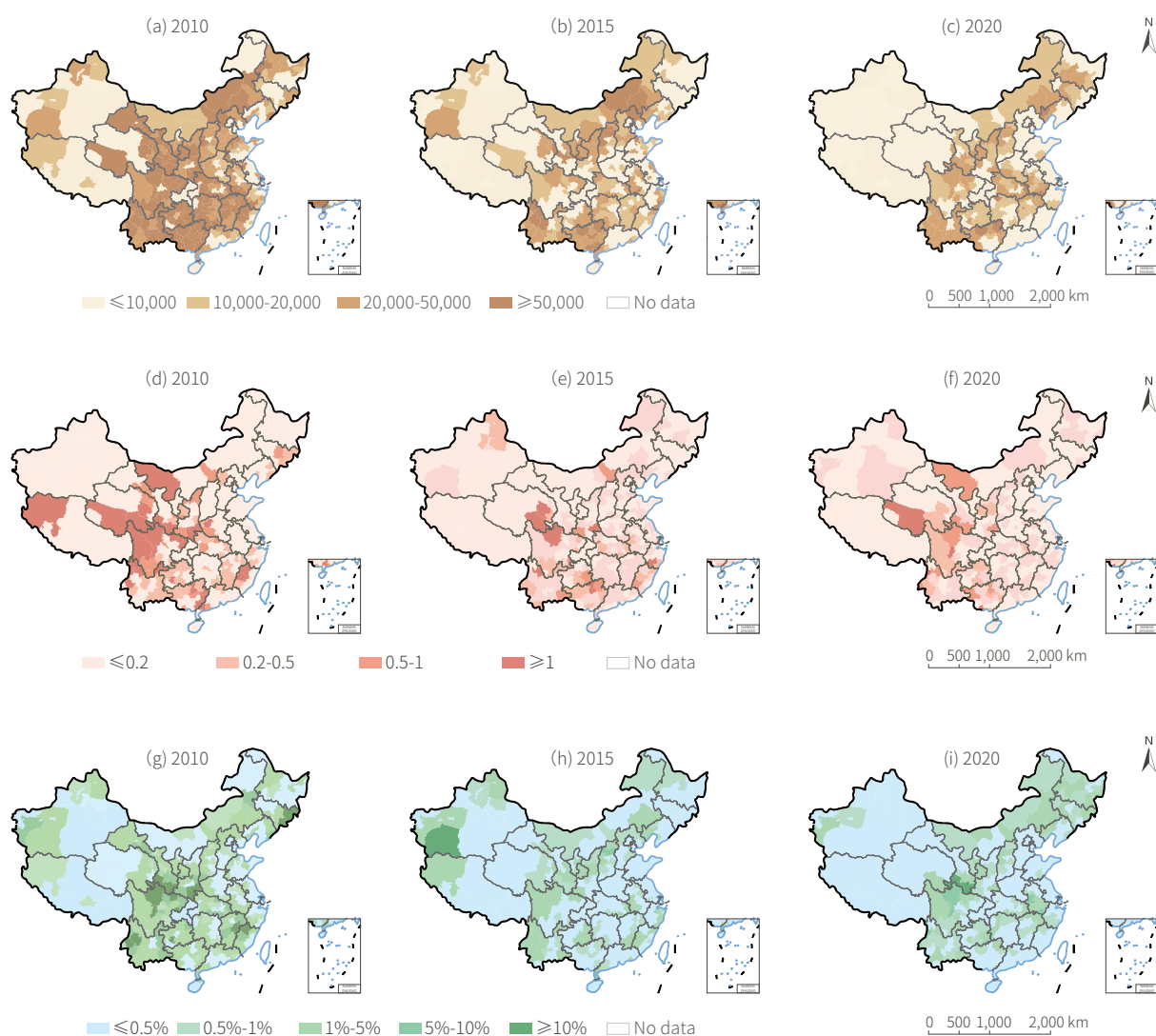
↑ Figure 4-4. Annual monitoring results of SDG 11.5 indicators in China from 2000 to 2020

(a) Number of affected persons per 100,000 population ; (b) Number of deaths and missing persons per 100,000 population; (c) Direct disaster economic loss in relation to GDP

monitoring, early warning, and resistance have been greatly improved, hence disaster-caused death and missing persons remarkably decrease year by year. By now, areas of high risks of fatalities concentrate in mountainous regions in the southwest and northwest, and flash floods and landslides are the main causes.

The temporal and spatial trend at the prefectural level for SDG 11.5.2, direct disaster economic losses in relation to Gross Regional Product, is shown in Fig. 4-5. Over 70% of disaster-affected prefectures and cities saw a decline in this Indicator during the period of 2010 to 2020 from the previous five years. According to the *National Program for Comprehensive Disaster Reduction (2016-2020)*, direct disaster economic losses in

relation to GRP should not exceed 1.3%. Between 2016 and 2020, prefectures and cities that failed to stay below that level decreased by 41.1% than in the previous five years, mainly due to enhanced capacities of disaster resistance and fast and major increase of GRP. Nevertheless, it should be noted that extreme disaster events may cause huge losses to a locality, representing a new risk that has emerged from global climate change.



↑ Figure 4-5. Temporal and spatial trend for SDG 11.5 indicators at prefectural level in China by every five years (2010-2020) (a)-(c) Number of affected persons per 100,000 population; (d)-(f) Number of deaths and missing persons per 100,000 population; (g)-(i) Direct disaster economic loss in relation to GRP

Outlook

Since 2010, China has notably enhanced its comprehensive capacities for disaster prevention, reduction and resistance. However, some regions with fragile economic and ecological systems in the southwest and northwest are still facing high disaster risks, while extreme disaster events pose big threats

to urban areas with high density of population and economic activities. As urban and rural areas are merging under rapid urbanization and rural revitalization in China, close attention should be paid to the coupling and chaining of disaster risks in such integrated urban-rural areas.

The patterns and dynamics of urban green space in China

Target: 11.7 By 2030, provide universal access to safe, inclusive and accessible, green and public spaces, in particular, for women and children, older persons and people with disabilities.

Highlights

- *Urban Green Space (UGS) fraction data products of 2000, 2010 and 2020 with 30 m spatial resolution in China were independently developed.*
- *The total areas of UGS in 93 typical Chinese cities have increased, from $0.35 \times 10^4 \text{ km}^2$ in 2000 to $1.19 \times 10^4 \text{ km}^2$ in 2020. Especially since 2010, the UGS has increased significantly, contributing to improved urban ecological environment.*

Background

Urban public open space can be improved through monitoring and analysis of its change, which promotes the sustainability of cities. Urban Green Space (UGS) is an important part of public open space. Timely and accurate monitoring UGS can provide important data sources for improving urban liveability and sustainability. However, a series of challenges must be overcome in monitoring SDG 11.7.1, such as the inconsistent statistical

sources, the long time required for acquiring information, and inability to characterize the geospatial information of UGS within the complex urban environment. Big Earth Data can accurately investigate the spatiotemporal patterns and changes of UGS, thus informing SDG 11.7.1 implementation and evaluation and related policy-making in China.

Data used

- The independently developed vector boundary data products of urban built-up areas in China in 2000, 2010 and 2020.
- The independently developed UGS fraction data products with 30 m spatial resolution in China in 2000, 2010 and 2020.
- The independently developed vector boundary data of public parks in built-up areas in China in 2020.
- Urban population data from *China Urban Construction Statistical Yearbook (2019)*.

Method

Urban built-up area is defined as land which has more than 35% of impervious surface as observed by satellite remote sensing and is closely connected to the central urban area. The impervious surface includes roofed structures, roads, squares and aprons which are impervious, covered by asphalt, concrete, brick or stone, and can be recognized by remote sensing. Urban green space refers to parks, woodland and vegetated land in urban built-up area, as acquired by satellite remote sensing.

1. Method for data production

Data products on the extent of urban built-up area and UGS in China were developed from multi-source data such as Chinese

satellite images of HJ-1A/B, GF-1/2, ZY-3, and Landsat TM/ETM+/OLI satellite images. The GF-1/2 and ZY-3 satellite images, supported by high-resolution remote sensing images, were used to produce training samples and validation samples in different geographical zones. The Landsat TM/ETM+/OLI images and auxiliary data were used to obtain Normalized Settlement Density Index (NSDI) using random forest method. Vector boundaries for urban built-up areas were derived by using density segmentation method and human-computer interaction interpretation. The UGS fraction data were obtained by applying vegetation cover index and vector boundaries for urban built-

up areas. Based on the above method, data products of UGS fraction in built-up areas with 30 m spatial resolution in China in 2000, 2010 and 2020 were generated. The dataset of UGS fraction adopted a unified coordinate system and storage format. The datum was D_WGS_1984; the projection coordinate system was Albert projection; the data format was Geotiff.

2. Method for data analysis

(1) The proportion of UGS

The proportion of UGS refers to the proportion of UGS area to the area of urban built-up areas. The formula is as follows:

$$UGS_p = \frac{UGS}{B} \times 100\%$$

where UGS_p is the proportion of UGS in built-up areas (%), UGS is the area of UGS in built-up areas (km^2), and B is the urban land area of built-up areas (km^2).

Results and analysis

1. UGS changes in built-up areas

The UGS areas of 93 Chinese cities have exhibited an ascending trend since the beginning of the 21st century (Fig. 4-6), increasing from $0.35 \times 10^4 km^2$ in 2000 to $0.59 \times 10^4 km^2$ in 2010, and then quickly to $1.19 \times 10^4 km^2$ in 2020. Since 2010, a series of strategies, as part of the deepening ecological conservation efforts, have remarkably increased UGS and improved urban living conditions.

In the past 20 years, the UGS proportion has increased due to a strong commitment to urban greening and ecological cities (Fig. 4-6). The average UGS proportion of 93 cities in China increased from 22.54% in 2000 to 29.71% in 2020. Among them, between 2000 and 2020, UGS proportion increased the fastest in metropolises from 22.29% to 30.56%, then in large cities to 29.59% up by 7.16 percentage points, and in megacities from 22.97% to 29.28%.

2. Green space pattern in public parks in built-up areas

In 2020, the total area of UGS in urban public parks in 93

(2) The growth rate of UGS

The growth rate of UGS refers to the annual growth area of UGS in built-up areas in a specific period of time, and the formula is as follows:

$$UGS_{t_1-t_2} = \frac{UGS_{t_2} - UGS_{t_1}}{t_2 - t_1}$$

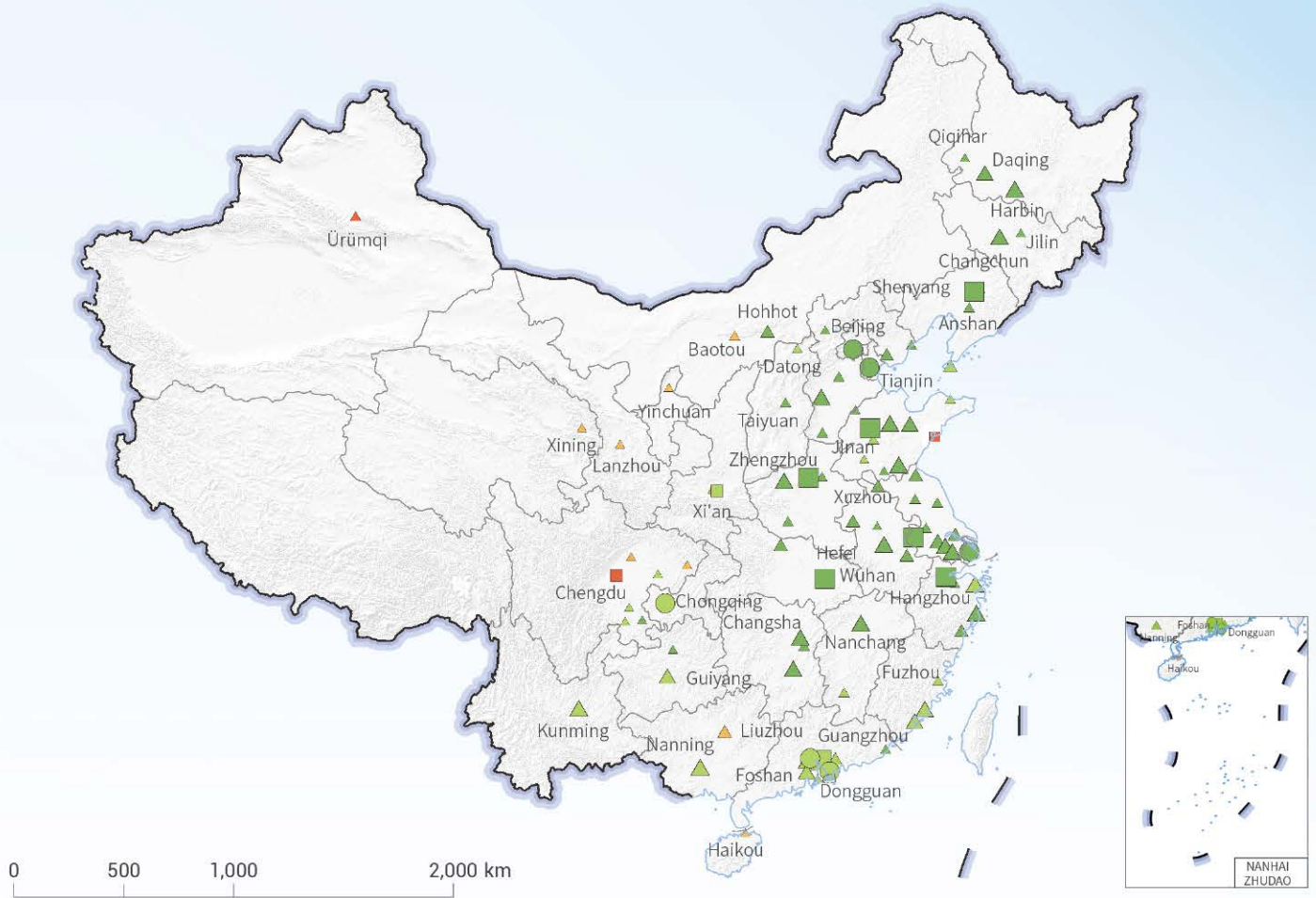
where $UGS_{t_1-t_2}$ is the growth rate of UGS in built-up areas from the year of t_1 to t_2 (km^2/a), and UGS_{t_1} and UGS_{t_2} are the areas of UGS in built-up areas in the year t_1 and t_2 , respectively (km^2).

In this study, 93 cities with an urban population of more than one million were selected as typical cities and divided into three categories: megacities (6), metropolises (10), and large cities (77), and their different levels of UGS were analyzed.

Chinese cities was $0.13 \times 10^4 km^2$, accounting for 3.20% of the total urban built-up areas (Fig. 4-7). In terms of the area of UGS in urban parks, the top ten cities included Beijing, Shanghai, Guangzhou, Shenzhen, Dongguan, Nanjing, Foshan, Suzhou, Hangzhou and Shenyang. Beijing had the largest areas of UGS in public parks, totaling $158.71 km^2$, making its built-up area the greenest, followed by Shanghai with $103.57 km^2$ of UGS in public parks.

In the process of urban construction, megacities paid more attention to the landscape mosaic of buildings and green spaces. The Beijing Olympic Forest Park, Shanghai Expo Park and Shenzhen Overseas Chinese Town Wetland Park stand out as examples of public parks that greatly increase and improve urban greening.

The above results show great progress in China's urban greening and fair and reasonable proportions of urban parks. In the process of urban development, cities of different sizes have improved urban environment by creating UGS and growing urban forest.

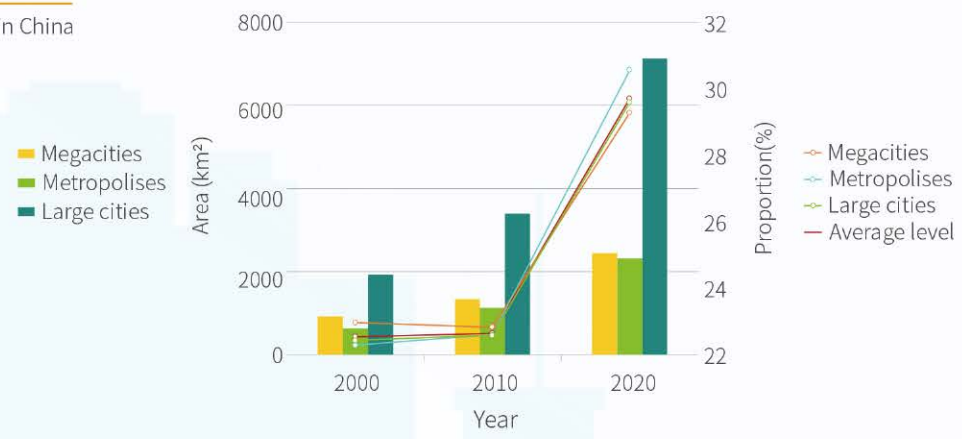


○ Megacities/Urban population: more than 10 million
 □ Metropolises/Urban population: 5-10 million
 △ Large cities/Urban population: 1-5 million

The change of UGS in built-up areas
 Area/km² ○□△ 25-50 ○□△ 50-75 ○□△ 75-100 ○□△ >100
 Proportion/% ●■▲ >5% ●■▲ 0-5% ●■▲ -5-0% ●■▲ <-5%

Figure 4-6.

● Changes of the area and proportion of UGS in China from 2000 to 2020 (No data for Hong Kong, Macau and Taiwan)



Outlook

A series of high-precision products for the UGS fractions in built-up areas in 2000, 2010 and 2020 were independently developed using the methods of big data, machine learning and human-computer interaction interpretation. They can provide important geoscience data for the evaluation of urban public

open space in China and facilitate the realization of SDG 11.7 with quick and accurate measuring of the area and proportion of UGS in built-up areas. The data and methodology used in this study provide a new insight on national evaluation and international comparison of SDG 11.



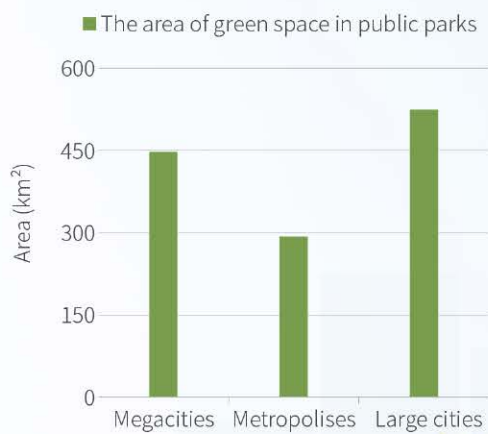


Figure 4-7.
 Green space in public parks in urban built-up areas in China in 2020 (No data for Hong Kong, Macau and Taiwan)



Community-scale urban landscapes' temporal change and sustainable development indicators in major Chinese cities

- Target:** 11.1 By 2030, ensure access for all to adequate, safe and affordable housing and basic services and upgrade slums.
- 11.2 By 2030, provide access to safe, affordable, accessible and sustainable transport systems for all, improving road safety, notably by expanding public transport, with special attention to the needs of those in vulnerable situations, women, children, persons with disabilities and older persons.
- 11.3 By 2030, enhance inclusive and sustainable urbanization and capacity for participatory, integrated and sustainable human settlement planning and management in all countries.
- 11.7 By 2030, provide universal access to safe, inclusive and accessible, green and public spaces, in particular, for women and children, older persons and persons with disabilities.

Highlights

- *A framework for urban landscape modeling and mapping at community scale was proposed.*
- *The first community-scale Chinese urban landscape datasets (in 2015 and 2020) were produced, covering 31 major Chinese cities (provincial capitals and municipalities directly under the Central Government) and 12 types of urban landscapes.*
- *It was found that from 2015 to 2020 shanty areas in the major cities were steadily upgraded (with their area decreasing by 4.5% but that of level-1 and level-2 residential areas increasing), transportation land use expanded significantly (increasing by 11.5%), public open spaces continued to improve (increasing by 2.7%) and land utilization rate improved significantly (with 74.5% decrease in the area of undeveloped land).*

Background

Urban landscapes are complex geographic structures formed through the interactions among man, nature and society. They are a basic factor of the city and are used as fundamental data in evaluating SDG 11.1, 11.2, 11.3, 11.7.

However, current studies on urban landscapes cover only limited categories and scales. Firstly, present evaluations for SDG 11 focus on single landscape categories (e.g., shanty areas or open spaces) and single indicators, and inconsistencies occur between different indicators due to varying extraction standards and overlapping spatial distributions. Secondly, existing urban

landscape data are mostly generated at the municipal scale and do not cover the community scale which is based on the functional zones within a city's boundary and represents the baseline scale for the evaluation of sustainable communities. The lack of valid urban landscape data negatively impacts SDG 11's monitoring and evaluation. Therefore, this study aimed to propose a method of urban landscape modelling and extraction at the community scale to produce community-scale, consistent, baseline data covering all categories of urban landscapes for evaluating SDG 11 in major Chinese cities.

Data used

© Satellite images of GF-1 (2015) and ZY-3 (2020), covering 31 major Chinese cities (provincial capitals and municipalities directly under the Central Government).

© Independently-developed urban landscape sample data set, including more than 200,000 sites of urban landscapes.

Method

1. Geoscene modeling and heuristic example learning for urban landscapes

This study proposed the geoscene model and automatic extraction method of urban landscapes to solve the problem that current GIS feature representations and remote sensing analysis methods cannot model and extract urban landscapes.

(1) Geoscene model of urban landscapes: the geoscene model was established on a hierarchical semantic cognition structure, i.e., object features → object categories → spatial object patterns → geoscenes → landscapes, to provide the data structure and knowledge model for representing landscape structures (Zhang *et al.*, 2017).

(2) Heuristic example learning for urban landscapes: heuristic example learning is a kind of example self-learning method, which can, under semi-supervision, generate samples for urban landscapes by human-computer gaming and active learning methods. It can extract large, balanced, representative, and distinguishable urban landscape samples (Zhang *et al.*, 2020b).

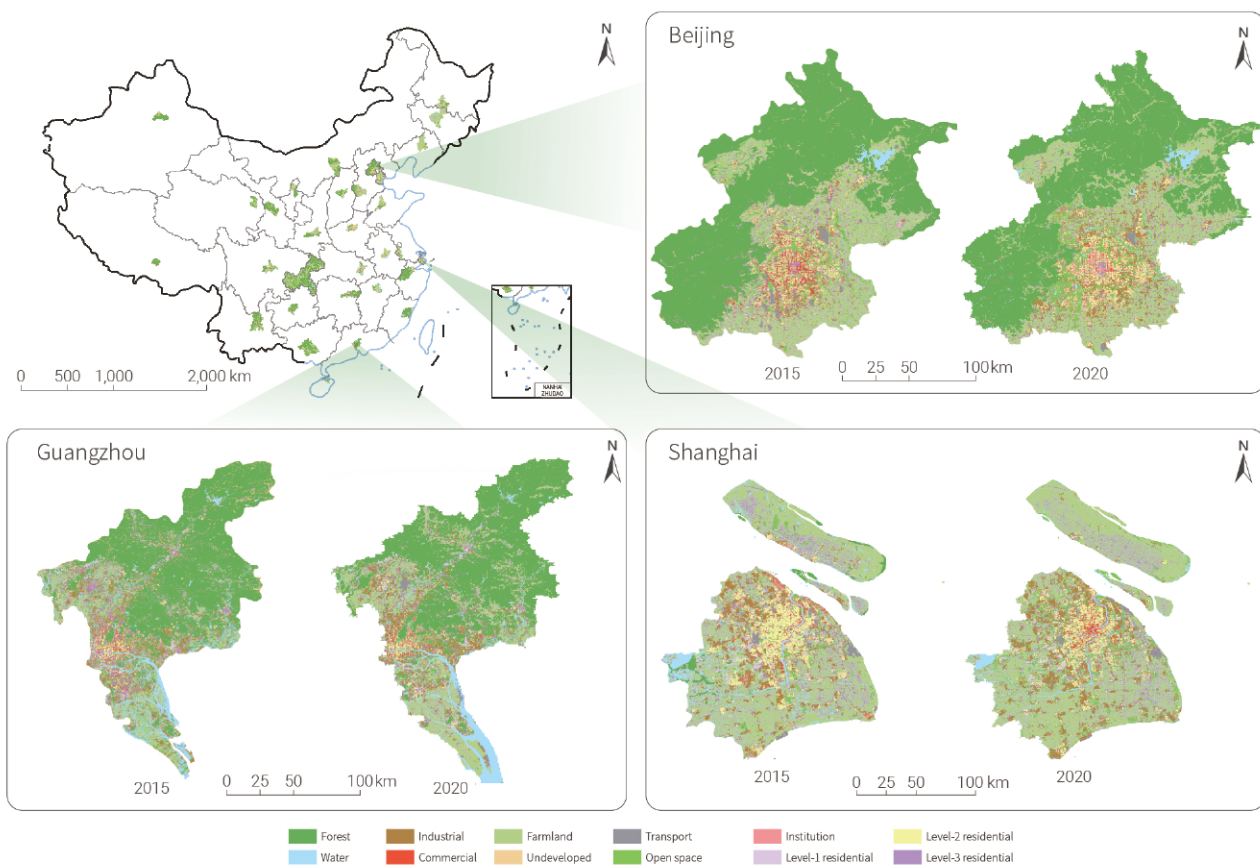
2. Automatic extraction and data production of community-scale urban landscapes

Currently urban landscape datasets are either lacking or at the coarse scale (city aggregation level), unable to support calculation for SDG 11 indicators. This study extracted community-scale urban landscape data on shanty areas and open spaces, which can be used as fundamental dataset for SDG 11 evaluation.

(1) Optimized landscape extraction method using multimodal geographic data: a multimodal data fusion method was developed to automatically identify and extract urban landscape based on geoscene model (Du *et al.*, 2021).

(2) Production of community-scale urban landscape datasets: community-scale urban landscape data sets were automatically generated by the optimized landscape extraction method using multimodal geographic data and urban landscape samples. Then, we extracted landscape indices related to SDG 11, such as the proportions of diverse urban landscapes, e.g., shanty areas, transportation lands and open spaces, as well as their temporal changes.

Results and analysis

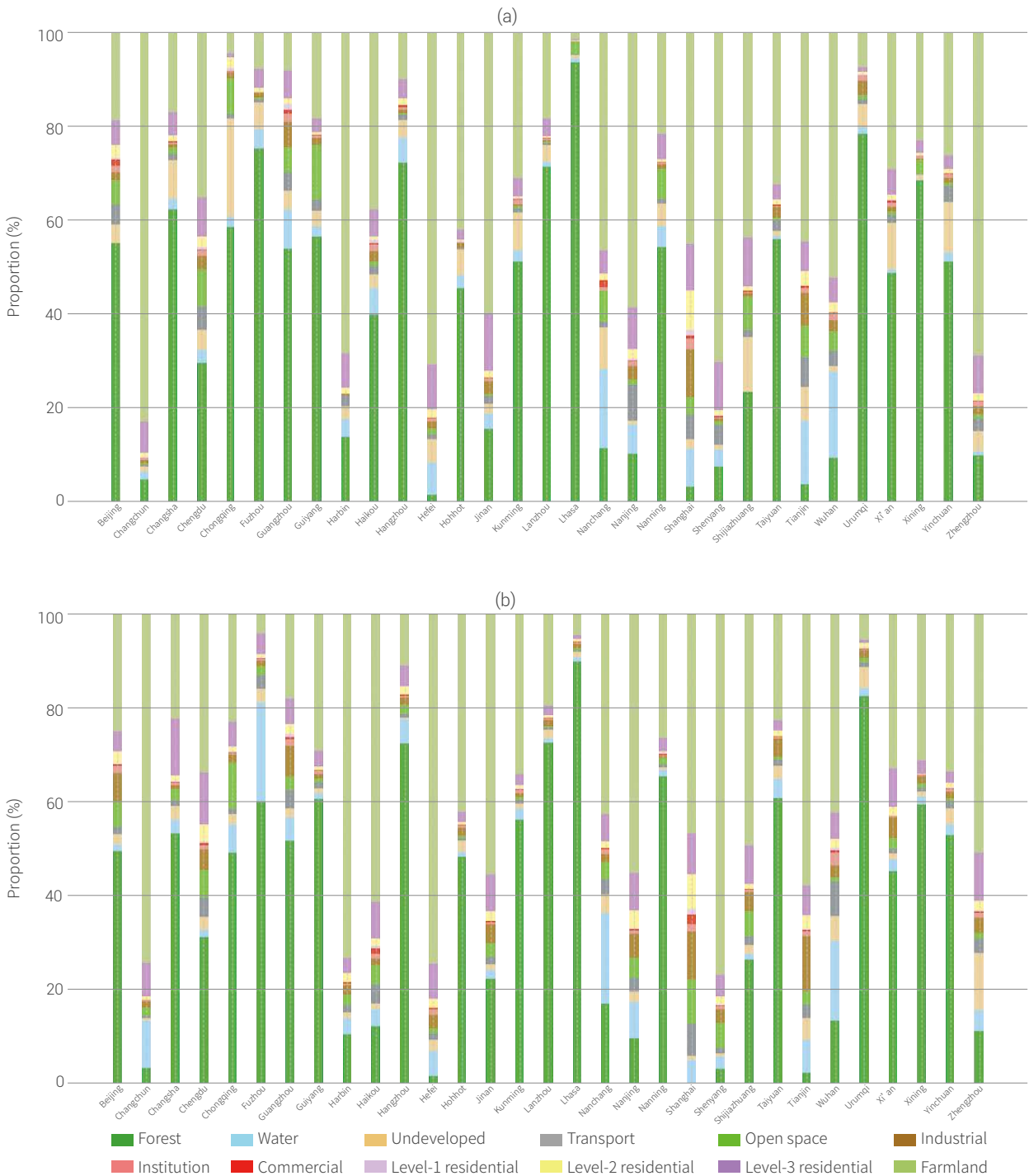


↑ Figure 4-8. Change in typical urban landscapes of Chinese cities from 2015 to 2020

The community-scale urban landscape data sets cover 31 major Chinese cities in 2015 and 2020, with an overall classification accuracy of 85% and a spatial resolution of 2 m (Fig. 4-8). The data sets contain 12 typical categories of urban landscapes, as defined by the *Code for Classification of Urban Land Use and Planning Standards of Development Land* (The Ministry of

Housing and Urban-Rural Development of China, 2012).

Based on the data sets (Fig. 4-8), proportions of diverse urban landscapes in these cities were calculated (Fig. 4-9). There are huge differences in the landscape type and structure among these 31 cities. For example, for the cities located on the Northeast Plain, North China Plain, Jiangnan Plain and Mid-lower



↑ Figure 4-9. Proportions of 12 types of urban landscapes in 31 major Chinese cities in (a) 2015; (b) 2020

Yangtze Plain, the main landscape is farmland, while forest is the main landscape of other cities. As presented in Fig. 4-8, the landscape structures in these cities changed significantly from 2015 to 2020, especially because 1) increase in urban areas: cities expanding outwards, with large industrial construction on urban boundaries; 2) redevelopment of urban functional zones: shanty areas in the urban center shrinking while commercial

districts growing. Generally, from 2015 to 2020, undeveloped lands decreased by 74.6%, forests 3.2%, and shanty areas 4.5%, while farmlands increased by 15.8%, industrial lands 25.1%, commercial lands 1.5%, open spaces 2.7%, transportation lands 11.5%, lands for research, educational, cultural and healthcare institutions 11.1%, level-1 residential lands 0.2%, and level-2 residential lands 0.7%.

Outlook

This study developed the geoscene modeling and urban landscape extraction methods, and produced urban landscape data sets of 2015 and 2020. The data sets cover comprehensive categories in 31 major cities by consistent standards, at the community scale with a spatial resolution of 2 m, which can support SDG 11 evaluation.

The study found that from 2015 to 2020, for SDG 11.1, shanty area renovation progressed steadily in major Chinese cities (with the area of shanty areas decreasing by 4.5%, and level-1

and level-2 residential lands increasing by 0.2% and 0.7%, respectively); for SDG 11.2, transportation lands expanded significantly by 11.5%; for SDG 11.3, the urban land use rate improved remarkably (with undeveloped land decreasing by 74.5%); for SDG 11.7, open spaces were enlarged by 2.7%. Future studies are planned to develop urban landscape data sets for the whole country and even the countries involved in the Belt and Road Initiative for SDG 11 evaluation.

Integrated evaluation of SDG 11 indicators in Chinese cities from 2015 to 2020

- Target:** 11.2 By 2030, provide access to safe, affordable, accessible and sustainable transport systems for all, improving road safety, notably by expanding public transport, with special attention to the needs of those in vulnerable situations, women, children, persons with disabilities and older persons.
- 11.3 By 2030, enhance inclusive and sustainable urbanization and capacity for participatory, integrated and sustainable human settlement planning and management in all countries.
- 11.5 By 2030, significantly reduce the number of deaths and the number of people affected and substantially decrease the direct economic losses relative to global gross domestic product caused by disasters, including water-related disasters, with a focus on protecting the poor and people in vulnerable situations.
- 11.6 By 2030, reduce the adverse per capita environmental impact of cities, including by paying special attention to air quality and municipal and other waste management.
- 11.7 By 2030, provide universal access to safe, inclusive and accessible, green and public spaces, in particular for women and children, older persons and persons with disabilities.

Highlights

- *The integrated evaluation was undertaken at the municipal scale of the five targets and seven indicators under SDG 11 by utilizing Big Earth Data and national statistical data.*
- *Compared with 2015, sustainability improved in 2020 at the municipal level. The SDG 11 integrated index was higher in the eastern cities than in the western ones. It increased in 300 cities but decreased in 29 others. The average value of SDG 11 integrated index increased from 0.64 to 0.73.*

Background

The 2030 Agenda for Sustainable Development proposed by the United Nations in 2015 includes 17 SDGs and 169 targets. Among them, SDG 11 is about building inclusive, safe, resilient and sustainable cities and human settlements, and it includes seven technical targets and three targets on cooperation, with a total of 15 indicators. Cases 1 and 2 analyzed urban public transportation (SDG 11.2.1) and urban disasters (SDG 11.5.1/11.5.2). Although each indicator can reflect the problems in urban development that it focuses on, there is no index to evaluate the overall sustainable development of a city.

The Sustainable Development Solutions Network (SDSN) calculated the integrated index of the 17 SDGs for every country

in the world, using an equal weight method (Sachs *et al.*, 2019). Xu *et al.* (2020) used the same approach to calculate the index for every provincial-level administrative division of China. However, there are few academic researches on the integrated index of SDG 11 at the municipal scale of China. This study combined the results of cases 1 and 2 presented in this chapter and statistical data of the corresponding years and carried out integrated evaluation of the five targets and seven indicators under SDG 11 at the municipal scale in 2015 and 2020. This study pointed out, for each city, the key targets and indicators where special attention is required in order for SDGs to be achieved by 2030.

Data used

- ◎ Public transportation information data of China (2015/2020).
- ◎ Data product of ratio of land use rate to population growth rate (2010-2015/2015-2020).
- ◎ Hazard data of prefecture-level cities in China (2015/2020).
- ◎ Annual average PM_{2.5} (2015/2020).
- ◎ Land use data (2015/2020).
- ◎ Gridded population data (2015/2020).
- ◎ China Urban Construction Statistical Yearbook (2015/2019).

Method

1. Normalization

In order to eliminate residuals caused by different dimensions, self-variation or extreme values of indicators, it was necessary to standardize the original indicators between 0 and 1 with the following equation:

$$x^* = \frac{x - \min(x)}{\max(x) - \min(x)}$$

A value of the normalized indicators closer to 0 indicates a worse performance while a value closer to 1 indicates a better performance. To remove the effects of extreme values, data at the bottom 2.5th percentile were selected as the lower bound for normalization, as proposed by Organisation for Economic Cooperation and Development (OECD) and JRC (2008). The selection of the upper bound drew on the method from *the Sustainable Development Report 2019* (Sachs *et al.*, 2019) and Xu *et al.* (2020).

2. Calculation of the integrated index

The following equation was used to calculate the integrated index according to the method in *the Sustainable Development Report 2019* (Sachs *et al.*, 2019):

$$I = \frac{1}{N} \sum_{k=1}^N I_k$$

where I is SDG 11 integrated index; N indicates the number of indicators; I_k denotes the value of indicators.

3. Quantifying the sustainable progress of indicators

To get an insight into the progress on indicators at the municipal scale, we separately assessed the trend of SDG 11 indicators from 2015 to 2020 and the distance between the 2020 level

(hereinafter referred to as the current level) and its target by drawing on the method from the United Nations' Sustainable Development Goals Progress Chart 2020 (UN, 2020b). Evaluations were made with distinction between two categories of indicators:

(1) indicators without an explicit numerical target

$$TR_a = \left(\frac{x_t}{x_{t_0}} \right)^{\frac{1}{t-t_0}} - 1$$

where TR_a is actual annual growth rate; t denotes current year (2020/2019); t_0 indicates baseline year (2015); x_t is the numerical value of the indicator in year t ; x_{t_0} means the numerical value of the indicator in year t_0 .

(2) indicator with an explicit numerical target (SDG 11.6.2)

$$TR = \frac{TR_a}{TR_r}$$

$$TR_r = \left(\frac{x^*}{x_{t_0}} \right)^{\frac{1}{2030-t_0}} - 1$$

where TR is the ratio between real annual growth rate and annual growth rate needed for the target; TR_r indicates the ideal annual growth rate to reach the target in 2030; x^* denotes the indicator value in 2030.

According to the above formulas, trends are represented by four levels, i.e., rapid progress, slow progress, no progress, and negative progress. Based on consultation with experts, and according to the distribution characteristics of data, statistical techniques were used to divide the current level into five tiers, i.e., almost met, close to target, moderate distance to target, far from target, and very far from target.

Results and analysis

1. Integrated Index

Figure 4-10 shows the spatial distribution of SDG 11 integrated index at the municipal scale. In general, the integrated index was significantly higher in the eastern cities than in the western ones. It went up in 300 cities and down in 29 in 2020 compared

with 2015, with its average value increasing from 0.64 to 0.73. The number of cities with an integrated index value below 0.6 decreased from 90 to 14, while the number of those above 0.75 increased from 8 to 118.

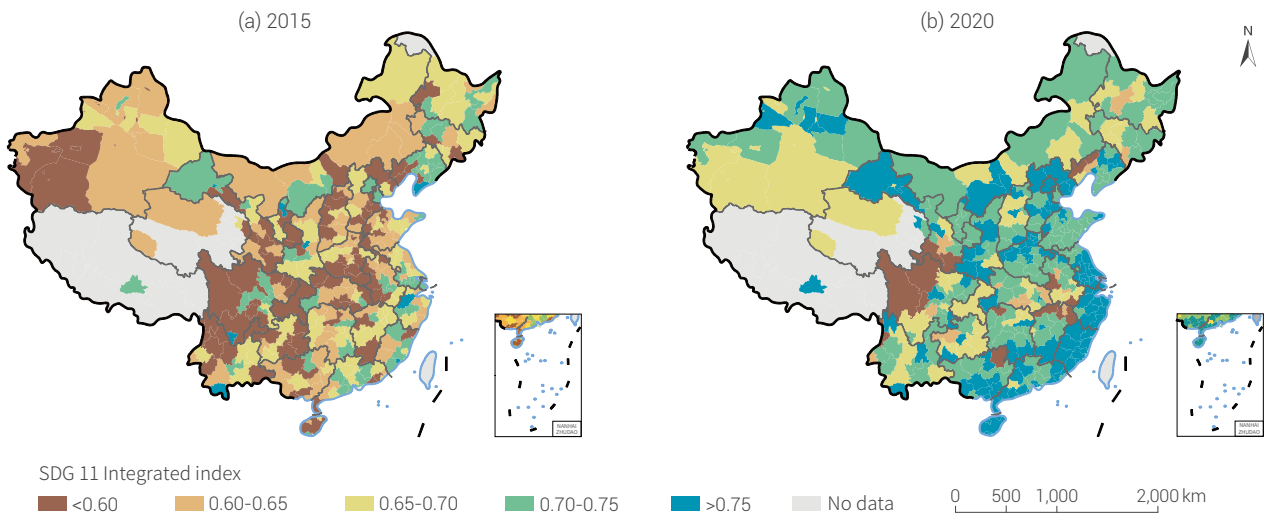


Figure 4-10. The spatial distribution of SDG 11 integrated index at municipal scale

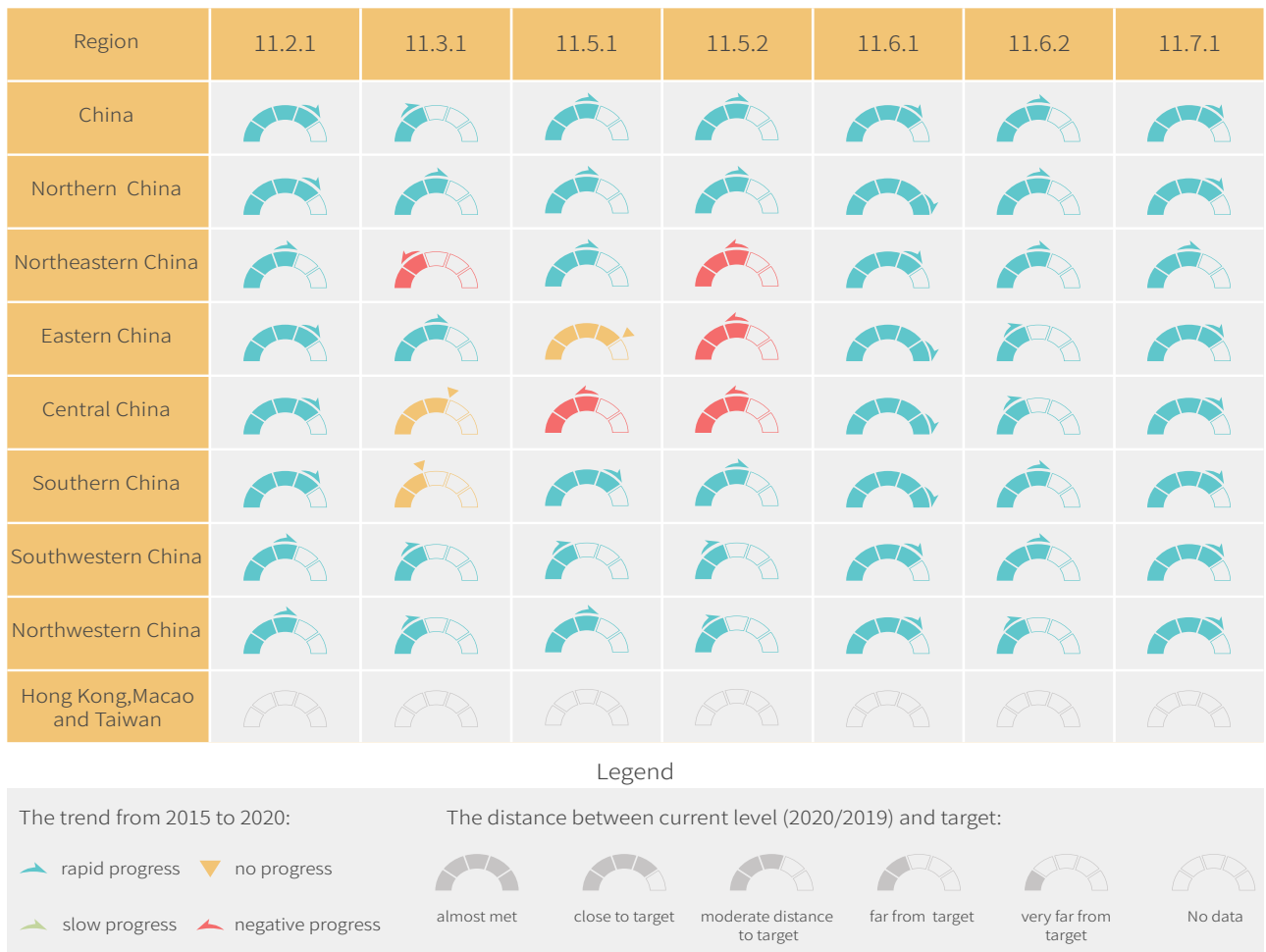


Figure 4-11. The dashboard of SDG 11 indicators

2. Progress toward indicators

Figure 4-11 shows the progress toward SDG 11 indicators. In general, SDG 11.2.1/11.6.1/11.7.1 had good trends and current level, while SDG 11.6.2 had a good trend but required more effort to improve the current level. Other indicators exhibited certain regional differentiation. Nationally, rapid progress was made from 2015 to 2020 toward all indicators. Except SDG 11.3.1, the current level of all indicators in 2020 was close to target, especially SDG 11.2.1/11.6.1/11.7.1.

Regionally, northern, southwestern and northwestern China performed well in both trend and current level and had almost

met target on SDG 11.6.1. Northeastern China made fast progress toward SDG 11.2.1/11.5.1/11.6.1/11.6.2/11.7.1 and was close to target, but progress was negative toward SDG 11.5.2 with moderate distance to target. Eastern China saw no change in the trend and was close to achieving SDG 11.5.1, but it made negative progress towards SDG 11.5.2; it made fast progress toward all the other indicators. Central China had uneven performance on different indicators, with rapid progress toward SDG 11.2.1/11.6.1/11.6.2/11.7.1, no change on SDG 11.3.1 and negative progress toward SDG 11.5.1/11.5.2, with the current level being good for all indicators. Southern China had good trend and current level for all indicators except SDG 11.3.1.

Outlook

This study calculated the SDG 11 integrated index, using the method of SDSN in *the Sustainable Development Report 2019*, which can serve as a tool for the evaluation of overall sustainability under SDG 11. Cities' performance in achieving SDG 11 was clearly measured by the value of each indicator and on the dashboard. As the trend of each indicator was calculated through the comparison of data from 2015 and 2020 (not the

continuous multi-year average), and given the unexpectedness of disasters, negative progress toward indicators SDG 11.5.1/11.5.2 in some cities can only indicate that they suffered more serious disaster losses in 2020 than in 2015 and cannot reflect the overall performance during the five years between 2015 and 2020. In addition, due to the data availability, the current levels for SDG 11.6.1 and SDG 11.7.1 were based on data in 2019.



Summary

This chapter presents the Big Earth Data-enabled index evaluation datasets, methods and models around three specific targets and four indicators, i.e., SDG 11.2 urban transportation, SDG 11.5 urban disaster and SDG 11.7 urban public open space, making the dynamic, spatially refined and quantitative monitoring of multiple indicators under SDG 11 possible. Integrated evaluation of multiple indicators was carried out at the provincial and prefectural levels in China, providing strong support for the realization of SDG 11.

Through the cases studies, we have drawn the following main conclusions:

(1) In terms of urban transportation, the overall proportion of the Chinese population with convenient access to public transportation was 90.15% in 2020, an increase of 9.59% over 2018, based on calculation using the independently-produced high-precision population kilometer gridded data by gender and age (2015, 2018 and 2020) and the vector data of China's public transportation network (bus, subway, etc.) of the corresponding years.

(2) In terms of urban disasters, based on the annual disaster and population economic data at the prefectural level in China, with spatial granularity of SDG 11.5 monitoring refined to the prefectural level, the findings show that the overall natural disaster risk in China exhibits a clear downward trend, and there has been significant improvement in the comprehensive disaster

prevention and reduction capability and urban resilience. However, special attention should be given to extreme weather events.

(3) In terms of urban public open space, the UGS in the built-up areas of 93 typical Chinese cities has shown an upward trend since 2000. Especially since 2010, the UGS has increased significantly, as part of the remarkable results of urban greening efforts.

(4) In terms of integrated evaluation of SDG 11 in cities, the sustainability performance of administrative divisions at the municipal level in 2020 was better than in 2015, and the average value of the integrated index increased from 0.64 to 0.73. The SDG 11 integrated index of the eastern cities was higher than that of the western cities.

The rapid urbanization in the world has given rise to many problems and challenges on the way toward economic, social and environmental sustainability in cities. Therefore, it is necessary to understand the transformation process of shaping sustainable urbanization, to which science and technology is an important lever of support. In particular, as an important outcome of scientific and technological innovation, the Big Earth Data can support the realization of SDG 11 by filling data gaps, expanding the index system and informing government decisions.



Satellite image of Fuzhou City (Gaofen-1, April 8, 2018)



SDG 13



SDG 13

Climate Action

Background	76
Main Contributions	77
Case Study	78
Summary	93



Background

SDG 13 was established to "Take urgent action to combat climate change and its impacts" in the UN sustainable development agenda. The main task is to mitigate and adapt to climate change and improve response capacity. Given the advantage of Big Earth Data, this chapter focuses on three specific objectives of climate action: strengthen capacity to natural disasters (SDG 13.1), climate change measures (SDG 13.2) and climate change adaptation and early warning (SDG 13.3).

The average temperature between 2016 and 2020 reached the highest value ever recorded, 1.1 °C higher than the pre-industrial level (WMO, 2020). Climate change has been a major driver of disaster losses for mankind (UNDRR, 2019). Climate change and extremes aggravate the imbalance of temperature and precipitation distribution, resulting in frequent disasters such as heat waves, droughts and floods. In addition to the direct impact of natural disasters caused by extreme weather, climate change also has far-reaching impacts on natural ecosystems and biodiversity, food security, water security and energy security (IPCC, 2019). The impact of some changes is not fully understood yet, and monitoring and early warning need to be strengthened.

The continuous emission and accumulation of greenhouse gases is the most important factor in global warming. Therefore, the most effective way to mitigate climate change and prevent it from getting out of control is to reduce emissions and achieve carbon neutrality as soon as possible (IPCC, 2018). In September

2020, China announced that it would adopt more effective policies and measures and strive to reach the peak of carbon dioxide emissions by 2030 and achieve carbon neutrality by 2060. The achievement of these objectives is projected to lower global warming by 0.2 to 0.3 degrees at the end of this century compared with the business-as-usual scenario, thus bringing the whole world closer to the Paris Agreement target (CAT, 2020).

At present, among all SDG 13 indicators, only indicator 13.1.1 (number of deaths caused by disasters) and indicator 13.2.2 (total greenhouse gas emissions) are Tier I indicators with established methodology and regularly produced data; the other six are Tier II indicators with established methodology but without regularly produced data. The limited available data are mostly statistics without clear spatiotemporal variations, therefore it is difficult to use them in support of climate change response and science-based decision-making.

The impact of climate change is far-reaching in both space and time. It takes Big Earth Data for researchers to trace past signatures, monitor current dynamics and identify the future direction and trend for climate action. In this year's report, we focus on changes and impacts of sandstorms, patterns of carbon emissions, potentials of natural carbon sink and response of oceans to climate change. Through continuous observation, the changes and spatial patterns were revealed to provide decision support for sustainable development.





Main Contributions

With regard to strengthen capacity to natural disasters (SDG 13.1), climate change measures (SDG 13.2) and climate change adaptation and early warning (SDG 13.3), researches were

carried out at both national and global scales. Five cases are presented here, with five sets of data products, one innovative method and four decision supports for SDG 13 (Table 5-1).

Table 5-1 Cases and Their Main Contributions

Target	Case	Contributions
13.1 Strengthen resilience and adaptive capacity to climate-related hazards and natural disasters in all countries	Interannual changes of sand and dust weather in China in the past 10 years	<p>Data product: Interannual range data of sand and dust weather from 2010 to 2020</p> <p>Decision support: It provides a theoretical basis for dust weather control and dust source transformation</p>
13.2 Integrate climate change measures into national policies, strategies and planning	Spatiotemporal variations of greenhouse gas concentration in China	<p>Data product: Spatiotemporal variations data of CO₂ and NO₂ in China in recent 5 years</p> <p>Decision support: Evidence to support the carbon peaking decision</p>
	Impacts of climate change on net ecosystem productivity of forest in China	<p>Data product: National forest net primary productivity and net ecosystem productivity products from 1981 to 2019</p> <p>Decision support: Forest carbon sink potential was estimated to provide basis for natural carbon sink</p>
	Impacts of land cover change on global net ecosystem productivity	<p>Data product: Global net ecosystem productivity estimations from 2001 to 2019</p> <p>Decision support: Information on variations of global net ecosystem productivity and their drivers to support the realization of the carbon neutrality objective</p>
13.3 Improve education, awareness-raising and human and institutional capacity on climate change mitigation, adaptation, impact reduction and early warning	Global ocean heat content change	<p>Data product: Remote sensing data set of global ocean heat content from 1993 to 2020</p> <p>Methods: A multi-level remote sensing inversion model of ocean heat content applicable at the global scale and for long time series, constructed by combining satellite remote sensing of ocean surface with float observations based on artificial neural network method</p>



Case Study

Interannual changes of sand and dust weather in China in the past 10 years

Target: 13.1 Strengthen resilience and adaptive capacity to climate-related hazards and natural disasters in all countries.

Highlights

- *The research team independently developed methodology to extract sand and dust information based on a variety of remote sensing images and obtained the interannual range of sand and dust weather from 2010 to 2020 on the basis of data in real-time reports from 13 northern provinces, regions and cities.*
- *We analyzed the time series trend of the number of sand and dust weather occurrences and their causes in the past ten years and found a downward trend. The reasons included Chinese sand prevention and control effort in recent years, leading to vegetation recovery in the main sand and dust source areas, increased precipitation and lower number of strong wind days against the general background of global climate change.*

Background

Sandstorm is one of the main catastrophic weathers that affect northern China in spring. Sandstorm disasters often bring extremely serious harm to industrial and agricultural production, transportation and people's life, safety and property, and sometimes cause catastrophic consequences. In order to reduce sandstorm hazards, China has taken measures to treat and ecologically restore sand and dust source areas and routinely

conduct hazard monitoring and assessment. By developing a three-in-one sandstorm-monitoring network consisting of satellite remote sensing systems, ground monitoring stations and field informants, China now has all-weather real-time three-dimensional monitoring of sandstorm disasters and is more resilient to sandstorm disasters.

Data used

© Data from National Oceanic and Atmospheric Administration (NOAA), FY-3A and FY-3B polar orbiting satellites as well as FY-4 satellite and Himawari-8 satellite.

© National Weather Service's precipitation, temperature and winds data from 2010 to 2020.

© Independently generated sandstorm distribution and frequency maps of China from 2010 to 2020 .

© Normalized Difference Vegetation Index (NDVI) data from NASA.

Method

On the basis of remote sensing images from NOAA, FY series and Himawari 8 satellites, the sandstorm automatic identification system analyzed the occurrence and development of sand and dust weather affecting northern China every year, and with

additional information reported by field informants determined the scope of each event and the number of incidences in northern China each year in light of the NWS Classification of Sand and Dust Weather (GB/T20480-2017).

Then, the Mann-Kendall (MK) non-parametric estimation model (Wang, 2016) and the relative change rate model were used to analyze the time series trend of the occurrence of sand and dust weather in the past ten years and calculate the trend of frequency change. A correlation model between the driving factors and the frequency of sand and dust weather was constructed to further analyze the internal factors driving changes.

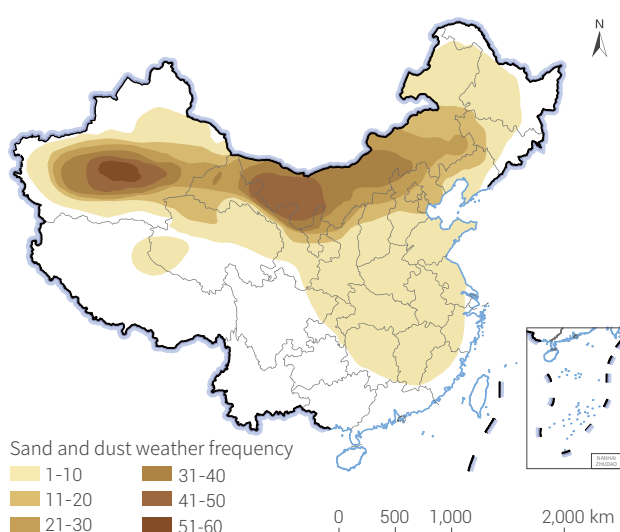
Samples for the MK test do not attenuate a certain degree of distribution and are not affected by a few outliers. It is suitable for data with abnormal distribution (Asrar, 1984). In the analysis of long time series data sets, non-parametric estimation slopes are often used to detect the magnitude of change trends (Wu, 2013). The formula for calculating the slope of the variable in the non-parametric estimation model of the MK time series was:

$$\text{slope} = \text{Median}(Q_i) = \text{Median}\left(\frac{x_j - x_i}{j - i}\right)$$

Results and analysis

Areas with high frequencies of sand and dust weather are mainly in arid and semi-arid north. The deserts and sandy lands have fragile ecological conditions and are the sources of sand and dust for the occurrence of sand and dust weather. Figure 5-1 shows the overall frequencies of sand and dust weather in the spring from 2010 to 2020. The Southern Xinjiang Basin and the Alxa Plateau in Inner Mongolia experienced the most frequent sandstorms.

According to the results of the MK model, the sand and dust weather frequency change rate (slope) from 2010 to 2020 was -0.1111, and the Relative Change Rate (RCR) was 13.58%. The frequency has shown a downward trend in fluctuations since



↑ Figure 5-1. Frequency map of sand and dust weather in spring (March to May) in China from 2010 to 2020

Among them: x_i and x_j represented the cumulative value of the i^{th} year and the j^{th} year ($j > i$) respectively.

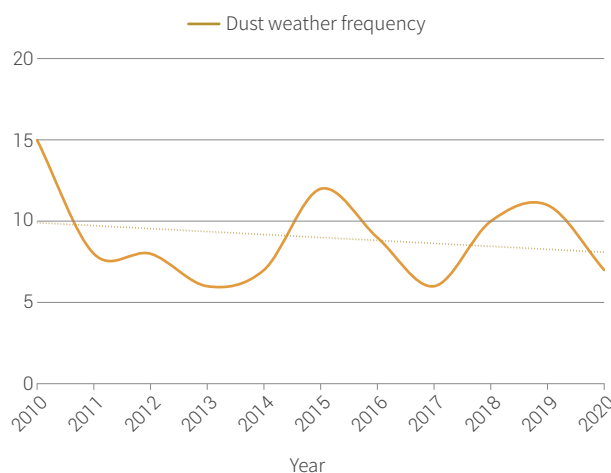
Given the differences among regions, the relative rate of change was introduced based on the MK non-parametric estimation model to analyze the ratio of the rate of change to the multi-year average. The calculation formula of the relative change rate was:

$$\text{RCR} = \frac{\text{slope}}{\text{mean}} \times N \times 100\%$$

Among them: RCR represented the relative rate of change from the start year to the end year, mean represented the multi-year average, N was the length of the time series in years, and slope represented the rate of change of the factor.

2010 (Fig. 5-2).

A sand and dust weather process is formed mainly out of unstable air mass, cold air and underlying surface, as reflected in four elements: the number of windy days, the number of cold air processes, vegetation growth and precipitation. The four elements were used to have a correlation analysis of the causes of the change trend of sand and dust weather. The number of sand and dust weather days and strong wind days were found to show a fluctuating downward trend as a whole, and there was a positive correlation, with the highest correlation coefficient ($R^2=0.5486$). This was because the ground surface in northern China is dry in spring and has poor sand fixation ability while



↑ Figure 5-2. Trend chart of the frequency of sand and dust weather in spring (March to May) in China from 2010 to 2020

gales, as the source of power, tend to cause sand and dust weather processes. The correlation between the frequency of sand and dust weather and the vegetation index was second ($R^2=0.3907$), and the correlation was negative. With further sand prevention and control efforts in recent years, the vegetation index has increased and the number of sand and dust weather has shown

a downward trend. Overall vegetation in north China has been significantly increasing and surface vegetation stocks in spring have also increased correspondingly, effectively suppressing the occurrence of sand and dust weather. The correlation between the number of sand and dust weather and precipitation in the same period is the lowest ($R^2=0.0045$).

Outlook

On the basis of meteorological satellites' remote sensing data plus real-time monitoring information, the research generated remote sensing image data sets from 2010 to 2020, data sets reported by informants and a collection of sandstorms monitoring and evaluation briefings from 2010 to 2020. Sandstorms trends from 2010 to 2020 were analyzed. The results showed that the number of sand and dust weather in China from 2010 to 2020 went downward, with good correlations with the number of windy days and vegetation status. Since vegetation cover has increased in north China in recent years, sand and dust from outside of China has become an important source of spring sandstorms in China, which will be closely followed in the future.

We plan to use more advanced sand and dust identification algorithms and domestic satellite FY-4 remote sensing data for independent, real-time and automatic monitoring. As scientific measures are adopted to treat desertification and improve the ecological environment of source areas, we must better monitor and study vegetation growth, changes in land degradation and desertification, strong winds and precipitation and other meteorological and climatic factors, further understand and predict the development trend of sand and dust weather, and effectively improve emergency response to sandstorm disasters, thus protecting people's lives and property to the maximum.

Spatiotemporal variations of greenhouse gas concentration in China

Target: 13.2 Integrate climate change measures into national policies, strategies and planning.

Highlights

- Greenhouse gas concentration data obtained by remote sensing has obvious spatiotemporal features useful for the change analysis of emissions and the tracking of emission sources.
- Since 2015, CO₂ concentrations in China has been increasing, but with significantly lower growth rate.
- In 2020, the concentration of greenhouse gases fluctuated in large scale. It touched the bottom in February under the influence of the COVID-19 pandemic and reached the peak in December due to economic recovery and the cold wave.

Background

China will have to work very hard to achieve its strategic carbon peaking and carbon neutrality objectives. It is making action plans and has started to take specific measures to ensure the achievement. Efficient and accurate monitoring of greenhouse gas emissions is essential to secure a smooth implementation of the national strategy.

Compared with the traditional emission statistics by industries, monitoring the concentrations of greenhouse gases such as CO₂ through satellite remote sensing enjoys good timeliness and wide spatial coverage, which enables rapid concentration change monitoring and emission sources tracking. It therefore provides efficient data and method support for emission reduction.

Data used

© Satellite data: OCO-2 carbon dioxide satellite data with a resolution of 0.5°; Sentinel-5P multispectral inversion of NO₂ products with a resolution of 0.01°.

© Statistics: World Bank China's carbon emission data; Carbon Emission Account & Datasets (CEADs) provincial emission inventory.

Method

CO₂ is a main greenhouse gas, accounting for about 65% of all greenhouse gases in the world. NO₂ mainly comes from high-temperature combustion of fossil energy, often accompanied by CO₂ emission. NO₂ can only exist in the air for a few hours and the data resolution of satellite observation is higher, which benefits emission sources tracking. In contrast, CO₂ is more stable, exists in the air for a longer time, and has obvious diffusion effect, making it rather difficult to track the carbon sources. Therefore, this study combined CO₂ and NO₂ data to explore the effect of satellite monitoring of carbon emissions.

The level 2 products of Orbiting Carbon Observatory 2 (OCO-2) generated through Kriging interpolation CO₂ image data, on the basis of which the monthly mean value was calculated. Sentinel-5P receives more than 500 scenes of NO₂ data every month and monthly median concentration data were generated on the basis of the median values of each pixel. Then the CO₂ concentration data obtained by OCO-2 satellite and the NO₂ concentration data obtained by Sentinel-5P were analyzed and the relationship between their concentrations and emissions was explored through provincial regional integration. First, the overall

national concentration distribution of CO₂ and NO₂ was analyzed and the median value was chosen as the threshold to distinguish the emission source (above the threshold value) and the diffusion area (below the threshold). Then only the emission source pixels were considered, and then the emission concentrations of each pixel were generated by subtracting the threshold value

from the pixel value. Finally, the emission concentration values of all the provinces were calculated by integration. A further correlation analysis was conducted against CEADs' statistical values of carbon emission in every province, thus generating the quantitative relationship between cumulative concentration and emissions.

Results and analysis

As can be seen from Figure 5-3, both CO₂ and NO₂ data showed that the concentration of greenhouse gases in eastern China was higher. In comparison, NO₂ has a shorter lifetime in the air and data resolution was better. Therefore, NO₂ concentration map showed emission sources with finer granularity, with obviously higher concentration in central cities in central and western China and urban agglomerations in eastern China than in their

surrounding areas. North China Plain had the most concentrated greenhouse gas emissions. Through quantitative analysis of correlation between the cumulative concentration from the satellites and emission statistics in various provinces, it was found that the correlation of NO₂ was higher than that of CO₂ (the correlation coefficients are 0.86 and 0.55 respectively), that is, NO₂ showed better spatial difference of CO₂ emissions.

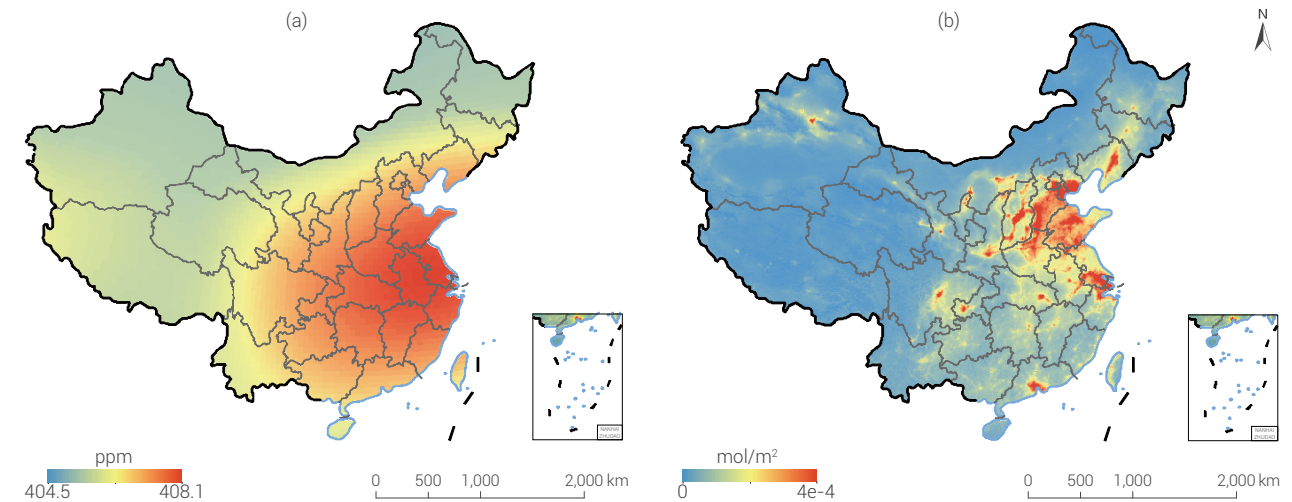


Figure 5-3. (a) Average concentration of CO₂ in 2018; (b) Average concentration of NO₂ in 2019

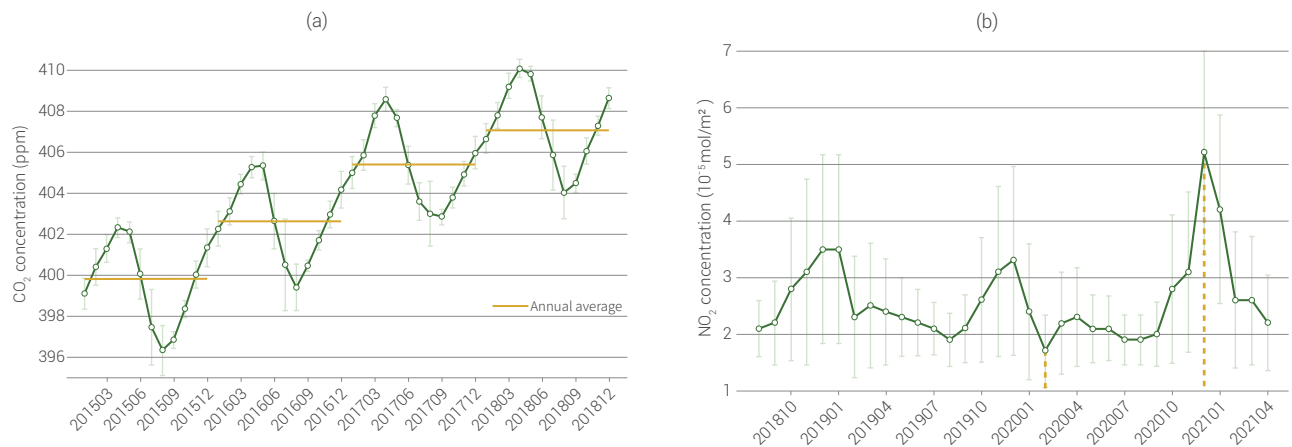


Figure 5-4. (a) CO₂ concentration changes in China from 2015 to 2018; (b) NO₂ concentration changes from August 2018 to April 2021 in China.

On the time scale (Fig. 5-4), the CO₂ concentrations showed a wavy upward trend from January 2015 to December 2018, reaching the annual maximum in April and the annual minimum in August. Judged from the annual average level (red horizontal line), although the concentration was still increasing, the range of increase was gradually decreasing. NO₂ concentration also showed a wavy trend between 2018 and 2019, reaching the annual peak in December and the annual bottom in August. Monthly fluctuations were mainly affected by the economic cycle, winter heating, absorption by plants and other factors.

Outlook

There are many advantages to use satellite data in monitoring greenhouse gas concentration since they are more time-efficient and contain richer spatial information. The spatial distribution of greenhouse gas concentrations monitored by satellites has a high correlation with regional emissions. The temporal variations of greenhouse gas concentration and regional emission are highly synchronic. The growth of CO₂ concentration in China has

During 2020, the concentration of NO₂ experienced great fluctuations. Affected by the COVID-19 pandemic, NO₂ concentration fell to the bottom of the past 3 years in February 2020. In the second half of 2020, China's economy began to recover rapidly. In December, it experienced the strongest cold wave in recent years, leading to increased fossil energy consumption for heating. As the result, the NO₂ concentration reached the peak in recent three years. The annual average NO₂ concentration in 2020 is slightly lower than that in 2019.

gradually slowed down since 2015. Greenhouse gas emissions are affected by economic development, energy structure and seasonal factors and demonstrate great volatility and complexity. Satellite data can be used to support the judgment on when China will reach its peak in carbon emission. Such a judgment must be science-based and with multiple factors considered.

Impacts of climate change on net ecosystem productivity of forest in China

Target: 13.2 Integrate climate change measures into national policies, strategies and planning.

Highlights

- *Dynamic assessment of net primary productivity (NPP) and net ecosystem productivity (NEP) of forests in China since 1981 was completed.*
- *The forest ecosystems in China had great carbon sink potential. Compared with the baseline climate period (1981-2010), the average NPP of forest ecosystems from 2011 to 2019 increased overall. The annual average NEP of Chinese forests from 2011 to 2019 was 199.54 TgC/a (1 Tg=10¹² g) or 0.199 PgC/a (1Pg=10¹⁵ g).*
- *There were obvious regional differences in NEP of forests in China. Forests in Yunnan had sequestered the largest NEP, followed by Guangxi and Guangdong.*

Background

The impacts of warming on global ecological environment are attracting more and more attention. As a principal part of terrestrial ecosystems, forests play irreplaceable roles in regulating global carbon balance and maintaining global climate. There are close relationships between forests and climate. Research showed that CO₂ exchanges between the atmosphere and the terrestrial biosphere through photosynthesis took about seven years on average and that 70% of the exchange was with forests (Zhao *et al.* 2019). Therefore, changes in forest distribution, soil respiration, productivity, and carbon budget caused by climate change can in turn produce significant

feedback on Earth's climate. Hence, it is of great significance to study the carbon sink potential of forest ecosystems in China with the carbon neutrality target in mind.

The methods and techniques for researches on forest carbon cycles have been constantly improving and more researchers have shifted their interests from individual ecosystems to larger zones. In this case study, the impacts of climate change on NPP and NEP of forests in China since 1981 were quantitatively evaluated based on Big Earth Data and forest ecosystem carbon budget model.

Data used

© Meteorological data: provided by the National Meteorological Information Centre (NMIC), including daily precipitation, daily maximum temperature, daily minimum temperature, daily average temperature, daily air relative humidity, daily average wind speed and daily surface solar radiation from 1981 to 2019 collected at 2100 meteorological stations in China, plus their longitude, latitude and altitude.

© Soil data: obtained from the soil texture map (1:14 000 000)

produced by the Institute of Soil Science, Chinese Academy of Sciences, including soil particle composition (percentages of sand, silt and clay), soil field capacity, wilting water content, bulk density, soil carbon storage and soil nitrogen storage.

© Remote sensing data: The vegetation feature data were calculated by remote sensing model based on NDVI data from the NOAA Advanced Very High Resolution Radiometer (AVHRR).

Method

The FORCCHN (FOREst ecosystem Carbon budget model for CHiNa) model based on individual tree species was used in this study to simulate the impacts of climate change on carbon sequestration potential of forest ecosystems in China. The model is based on the basic principles of plant physiology, forest ecology and soil environment science and reasonably explains the dynamic mechanisms of the carbon budget of young forests in forest ecosystems (Yan and Zhao, 2007). FORCCHN has a resolution of 10 km×10 km. It has been used to simulate forest carbon cycles at national and global scales (Zhao *et al.*, 2019, 2020).

In FORCCHN, the main control equations of NPP and NEP of individual trees were as follows:

$$NPP_i = GPP_i - RA_i$$

$$NEP_i = NPP_i - RH_i$$

where NPP_i , GPP_i and RA_i represented the net primary productivity, gross primary productivity and autotrophic respiration of the i^{th} individual tree, and the physical dimension is (gC/d); NEP_i represented the NEP of the i^{th} individual tree (gC/d); and RH_i represented soil heterotrophic respiration (gC/d).

Results and analysis

1. Impacts of climate change on NPP of forests in China

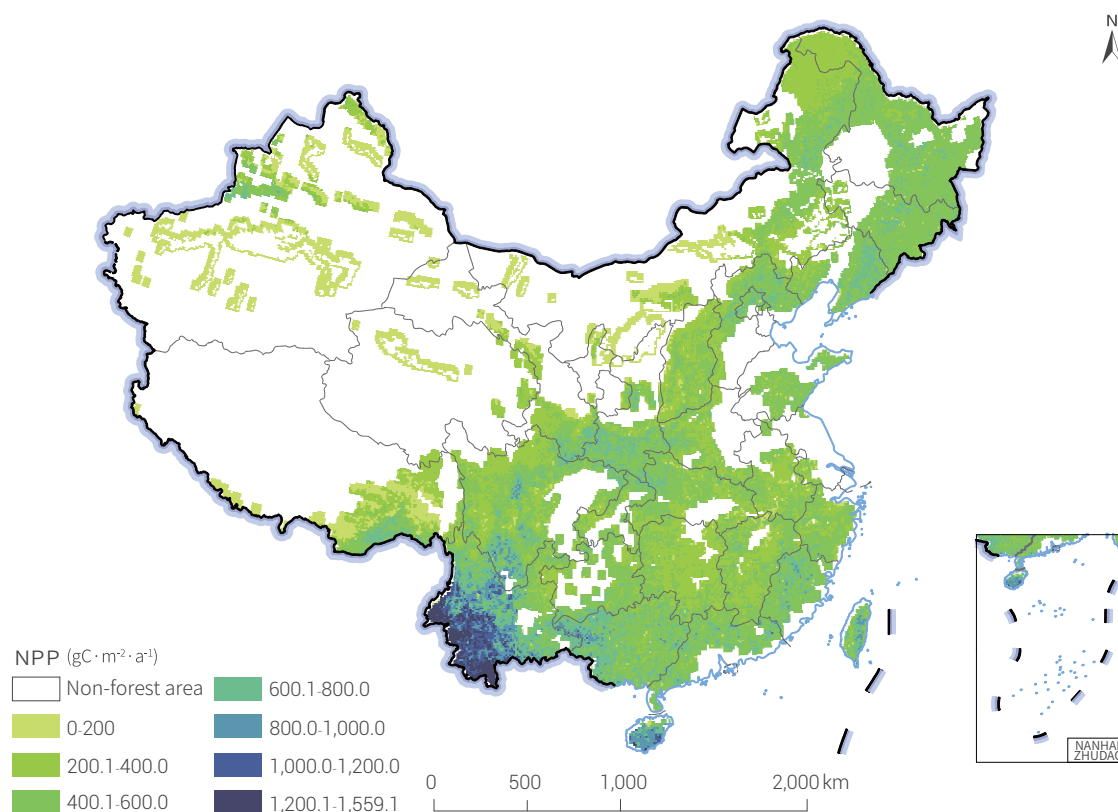
Compared with the baseline climate period (1981-2010), the average NPP of forests in China increased from 2011 to 2019 overall. The most obvious increases were in Southwest China and Southeast China: 3.10% - 6.00%. In particular, NPP increased by 6.10%-9.00% in Southwest China during 2011-2015 and in Southeast China during 2016-2019. However, in Northeast China decreased obviously, by more than 6.00% in some areas.

In terms of regional average, NPP per unit area of forests was high in the Southeast and low in the Northwest. From 2011 to

2019, the average NPP per unit area was $530.25 \text{ gC}\cdot\text{m}^{-2}\cdot\text{a}^{-1}$. It was the highest in Southwest China, followed by the Northeast and Southeast, and then the Northwest (Fig. 5-5).

2. Effects of climate change on NEP of forests in China

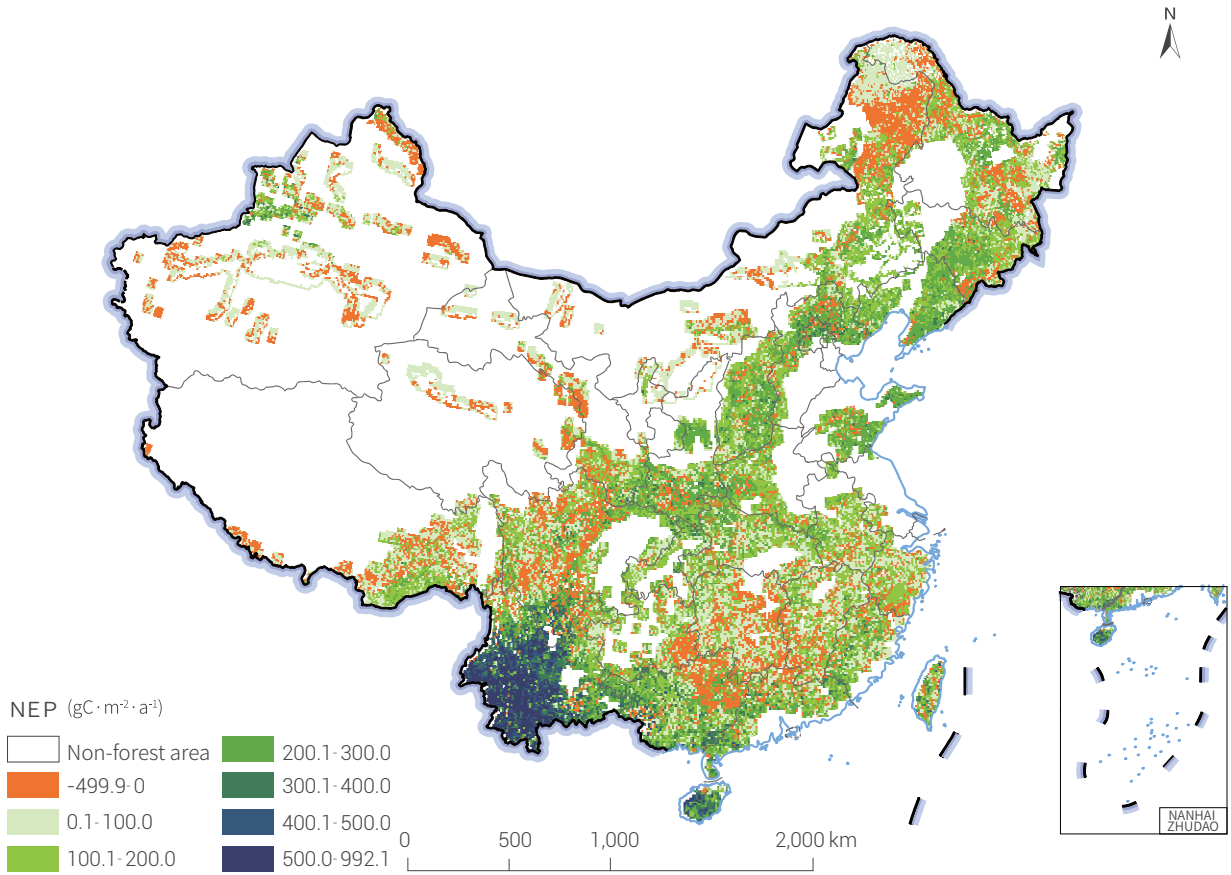
Climate change generally contributes to carbon sequestration in forest vegetation in China. In the past 39 years, the forest ecosystems in China have in general sequestered carbon. From 2011 to 2019, the annual average NEP was 199.54 TgC/a and the NEP per unit area was $109.25 \text{ gC}\cdot\text{m}^{-2}\cdot\text{a}^{-1}$. Affected by climate, soil type, vegetation type and other factors, there were significant



↑ Figure 5-5. Average NPP of forests in China during 2011-2019

differences in NEP among different regions in China, with an upward trend from the Northwest to the Southeast (Fig. 5-6). From

2011 to 2019, Yunnan Province had the largest NEP (72.79 TgC/a), followed by Guangxi (18.49 TgC/a) and Guangdong (10.01 TgC/a)



↑ Figure 5-6. Average NEP of forests in China during 2011-2019

Outlook

In the case study, internationally shared Big Earth Data were used and a dynamic assessment of the carbon sequestration potential of forests in China was conducted using the FORCCHN model based on individual tree growth processes. The results showed that compared with the baseline climate period (1981-2010), the NPP of forests in China increased in the 2011-2019 period. The most obvious increases were in Southwest China and Southeast China, at around 3.10%-6.00%. In the past 39 years, forest ecosystems in China have sequestered carbon. There were significant differences in NEP among different regions in China. From 2011 to 2019, Yunnan Province had the largest NEP (72.79 TgC/a), followed by Guangxi (18.49 TgC/a) and Guangdong (10.01 TgC/a). The results will inform accurate assessment of the role of forest carbon sinks in regulating global carbon balance and maintaining global climate, thus contributing to the realization of China's carbon neutrality goal. They can also provide scientific basis for the evaluation of the roles of forests in ecological environment construction and global climate

change research.

Forest vegetation is the main body of terrestrial biological carbon sequestration, which features low cost, large carbon sink and high ecological values. Through a series of measures such as increasing forest area, artificial afforestation, natural forest protection and restoration, the forest stock and carbon sequestration in China have both greatly increased, thus playing an increasingly important role in coping with climate change and contributing to the carbon neutrality goal. However, there are still significant differences in carbon sequestration potentials in different regions. For example, Northwest China is very important as an ecological security barrier and for expansion of carbon sink development, but its NPP and carbon sequestration potential are still relatively low. In light of this, it is imperative to improve forest carbon sink through enhanced forest tending and science-based forest management so as to further increase the carbon sink potential of forests in Northwest China against the backdrop of climate change.

Impacts of land cover change on global net ecosystem productivity

Target: 13.2 Integrate climate change measures into national policies, strategies and planning.

Highlights

- *Net ecosystem productivity (NEP) computed through BEPS is often used to describe carbon sink. This study analyzed global NEP changes and found that global NEP increased significantly from 2001 to 2019, especially in the northwestern and northeastern Eurasian continent, southern and central China, South Asia, Central Africa, northern North America, western South America, etc.*
- *The importance of land cover change to global NEP from 2001 and 2019 was significant. The importance in China was about 32%. Forest, cropland, and other land uses contributed 17%, 8% and 7% respectively to carbon sink.*

Background

Climate change is a global issue confronting mankind. Greenhouse effect has driven significant global warming due to carbon dioxide emissions. By 2020, the global average atmospheric concentration of carbon dioxide had reached 415 ppm, significantly higher than the pre-industrial level of 285 ppm in 1850. The global average surface temperature rose by about 1.2 °C from 1850 to 2020. Global warming has accelerated the melting of polar glaciers, raised the sea level and aggravated natural disasters, all of which ultimately threaten the survival of human beings and other living organisms (Chen, 2021; NOAA, 2020).

The terrestrial ecosystems play an important role in the

climate system. The carbon sources, carbon sink and their spatiotemporal changes in the terrestrial ecosystem are affected by many factors, such as climate and human activities (Chen *et al.*, 2019; Peng *et al.*, 2017). Researches on carbon sources and carbon sink to reveal the carbon sink driving mechanism in terrestrial ecosystems will inform carbon neutralization policies. The net ecosystem productivity (NEP) computed through the Boreal Ecosystem Productivity Simulator (BEPS) is often used to describe the state of carbon sink. In this study, we analyzed the global NEP variations and the driving mechanisms from 2001 to 2019 with a view to providing macro decision support in response to climate change.

Data used

© Global daily maximum temperature, minimum temperature, average relative humidity, daily total precipitation, daily total radiation, leaf area index (LAI), CO₂ concentration, nitrogen

deposition from 2001 to 2019.

© MODIS annual land cover products.

Method

We used the daily maximum temperature, minimum temperature, average relative humidity, daily total precipitation, daily total radiation, LAI, CO₂ concentration and nitrogen deposition in the BEPS to calculate NEP, and then quantified the importance of these (land cover, climate, CO₂ concentration and nitrogen

deposition) changes to global NEP with random forest algorithm. For China, we went further to analyze also the importance of forest, cropland, other vegetations, various meteorological factors, CO₂ concentration and nitrogen deposition to NEP changes.

Figure 5-7.

● Interannual variations in global NEP from 2001 to 2019

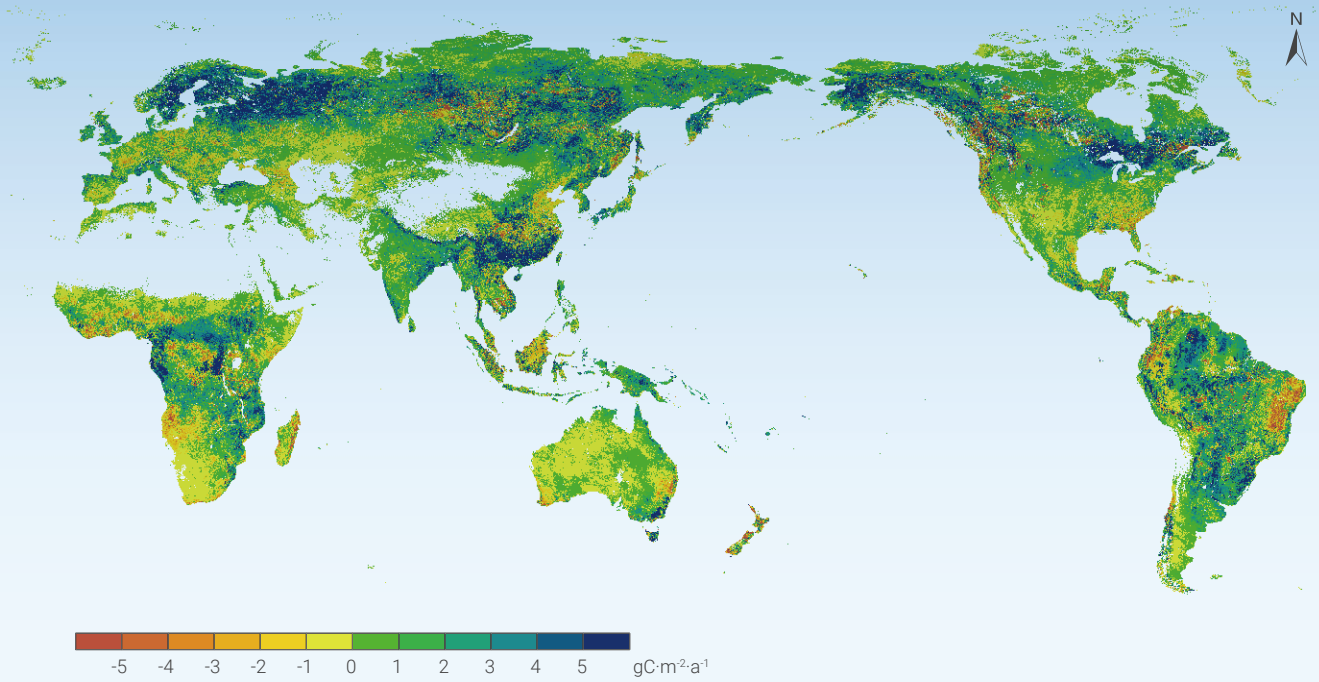
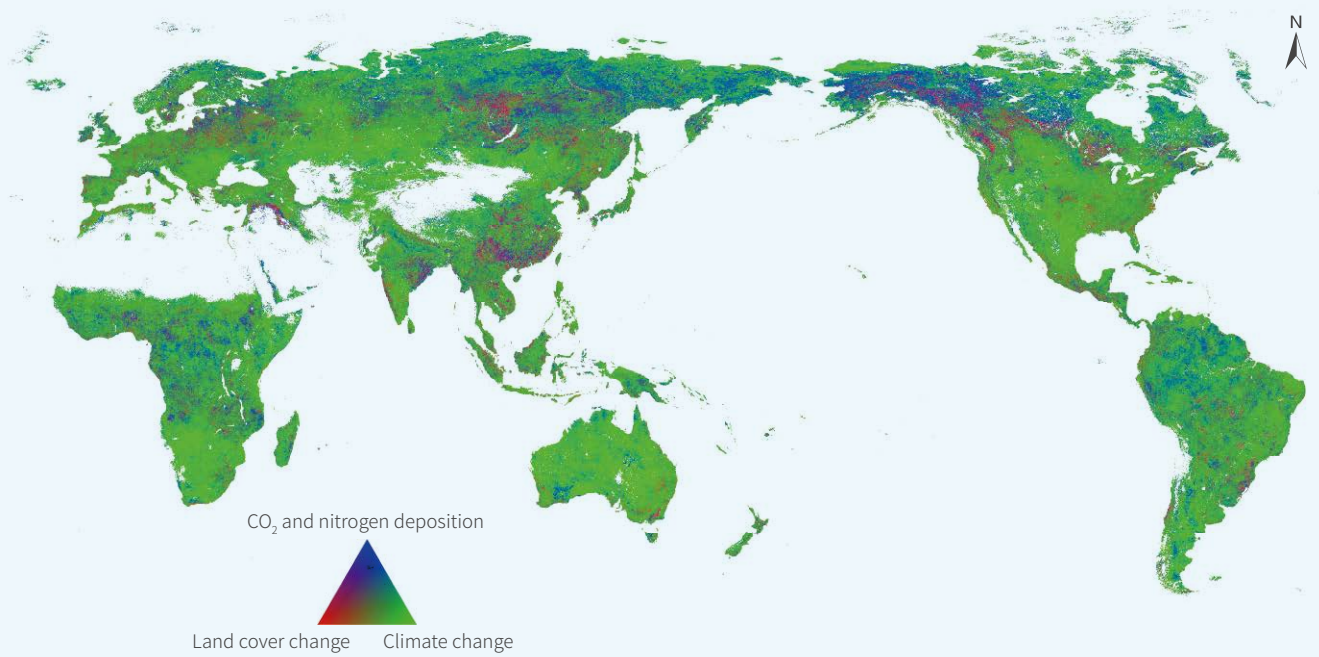


Figure 5-8.

● Contributions of land cover change, climate change, CO₂ and nitrogen deposition change to global terrestrial ecosystems NEP from 2001 to 2019



Results and analysis

1. Global NEP variations at pixel level

Figure 5-7 shows the interannual variations in global NEP. Obviously it increased from 2001 to 2019 in most regions, especially in southern and central China, the northwestern and northeastern Eurasian continent, South Asia, Central Africa, northern North America and western South America. In general, global NEP showed an upward trend, from 1.57 Pg in 2001 to 2.84 Pg in 2019, with an interannual linear increase of 0.08 Pg. China saw a significant increase from 63.95 Tg in 2001 to 223.81 Tg in 2019, with an interannual linear increase of 8.72 Tg.

2. Driver analysis

The importance of the main driving factors to global NEP variations are shown in Figure 5-8. Land cover change played a major role primarily at the middle and high latitudes in Europe and North America as well as central and southern China. Climate change played a major role in Central Asia, Oceania and southern Africa. The effects of CO₂ and nitrogen deposition were more visible at the middle and high latitudes. Comparison between Figures 5-7 and 5-8 suggested that the annual change rate of NEP in areas where land cover change plays a major role

was relatively large. For example, southern and central China, northwest and northeast Eurasian continent, and northern North America demonstrated a relatively large increase in NEP ($> 5\text{gC}\cdot\text{m}^{-2}\cdot\text{a}^{-1}$). Some land cover changes, such as deforestation in tropical areas such as Amazon, led to NEP decrease, that is, a negative contribution to NEP. Since the importance calculated with random forest algorithm did not distinguish positive and negative effects, but was the sum of absolute values, this study indicated that global land cover change was of great importance to the variations of the NEP of the global terrestrial ecosystem from 2001 to 2019.

In China, the importance of these driving factors was 32% (land cover), 32% (climate) and 36% (CO₂ concentration and nitrogen deposition) respectively for the same period. Among different land covers, forest, cropland and other land use types accounted for 17%, 8% and 7%, respectively. The percentages have been the results of large-scale ecological projects (such as the Three-North Shelterbelt, Returning Cultivated Land to Forests, and Natural Forest Protection, etc.) since 2000 (Bryan *et al.*, 2018; Chi *et al.*, 2019).

Outlook

Carbon neutralization refers to the realization of net zero CO₂ emissions by balancing or eliminating carbon dioxide emissions and preventing its increase in the atmosphere, which leads to global warming. For developing countries, direct emission reduction is in conflict with economic development to some extent. Carbon sequestration through land use or cover change and the vegetation ecosystem can be adopted as a strategic choice for indirect emission reduction. In addition to reducing fossil fuel consumption, the development of renewable energies such as wind, solar, biomass, geothermal, tidal and hydrogen is also an effective way to achieve carbon neutrality. Policy and

economic incentives are important to promote carbon neutrality. The cost of afforestation and forest management is much lower than that of industrial carbon removal. Therefore, increased carbon sink with the terrestrial ecosystem is a low-cost option to eliminate carbon dioxide in the atmosphere. Building on the analysis of NEP, which reflects terrestrial ecosystem carbon sink, and its drivers, we focused on the quantitative impacts of land cover change on NEP in recent decades. In the future, with data of finer resolution and better precision, such quantitative studies will be more accurate and targeted to guide decisions.



Global ocean heat content change

Target: 13.3 Improve education, awareness-raising and human and institutional capacity on climate change mitigation, adaptation, impact reduction and early warning.

Highlights

- A new dataset of global ocean heat content from 1993 to 2020 based on remote sensing data was produced.
- In the past 30 years, the upper 2000 meters of the global ocean have been warming significantly, with a warming rate of $2.25 \times 10^8 \text{ J} \cdot \text{m}^{-2} \cdot \text{decade}^{-1}$. In 2020, the upper 2000 meters absorbed $13.95 \times 10^{22} \text{ J}$ of heat (over 1993-2015 baseline). The warming rate of the subsurface and deeper ocean was higher than that of the upper ocean, and more and more heat was absorbed by the deeper ocean.
- In the global warming process, heat uptake significantly and unevenly occurred in different ocean basins. Ocean heat content was currently the most effective indicator to measure global warming and directly reflected global climate change.

Background

With the continuous emission of greenhouse gases, global warming is accelerating and the ocean, as an essential "conditioner" of global climate, is absorbing heat and warming up. The ocean absorbs and stores more than 90% of the global warming energy, which significantly increases global ocean heat content. Recent evidence shows that the ocean continued to warm up in 2020, making the year the warmest since the start of modern ocean observation records (Cheng *et al.*, 2021). Meanwhile, the past five years have also been the warmest five years in modern ocean observation records, and ocean warming is still accelerating (Cheng *et al.*, 2019). Ocean warming has had a serious impact on the marine ecosystem and the sustainable

development of mankind, resulting in serious consequences such as rising sea levels, more extreme climate events, coral bleaching and marine ecology deterioration. Ocean Heat Content (OHC) is one of the most direct and effective indicators to measure global warming and directly reflects global climate change. Due to the sparseness and insufficiency of ocean interior observation data, there are still large uncertainties and controversies in the estimation and study of ocean warming, which should be supported with subsurface and deeper ocean observation data. Therefore, there is an urgent need to develop subsurface and deeper ocean remote sensing technology so as to accurately retrieve global ocean heat content change.

Data used

◎ Sea Surface Height (SSH): from Archiving, Validation and Interpretation of Satellite Oceanographic data (AVISO) satellite altimeter products, with spatial resolution: $1^\circ \times 1^\circ$; temporal resolution: daily; and time span: from 1993 to the present.

◎ Sea Surface Temperature (SST): from NOAA Optimum Interpolation Sea Surface Temperature (OISST) products, spatial resolution: $1^\circ \times 1^\circ$; temporal resolution: daily; and time span: from 1981 to the present.

◎ Sea Surface Wind (SSW): from Cross-Calibrated Multi-Platform (CCMP) ocean wind field data, spatial resolution: $1^\circ \times 1^\circ$; temporal resolution: daily; and time span: from 1987 to the present.

◎ Array for Real-time Geostrophic Oceanography (ARGO) observations: temperature observations for the upper 2000 meters of the global ocean, spatial resolution: $1^\circ \times 1^\circ$; temporal resolution: monthly; and time span: from 2005 to the present.

Method

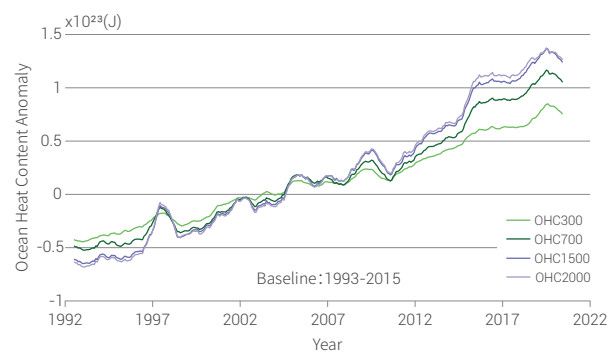
The artificial neural network approach was used in combination with multisource satellite observations and ARGO float data to build a remote sensing inversion model for global-scale, multi-layered, and long-time series estimation of OHC. A series of sensitivity tests for input factors were performed and the network structure was optimized to generate the optimal model. Based on this model, a new long-time series remote sensing dataset of global OHC from 1993 to 2020 was reconstructed (named OPEN, for the upper 2000 meters, with monthly temporal resolution and

$1^{\circ}\times 1^{\circ}$ spatial resolution), which improved the accuracy of OHC estimation, supplemented ARGO observations in the length of time series, and filled the gap in ocean observation before ARGO. Based on the OPEN data, OHC changes were examined from multiple perspectives (such as the warming rate, linear trend and spatial heterogeneity) to quantitatively understand the current status, characteristics and processes of ocean warming in the context of global warming.

Results and analysis

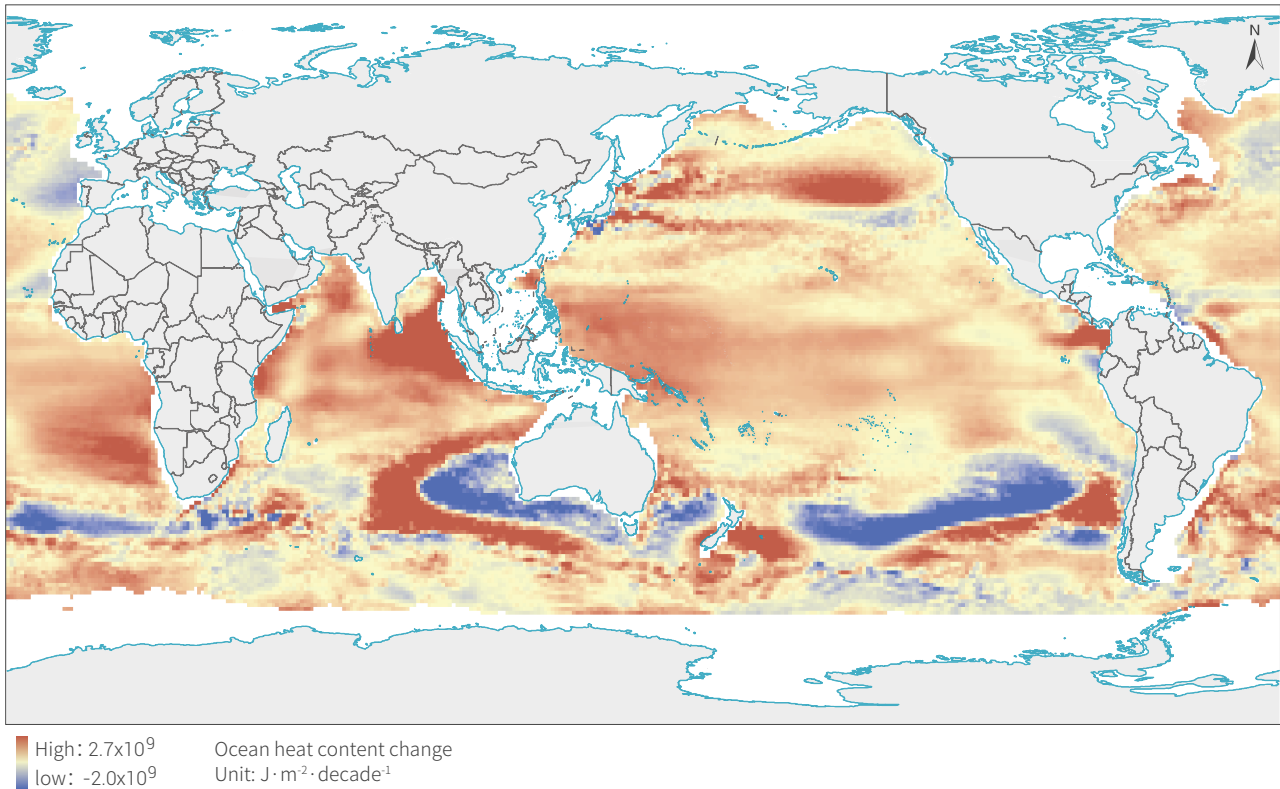
The OPEN dataset reconstructed on satellite remote sensing data and an artificial neural network was employed to calculate the OHC anomaly trend (Fig. 5-9) and change rate (Fig. 5-10) of the global ocean in different depth ranges (1993-2015 baseline). Figure 5-9 shows the trend of global ocean heat content anomaly for the upper 2000, 1500, 700, 300 meters from 1993 to 2020. The results showed that during the past 30 years, the upper 2000 meters of the global ocean had been warming significantly and continuously, with a warming rate of $2.25\times 10^8 \text{ J}\cdot\text{m}^{-2}\cdot\text{decade}^{-1}$. The global warming rates for the upper 1500, 700 and 300 meters were 2.22×10^8 , 1.76×10^8 , and $1.37\times 10^8 \text{ J}\cdot\text{m}^{-2}\cdot\text{decade}^{-1}$, respectively. The deeper layers of the ocean were warming up at a faster rate than the upper layers as more and more heat had been absorbed by the subsurface and deeper ocean. In 2010, 2015, and 2020, the global ocean absorbed 3.25×10^{22} , 8.19×10^{22} , and 13.95×10^{22} J of heat at upper 2000 meters (1993-2015 baseline), indicating a heat uptake of 10.70×10^{22} J in the past 10 years (2010-2020). A rapid warming trend was maintained. With global warming, the situation of ocean warming was very severe, and such a huge heat storage will pose a serious threat to marine ecosystems, sea-level rising and sustainable development of human beings.

Figure 5-10 shows the spatial distribution of global OHC variations for upper 2000 meters from 1993 to 2020. It was found in the study that in the past 30 years, all ocean basins (including



↑ Figure 5-9. Trends of global ocean heat content anomaly for upper 2000, 1500, 700, 300 meters from 1993 to 2020

the Pacific, Atlantic, Indian and Southern Oceans) had warmed up significantly during the global warming process, but there was a certain degree of spatial heterogeneity across the global ocean. The warming characteristics of different ocean basins varied, and cooling also occurred in some areas. OHC is currently the most direct and effective indicator to measure global warming. To track the global warming process, more attention should be given to OHC changes, especially in the subsurface and deeper ocean. It is more urgent than ever to enhance the observation of the subsurface and deeper ocean and improve the accuracy of observations.



↑ Figure 5-10. Rates of global ocean heat content change for upper 2000 meters from 1993 to 2020

Outlook

As the heat reservoir of global warming, the ocean plays an important role as a conditioner of global climate change. The OHC change is the most effective indicator to measure climate change and it directly reflects the status of global warming. To understand global warming, we must pay attention to ocean warming. Strengthening the observation of the subsurface and deeper ocean is critical to improving the accuracy of OHC estimation and reducing uncertainties in ocean warming analysis, thus contributing to a deeper understanding of global warming and a better response to global climate change. Ocean warming will seriously threaten marine ecosystems (causing coral bleaching and reducing fishery productivity), fuel extreme weather events (increased frequency of super typhoons and extreme heatwaves), cause sea-level rising (threatening the living space of islands and coastal zones), and ultimately affect the

sustainable development of mankind. The series of ecological and environmental issues caused by ocean warming should be given more attention and publicity.

In recent years, the ever-increasing ocean warming has supported global warming as an indisputable fact, which is serious and ongoing. Mankind still faces severe challenges in coping with climate change. The ultimate solution to global warming is to reduce carbon dioxide and other greenhouse gas emissions. Pursuing the carbon peaking and neutralization goal is the most effective way for mankind to cope with climate change and reduce the risk of global warming. The global warming revealed by ocean warming once again suggests that there is still a long way to go and it will take concerted efforts of all mankind to achieve the temperature control target of *the Paris Agreement*.



Summary

The chapter is structured around three topics: strengthen capacity to natural disasters (SDG 13.1), climate change measures (SDG 13.2) and climate change adaptation and early warning (SDG 13.3). It describes studies through Big Earth Data on the progress of China and the world in coping with climate change. Those studies generated the following datasets: national spatial distribution of sandstorms, greenhouse gases, forest NEP, global NEP change and global OHC.

Through the case studies, we draw the following main conclusions:

- (1) Extreme weather events caused by climate change are increasing disaster risks everywhere, but science-based responses may minimize their impact on food security and human life. Over the past 10 years, the frequency of dust storms has shown a downward trend in fluctuations, mainly due to the increase of vegetation coverage and sand fixation capacity in north China, which is a reflection of China's effective response to climate related disasters.
- (2) Emission reduction by mankind remains the most urgent task in controlling global warming. Meanwhile, increasing ecological carbon sink in the natural environment is also an important

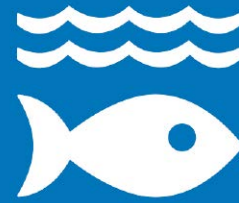
means to reduce CO₂ concentration. CO₂ emissions have been increasing in China since 2015, but at a slower rate. In 2020, due to the impact of COVID-19, emissions decreased slightly compared with 2019. Climate change has increased the carbon sequestration capacity of China's forests in the recent 10 years. The global terrestrial carbon sequestration capacity has also been significantly enhanced.

- (3) Climate change is having a profound impact on multiple spheres of the Earth. Mankind must be vigilant to the warming of the oceans and its future impact. In the past 30 years, global OHC has been rising at faster speed. It is necessary to strengthen early warnings of marine super storms, sea level rise and marine ecological environment.

Climate change is posing an unprecedented threat to human sustainable development. Science and technology are the key to mankind's response to climate change. In particular, Big Earth Data can provide rich data in the spatiotemporal distribution of disasters, carbon sources, carbon sink and multi-sphere responses. These data will inform future decision-making and early warning and support the effort to mitigate and adapt to climate change.



STRA



SDG 14

Life below Water

Background	96
Main Contributions	97
Case Study	98
Summary	108

Satellite image of coastal farming area in Ningde, Fujian Province (Gaofen-7, January 9, 2021)



Background

The safety of marine ecosystems directly bears on the health and well-being of all mankind. In 2015, SDG 14 (Conserve and sustainably use the oceans, seas and marine resources for sustainable development) was written into the UN 2030 Agenda for Sustainable Development and became one of the hot issues of concern to the international community.

However, global progress in the implementation of most of the SDG 14 targets has not been satisfactory. According to the report on *the Second World Ocean Assessment* released by the UN on 21 April 2021, since 2015, stresses generated by human activities have continued to degrade marine ecosystems, such as mangroves and coral reefs. The stresses are related to climate change, unsustainable fishing, introduction of invasive species, air pollution that causes acidification and eutrophication, excessive input of nutrients and harmful substances, increasing man-made noise, and poorly managed coastal development and natural resources exploitation, etc. (UN, 2021c). UN Secretary-General António Guterres called on all countries and stakeholders around the world to pay more attention to the warnings in the report.

The Chinese government has always attached great importance to and supported the relevant UN agenda for sustainable ocean development. Bearing in mind its strategic goal to become a maritime power, China has developed marine industries rapidly

and achieved significant results in vigorously reducing marine pollution, restoring marine ecology with science-based measures and rationally expanding the marine economy. However, the dense population in coastal areas, the rapid economic development and the huge demand for marine resources challenge sustainable ocean development in China. There is hence a need to better use data and innovative technologies at the service of SDG 14.

Big Earth Data, with its huge potential in macroscopic and dynamic monitoring, has already become a new key to our understanding of the ocean and a new engine for knowledge discovery (Guo *et al.*, 2016). In the past two years, we have made a lot of efforts and explorations to support SDG 14 by using Big Earth Data and related technologies and methods and accumulated good practical experience in data set production and evaluation model construction. In the studies, researchers built on the models and methods used in 2019 and 2020 as well as regional and national evaluations and demonstrations, focused on SDG 14.2 (protection of marine ecosystems), and evaluated the effects of mangrove protection, coastal aquaculture pond management and algal bloom monitoring and early warning. The results of the case studies in this report provide new data and technical support for better understanding major issues related to sustainable ocean development and making response strategies.

SDG 14





Main Contributions

The studies tackled SDG 14.2 (protection of marine ecosystems). Big Earth Data were used to monitor and evaluate the relevant indicators in China's coastal waters and typical areas. The data

products, methods and decision support provided are presented here through three cases (Table 6-1).

Table 6-1 Cases and Their Main Contributions

Target	Case	Contributions
14.2 By 2020, sustainably manage and protect marine and coastal ecosystems to avoid significant adverse impacts, including by strengthening their resilience, and take action for their restoration in order to achieve healthy and productive oceans	Monitoring and forecasting macroalgal blooms in the Yellow Sea	<p>Method: A methodological system for monitoring and forecasting macroalgal blooms in the Yellow Sea, including rapid extraction of the spatial distribution data of floating algae from the Big Earth Data cloud platform and real-time prediction of the drift trajectories of macroalgal blooms based on a four-dimensional variational assimilation forecast model</p> <p>Decision support: Informing early warning and prediction of harmful algal bloom hazards and integrated decision-making in coastal municipalities</p>
	Changes of Mangrove forests in China	<p>Data product: Data sets on mangrove forest distributions in China for 2015, 2018 and 2020</p> <p>Method: Rapid interpretation of mangrove forests using machine learning method</p> <p>Decision support: Cyclical monitoring of mangrove forests and informing measures to protect biodiversity and enhance disaster resilience of marine ecosystems</p>
	Changes of coastal aquaculture ponds in China	<p>Method: A rapid identification method for large-scale coastal aquaculture ponds based on Big Earth Data and cloud platform</p> <p>Decision support: Analysis of the spatial and temporal variations of coastal aquaculture ponds to scientifically inform decision-making on sustainable management of coastal zones and aquaculture</p>



Case Study

Monitoring and forecasting macroalgal blooms in the Yellow Sea

Target: 14.2 By 2020, sustainably manage and protect marine and coastal ecosystems to avoid significant adverse impacts, including by strengthening their resilience, and take action for their restoration in order to achieve healthy and productive oceans.

Highlights

- A system of technologies and methods to monitor and forecast macroalgal blooms in the Yellow Sea was established and applied in mitigation of *Ulva prolifera* green tides in the Yellow Sea from May to July in 2021.
- Quasi-real-time extraction of floating macroalgal bloom signals from remote sensing products was combined with forecasting of drift trajectory of floating macroalgae based on four-dimensional variational (4DVar) data assimilation to effectively inform the monitoring and forecasting of harmful algal blooms for coastal cities along the Yellow Sea.

Background

Macroalgal blooms, particularly large-scale green tides of *Ulva prolifera* has occurred every year in the Yellow Sea since 2007, seriously disrupting the landscape, environment and aquaculture and becoming a regular ecological disaster in the Yellow Sea. Based on previous studies (Liu *et al.*, 2009; Zhou *et al.*, 2015), the Ministry of Natural Resources, Ministry of Ecology and Environment and the provincial governments of Shandong and Jiangsu jointly took a series of control measures, including green algae treatment at the source region of green tides, preventing the expansion of green algae before the formation of intense green tide, development of monitoring and forecasting methods,

and interception, collection, processing and utilization of green algae etc. The results of these measures were seen in 2020, as the volume and scope of green tides were remarkably smaller than the previous years. However, a large-scale green tide broke out again in June 2021, which fully demonstrated the complexity of macroalgal bloom treatment. Therefore, effective monitoring and forecasting of macroalgal blooms is of great value. In this study, satellite remote sensing was used to rapidly identify floating macroalgal blooms and a 4DVar data assimilation model was used to forecast the drift trajectories of floating macroalgae.

Data used

- MODIS/Terra Surface Reflectance Daily L2G Global 1 km and 500 m SIN Grid Product, MOD09GA (2021).
- Sentinel-2 multi-spectral instrument level-1C data from European Union ESA Copernicus (2021).
- Gaofen and Haiyang satellite images (2021).
- Global model data (1/12°) from HYbrid Coordinate Ocean Model (HYCOM).
- Global Forecast System (GFS) from NCEP.
- Satellite sea surface heights from AVISO.
- Infrared and microwave combined sea surface temperature measurements from the Group for High Resolution Sea Surface Temperature (GHRSSST).
- Ocean temperature and salinity profiles from ARGO.
- Real-time observed water salinity and temperature data from the Yellow Sea Stations of Offshore Marine Observation Research Network (OMORN), Chinese Academy of Sciences.

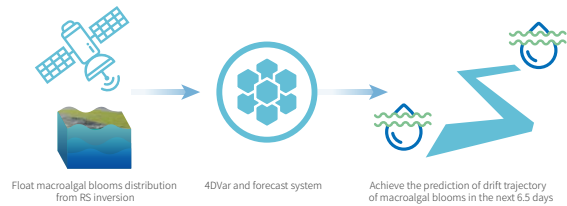
Method

1. Quasi-real-time monitoring of the spatial distribution of macroalgal blooms based on satellite RS data

Based on the CASEarth platform, the satellite images from MOD09GA, Sentinel-2 and Gaofen-1 were processed by removing pixels with cloud and no-data values, clipping land boundary, masking water area, calculating NDVI, selecting thresholds and conducting discriminant analysis to get quasi-real-time distribution data of floating macroalgae in the Yellow Sea. Zonal statistics was then performed to convert the distribution raster layer into a vector point layer, with a resolution of 1 km, as the input dataset for the 4DVar model to forecast floating macroalgal trajectories.

2. Forecasting of floating macroalgal trajectories based on the 4DVar data assimilation model

To improve the simulation of nearshore region at mesoscale and sub-mesoscale, the Regional Ocean Modeling System (ROMS) 4DVar assimilation method was used to assimilate sea surface temperature, sea surface height and measurements from ARGO and OMORN to obtain the optimal initial field. HYCOM data were used as the boundary condition and GFS data as the forcing



↑ Figure 6-1. Quasi-real-time prediction of floating macroalgal trajectories based on RS data and a 4DVar data assimilation model

field. The model initial field was combined with the prediction field provided by HYCOM and GFS and then tidal forcing was added to give a forecast for the next 6.5 days. The flow chart is shown in Figure 6-1. The distribution of algae blooms retrieved through RS inversion was added to the model as floats and then the drift trajectory of macroalgal blooms was given with continuous integration of the model. Factors such as natural growth, mortality and manual collection of macroalgal blooms were not considered in the model.

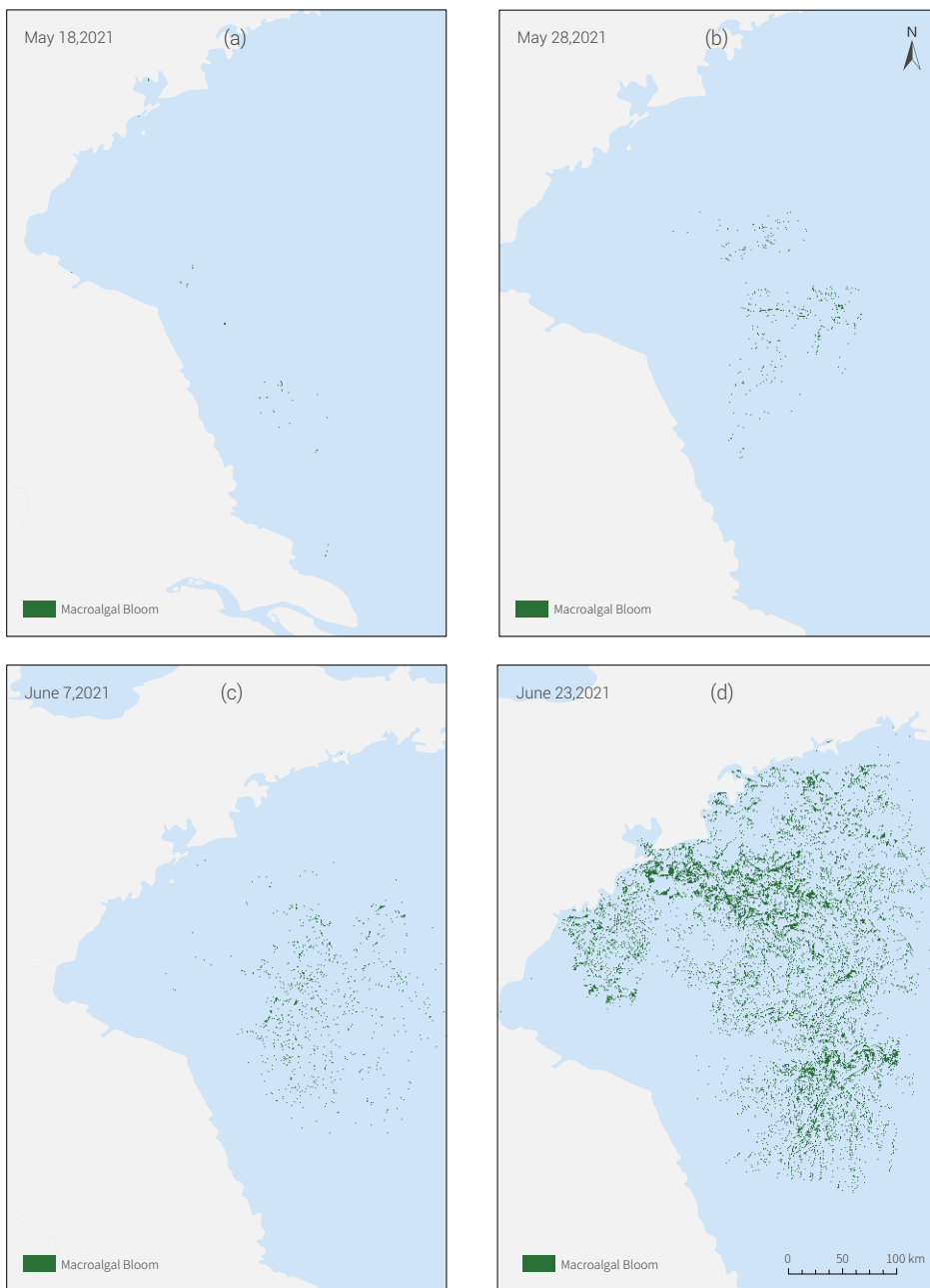
Results and analysis

By extracting information from the distribution updates of floating macroalgae in the Yellow Sea on the CASEarth platform, researchers established datasets on green tide distribution from May to June 2021. Data on May 18, May 28, June 7, and June 23, when there was relatively low cloud cover, were displayed in Figure 6-2.

On 18 May 2021, floating macroalgae was detected through RS in areas near Subei Shoal for the first time. The macroalgal bloom expanded rapidly in the next 10 days, and the affected area increased by about 30 times by 28 May. On 7 June, a small proportion of floating green algae already arrived at the coast of

Rizhao and Qingdao on the Shandong Peninsula. By 23 June, the total affected area had reached 2,500 km².

The distribution data of floating macroalgae retrieved from RS products were used as the inputs to forecast macroalgal trajectories. With continuous integration on the basis of the 4DVar model, the projected distribution of floating macroalgae was largely aligned with the actual trajectory from RS. The monitoring results and simulation predictions were both submitted to the relevant government agencies as an information and technical support for the prevention and treatment of green tides in 2021.



↑ Figure 6-2. Distribution of macroalgal blooms in the Yellow Sea derived from remote sensing data in 2021
 (a) May 18; (b) May 28; (c) June 7; (d) June 23

Outlook

The study constructed a monitoring and forecasting system including a quasi-real-time method to extract relevant data from the CASEarth platform and a prediction method for drift trajectories based on 4DVar data assimilation model. The system was applied and tested in monitoring and forecasting green tide outbreaks in the Yellow Sea from May to July 2021 and may support early warning and decision-making in coastal cities.

The distribution of macroalgal blooms, as well as its relationship with aquaculture rafts, water temperature, salinity and other environmental factors in the Yellow Sea, will be further explored. An improved prediction method based on the 4DVar model plus the biomass growth data will provide full-fledged and efficient decision support for the monitoring and prediction of macroalgal blooms in coastal cities.

Changes of mangrove forests in China

Target: 14.2 By 2020, sustainably manage and protect marine and coastal ecosystems to avoid significant adverse impacts, including by strengthening their resilience, and take action for their restoration in order to achieve healthy and productive oceans.

Highlights

- *A method for rapid extraction of mangrove forests from remote sensing images was developed on the basis of machine learning and the spatial distribution and features of changes in 2015, 2018 and 2020 were analyzed. It was found that from 2015 to 2020, the area of mangrove forests in China increased by 16% and the increases were mainly along Guangdong and Guangxi coasts. Mangrove forests inside nature reserves had been well protected and restored. China has made remarkable achievements in mangrove conservation and restoration since the start of implementation of SDGs.*

Background

Mangroves form wetland woody plant communities in tropical and subtropical intertidal zones and mouth of rivers and are among the most productive ecosystems on the planet (Jia *et al.*, 2021). Owing to their intermediate position between the terrestrial and marine environments, mangroves play a vital role in maintaining littoral ecological stability and promoting the energy cycle between land and ocean. They have thus been identified as important targets of global wetland and biodiversity protection. Due to destruction of mangroves, coastal residents and animals have no habitat to breed and live. Thus, mangrove

restoration, conservation and sustainable management is critical to SDG 14.2.

In this study, an object-oriented method and random forest classifier were used in combination with expert knowledge to construct the first 10 m resolution datasets of mangrove forest distributions in 2015, 2018, and 2020 in China. Then the spatiotemporal changes of mangroves were analyzed. The study offered reliable research methods and data products to support the evaluation of SDG 14.2 and inform the restoration and conservation mangroves and even coastal ecosystems in China.

Data used

- © Multi-temporal Sentinel-2 images covering mangrove regions in China in 2015, 2018, and 2020.
- © Digital Elevation Model, administrative division vector data,

1:1,000,000 vegetation type map, coastline vector data.

- © Field samples, governmental statistics and monitoring data.

Method

An object-oriented method and random forest classifier were used in combination with manual modification to classify mangroves in China. The 2015 coastline plus buffer zones of 2 km seaward and 5 km landward was identified as the area of interest and images were selected accordingly. Then remote sensing images acquired in seasons when mangroves are

easily distinguishable from other vegetations were taken as the classification data source. These images were put to multi-scale segmentation and random forest classification to identify mangroves. The classification results were validated against massive field survey samples. More specifically, images from not-so-rainy seasons, with low tide and withered *Spartina*

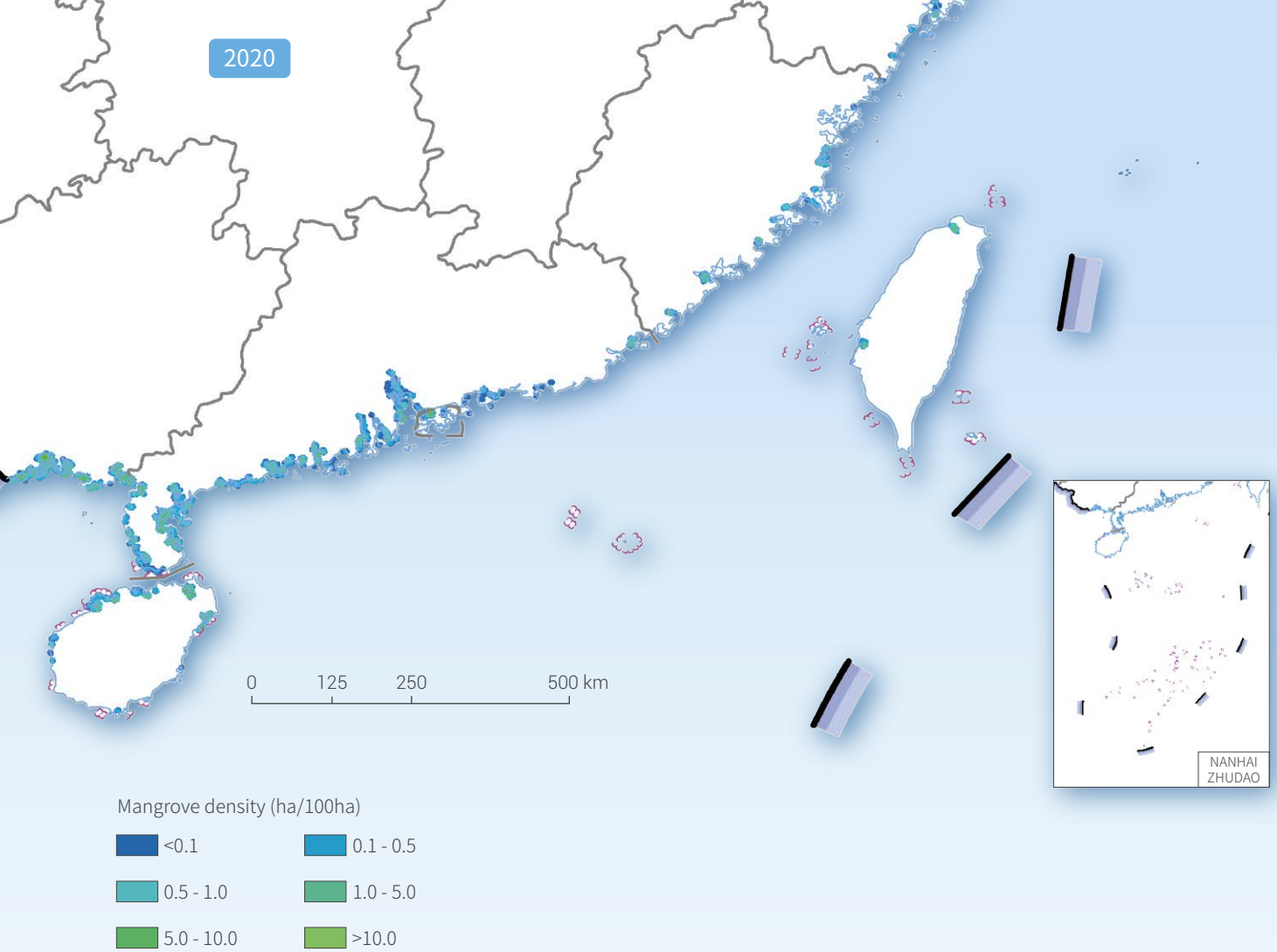


Figure 6-3.

● Spatial distribution of mangrove forests in China

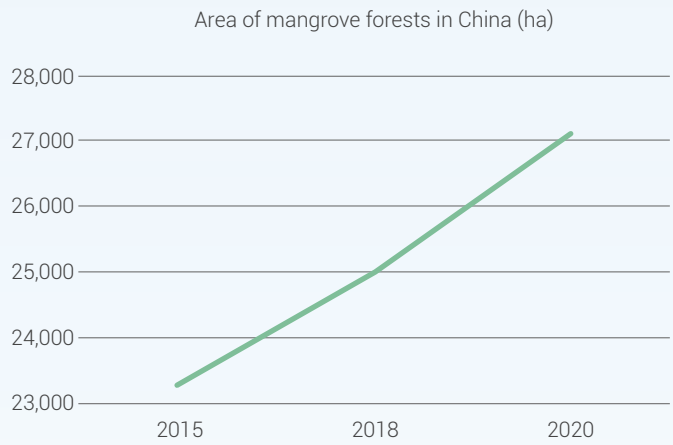
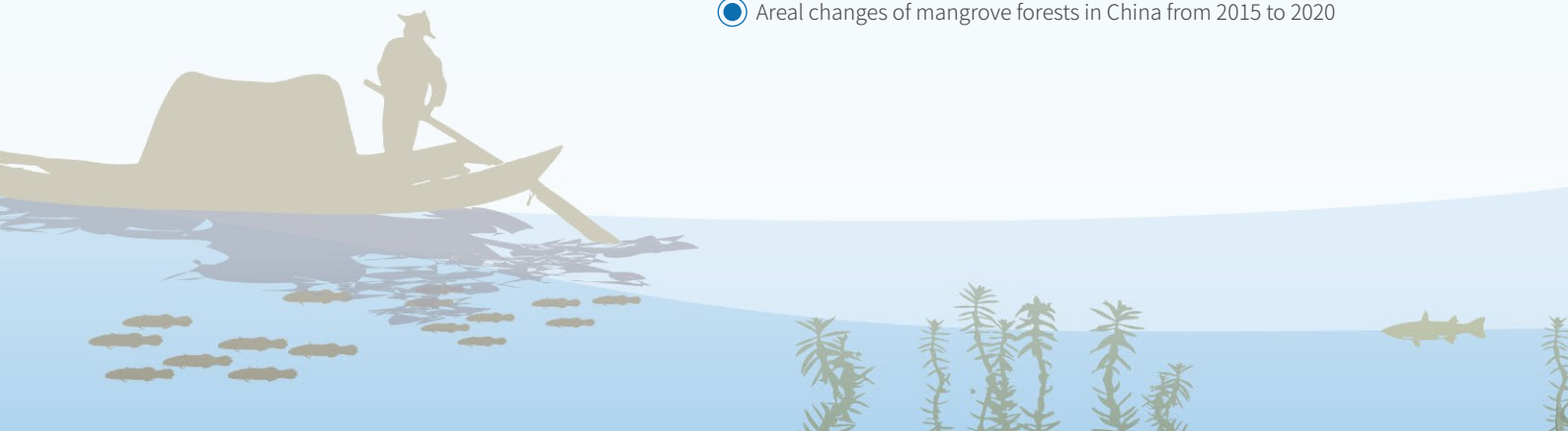
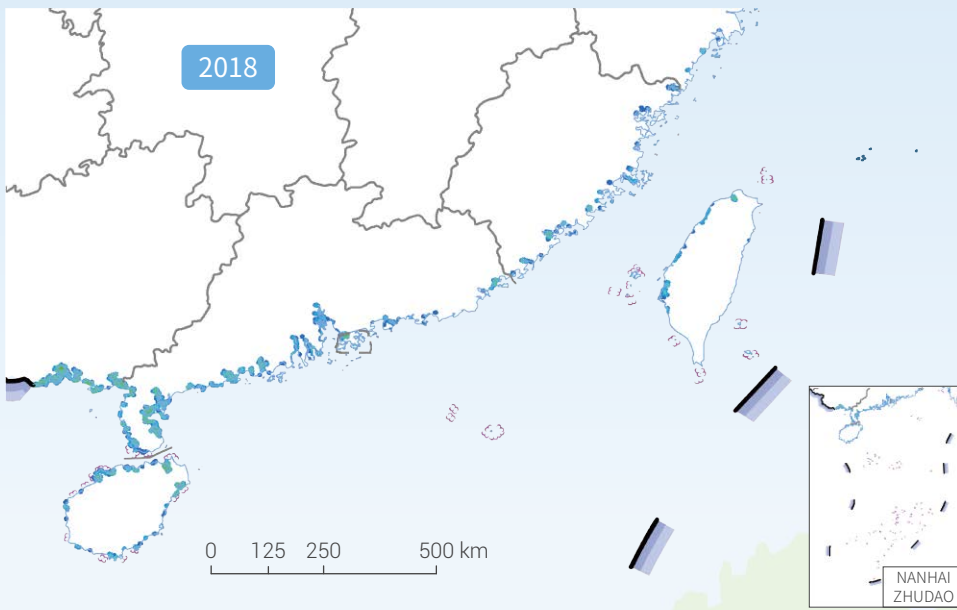
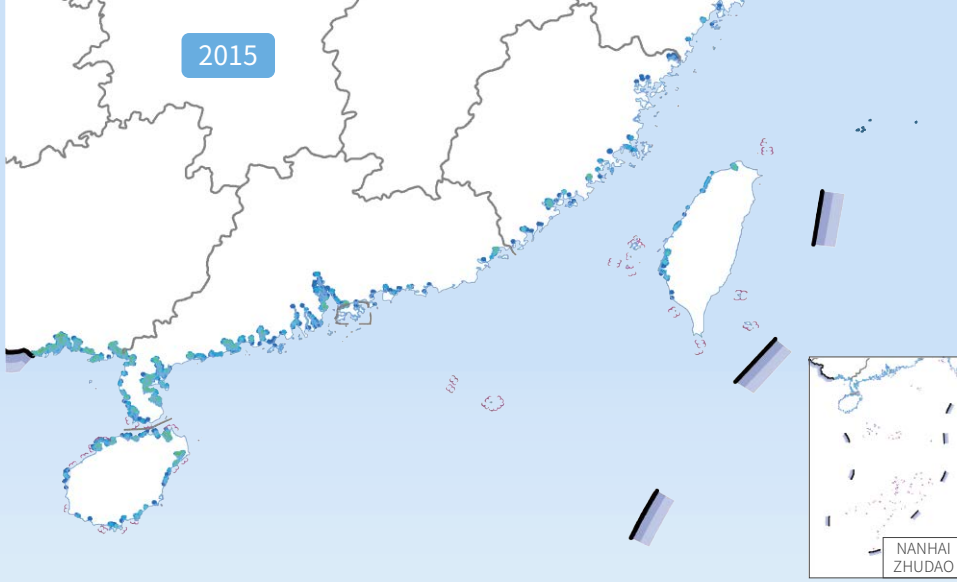


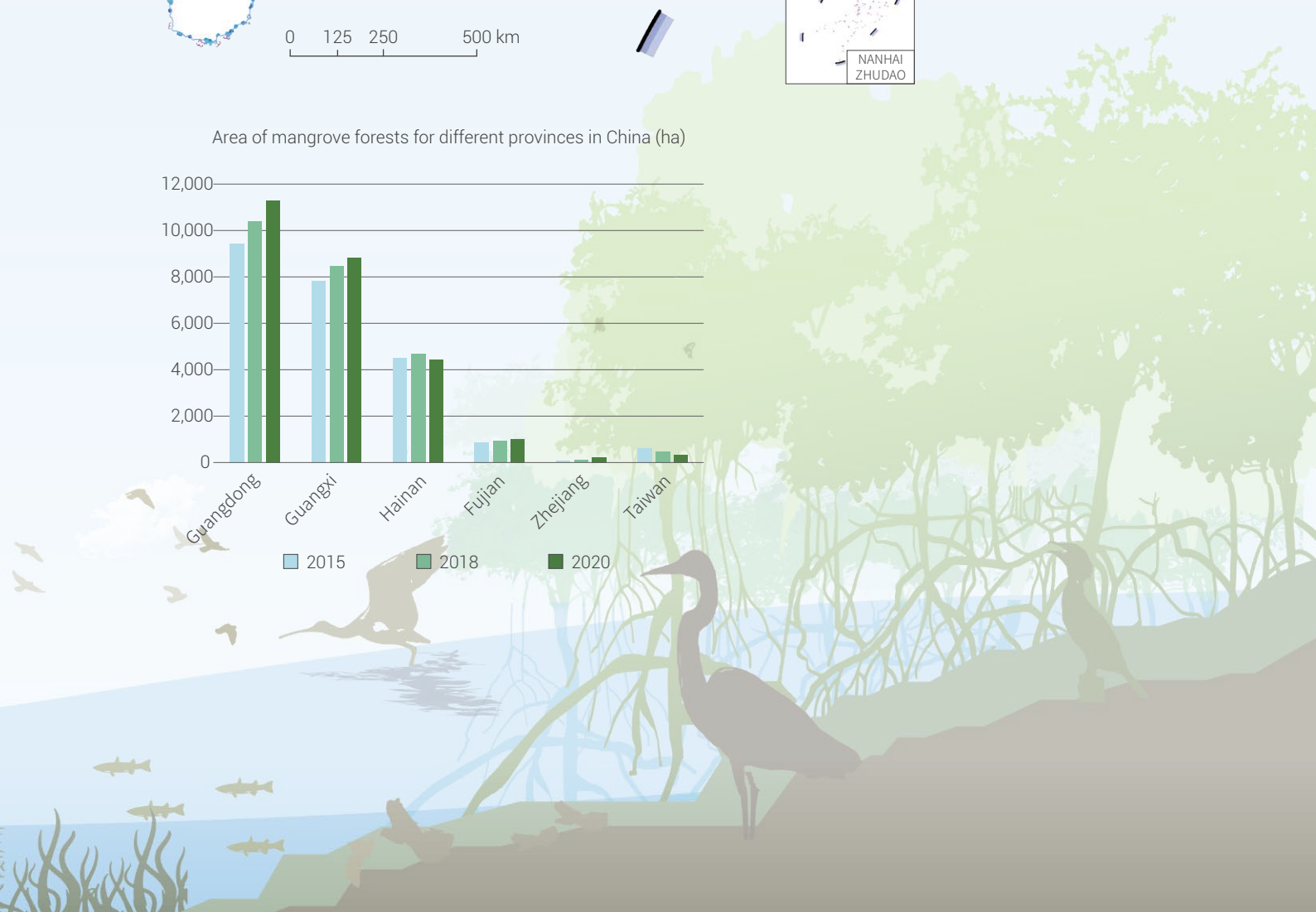
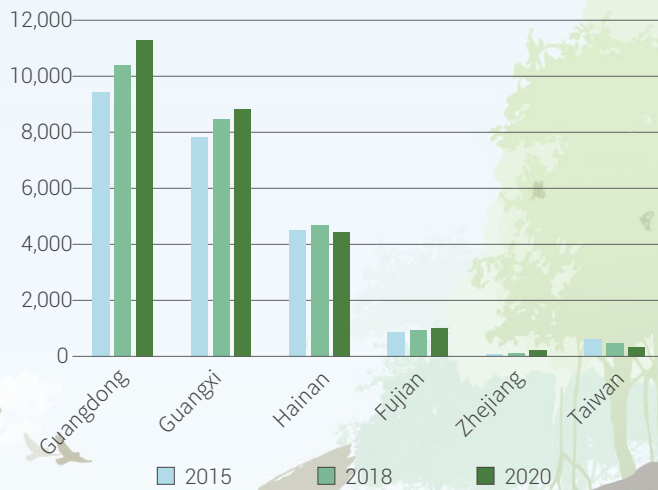
Figure 6-4.

● Areal changes of mangrove forests in China from 2015 to 2020





Area of mangrove forests for different provinces in China (ha)



alterniflora and without clouds, were selected; field survey sites in 2015 (40 mangrove forests, 127 other forests), 2018 (60 mangroves, 226 others) and 2020 (60 mangroves, 331 others) were selected as samples for random classification; and 14 spectral features and 5 texture parameters were used in classification trainings.

In the end, mangrove distribution datasets for years 2015, 2018 and 2020 were obtained. Upon validation against over 5000 field samples, the classification accuracy of the mangrove forest datasets for the three years were 92%, 95% and 96% respectively.

Results and analysis

1. Spatial distribution changes

Spatial distributions of mangrove forests in China are shown in Figure 6-3. Mangrove forests along the coasts of Guangdong, Guangxi and Hainan are relatively dense. Fuding County (27°20'N), Fujian Province, is the northern boundary of natural mangrove forests, and Lujiazhi Island (29°32'N) at Zhoushan, Zhejiang Province is the northern boundary of planted mangroves. From 2015 to 2020, mangroves increased visibly, primarily along the coasts of Guangxi, Yangjiang (Guangdong), and local coasts of Zhejiang; losses mainly happened in Leizhou Peninsula (Guangdong), Qinzhou (Guangxi) and Northwest coasts of Hainan.

2. Areal changes

The areas of mangrove forests in the relevant provinces and their changes are shown in Figure 6-4. Guangdong has the largest area of mangroves, followed by Guangxi and Hainan. These three provinces accounted for 94% in the national total area of mangroves in 2020. From 2015 to 2020, the net increase of mangrove forests was 16%. Mangrove forests in Guangdong and Guangxi increased significantly, and those in Zhejiang and Fujian increased slightly, while those in Hainan increased first and then decreased and those in Taiwan showed a downward trend.

Outlook

This study combined object-oriented method and random forest classifier to establish accurate datasets of China's mangrove forests in 2015, 2018, and 2020. The rapid and accurate classification method could be used to track the implementation of mangrove-related SDGs for a long period time, and it is also applicable to other studies. The datasets produced in this study are relevant to evaluate SDG 14.2. Future updates will be useful for further evaluation of SDG targets.

The findings of this study include the following. First, since

2015, the area of mangrove forests in China had increased markedly, which was a great contribution to global mangrove protection and restoration. Second, from 2015 to 2020, new mangroves grew mainly along the coasts of Guangxi and Guangdong. Results of the study are useful to support SDG 14.2 evaluation and inform mangrove ecosystem conservation and science-based management. They could also be used in support of decision-making and evaluation related to SDG 6.6, 13.1, 14.5, 15.2, 15.5, 15.8 and 15.9.

Changes of coastal aquaculture ponds in China

Target: 14.2 By 2020, sustainably manage and protect marine and coastal ecosystems to avoid significant adverse impacts, including by strengthening their resilience, and take action for their restoration in order to achieve healthy and productive oceans.

Highlights

- *In this study, by applying the Big Earth Data cloud service platform, a hybrid object-based and hierarchical classification approach was developed to accurately and rapidly delineate the distribution of coastal aquaculture ponds in China.*
- *The spatial patterns and temporal changes of coastal aquaculture ponds in China between 2015 and 2020 were examined. Results revealed clear spatiotemporal heterogeneity in the period of interest. Given the background of Restoring Aquaculture Pond to Natural Wetland policy, the total area of aquaculture ponds consistently declined, especially in Zhejiang province.*

Background

Since the beginning of reform and opening-up, aquaculture has developed rapidly in China. Rapid expansion of coastal aquaculture ponds has strongly supported the rapid socio-economic development of coastal areas, but also caused the loss of natural coastal wetlands, thus exerting a major impact on the habitats of water birds (Ren *et al.*, 2019). Accurate monitoring of the spatiotemporal dynamics of coastal aquaculture ponds in China is of great scientific and practical significance to support the sustainable management of coastal ecosystems. However, China, the largest and most populous developing country in the world, still lacks accurate datasets on the spatial distribution of coastal aquaculture ponds at national scale. Especially in the context of strengthened coastal ecological protection, evaluation of the spatiotemporal changes of coastal aquaculture ponds since

2015 is still lacking.

The research team developed a Hybrid Object-based and Hierarchical Classification approach (HOHC) to establish datasets characterizing the spatial distribution of coastal aquaculture ponds in China (10 m spatial resolution). The spatiotemporal heterogeneity of changes from 2015 to 2018 and 2020 was analyzed. The study has resulted in a reliable and scalable research method for SDG 14.2. The relevant data products are directly usable in the evaluation of SDG 14.2, may inform the evaluation of SDG 2, 13 and 15 (food safety, greenhouse gas emissions and alternative habitat respectively), and support the formulation of coastal wetland ecosystem conservation and restoration strategies in China.

Data used

© Sentinel-2 satellite images (10 m resolution) in 2015/2016, 2018 and 2020.
© Digital elevation model data, vector data of administrative divisions, global water distribution products (2015, 2018 and

2020), and Chinese coastlines data.

© Field survey samples, industrial statistics and monitoring data.

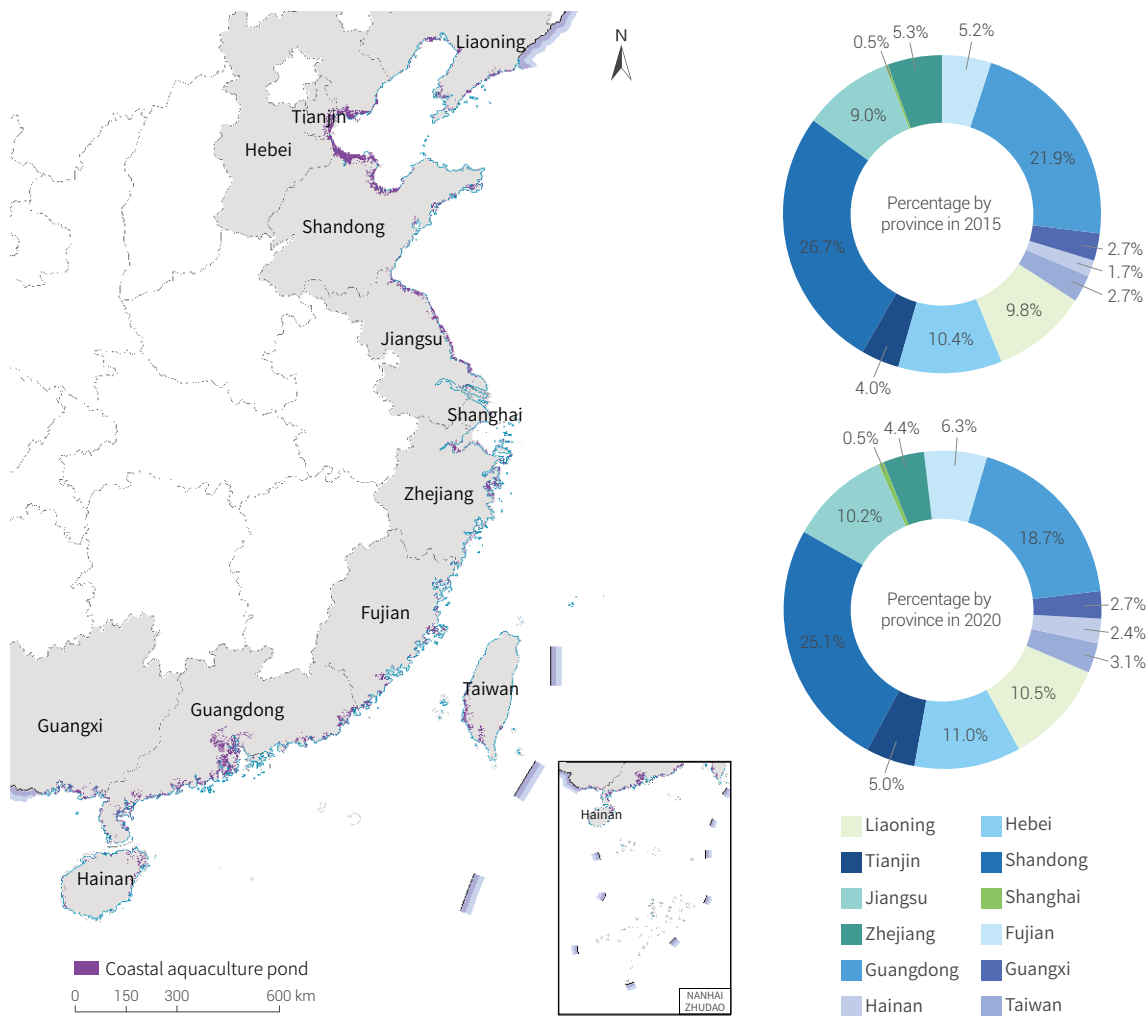
Method

It is difficult to distinguish a coastal aquaculture pond from other water bodies in spectrum and therefore hard to rapidly and accurately extract the relevant information by way of machine learning. But coastal aquaculture ponds do have obvious geometric features and geographical location features (Mao *et al.*, 2020). In this case, HOHC was developed to extract the distribution information of coastal aquaculture ponds with 10 m spatial resolution at national scale of China with high precision.

The following steps were taken: (1) Grid analysis of the study area: areas of interest were delimited on the basis of coastline data and DEM data and historical waterbody datasets were then applied to identify the grids that potentially contained coastal aquaculture ponds; (2) Sentinel-2 satellite image data screening and processing: images with low cloud cover and the most abundant water information and obtained in the past year were selected as the primary image data source; (3) Construction of feature vectors library for extracting aquaculture ponds: Normalized Difference Water Index (NDWI), Normalized

Difference Vegetation Index (NDVI), Normalized Difference Building Index (NDBI) and other normalized indices were calculated to support the extraction of potential coastal aquaculture ponds; (4) Image segmentation based on K-means algorithm: images containing potential coastal aquaculture ponds were segmented; (5) Distribution information extraction based on hierarchical decision trees: accurate extraction was further completed, using the shape index; (6) Data integration and accuracy evaluation of classification results: the classification results of coastal aquaculture ponds in each grid were merged and their accuracy was evaluated against field survey samples.

Through the afore-mentioned steps, the spatial distribution datasets of China's coastal aquaculture ponds with 10 m spatial resolution were completed for 2015, 2018 and 2020. Upon validation against more than 6,000 field survey samples, the overall classification accuracy for the three datasets was above 95%.

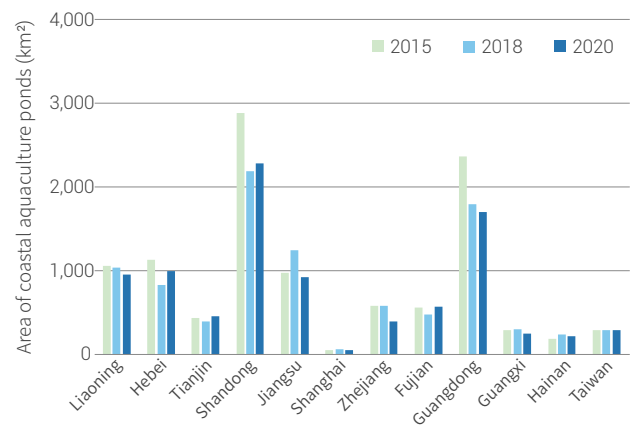


↑ Figure 6-5. Spatial pattern of coastal aquaculture ponds in China (2020)

Results and analysis

Figure 6-5 shows the spatial distribution of coastal aquaculture ponds in China, mainly in Shandong, Guangdong, Hebei, Jiangsu and Liaoning. The five provinces account for 75.5% of the total area of coastal aquaculture ponds in China. Shandong province had the largest area of coastal aquaculture ponds.

From 2015 to 2020, coastal aquaculture ponds decreased consistently in China, with a relative decline of 15.9%. The loss between 2015 and 2018 was 12.5% and that between 2018 and 2020 was 3.7%. During the five years, coastal aquaculture ponds increased in Tianjin, Fujian, and Hainan, especially Hainan province (Fig. 6-6).



↑ Figure 6-6. Areal changes in coastal aquaculture ponds among various provinces (2015, 2018 and 2020)

Outlook

In terms of methodology and data, this study developed the HOHC supported by Big Earth Data and cloud computing and achieved accurate and rapid extraction of coastal aquaculture ponds in 2015, 2018 and 2020 from satellite images. The generated data are useful to support SDG 14.2 evaluation for China and inform the evaluation of SDG 6.6, 13.1 and 15.5. The method developed in this study is potentially scalable to monitor spatiotemporal changes of coastal aquaculture ponds at a global scale, thus supporting the sustainable management of global aquaculture.

In terms of decision support, this study revealed that the area of coastal aquaculture ponds in China had consistently declined since the SDG baseline year (2015). On the one hand, some ponds were converted into natural wetlands driven by the policy of Returning Aquaculture Ponds to Natural Wetlands (Mao *et al.*, 2019). On the other hand, the expansion of built-up lands due to urbanization and industrialization destroyed many coastal aquaculture ponds (Mao *et al.*, 2018). The findings in this research are beneficial to not only SDG 14 evaluation but also the conservation of coastal ecosystems and migratory water birds diversity.



Summary

This chapter focuses on the protection of marine ecosystems. Through the Big Earth Data method, we carried out research on the progress of the implementation of marine sustainable development goals in typical regions of China and generated data sets of spatial distribution of mangroves in China (2015, 2018, 2020, at 10 m resolution), spatial distribution of coastal aquaculture ponds in China (2015, 2018, 2020, at 10 m resolution) and other data products.

The studies led to the following findings: China has made remarkable progress in mangrove protection and restoration. Between 2015 and 2020, the area of mangroves increased by 16%, which was an important contribution to global mangrove protection and restoration. Driven by policy to return aquaculture ponds to wetlands, these ponds have continuously decreased, effectively facilitating the restoration of coastal ecosystems. Through the Big Earth Data cloud platform, the spatial distribution of macroalgal blooms was extracted from

remote sensing images and the real-time prediction of the drift trajectories of macroalgal blooms was made possible with the four-dimensional variational assimilation forecast model, thus providing effective information support for the monitoring and early warning of harmful algal bloom disasters in coastal areas.

The three cases reported exemplify the potential of monitoring and evaluating the implementation of the national and global marine sustainable development goals based on Big Earth Data. To follow up, uses of Big Earth Data, artificial intelligence and other technologies will be further pursued in the monitoring and evaluation of SDG 14 indicators. More useful and applicable data products will be produced to support the realization of marine sustainable development goals. It is hoped that the relevant researches will be extended from Chinese offshore waters to more distant waters with a view to developing a more complete system of monitoring and evaluation data, technologies and methods for sustainable development.



Aerial image of the Yellow River Estuary (ADS80, November 2019)



SDG 15



SDG 15

Life on Land

Background	112
Main Contributions	113
Case Study	114
Summary	128



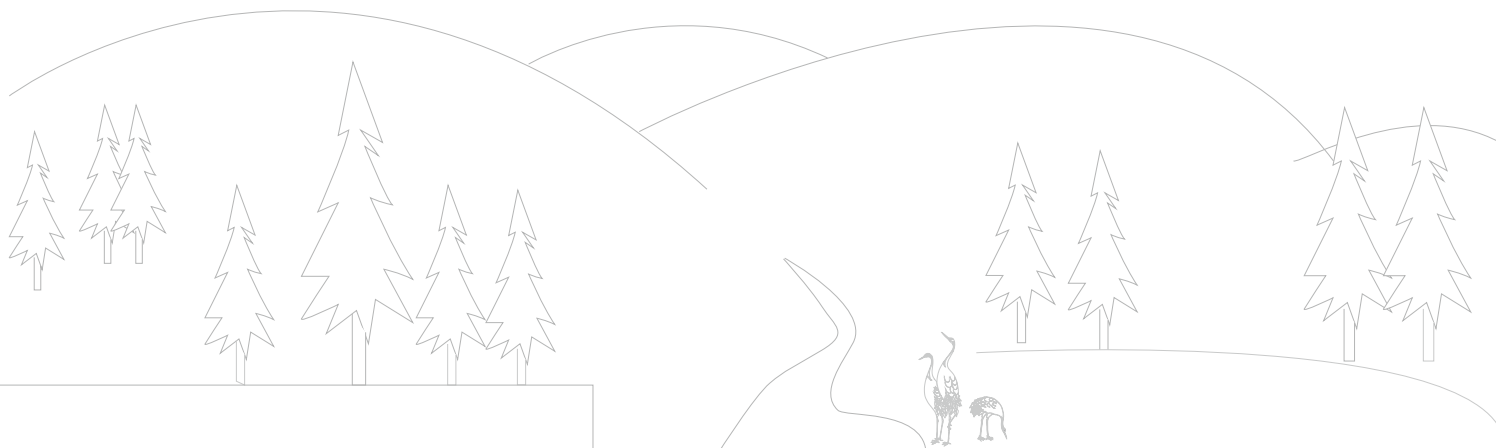
Background

SDG 15 is to "protect, restore and promote sustainable use of terrestrial ecosystems, sustainably manage forests, combat desertification, and halt and reverse land degradation and halt biodiversity loss". The 2030 Agenda for Sustainable Development has been adopted for 6 years, yet mankind still faces a stern situation. Global forest area (SDG 15.1.1) is steadily declining (FAO, 2020c). About 75% of the global land surface is degraded (SDG 15.3.1) (IPBES, 2018). Despite continued increase of the proportion of key biodiversity areas covered by protected areas (SDG 15.1.2, SDG 15.4.1), the Red List Index (SDG 15.5.1) continues to decrease (UNEP, 2021). At the current speed of progress, the world is not on track to achieve SDG 15 in 2030 (UN, 2019).

Evaluation of progress is the key to understand where we are now, identify gaps and adopt effective interventions. With increased data availability and technical methods, 8 of the 14 SDG 15 indicators are at Tier I status (with both data and methodology). However, these indicators are mainly obtained on the basis of statistical methods, which are not scalable

across different scales (global-regional-national-local), and many countries with limited data acquisition capabilities cannot provide data on a regular basis. Therefore, it is necessary to use cutting-edge technologies, such as Earth observation, artificial intelligence and citizen science, to further carry out multi-scale spatial monitoring and evaluation of indicators and contribute data, methods, tools and policy recommendations in support of SDG 15.

This report presents 5 case studies on the establishment of a large-scale ecosystem quality and dynamics assessment system, identification of gaps in species-level important grassland ecosystem protection, refined spatial distribution simulation of important endangered plants, dynamic monitoring of global Mountain Green Cover Index (MGCI), and evaluation of habitat area and quality of important species. Big Earth Data were used to identify critical data and method gaps with a view to providing data products, models, methods and decision support for UN agencies and related countries in the monitoring and evaluation of SDG 15 indicators.





Main Contributions

For three different scales (global, China and typical regions), dynamic and quantitative monitoring and evaluation of SDG 15 multiple indicators with fine spatial granularity were realized to facilitate SDG 15 with data products, methodology and decision support. For SDG 15.1, a national-scale ecosystem quality and dynamics assessment system was constructed, the current status of and gaps in the protection of grassland ecosystems in China were identified. For SDG 15.1.2 and SDG

15.4.1, a breakthrough in the precision simulation of the spatial distribution of endangered species was realized. For SDG 15.4.2, high-resolution MGCI data sets were produced for 2015 and 2020. For SDG 15.5, spatiotemporal dynamic monitoring of the habitat of wintering white cranes was carried out, which provided important support for the effective protection of the habitats of precious species (Table 7-1).

Table 7-1 Cases and Their Main Contributions

Indicator	Tier	Case	Contributions
15.1 By 2020, ensure the conservation, restoration and sustainable use of terrestrial and inland freshwater ecosystems and their services, in particular forests, wetlands, mountains and drylands, in line with obligations under international agreements	/	Changes in ecosystems and their quality in China	Data product: Ecosystem quality data sets for 2000 and 2015 Decision support: The effectiveness of ecological protection and restoration in the context of large-scale efforts was revealed to inform ecosystem conservation in China
		Current status of and gaps in grassland ecosystem conservation in China	Data product: Important grassland ecosystems directory and spatial distribution data sets Decision support: Gaps in grassland conservation were identified to inform future protection measures
15.1.2 Proportion of important sites for terrestrial and freshwater biodiversity that are covered by protected areas, by ecosystem type 15.4.1 Coverage by protected areas of important sites for mountain biodiversity	Tier I	Big data simulation to generate high-resolution distribution of rare and endangered plants	Method: Big data simulation model of rare and endangered plants distribution
15.4.2 Mountain Green Cover Index	Tier I	High-resolution monitoring of global mountain green cover index	Data product: Global MGCI data sets for 2015 and 2020
15.5 Take urgent and significant action to reduce the degradation of natural habitats, halt the loss of biodiversity and, by 2020, protect and prevent the extinction of threatened species	/	Monitoring spatiotemporal variations of wintering Siberian crane habitats	Data products: Data sets of crane habitat distribution in Poyang Lake wetland from 1993 to 2018



Case Study

Changes in ecosystems and their quality in China

Target: 15.1 By 2020, ensure the conservation, restoration and sustainable use of terrestrial and inland freshwater ecosystems and their services, in particular forests, wetlands, mountains and drylands, in line with obligations under international agreements.

Highlights

- *The study was the first-ever evaluation of the changes in ecosystem quality at the national scale and revealed the effectiveness of ecological protection and restoration in the context of large-scale efforts in China.*
- *From 2000 to 2015, a total of 51,668 km² of artificial ecosystems were restored to natural ecosystems. Ecosystem quality improved significantly and the integrated ecosystem quality index increased by 21% approximately year-on-year.*

Background

The natural environment in China is fragile. The huge population, high-speed urbanization and intensive resource development exert tremendous pressure on the ecosystems and ecosystem degradation is serious. Since 2000, China has implemented massive ecological protection and restoration programmes, such as the Grain for Green Programme (conversion of cropland to forest and wetland, and of grazing land to

grassland) and the Natural Forest Protection Project. It is necessary to comprehensively assess the corresponding changes of ecosystems and their quality. In this connection, the research team assessed the dynamics of Chinese ecosystems and their quality from 2000 to 2015 with a view to inform the relevant policy reviews.

Data used

© National ecosystem classification data (30 m, 2000 to 2015) from national ecosystem surveys.

© Remote sensing inversion products (aboveground biomass, vegetation coverage etc.) (250 m, 2000-2015) from national ecological surveys.

Method

The evaluation method drew references from the relevant technical methods used in the national ecological survey (Ouyang *et al.*, 2017). First, the area of ecosystem restoration was estimated by calculating the area of artificial ecosystems (cropland and built-up areas) converted into natural ecosystems (forests, shrubs, grasslands and wetlands). Then biomass and vegetation coverage indicators were used to evaluate the quality of ecosystems. An Ecosystem Quality Index (EQI) was

constructed based on the areas of ecosystems of different quality levels.

The calculation method of the Ecosystem Quality Index was as follows:

$$EQI_i = \frac{\sum_{j=1}^5 (EA_{ij} \times j)}{(EA_i \times 5)}$$

$$EQI = \frac{\sum_{j=1}^5 (EA_j \times j)}{(EA \times 5)}$$

Where EQI_i was the Ecosystem Quality Index of the i^{th} ecosystem, EA_{ij} was the area of the i^{th} ecosystem with the j^{th} quality level and EA_i was the total area of the i^{th} ecosystem; and the national integrated index EQI was calculated after adding

up the areas of all types of ecosystems, where EA_j was the total area of the j^{th} quality level and EA was the total area of all ecosystems.

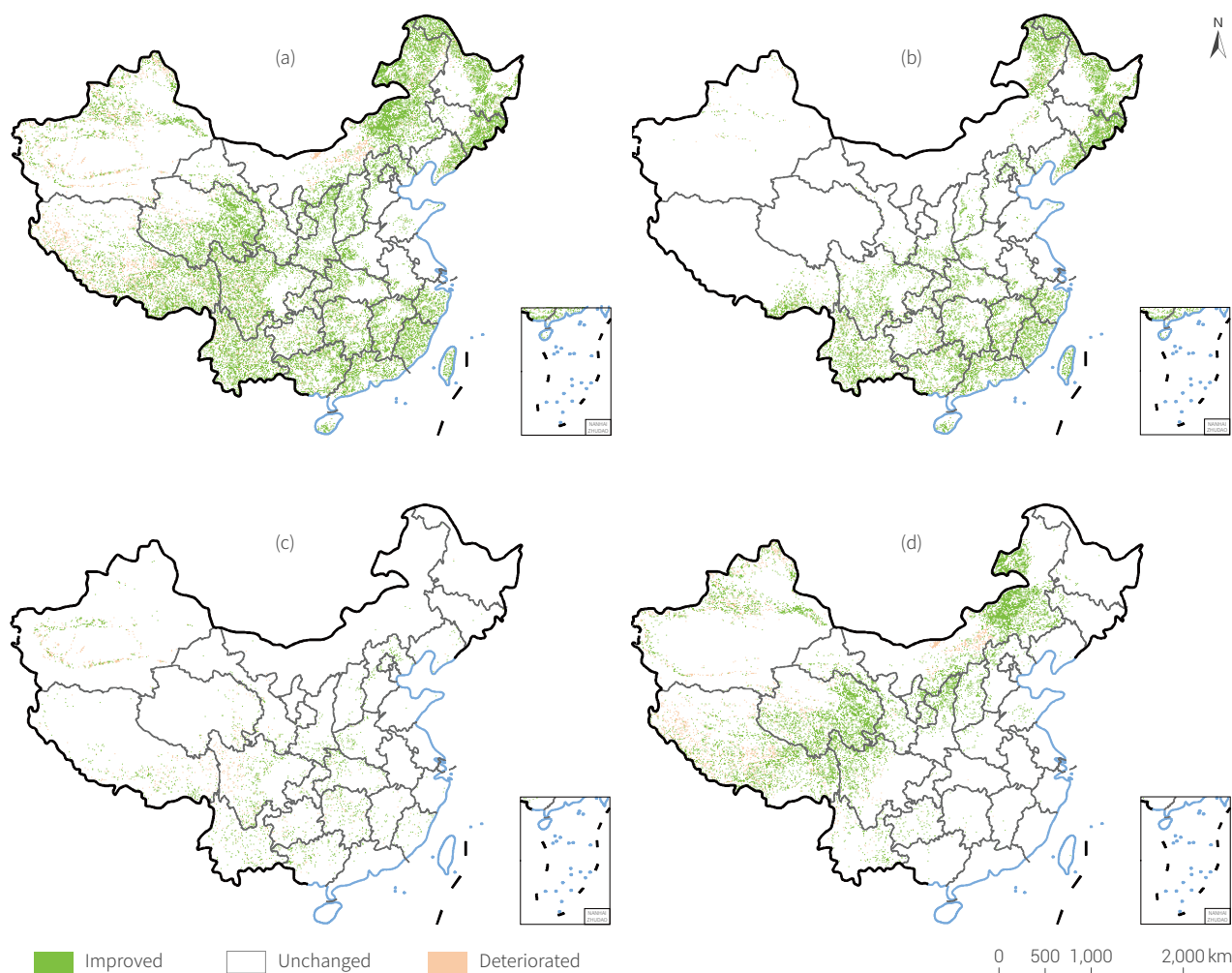
Results and analysis

From 2000 to 2015, thanks to the protection programmes and other conservation and restoration programs, ecosystems recovered extensively. A total of 51,668 km² of artificial ecosystems were turned into natural ecosystems as: forests and shrubs: 26,546 km², accounting for 52% approximately; grasslands: 20,853 km², accounting for 40% approximately; and wetlands: 4,269 km², accounting for 8% approximately.

In the same period, the overall quality of forest, shrub and grassland ecosystems in China improved significantly. The spatial distribution of changes in the quality of terrestrial

ecosystems across the country is shown in Figure 7-1. The area of excellent and good ecosystems increased by 88% approximately, from 0.7239 to 1.3587 million km², and the area of poor and low-quality ecosystems decreased by 24% approximately, from 3.8065 to 2.8783 million km². Low-quality ecosystems are mainly at the Loess Plateau, the Sanjiangyuan, Daxinganling Mountains, Changbai Mountains, Taihang Mountains, Nanling Mountains, Hengduan Mountains, Qinling Mountains, etc.

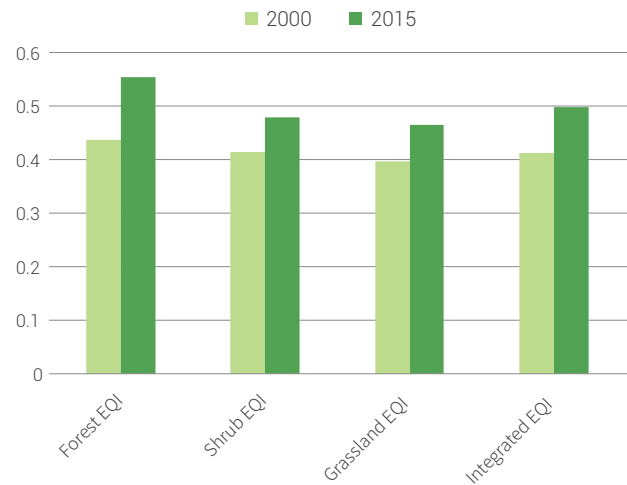
From 2000 to 2015, the national EQI increased from 0.413 to



↑ Figure 7-1. Ecosystem quality changes in China from 2000 to 2015
 (a) Change of ecosystem quality; (b) Change of shrub ecosystem quality; (c) Change of forest ecosystem quality;
 (d) Change of grassland ecosystem quality

0.499, up 21% approximately. The forest EQI increased from 0.437 to 0.555, up 27% approximately, the grassland EQI increased from 0.397 to 0.465, up 17% approximately, and the shrub EQI increased from 0.414 to 0.478, up 15% approximately.

The overall improvement in terms of ecological restoration area and ecosystem quality were a remarkable result of massive ecological protection and restoration efforts in China since 2000. The areas of forests, grasslands and other ecosystems in key protected and restored areas across the country increased greatly. The overall low quality of ecosystems had begun to significantly improve, especially for forest ecosystems, the total area and quality of which increased the most. The forest EQI also grew faster than the national integrated EQI.



↑ Figure7-2. EQIs from 2000 to 2015

Outlook

In this study, researchers assessed the overall changes in ecosystems and their quality from 2000 to 2015 and proposed an ecosystem quality index to comprehensively reflect the general trend of improving ecosystem quality in China. Results showed extensive natural ecosystem restoration, significant quality

improvement and remarkable results from interventions since 2000. However, ecosystem degradation in the form of quality deterioration still existed in some areas. China needs to take further measures to curb degradation.

Current status of and gaps in grassland ecosystem conservation in China

Target: 15.1 By 2020, ensure the conservation, restoration and sustainable use of terrestrial and inland freshwater ecosystems and their services, in particular forests, wetlands, mountains and drylands, in line with obligations under international agreements.

Highlights

- *With the help of data interpreted from remote sensing imagery and vegetation map, high-precision grassland classification map was obtained. A directory of important grassland ecosystems and their spatial distribution in China was developed.*
- *The existing protected areas in China covered all 21 types of grassland ecosystems for priority conservation. Good overall conservation effect had been achieved for those. However, the proportions of protection for five types of grasslands remained low and conservation efforts were still absent in certain parts of eastern Inner Mongolia and eastern Qinghai-Tibet Plateau.*

Background

The proportion of critical sites for terrestrial and freshwater biodiversity covered by protected areas (SDG 15.1.2) is an important indicator for the effectiveness of ecosystem conservation. In this regard, the types and spatial distribution of important ecosystems are key measures to assessing the effect of protected areas. However, there is still not an effective way to identify important ecosystem types and key protected areas. In addition, currently, protected areas account for more than 18% of

the country's total land area, but it is still unclear whether their spatial distribution is reasonable and how much they contribute to natural ecosystems conservation. Taking grassland ecosystem as its main object, this study proposed a method to identify important ecosystem types and key areas for conservation, which can provide scientific support to assess the effectiveness of protected areas and optimize the spatial distribution of these areas.

Data used

© Land cover data obtained from interpreting the HJ-1 A/B data and Landsat OLI data (at 30-m resolution), as well as biomass and vegetation coverage data.

© Vegetation Map of China (1:1 000 000) and its updates (2001, 2020).

© Data on the distribution of protected areas in China in 2020.

Method

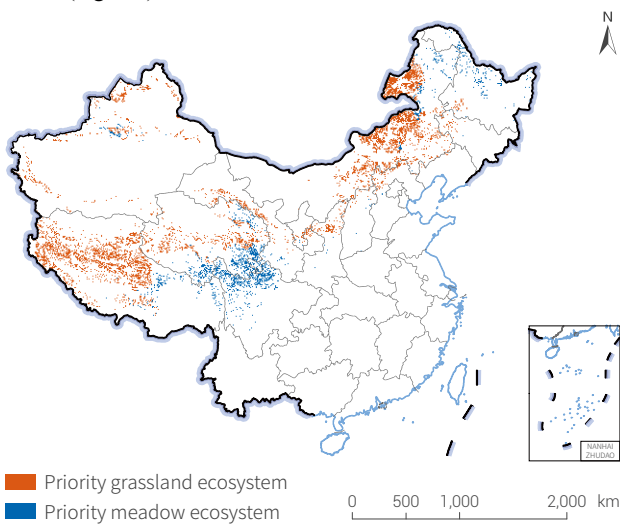
First, a directory of grassland ecosystems in China was developed on the basis of *the Vegetation Map of China* (1:1 000 000) and its updates. The criteria of ecosystems requiring prioritized conservation were set up, i.e., the dominant ecosystem type; the special climatic-geographical and soil characteristics as reflected in the ecosystem; and its sole existence in China. A directory of grassland ecosystems in need of priority conservation was developed on the basis of the afore-mentioned criteria and expert opinions. Second, based on

grassland classification data interpreted from the *Vegetation Map of China* (1:1 000 000), the HJ-1 A/B (30 m resolution) data and the Landsat OLI data, distribution map of important grassland ecosystems and key areas for conservation was developed and calibrated against field survey data and published literature. And last, the distribution map was overlaid with the map of existing protected areas to verify the conservation status of grassland ecosystems in China and identify conservation gaps.

Results and analysis

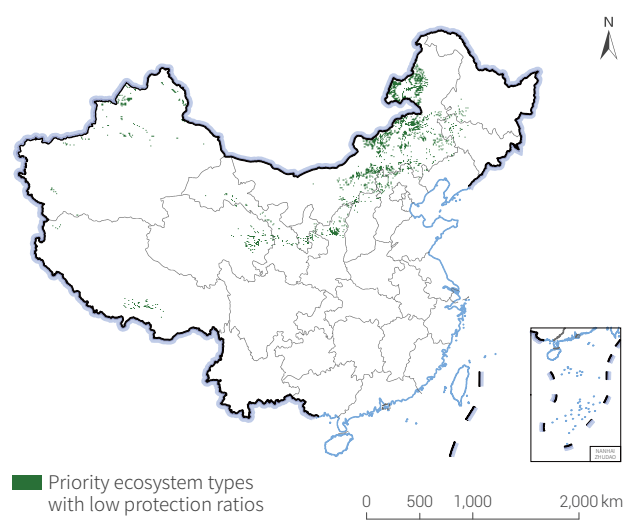
At present, there were 220 types of grassland ecosystems in China, among which 21 types, with a total area of 513,700 km², are in need of priority conservation. Five priority grassland ecosystems had an area larger than 30,000 km² each, namely, *Stipa purpurea* alpine grassland, *Leymus chinensis* grassland, *Kobresia parva* alpine meadow, *Stipa krylovii* grassland and *Stipa bungeana* grassland. They accounted for 69.5% of the total area for priority conservation. On the other hand, four types of grasslands, namely, *Stipa basiplumosa* alpine grassland, *Stipa roborowskyi* grassland, *Achnatherum splendens* grassland and *Suaeda salsa-Salicornia europaea* meadow, had an area of less than 1,000 km² each.

The grassland ecosystems for priority conservation were located in 14 provinces/regions across China. These ecosystems were mainly in Hulunbuir Grassland, Hunshandak Sandy Land, Horqin Sandy Land and the north of Yinshan Mountains in Inner Mongolia, the southwest edge of Tianshan-Jungar Basin, Altai District and Tarim River Basin in Xinjiang, Qiangtang area of Qinghai-Tibet Plateau, Qilian Mountains at the Source of Three Rivers, and the Loess Plateau (Fig. 7-3).



↑ Figure 7-3. Spatial distribution of grassland ecosystems for priority conservation in China

The existing protected areas in China covered all 21 types of grassland ecosystems for priority conservation and 24% of the key areas for grassland conservation while protected areas accounted for only 18% of China's total land area. The conservation effect was generally good. Eleven types of ecosystems had a conservation proportion of over 18%. The conservation proportions of *Carex moorcroftii* alpine grassland, *Kobresia setschwanensis* alpine meadow, *Stipa purpurea* alpine grassland and *Sanguisorba tenuifolia-Trollius chinensis-Gramineous* weeds meadow all exceeded 30%. However, the conservation proportions of five types of grasslands with smaller areas, namely, *Stipa roborowskyi* grassland, *Stipa breviflora* grassland, *Orinus thoroldii* grassland, *Stipa basiplumosa* alpine grassland, and *Suaeda salsa-Salicornia europaea* meadow, were still low and conservation effort should be strengthened accordingly. In particular, the areas of *Stipa roborowskyi* grassland and *Suaeda salsa-Salicornia europaea* meadow were less than 1,000 km² each, with the proportion covered by protected areas lower than 10%. Conservation for these two ecosystems should also be strengthened.



↑ Figure 7-4. Distribution of grassland ecosystems for priority conservation yet with low protection ratios

Outlook

This study focused on grassland ecosystems and generated a high-precision distribution map on the basis of land cover and vegetation information from remote sensing images and existing vegetation map. Key areas for grassland ecosystem conservation were also identified. The research results will provide methods and data support for accurate assessment of the effectiveness of grassland ecosystem conservation. The approaches and methods adopted in the study will inform similar efforts in other parts of the world and contribute to the conservation of grassland ecosystems worldwide.

The identification of key areas of and gaps in grassland ecosystem

conservation may help optimize the spatial distribution of protected areas for grasslands. The existing protected areas in China cover all 21 types of grassland ecosystems in need of priority conservation and have achieved a good overall protection effect. However, there are still five types of grasslands with smaller areas having a low proportion of protection. The spatial distribution of protected areas may be optimized by creating grassland parks and other nature reserves. Priority grassland ecosystems not yet covered by protected areas but with high biological authenticity and integrity may also be placed under protection, thus increasing the area and proportion of conservation.

Big data simulation to generate high-resolution distribution of rare and endangered plants

Target: 15.1 By 2020, ensure the conservation, restoration and sustainable use of terrestrial and inland freshwater ecosystems and their services, in particular forests, wetlands, mountains and drylands, in line with obligations under international agreements.

15.4 By 2030, ensure the conservation of mountain ecosystems, including their biodiversity, in order to enhance their capacity to provide benefits that are essential for sustainable development.

Highlights

- *The occurrences of IUCN Red List species were obtained through big data analysis such as metadata extraction from literature, semantic analysis and mining, web crawling and data cleaning. The distribution of individual species was modeled by MaxEnt or BIOMOD2 and simulated, generating with highest confidence high-resolution, clear and dynamic species distribution data within 1 km × 1 km grids.*

Background

SDG 15.1.2 (Proportion of important sites for terrestrial and freshwater biodiversity that are covered by protected areas, by ecosystem type) and SDG 15.4.1 (Coverage by protected areas of important sites for mountain biodiversity) emphasize the creation of nature protected areas as an important measure and mechanism for biodiversity conservation, with latter focusing specifically on mountain biodiversity conservation. The two indicators build on indicator 26 of Millennium Development Goal (MDG) Target 7.9 (Ratio of area protected to maintain biological diversity to surface area) (UN, 2015a). They reflect advances in protecting, restoring and sustainably using terrestrial and freshwater ecosystems and their services, especially in wild endangered species protection, biodiversity conservation and forest, wetland, mountain and dryland protection (Wei *et al.*, 2018; Zheng *et al.*, 2021). The UN defined the calculation

formulas for the two indicators and provides the statistical results of each country at the UNEP – World Conservation Monitoring Centre (UNEP-WCMC) website. Calculations can be done for a single species or the combination of several species. However, the two indicators are still classified as Tier II, meaning an internationally established methodology and standards are available but data are not regularly produced by countries (UN, 2015b), because when countries try to do their own calculations, they still do not have high-confidence data with regard to the spatial distribution of rare and endangered plants and animals. Available distribution data are mostly from traditional, occasional investigations generally with low accuracy and very coarse description of geographical boundaries (Rodrigues *et al.*, 2006).

Data used

© Species data: International Union for Conservation of Nature (IUCN) Red List (<https://www.iucnredlist.org/>).

© Species occurrence data: Chinese Virtual Herbarium (CVH) (<http://www.cvh.ac.cn/>), National Specimen Information

Infrastructure (<http://www.nsii.org.cn/2017/home.php>), Global Biodiversity Information Facility, (<https://www.gbif.org/>) and literature reports.

Method

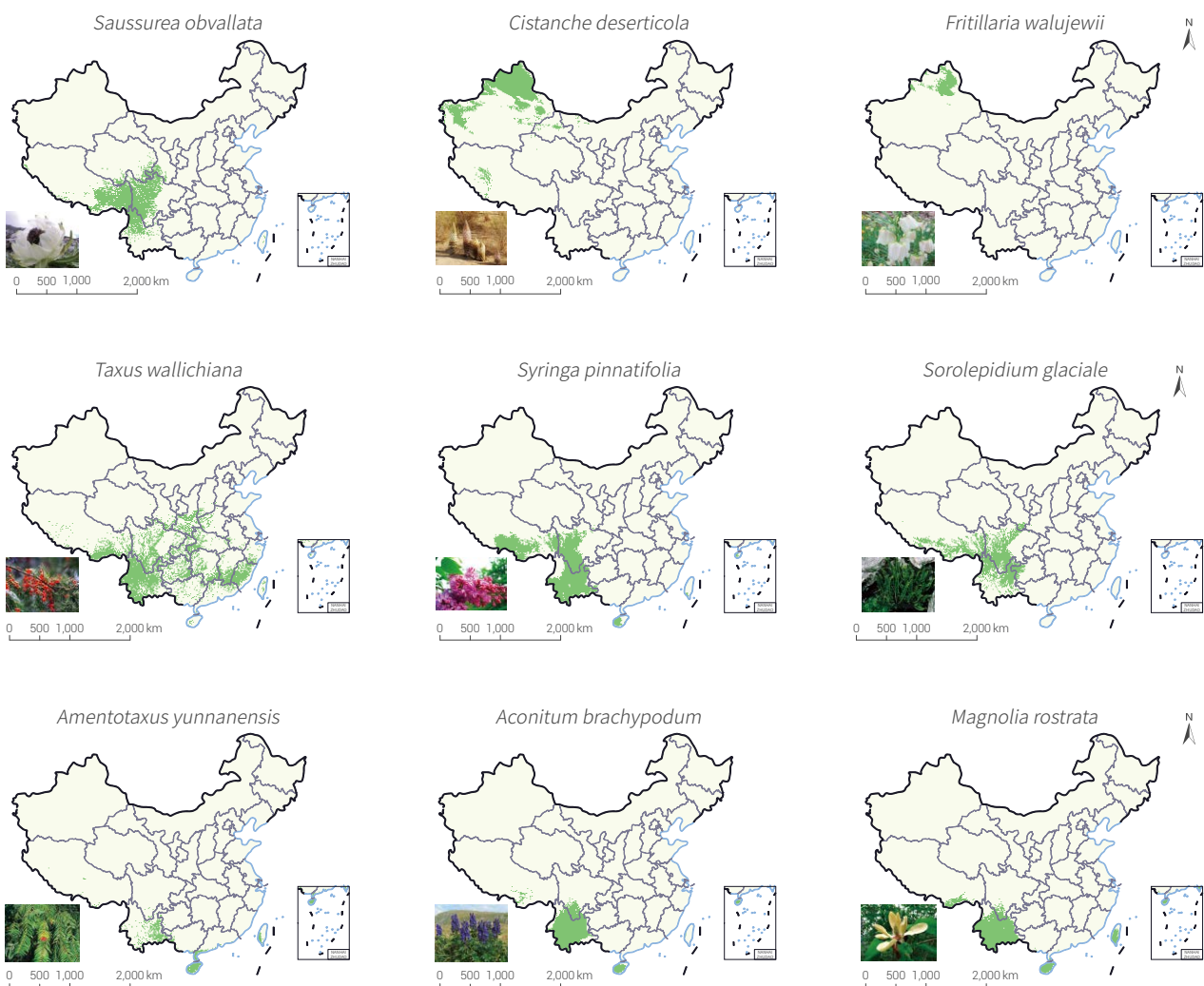
The study was based on data acquisition and processing methods supported by Big Earth Data. Through metadata extraction from literature reports, semantic analysis, web crawling and data cleaning, the occurrences of species on the IUCN *Red List of Endangered Species* (<https://www.iucnredlist.org/>), *List of National Key Protected Wild Animals* (<http://www.forestry.gov.cn/main/3954/content-1063883.html>) and *List of National Key Protected Wild Plants* (<http://www.forestry.gov.cn/main/3954/20180925/143410933280757.html>) were obtained. The four groups of critical habitat factors, i.e., terrain, climate, vegetation and

soil, were extracted by Principal Component Analysis (PCA). These critical factors were the inputs in MaxEnt or BIOMOD2 to simulate the distribution of each single species. The suitability threshold was limited to 0.6 or more to ensure reliability of the simulation results. Finally, the spatial distribution of each species with highest confidence was obtained with a spatial resolution of 1 km × 1 km (Wei *et al.*, 2021). By using the advantages of Big Earth Data, the method enabled a highly accurate, fine, clear and dynamic spatial distribution of each species in a 1 km × 1 km grid format.

Results and analysis

This study took 75 endangered, vulnerable, or near threatened plants and fungi from the IUCN Red List as species of interest. The occurrences of each of the 75 were obtained through Big

Earth Data analytics and its current (2020) spatial distribution was simulated through a species distribution model (Fig. 7-5). The results demonstrated the spatial distributions acquired

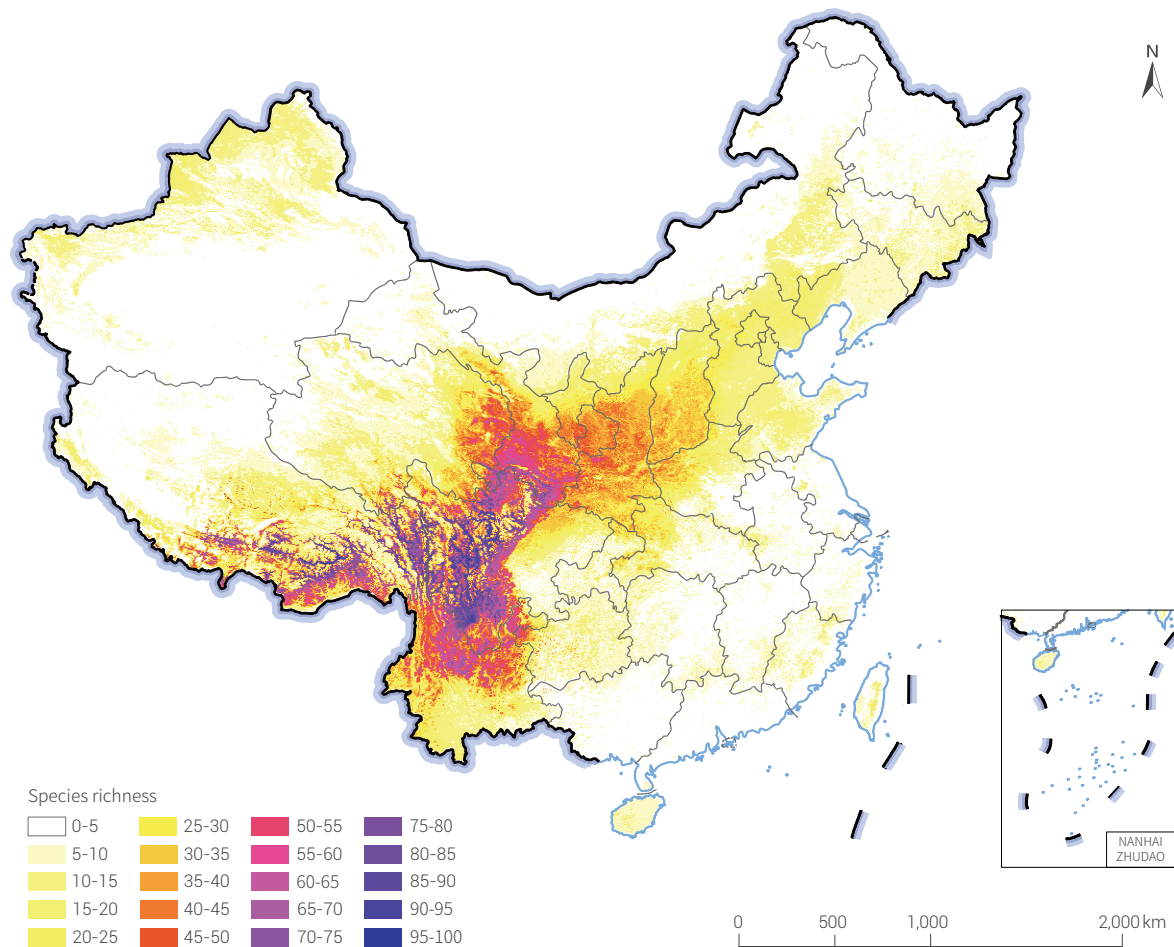


↑ Figure 7-5. Spatial distributions of 9 representative endangered plants/fungi

through modelling were more reasonable and with better resolution (1 km×1 km) than those obtained through traditional investigations. Extraction and simulation based on big data methods was proven to be a timesaving and highly efficient method to obtain the distributions of endangered species through an engineering approach.

Then the spatial distribution map of each species was binarized: 1 with distribution and 0 without. The total value of each 1 km×1 km pixel was the sum of all 75 endangered plants and fungi normalized as 0 to 100%, ultimately producing a species richness map at a spatial resolution of 1 km×1 km (Fig. 7-6). The

map showed clearly the occurrences of the 75 IUCN endangered species mainly in the transition between the first and second steps in the three-step "staircase" of the Chinese terrain. They lived in the northeast, southeast and south of the Qinghai-Tibet Plateau, mainly the Qilian Mountains and the south of Gansu Province, the Hengduan Mountains, the east part of the Himalayas and the northwest of Yunnan Province. These regions were thus critical to the conservation of endangered species in China. Another key biodiversity areas identified in this study was the zone extending from the south of Gansu Province to Qinling Mountains in the east. Most of these regions are mountainous (over 96%).



↑ Figure 7-6. Species richness map based on the 75 endangered plants and fungi

Outlook

The study used big data methods to obtain spatial distribution samples of rare and endangered species and extracted their habitat information including terrain, climate, vegetation and soil. Critical habitat factors were then extracted by PCA and used as inputs in MaxEnt or BIOMOD2 to simulate the distribution of each species. Finally, the spatial distribution of each selected species was obtained in 1 km×1 km grids with the highest confidence. The method's timesaving, high-efficiency advantages

demonstrate its feasibility, but all of the habitat indicators are only focused on terrain, climate, vegetation, and soil, while human activities, e.g., increasing market demand, trading, and overexploitation, present a more and more prominent influence on species spatial distribution. Further research should emphasize anthropogenic indicators, e.g., land use types and intensity, artificial picking, and overexploitation of endangered species, for comprehensive modeling.

High-resolution monitoring of global mountain green cover index

Target: 15.4 By 2030, ensure the conservation of mountain ecosystems, including their biodiversity, in order to enhance their capacity to provide benefits that are essential for sustainable development.

Highlights

- *The research team was the first in the world to produce globally consistent and spatially comparable high-resolution mountain green cover index datasets for 2015 and 2020.*
- *The study went beyond individual countries and analyzed the mountain green cover index spatiotemporal distribution and variation trend for different mountain types at varying elevations.*

Background

Under the combined influence of climate change and human activities, mountain ecosystems are undergoing significant changes (Immerzeel *et al.*, 2020). SDG 15.4.2 Mountain Green Cover Index (MGCI) aims to measure the extension and changes of green vegetation cover (including forest, shrub land, grassland and cropland) in mountain areas and serves SDG 15.4.

The Food and Agriculture Organization (FAO) and the International Scientific Committee on Research in the Alps (ISCAR) have established the method to monitor SDG 15.4.2 at both mountain descriptor layer and vegetation descriptor layer (FAO, 2017). Although country profiles have been released at the global level (data available for 2000, 2010, 2015 and 2018), dynamic changes data with clear spatial locations are still lacking. The SDG 15.4.2 official data use European Space Agency-Climate Change Initiative (ESA-CCI) land cover data at a 300-m resolution, with much uncertainty in monitoring

smaller massifs or highly heterogenous mountain vegetation. In this situation, the FAO suggested to use data with higher spatial resolution where they are available. Nevertheless, it is valuable to establish a set of standardized, universally comparable and spatially identifiable high-resolution time series SDG 15.4.2 monitoring framework at a global scale.

In 2020, within the CASEarth program, the MGCI of major economic corridors of the Belt and Road Initiative (BRI) were computed on the basis of remote sensing (Guo, 2021). Continuous tracking of the SDG 15.4.2 process is a necessary prerequisite for achieving SDG 15.4 globally. Therefore, drawing references from the MGCI metadata designed by the FAO and using the high-resolution MGCI monitoring model, in 2021, we continue to assess the global MGCI dynamics (using 2015 as the baseline year) and analyze MGCI changes of different mountain types at different latitudes and altitudes.

Data used

- Landsat-8 OLI surface reflectance data at 30 meters spatial resolution (2015-2020).
- ASTER GDEM Version 2 Data at 30 meters.

- UNEP-WCMC 500 m mountain classification data (Classification system in Table 7-2).
- FROM-GLC global sample sets for land cover classification in 2015.

Table 7-2. UNEP-WCMC criteria for mountain classification (Kapos *et al.* 2000).

Mountain types	Elevation	Slope	LER (local elevation range) 7-kilometer Radius
1	>4,500 m	Not used	Not used
2	3,500-4,500 m	Not used	Not used
3	2,500-3,499 m	Not used	Not used
4	1,500-2,499 m	>2°	Not used
5	1,000-1,499 m	>5°	OR >300 m
6	300-999 m	Not used	>300 m

Method

Based on our previous research in time series MGCI monitoring of economic corridors in the BRI framework, we monitored MGCI spatiotemporal dynamics in the years of 2015 and 2020 by using global Landsat-8 OLI surface reflectance data and mountain classification data in combination with the FAO's SDG 15.4.2 Metadata and the MGCI monitoring model (FAO, 2017; Bian *et al.*, 2020). The detailed steps were: (1) Extracting vegetation cover in mountainous regions through a model based

on Big Earth Data platform and with due attention to remote sensing observation frequency and vegetation phenology. (2) Calculating global high-resolution spatial distribution of MGCI for 2015 and 2020 based on MGCI computing model which considered the mountain surface area in a mountain grid. (3) Analyzing MGCI variation trend for different mountain types, altitudes and latitudes.

Results and analysis

The global MGCI for 2015 and 2020 were shown in Figure 7-7. The grid-based high-resolution MGCI data provided information beyond administrative boundaries and clearly reflect mountain green vegetation cover of different ranges. MGCI aggregations for different administrative regions, river basins or protected areas allowed deeper understanding of the state of regional development. The research results showed a mean global MGCI of 80.56% in 2020. 16.94% of global mountain regions were without green vegetation cover, mainly in the Qinghai-Tibet Plateau, Central Asian mountains, Chilean mountain ranges, north Canada and Greenland.

Accord to statistics, SDG 15.4.2 didn't change very obviously but spatial variations did exist from 2015 to 2020. Compared with 2015, in general, the MGCI of about 13.06% global mountains showed a minor upward trend, up 5.7% on average, while that of about 15.04% global mountains showed a minor

downward trend, down 5.5% on average.

In terms of latitudes, the MGCI differed widely from 60°S to 70°N due to the existence of different mountain types and ecosystems. At latitudes higher than 80°N, tundra was the main green vegetation cover and the MGCI showed a slightly upward trend in the past five years. In terms of altitudes, the MGCI was higher than 80% when the elevation was below 2,500m and decreased when the elevation was above 4,500m. The variations were mainly affected by temperature and humidity. For different mountain types (Table 7-2), types 1, 2 and 3 had lower MGCI due to their higher elevations, on average 37.15%, 60.73% and 57.28% respectively in 2020. The MGCI for mountain types 4, 5 and 6 were 82.46%, 84.13% and 89.77% on average, respectively. From 2015 to 2020, MGCI variations for all mountain types were below 1%.

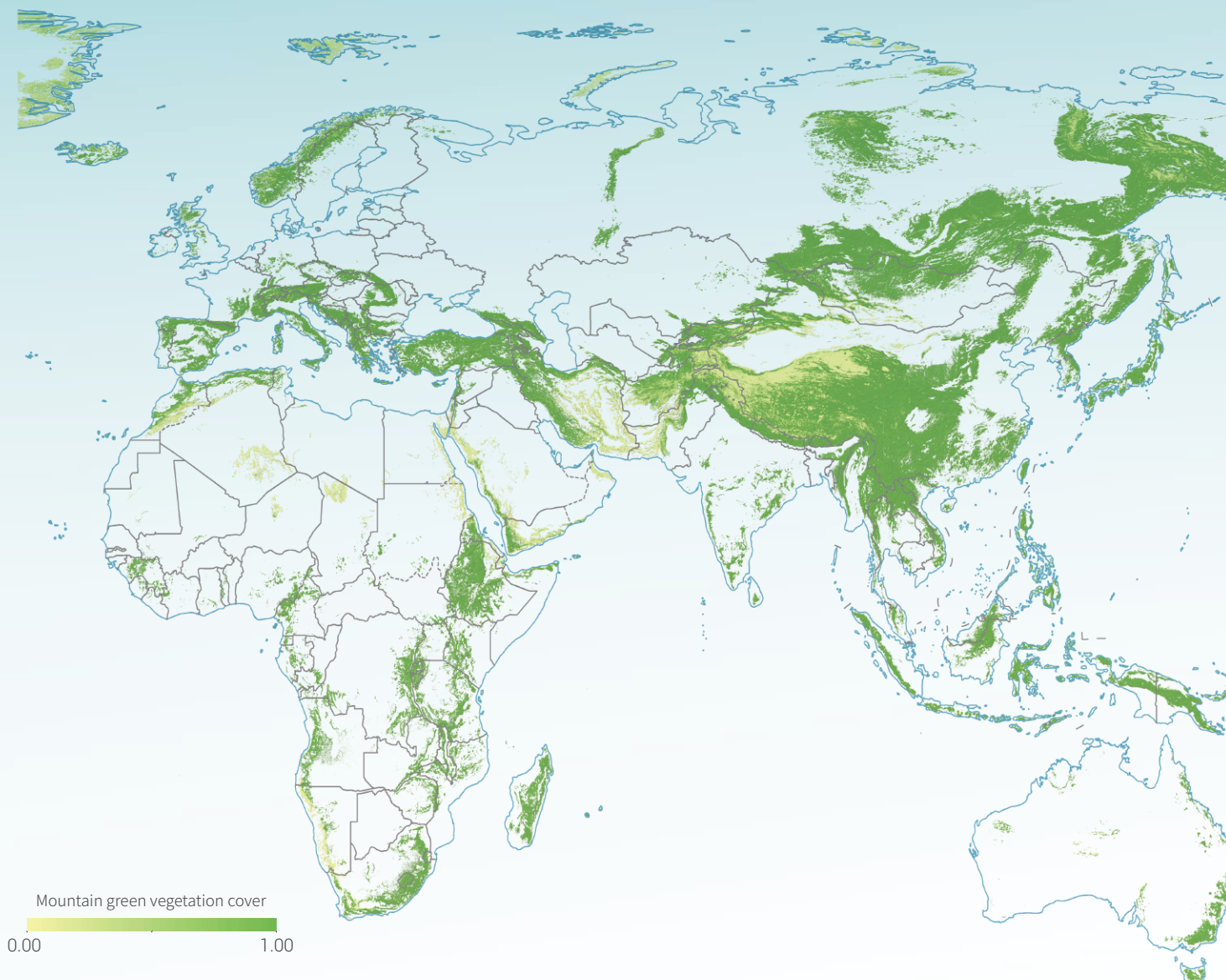


Figure 7-7.

● Global distribution of MGCI in 2020





Outlook

As an important part of the global environmental commons, mountain ecosystems are crucial for protecting global water resources and biodiversity and need urgently SDG monitoring supported with Big Earth Data. This study drew references from the FAO's definition of MGCI and used open-source Landsat-8 OLI images and DEM data to develop a high-resolution monitoring model that took into account the mountain surface area. Dynamic monitoring of SDG 15.4.2 was realized. Global MGCI variations in recent 5 years were then assessed, thus providing an important technical and data support for SDG 15.4 (conservation of mountain ecosystems).

MGCI increases in most cases can be interpreted as stringent controls over damages to ecosystems having led to the expansion of forest, shrub and grassland ecosystems. It is

noteworthy though that in some rare cases, MGCI increases at higher elevations may have been caused by green vegetation growth upon the retreat of glaciers or permanent snow in the context of global warming. Since the changes of glacier and snow tend to occur at smaller scales, the use of land cover data with higher resolution may better reveal the mountain classifications and MGCI variations at different elevations. In addition, transitions between different ecosystems may result in situations where the index remains unchanged but natural ecosystems are still threatened (for example, changes from forest to grassland/farmland or from grassland to farmland). In the future, it is necessary to further define the index to enable expression of more diversified trends, which can also be an important area of further research.

Monitoring spatiotemporal variations of wintering Siberian crane habitats

Target: 15.5 Take urgent and significant action to reduce the degradation of natural habitats, halt the loss of biodiversity and, by 2020, protect and prevent the extinction of threatened species.

Highlights

- A long time series dataset of the suitable habitat distributions of Siberian cranes in the Poyang Lake wetland from 1993 to 2018 was produced.
- The hot spots of the Siberian crane habitats exhibited a consistent sheet structure around the Qianqihu sub-lakes of Poyang Lake, whereas the cold spots indicated a spatial pattern of axial distributions primarily along the main channel. As the water level of Poyang Lake increased, the stability and variety of crane habitats decreased and their aggregation feature was weakened.

Background

The Siberian crane (*Leucogeranus leucogeranus*) is one of the most endangered species in the world. It was identified as a Class I protected species by China in 1989 and put in the IUCN Red List as a critically endangered species in 2010. The Poyang Lake wetland is a unique wetland ecosystem located in the middle and lower reaches of the Yangtze River and provides important habitats for millions of wintering waterbird species. It is the largest wintering destination for the Siberian crane, a critically endangered species. Approximately 98% of the Siberian cranes in the whole world spend the winter here (Wang, 2020). The

hydrological situation of Poyang Lake is the main determinant of the quality of Siberian crane habitats. Autumn/winter droughts in recent years significantly affected their main food sources and habitat condition (Jiang *et al.*, 2014). It is therefore of great importance to monitor and analyze the spatiotemporal variations of Siberian crane habitats and their response to water-level changes. This study aimed to inform and support ecosystem conservation and treatment at Poyang Lake wetland and provide novel approaches and methods to monitor migratory bird habitats and protect biodiversity in typical wetlands.

Data used

- © Landsat TM/ETM+/OLI remote sensing images acquired in autumn/winter from 1993 to 2018, covering water levels from 5 m to 15 m, with a spatial resolution of 30 m.
- © Daily water level data at the Xingzi gauging station in Poyang

Lake from 1993 to 2018.

- © Vector data, including the boundaries of natural Poyang Lake wetland, sub-lakes, and Nanji wetland and Poyang Lake national nature reserves.

Method

Shallow water, wet grassland and mudflat of the Poyang Lake wetland are ideal habitats for wintering Siberian cranes. Remote sensing classification of the Siberian crane habitats in the Poyang Lake wetland was conducted for varying water levels in different years. Wet grasslands, waterbodies and

bare soils were extracted from the remote sensing images. Shallow waters were then extracted from the waterbody images by way of water depth estimations and mudflats were extracted from bare soil images using the NDWI threshold. The landscape metrics were used to describe the spatial

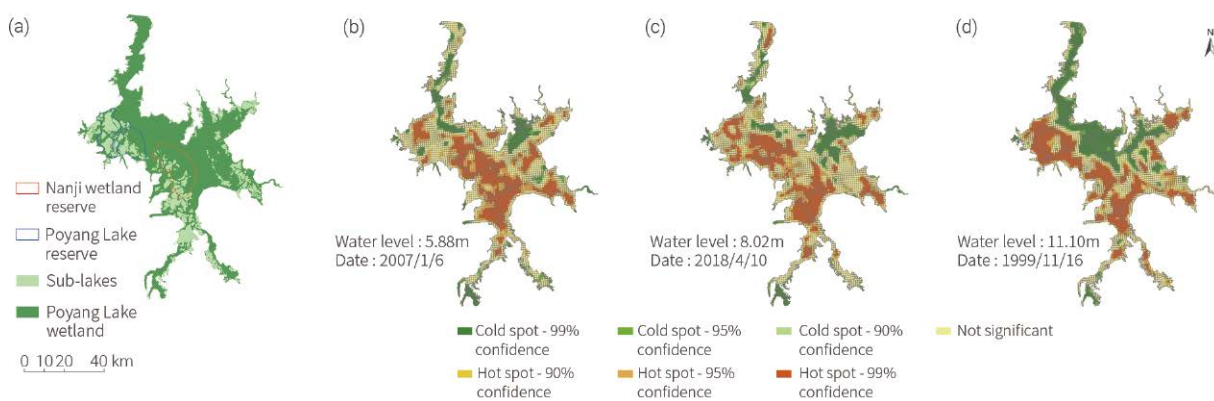
structure of the crane habitats and the spatial autocorrelation indicators were applied to explore the hot and cold spots of habitat distributions. Three vulnerability evaluation indicators including sustainability, stability and variety were constructed to evaluate the vulnerability of the Siberian crane habitats under various water-level conditions (Zou *et al.*, 2021). The

water levels were divided into 1m intervals under different hydrological conditions. Subsequently, the spatiotemporal variational characteristics and spatial clustering patterns of the Siberian crane habitats were analyzed and the corresponding vulnerability evaluation and comparative analysis were conducted.

Results and analysis

Siberian crane habitats in the Poyang Lake wetland exhibited a consistent spatial distribution pattern with extremely low, low and average water levels. The hot spots formed multiple sheets

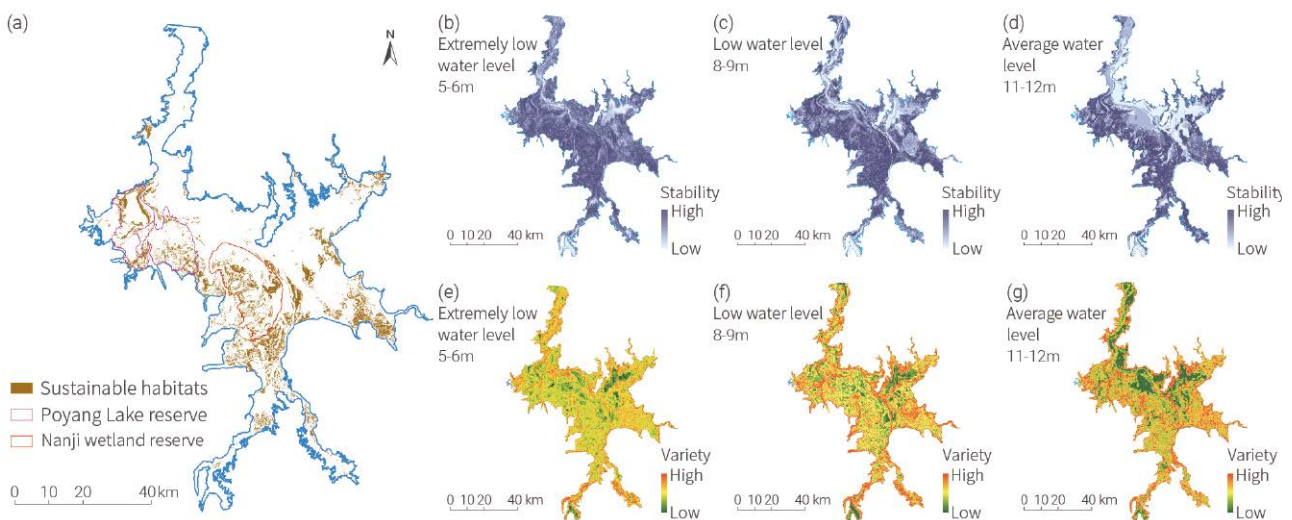
centering on the Qianqiuhu sub-lakes of Poyang, whereas the cold spots were distributed axially around the main channels of Poyang Lake (Fig. 7-8).



↑ Figure 7-8. Hot and cold spots of Siberian crane habitats in Poyang Lake wetland

Based on the dataset of the Siberian crane habitat distributions in the Poyang Lake wetland from 1993 to 2018, including 11 images with extremely low water level, 11 with low water level and 10 with average water level, the vulnerability of the crane habitat distributions was evaluated for different water levels. More sustainable crane habitats were mainly distributed in Qianqiuhu sub-lakes of Poyang, and intensively aggregated in

Nanji wetland reserve and Poyang lake national nature reserve (Fig. 7-9a). At all water levels, the stability and variety of crane habitats gradually decreased as water level increased (Fig. 7-9b-g). In the main lake of Poyang and close to the main channels in particular, the decrease was obvious and expansionary. Increases of water level significantly weakened the aggregation characteristic of the crane habitats.



↑ Figure 7-9. Vulnerability distributions of the Siberian crane habitats in the Poyang Lake wetland

Outlook

The Siberian crane is a very special species among hundreds of wintering migratory birds in Poyang Lake. It is highly dependent on shallow water wetlands and has very stringent requirements on the ecological environment of the habitats. This study focused on the spatiotemporal variations of the Siberian crane habitats in the Poyang Lake wetland and changes caused by varying water levels during the past 30 years. The vulnerability of those habitats was then evaluated. The findings are of great value for wetland ecosystem management and migratory bird habitat protection. The unique hydrological features of Poyang Lake caused the fluctuations and complexity of the landscape structure of the crane habitats. The hot spots of the crane habitats showed obvious continuity under different water level conditions, especially in the national nature reserves. In this connection, strengthening the protection of nature reserves is of

great importance to the protection of the Siberian crane habitats. The construction and protection of man-made wetlands in Poyang Lake region in recent years provided more habitats for wintering cranes. In Wuxing Siberian crane conservation zone, large areas of protected lotus roots became an important food source for over 30% of the wintering Siberian cranes in Poyang Lake. Meanwhile, sand dredging activities were regulated with coordinated planning of the timing, location and output, which significantly reduced their impacts on the Siberian crane habitats in the main lake area and close to the main channels. Besides the current nature reserve management and man-made wetland construction, future conservation strategies should be focused on improving the ecosystem service function of the Poyang Lake wetland as its hydrological condition in low-water season goes through significant changes.



Summary

This chapter focuses on gaps in data and methodology to evaluate the progress towards SDG 15. With Big Earth Data, the relevant research teams obtained two important datasets: the global MGCI and the fine distribution of endangered species in kilometer grids, analyzed the ecosystem quality dynamics and grassland protection status and gaps in China and assessed the spatiotemporal variations of wintering Siberian crane habitats.

The research findings are as follows.

- (1) The quality of ecosystems in China improved significantly from 2000 to 2015. The integrated EQI increased by 21% approximately year-on-year. The conservation of important grassland ecosystems was generally good, but five types of grasslands with smaller areas still have a low protection ratio.
- (2) The habitats of wintering Siberian cranes in Poyang Lake wetland have been degraded since 1993. It is necessary to

study and identify targeted strategies to tackle the weakening aggregation of crane habitats.

There are fewer than 10 years to go before the 2030 SDG target year. Given that it takes a long time for ecosystems to recover under protection and then generate benefits, only by urgently taking consistent and effective actions to protect and restore ecosystems will it be possible to fully realize the SDG 15 in the 2030 Agenda. Science and technology are important means to facilitate the sustainable development of life on land. In the future, in response to the needs for spatial data at different scales in the evaluation of SDG 15, the advantages of Big Earth Data should be further explored to provide better data, products and tools supporting SDG 15 evaluation, thus contributing to the realization of SDG 15 in 2030.



Jiuzhaigou Valley

Interactions among SDG indicators

Background

The complex interactions among the UN SDG indicators are a key challenge affecting the implementation of the SDGs. Tracking and understanding these interactions is of great significance to achieving the goals and dynamically adjusting the path to sustainable development.

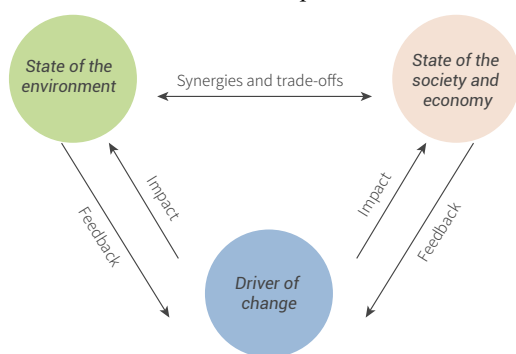
Interactions occur both between different SDGs and within the same SDGs. They are manifest as synergies or trade-offs, which vary spatially and temporally, affect the factors of production and then shape the sustainable development process. When there are synergies between indicators, the achievement of one indicator facilitates the improvement of others. In other words, synergistic indicators promote one another. Trade-offs and counterbalances occur when an indicator is achieved at the expense of others. In light of the UNEP's SDG indicators classification system (UNEP, 2021), the existing indicators can be roughly put into three groups: those relating to the state of the environment, those relating to the state of the society and economy, and those driving changes. The interactions among the three groups are shown in Figure 8-1. The driver indicators lead changes to the environmental and socio-economic indicators. The latter two groups measure the achievement of the SDGs, with both synergies and trade-offs between themselves and affect the implementation of the drivers through feedbacks. At the same time, there are complex synergy and trade-off relationships within each of the three groups.

At the global scale, most countries in the world find more synergies than trade-offs among SDG indicators, which is the solid foundation for the implementation of the 2030 Agenda. In general, trade-offs between SDGs may be linked to the traditional mode of development, which stresses socio-

economic growth over the environment and is not sustainable (Pradhan *et al.*, 2017). For example, some countries consume more non-renewable energy to increase power supply, leading to a significant negative correlation between SDG 7.2.1 (renewable energy share in the total final energy consumption) and SDG 7.1.1 (proportion of the population with access to electricity) at the global level. The increase of irrigation water to boost food production (SDG 2.4.1) is often at the expense of ecological and environmental water use, which leads to worsening regional indicators relating to the state of the environment (SDG 6.4 water security and SDG 15.1 ecosystems). Efforts to boost social production to improve health (SDG 3) and nutritional status (SDG 2) often result in increased greenhouse gas emissions (SDG 13.2.2). Therefore, it is particularly important to clarify the interactions among SDG indicators, monitor their dynamics and evaluate their development so as to provide decision support for SDG implementation and path adjustment.

Many international organizations and institutions have been attracted to studying the interactions among SDG indicators. For example, UN-Water analyzed the six targets of SDG 6 and other SDG targets with potential interactions and found 29 pairs of targets in potential trade-off relationships and 127 pairs being synergistic (UN-Water, 2016). UNEP took the 13 environmental SDG indicators, analyzed their relationships with indicators of the other two groups and evaluated the progress of the environmental indicators to support decision-making for their implementation (UNEP, 2021).

Big Earth Data integrates satellite observations, near-surface observations and ground surveys from multiple sources. Being magnanimous and multi-temporal, they provide important data support for the monitoring and evaluation of the SDGs. The study of interactions among SDGs may be supported with Big Earth Data in spatial and other analytics, including: to evaluate the synergy and trade-off relationships among SDG indicators, their correlations to start with, to discover potential scientific problems, and to evaluate the impact of policy measures; to analyze future environmental, economic and social development scenarios in the context of such interactions, temporal variations to start with, and to guide dynamic policy planning; to identify regional practices and develop an integrated evaluation of the regional SDGs in order to guide the regional path to sustainable development.



↑ Figure 8-1. Interactions among SDG indicators

Methods and practices of research on interactions among SDG indicators supported with Big Earth Data

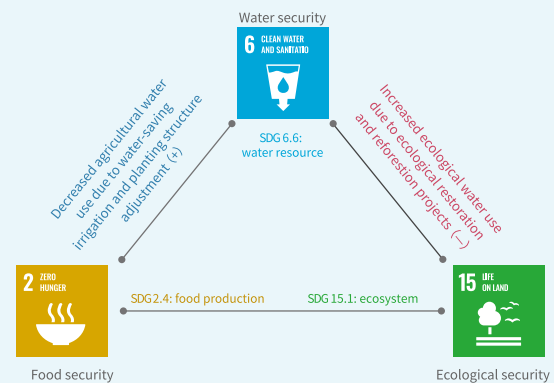
1. Quantification and evaluation of interactions among SDG indicators

Big Earth Data has significant advantages in spatial information mining. They enable not only the monitoring of the environmental indicators (such as SDG 6.4 water resources security, SDG 15.1.1 forest cover and SDG 13.2.2 greenhouse gas, etc.) (Avtar *et al.*, 2020) but also the monitoring and evaluation of socio-economic indicators (SDG 11.1.1 convenient transportation and SDG 13.1.1 disaster losses, etc.) through geographically decomposing and coupling multiple-

source demographic, economic and societal data (Chen *et al.*, 2019). The monitoring results of long time series data related to regional SDG indicators provide data support for the study of interactions among those indicators. On this basis, the synergy and trade-off among different indicators can be quantified through correlation analysis, network analysis and other methods (Weitz *et al.*, 2018). Meanwhile, the dynamics of SDG indicators with known trade-offs or synergies can be evaluated with Big Earth Data technologies to provide decision-making support for policy formulation and implementation effects evaluation.

Case study: Evaluation of interactions among water, food and ecological security indicators in North China

North China is a traditional grain production area in China and accounts for more than one-quarter of the national total grain output, population and GDP. But it has only 3% of the national total water resources. The trade-off between water resources security (SDG 6.4) and sustainable food production (SDG 2.4) is a major concern to be addressed for regional sustainable development. While massive ecological restoration programs (the Natural Forest Protection Project and the Grain for Green Project) since 1999 have improved regional ecological conditions, with significantly better vegetation (SDG 15.1) and a greater water conservation capacity, ecological water consumption have also increased, forming a trade-off relationship with water security (SDG 6.4) (Fig. 8-2). Continuous monitoring on the basis Big Earth Data technologies of the surface and groundwater resources (SDG 6.6) and ecosystems (SDG 15.1) in North China over the past 20 years revealed that North China had benefited from a series of policies and actions including agricultural water-saving irrigation, cropping structure adjustment and the South-to-North Water Diversion Project. While enjoying steady grain output increase for years, the region also saw decreased



↑ Figure 8-2. Interactions among water, food and ecological security indicators in North China

agricultural water consumption, improved water resources situation and expanded area of surface water. Obviously, the trade-off between water security and food security goals had been mitigated. It may therefore serve as a reference point for decision-making to address the trade-offs among water, food and ecological security targets in similar regions.

2. Scenario simulation and evolution analysis in the context of interactions among SDG indicators

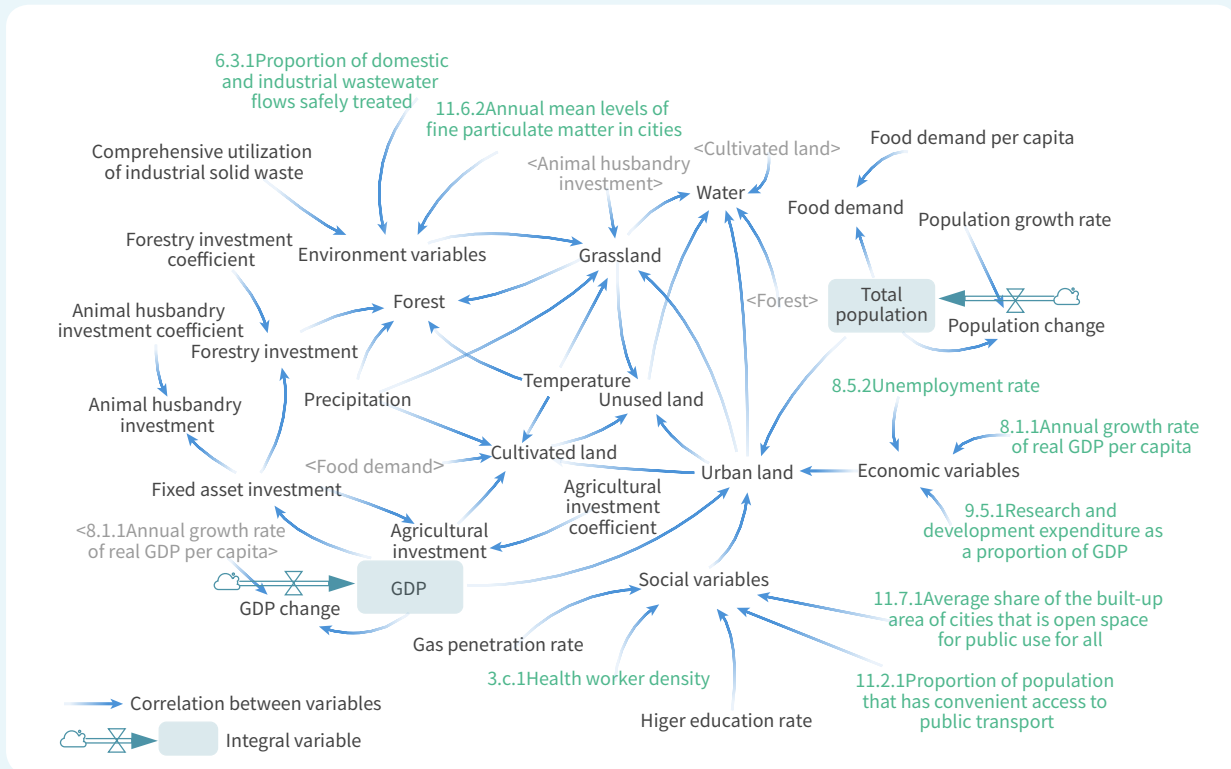
The broad scope of the SDGs and their inherent long-term, systemic and complex nature challenge policymakers to comprehensively assess their long-term impacts on economic, social and environmental development. Scenario simulation and evolution analysis embodies a long-term view to coordinate social, economic and environmental goals, thus serving as a theoretical basis and technical

support for sustainable development planning through quantitative modeling (Allen *et al.*, 2016). Big Earth Data features multiple scales, long time series, spatial attributes and massive data. Researchers may consider using Big Earth Data to analyze the interactive relationships among SDG indicators, model their evolution processes and simulate different development scenarios of the environment, economy and society from the geospatial perspective, thus informing dynamic policy planning.

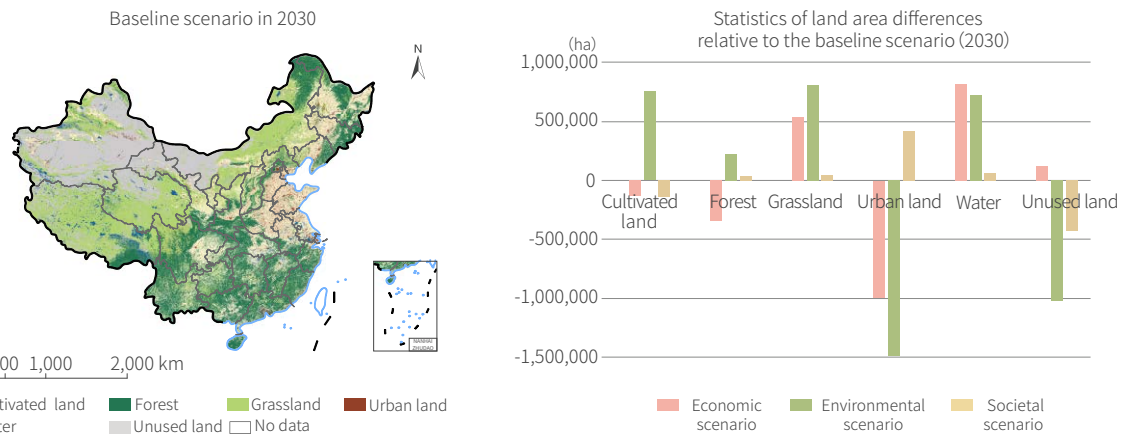
Case study: Scenario simulation and analysis of land use development in China with multi-SDG interactions

Sustainable utilization of land resources plays an important role towards sustainable development encompassing economic growth, social progress and environmental protection (Hong *et al.*, 2021). On the basis of the dynamics of land uses within the constraints of multiple SDGs in the past 20 years, a system dynamics model relating to land use needs in China was constructed to simulate future land use scenarios and analyze the evolution. The environmental (SDG 11.6.2), socio-economic (SDG 3.c.1, 11.2.1, 11.7.1, 8.1.1, 8.5.2) and driver indicators (SDG 6.3.1, 9.5.1) all constrained land uses such as urban land, cultivated land, forest and grassland respectively (Fig. 8-3). Four development scenarios were designed, including

a baseline one and three others prioritizing economy, environment and society respectively. The baseline scenario was deduced along historical trends (Fig. 8-4), the economic scenario was focused on GDP growth and expenditure, the environmental scenario was focused on pollution, emissions and environmental protection, and the societal scenario was focused on improving the living environments. A cellular automata model was used to generate series of spatial data on land uses in China under different sustainable development scenarios. The simulation results will inform the dynamic planning and adjustment of the country's pathway to sustainable development.



↑ Figure 8-3. Dynamics of land uses amid interactions among SDG indicators



↑ Figure 8-4. Scenario simulation results of land use types in China (2030)

3. Integrated evaluation of regional SDGs

A region has spatial systems at multiple scales and of different uses. It is the specific carrier of sustainable development and plays an important role in the implementation of sustainable development strategies. Factors affecting sustainable development of regions at different scales and of varying types are not completely the same. The purpose of conducting integrated evaluation of regional SDGs was to comprehensively and systematically sort out various SDG goals in a specific region and evaluate the state of sustainable development under a specific topic such as urbanization, ecological environment, water resources and agriculture or multiple topics in the entire region and various spatial units

within the region. In addition, specific researches can also be conducted to quantify and evaluate the interactions among SDG indicators or to simulate and analyze the evolution of regional development scenarios under such interactions. Another area of interest is the interactions among SDG indicators between various geographical spaces within and without a selected region as an open coupled system. CBAS has coordinated integrated evaluations of regional SDGs and relevant demonstrations in Hainan province, Shenzhen, Guilin, Lincang and other places in China. Preliminary results have been produced. Further work will be carried out on more topics and targets.

Case study: Integrated evaluation of urban sustainable development in Hainan Island

Hainan Island was taken as a demonstration area and the integrated evaluation was carried out by using data from multiple sources such as Earth observation and statistics. All cities and counties on Hainan Island were monitored and evaluated for urban sustainable development from 2010 to 2019. Researchers first screened data for extremums and obtained single index scores through normalization. Then they built single indicator dashboards and trend chart. The comprehensive sustainable development scores were finally calculated. The results showed obvious fluctuations

in those scores from 2010 to 2015 (Fig. 8-5). Since 2015, with the implementation of the 13th Five-Year Plan, the scores rose rapidly. From 2010 to 2018, spatially, the sustainable development level was high in the north and south of Hainan Island and low in the central and western regions (Fig. 8-6). Haikou, the administrative center, and Sanya, the tourism center, had the highest level of sustainable development. The evaluations offered pathways and solutions for other provinces and regions to implement the SDGs.



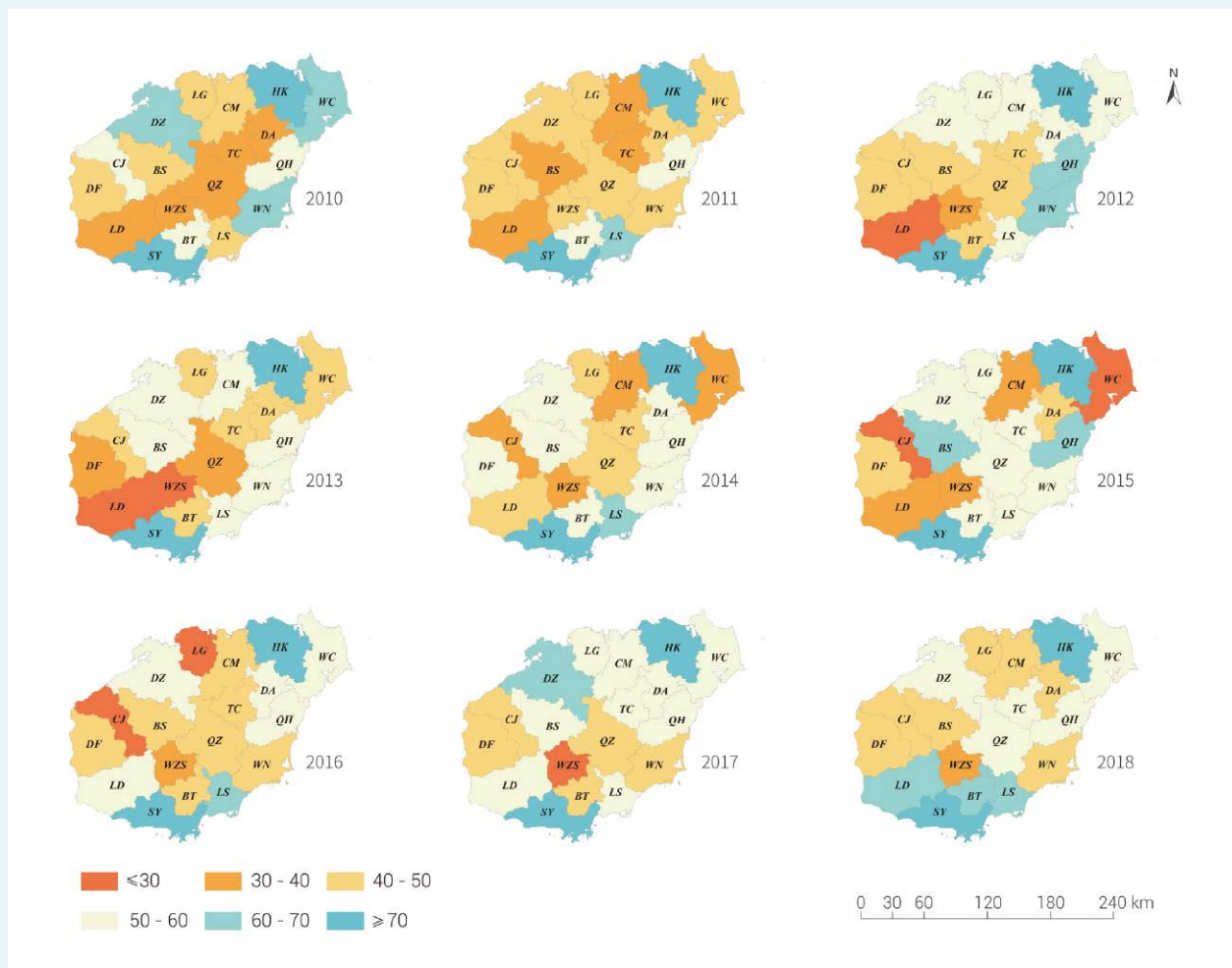
↑ Figure 8-5. Left: Urban sustainability score chart (2018); Right: Urban sustainability trend chart (2015-2018).

Summary

Interactions among the three dimensions of sustainable development (economic, social and environmental) are not simple, linear or compensable. They are manifest as synergies and trade-offs. Generally speaking, SDG indicators showing synergy with environmental sustainability should be prioritized in socio-economic development while we should guard against possible ecological and environmental risks in pursuing those in a trade-off relationship. This chapter presents three cases to analyze the main synergy and trade-off relationships among SDGs of different categories and discuss the methods and practices to use Big Earth Data in support of researches into the interactions.

In the first case, the North China region was used to analyze the relationships between grain yield (SDG 2.4), water use efficiency (SDG 6.4) and ecological protection (SDG 15.1). It was demonstrated that the South-to-North Water Diversion Project, agricultural structure adjustment and water-saving irrigation had helped to mitigate the conflicts among the three goals.

The second case involved development scenario simulation and evolution analysis. China at the national scale was the target of research. A land use evolution simulation model was constructed on basis of the internal correlations and interaction mechanisms among SDG indicators. Land uses



↑ Figure 8-6. Integrated evaluation results for cities and counties in Hainan Island (2010 to 2018)

Cities and counties in Hainan Island. HK: Haikou; SY: Sanya; DZ: Danzhou; WZS: Wuzhishan; QH: Qionghai; WCS: Wenchang; WN: Wanning; DF: Dongfang; DA: Ding'an; TC: Tunchang; CM: Chengmai; LG: Lin'gao; BS: Baisha; CJ: Changjiang; LD: Ledong; LS: Lingshui; BT: Baoting; QZ: Qiongzong.

under different sustainable development scenarios in China in 2030 were analyzed. The research results may inform future SDG implementation paths in China.

The last case was about integrated evaluation of regional SDGs. The states of urban sustainability in cities and counties in Hainan province were analyzed on the basis of Earth observation, statistics and other data. Single indicator dashboards and trend charts were generated. The research stands to provide other provinces and regions with methods and solutions to implement the SDGs.

To facilitate the implementation of the SDGs, the technical advantages of Big Earth Data should be fully tapped and technology facilitation mechanisms should be used to strengthen research on the interactions among SDGs and their indicators. New tools and methods should be explored to comprehensively quantify the extents of these interactions, thus supporting future decisions on the SDGs implementation pathways with more relevant and richer information.

Summary and Prospects

The COVID-19 pandemic, as a public health and security event, has had a tremendous impact on all aspects of global sustainable development. The global sustainable development score for 2020 fell for the first time since 2015. The pandemic is also putting at risk production of data critical to the achievement of SDGs as field data collection has been seriously disrupted in many countries. In this connection, it has been a natural and higher demand for science, technology and innovation to play a role in data collection and monitoring and evaluation of SDG indicators. This report addresses six SDGs (zero hunger, clean water and sanitation, sustainable cities and communities, climate action, life below water and life on land) and interactions among SDGs with case studies to evaluate the UN SDG indicators with Big Earth Data in terms of data products, methods and models, and decision support.

(1) SDG 2.4: The studies were focused on China national and local scales. Cropland cropping intensity was extracted annually from 2001 to 2020 and found to have decreased about 6% in the past 20 years. Spatial distributions of 14 major crops in 2000 and 2015 were mapped by integrating time-series remote sensing data with statistics of regional crop calendars and statistical crop planting areas. An efficient agroecological paradigm was proposed and its contribution to improving economic efficiency, reducing resource consumption and mitigating environmental impact was demonstrated through a field experimental farm, providing an example for the development of sustainable agriculture.

(2) SDG 6.3, 6.4, 6.5 and 6.6: The relevant indicators were monitored and evaluated on both the Chinese and global scales with the following findings. Since 2000, China's lakes with an area of more than 1 km² have become clearer, the water use efficiency of crops has increased, and the area of natural and artificial water bodies has increased, a visible slowing down in the loss of vegetated wetlands and markedly improved integrated water resources management. At the global scale, the water bodies of lakes bigger than 25 km² have become clearer and the crop water-use efficiency in agricultural areas has also shown an upward trend.

(3) SDG 11.2, 11.5 and 11.7: Studies were conducted at

the Chinese scale and the findings are as follows. 90.15% of the whole Chinese population had convenient access to public transport in 2020, up 9.59% from 2018. Since 2010, China had witnessed a general trend of declining impact of natural disasters as its comprehensive disaster prevention and mitigation capabilities and the resilience of cities against natural disasters improve markedly. Since 2000, green spaces in 93 typical urban built-up areas in China had been increasing as the result of urban ecological and greening actions. In terms of integrated evaluation of SDG 11 indicators, all cities had a sustainability performance in 2020 better than 2015, with the average integrated index increasing from 0.64 to 0.73 and cities in eastern China performing better than those in western China.

(4) SDG 13.1, 13.2 and 13.3: Studies were carried out in China and at the global scale with the following findings. In China, the frequency of sandstorms visibly decreased in the past 10 years; since 2015, CO₂ emissions had still been increasing, but the growth was slowing down; forest carbon sink capacity had been strengthened in the last decade, with forests in Yunnan province sequestering the most, followed by those in Guangxi and Guangdong. Globally, land cover change was important driver in the terrestrial carbon sink process. In the past nearly 30 years, due to climate change, ocean heat content had risen at an increasing rate.

(5) SDG 14.2: The studies were focused on coastal regions in China, with the following findings. Satellite remote sensing was used to rapidly identify large floating algal blooms and four-dimensional variational data assimilation was conducted to predict floating trajectories so as to provide decision support for the prevention and control of large algal blooms in the Yellow Sea. From 2015 to 2020, the area of mangroves in China increased by 16%, with the most significant growth along the coast of Guangxi. In the past five years, driven by incentives to transform mariculture ponds back to wetlands, the areas of such ponds have shown a downward trend, with the largest drop in Zhejiang Province.

(6) SDG 15.1, 15.4 and 15.5: Studies were conducted on the globe, China and selected typical areas with the following findings. From 2000 to 2015, China's ecosystem quality

improved markedly as the integrated index increased by 21% approximately year-on-year. Key grassland ecosystems in China were well protected on the whole while still 5 types of rare grasslands did not have sufficient protection. Global high-resolution MGCI was produced for 2015 and 2020, with the spatiotemporal change characteristics for different mountain types and elevation gradients analyzed. Through big data simulation, researchers generated species richness maps for 75 species of endangered plants and fungi, supporting with quantitative data the assessment of sites of biodiversity conservation importance. Spatiotemporal distribution data sets were produced on the basis of long time series of habitat data on wintering Siberian cranes and analysis was conducted on the dynamic change of out-of-control habitat and effective protection in the future.

(7) Interactions among SDGs: The main synergies and trade-offs among different types of SDG indicators were analyzed and the methods and practices of using Big Earth Data in the study of those intersections were discussed, including the quantification and evaluation of the intersectional relationships, the development of scenario simulation and evolution research and the comprehensive regional evaluation.

Over the past two years, the Chinese Academy of Sciences has conducted pilot studies on SDG indicators evaluation methods and data expansion. Many challenges remain, such as the lack of multi-type spatiotemporal data essential for the evaluation of the indicators as well as barriers in standards and security of and access to data sharing. To use Big Earth Data in support of the SDGs, we need to focus on the following in the future.

1. SDG-oriented Big Earth Data infrastructure

The 17 SDGs involve different types of data, which usually correspond to social phenomena or environmental problems at different spatial and temporal scales. At present, the main data sources used in SDG evaluation are statistical surveys, but they are not sufficient to meet the evaluation needs due to different survey times and varying data quantity and quality. In his SDG Report 2020, UN Secretary General

António Guterres highlighted the need to make better use of data, with particular emphasis on the role of science, technology and innovation in data collection. Therefore, we need to improve the existing statistical data acquisition methods and use Big Earth Data analysis to strengthen the data infrastructure for the SDGs. Open data storage, computing facilities and advanced data processing methods should be used to ensure global collection and analysis of SDG data and obtain high-quality and spatiotemporally consistent SDG data.

2. Improved data access and sharing capabilities

Many organizations are committed to establishing data and information platforms to support the evaluation of SDGs. However, due to the lack of common understanding on the sharing strategies at the policy level, no unified standards at the technical level have been developed, including for data structure and security. Users may not have access to data held by other institutions, or some data may be generated in statistical units not directly usable by others. SDG data access and sharing models and technical standards should be developed jointly by the scientific community, governments, private sector and civil society. The CASEarth Big Earth Data platform (<http://data.casearth.cn/>) was launched in January 2019 and now provides 10 petabytes of data for SDG analysis (such as satellite data, biological and ecological data, and omics data). Users are free to browse metadata, perform keyword search and download data.

3. Strengthened leverage of science and technology in the implementation of SDGs

The *UN Global Sustainable Development Report 2019* identifies six entry points and four levers to be coherently deployed through each entry point to bring about the necessary transformations for the 2030 Agenda for Sustainable Development. Science and technology are one of the levers. To promote the socio-economic transformations required for the achievement of the SDGs, it is necessary to make better use of Big Earth Data science. The science and technology lever will be better used by applying Big Earth Data technology to produce high-quality evaluation datasets and innovating to better monitor SDG indicators. In this

connection, we need to help people of all ages, genders, education levels and livelihoods to understand directly and clearly the advantages of applying Big Earth Data in support of the SDGs, to ensure the central role of science and technology as a lever.

4. Demonstration studies on integrated application of SDG indicators in different regions

The SDGs contain goals in social, economic and environmental dimensions. Different regions face different problems in achieving those goals. As Big Earth Data may be collected at different scales, it is necessary to select and adjust the indicators in the light of local conditions and

explore and construct a system of SDG indicators with the same temporal scales for different zones: national, provincial, municipal and county. The system of SDG indicators supported by Big Earth Data thus developed will include algorithms and standards for various demonstration zones, with corresponding series of technical products. Such a comprehensive and distinctive demonstration system for sustainable development and innovation will be useful point of reference for places with similar circumstances.

We believe that the Big Earth Data method, as a new approach to sustainability science, will be of great value to the implementation of the SDGs.

Acronyms & Abbreviations

AVISO	Archiving, Validation and Interpretation of Satellite Oceanographic Data
BED	Big Earth Data
BEPS	Boreal Ecosystem Productivity Simulator
CAS	Chinese Academy of Sciences
CASEarth	CAS Big Earth Data Science Engineering Program
CBAS	International Research Center of Big Data for Sustainable Development Goals
CCMP	Cross-Calibrated Multi-Platform
CEADs	Carbon Emission Account & Datasets
CGLS	Copernicus Global Land Service
COVID-19	Coronavirus Disease 2019
DEM	Digital Elevation Model
EEAP	Efficient Ecological Agricultural Paradigm
ELR	Environmental Loading Ratio
EMLS	European Multi Lake Survey
ESA-CCI	European Space Agency-Climate Change Initiative
EQI	Ecosystem Quality Index
ESI	Emergy Sustainability Index
ET	Evapotranspiration
EVI	Enhanced Vegetation Index
FAO	Food and Agriculture Organization of the United Nations
FAPAR	Fraction of Absorbed Photosynthetically Active Radiation
FUE	Fertilizer Use Efficiency
FORCCHN	Forest Ecosystem Carbon Budget Model For CHiNa
GDP	Gross Domestic Product
GFS	Global Forecast System
GHRSSST	Group for High Resolution Sea Surface Temperature
GLASS	Global Land Surface Satellite
GPM	Global Precipitation Measurement
GPP	Gross Primary Productivity
GRP	Gross Regional Product
GSW	Global Surface Water
GVG	GPS, Video, and GIS
HOHC	Hybrid Object-based and Hierarchical Classification
HYCOM	HYbrid Coordinate Ocean Model
IUCN	International Union for Conservation of Nature
IW	Irrigation Water

IWRM	Integrated Water Resources Management
JRC	European Commission's Joint Research Centre
LAI	Leaf Area Index
LPO	Land Profit Output
LULC	Land Use and Land Cover
MDG	Millennium Development Goals
MGCI	Mountain Green Cover Index
MK	Mann-Kendall
MODIS	Moderate Resolution Imaging Spectroradiometer
NDBI	Normalized Difference Building Index
NDVI	Normalized Difference Vegetation Index
NDWI	Normalized Difference Water Index
NEP	Net Ecosystem Productivity
NOAA	National Oceanic and Atmospheric Administration
NPP	Net Primary Productivity
OA	Overall Accuracy
OECD	Organisation for Economic Cooperation and Development
OHC	Ocean Heat Content
OISST	Optimum Interpolation Sea Surface Temperature
PA	Producer's Accuracy
PU	Pesticide USE
PCA	Principle Component Analysis
RCR	Relative Change Rate
ROMS	Regional Ocean Modeling System
SAR	Synthetic Aperture Radar
SDGs	Sustainable Development Goals
SOM	Soil Organic Matter
SDSN	Sustainable Development Solution Network
SRTM	Shuttle Radar Topography Mission
SSH	Sea Surface Height
SST	Sea Surface Temperature
SSW	Sea Surface Wind Vector
TP	Traditional Paradigm
UA	User's Accuracy
UN	United Nations
UNEP	United Nations Environment Programme
UNEP-WCMC	United Nations Environment Programme-World Conservation Monitoring Centre
UNSD	United Nations Statistics Division
VIIRS-DNB	Visible Infrared Imaging Radiometer Suite Day/Night Band
WUE	Water Use Efficiency

References

- Acuto, M., Parnell, S., Seto, K. (2018). Building a global urban science[J]. *Nature Sustainability* 1: 2–4. doi:10.1038/s41893-017-0013-9.
- Allen, C., Metternicht, G., Wiedmann, T. (2016). National pathways to the Sustainable Development Goals (SDGs): A comparative review of scenario modelling tools[J]. *Environmental Science & Policy* 66: 199–207. doi:10.1016/j.envsci.2016.09.008.
- Asrar, G., Fuchs, M., Kanemasu, E. T., *et al.* (1984). Estimating absorbed photosynthetic radiation and leaf area index from spectral reflectance in wheat[J]. *Agronomy Journal* 76(2): 300–306. doi:10.2134/agronj1984.00021962007600020029x.
- Avtar, R., Aggarwal, R., Kharrazi, A., *et al.* (2020). Utilizing geospatial information to implement SDGs and monitor their Progress[J]. *Environmental Monitoring and Assessment* 192(1): 35. doi:10.1007/s10661-019-7996-9.
- Bian, J., Li, A., Lei, G., *et al.* (2020). Global high-resolution mountain green cover index mapping based on Landsat images and Google Earth Engine. *Isprs Journal of Photogrammetry and Remote Sensing* 162: 63–76. doi: 10.1016/j.isprsjprs.2020.02.011.
- Bryan, B. A., Gao, L., Ye, Y. *et al.* (2018). China's response to a national land-system sustainability emergency[J]. *Nature* 559(7713): 193–204. doi:10.1038/s41586-018-0280-2.
- Chen, J., Peng, S., Zhao, X.S., *et al.* (2019). Measuring regional progress towards SDGs by combining geospatial and statistical information[J]. *Acta Geodaetica et Cartographica Sinica* 48(04): 473–479. doi: 10.11947/j.AGCS.2019.2018 0563.
- Chen, J. M. (2021). Carbon neutrality towards sustainable future. *The Innovation* 2(3): 100127. doi:10.1016/j.xinn.2021.100127.
- Chen, J. M., Ju, W., Ciais, P., *et al.* (2019). Vegetation structural change since 1981 significantly enhanced the terrestrial carbon sink[J]. *Nature Communications* 10: 4259. doi: 10.1038/s41467-019-12257-8.
- Cheng, L., Abraham, J., Hausfather, Z., *et al.* (2019). How fast are the oceans warming?[J]. *Science* 363 (6423): 128–129. doi: 10.1126/science.aav7619.
- Cheng, L., Abraham, J., Trenberth, K. E., *et al.* (2021). Upper ocean temperatures hit record high in 2020[J]. *Advances in Atmospheric Sciences* 38: 523–530. doi: 10.1007/s00376-021-0447-x.
- Cheng, R., Gao, J., Sun, Z.C., *et al.* (2021). A vehicle detection method based on deep learning: Wuhan during the COVID-19 pandemic as an example[J]. *Bulletin of Surveying and Mapping*.
- Chi, C., Park, T., Wang, X., *et al.* (2019). China and India lead in greening of the world through land-use management[J]. *Nature Sustainability* 2: 122–129. doi:10.1038/s41893-019-0220-7.
- Climate Action Tracker (CAT). (2020). The recent wave of net zero targets has put the Paris Agreement's 1.5°C within striking distance. <https://climateactiontracker.org/publications/global-update-paris-agreement-turning-point/>
- Crippa, M., Solazzo, E., Guizzardi, D., *et al.* (2021). Food systems are responsible for a third of global anthropogenic GHG emissions[J]. *Nature Food* 2: 198–209. doi: 10.1038/s43016-021-00225-9.
- Du, S., Liu, B., Zhang, X. (2021). Mapping large-scale and fine-grained urban functional zones from VHR images using a multi-scale semantic segmentation network and object-based approach[J]. *Remote Sensing of Environment* 261: 112480. doi:10.1016/j.rse.2021.112480.
- Elmqvist, T., Andersson, E., Frantzeskaki, N., *et al.* (2019). Sustainability and resilience for transformation in the urban century[J]. *Nature Sustainability* 2: 267–273. doi: 10.1038/s41893-019-0250-1.
- FAO. (2017). Metadata 15.04.02. <https://unstats.un.org/sdgs/metadata/files/Metadata-15-04-02.pdf> (Last updated: 12 February 2021, accessed on 26 May 2021).
- FAO. (2018). Guiding the Transition to Sustainable Food and Agricultural Systems. Rome, Italy. https://www.socioeco.org/bdf_fiche-document-7625_en.html.
- FAO (2020a). Factsheets on the 21 SDG Indicators Under FAO Custodianship. A Highlight of the Main Indicators with the Greatest Gaps in Country Reporting. Rome. <http://www.fao.org/documents/card/en/c/ca8958en>.
- FAO. (2020b). The State of Food and Agriculture(SOFA) 2020. Overcoming Water Challenges in Agriculture. Rome,

- Italy. <https://www.unwater.org/the-state-of-food-and-agriculture-2020-overcoming-water-challenges-in-agriculture>.
- FAO. (2020c). Global Forest Resources Assessment 2020: Main report. Rome, Italy.
- FAO, IFAD, UNICEF, WFP and WHO. (2021). The State of Food Security and Nutrition in the World 2021: Transforming Food Systems for Food Security, Improved Nutrition and Affordable Healthy Diets for All. Rome, Italy. <https://data.unicef.org/resources/sofi-2021>.
- Field, C. B., Randerson, J. T., Malmstrom, C. M. (1995). Global net primary production: Combining ecology and remote sensing[J]. *Remote Sensing of Environment* 51: 74–88. doi: 10.1016/0034-4257(94)00066-v.
- Global Water Partnership Technical Advisory Committee. (2016). *Integrated Water Resources Management*[M], translated by Global Water Partnership China. Beijing: China Water & Power Press.
- Guo, H. D., Wang, L. Z., and Liang, D. (2016). Big Earth Data from space: A new engine for Earth Science[J]. *Science Bulletin* 61 (7): 505–513. doi: 10.1007/s11434-016-1041-y.
- Guo, H. D. (2017). Big Earth Data: A new frontier in Earth and Information Sciences[J]. *Big Earth Data* 1(1–2): 4–20. doi:10.1080/20964471.2017.1403062.
- Guo, H. D. (2021). *Big Earth Data in Support of the Sustainable Development Goals (2021)*[M]. Beijing: Science Press and EDP Sciences.
- Guo H. D., Chen F., Sun Z. C., *et al.* (2021). Big Earth Data: A practice of sustainability science to achieve the Sustainable Development Goals[J]. *Science Bulletin* 66: 1050–1053. doi: 10.1016/j.scib.2021.01.012.
- Hong, C. P., Burney, J. A., Pongratz, J., *et al.* (2021). Global and regional drivers of land-use emissions in 1961–2017[J]. *Nature* 589: 554–589. doi:10.1038/s41586-020-03138-y.
- Hu, G. C., Jia, L. (2015). Monitoring of evapotranspiration in a semi-arid inland river basin by combining microwave and optical remote sensing observations[J]. *Remote Sensing* 7(3): 3056–3087. doi: 10.3390/rs70303056.
- IAEG-SDGS. (2021). Tier Classification for Global SDG Indicators. Interagency and Expert Group on SDG Indicators, New York.
- Immerzeel, W. W., Lutz, A. F., Andrade, M., *et al.* (2020). Importance and vulnerability of the world's water towers[J]. *Nature* 577: 364. doi: 10.1038/s41586-019-1822-y.
- IPBES. (2018). The IPBES Assessment Report on Land Degradation and Restoration. Montanarella, L., Scholes, R., and Brainich, A. (eds.). Secretariat of the Intergovernmental Science-Policy Platform on Biodiversity and Ecosystem Services, Bonn, Germany.
- IPCC. (2018). Summary for Policymakers. In: Masson-Delmotte, V., Zhai, P., Pötnner, H. O. *et al.* (eds.). Global Warming of 1.5°C. An IPCC Special Report on the Impacts of Global Warming of 1.5°C Above Pre-industrial Levels and Related Global Greenhouse Gas Emission Pathways, in the Context of Strengthening the Global Response to the Threat of Climate Change, Sustainable Development, and Efforts to Eradicate Poverty. <https://www.ipcc.ch/sr15/chapter/spm/>.
- IPCC. (2019). Summary for Policymakers. In: Pötnner, H. O., Roberts, D.C., Masson-Delmotte, V. *et al.* (eds.). IPCC Special Report on the Ocean and Cryosphere in a Changing Climate. https://www.researchgate.net/publication/336134726_Summary_for_Policy_Makers.
- Jia, M. M., Wang, Z. M., Zhang, Y. Z., *et al.* (2018). Monitoring loss and recovery of mangrove forests during 42 years: The achievements of mangrove conservation in China[J]. *International Journal of Applied Earth Observation and Geoinformation* 73: 535–545. doi: 10.1016/j.jag.2018.07.025.
- Jia, M. M., Wang, Z. M., Mao, D. H., *et al.* (2021). Spatial-temporal changes of China's mangrove forests over the past 50 years: An analysis towards the Sustainable Development Goals[J]. *Science Bulletin* doi: 10.1360/TB-2020-1412.
- Jiang, F., Qi, S. H., Ding, M. J., *et al.* (2014). Vulnerability of Siberian crane habitat to water level in Poyang lake wetland, China[J]. *Geoscience and Remote Sensing* 51: 662–676. doi: 10.1080/15481603.2014.978126.
- Jiang H., Sun Z., Guo H., *et al.* (2021). An assessment of urbanization sustainability in China between 1990 and 2015 using land use efficiency indicators[J]. *npj Urban Sustainability* 1: 34. doi: 10.1038/s42949-021-00032-y.
- Kapos, V., Rhind, J., Edwards, M., *et al.* (2000). Developing a Map of the World's Mountain Forests[G].//Price, M. F., Butt, N. Forests in Sustainable Mountain Development: A State of Knowledge Report for 2000(Vol. 5). Wallingford: CABI, 2000:4-19. ISBN: 0851994466.
- Kastner, T., Rivas, M. J. I., Koch, W., *et al.* (2012). Global changes in diets and the consequences for land requirements for food[J]. *Proceedings of the National Academy of Sciences of the United States of America* 109(18): 6868–6872. doi: 10.1073/pnas.1117054109.

- Li, J. H. and Shi, J. C. (2016). *2015 Global Ecosystems and Environment Observation: Annual Report from China (GEOARC)*[M]. Beijing: Science Press.
- Liu, C., Zhang, Q., Tao, S., *et al.* (2020). A new framework to map fine resolution cropping intensity across the globe: Algorithm, validation, and implication[J]. *Remote Sensing of Environment* 251: 112095. doi: 10.1016/j.rse.2020.112095.
- Liu, D., Keesing, J., Xing, Q., *et al.* (2009). World's largest macroalgal bloom caused by expansion of seaweed aquaculture in China[J]. *Marine Pollution Bulletin* 58(6): 888–895. doi:10.1016/j.marpolbul.2009.01.013.
- Mao, D. H., Wang, Z. M., Wu, J. G., *et al.* (2018). China's wetlands loss to urban expansion[J]. *Land Degradation & Development* 29: 2644–2657. doi: 10.1002/ldr.2939.
- Mao, D. H., Liu, M. Y., Wang, Z. M., *et al.* (2019). Rapid invasion of *Spartina alterniflora* in the coastal zone of mainland China: Spatiotemporal patterns and human prevention[J]. *Sensors* 19(10): 2308. doi: 10.3390/s19102308.
- Mao, D. H., Wang, Z. M., Du, B. J., *et al.* (2020). National wetland mapping in China: A new product resulting from object-based and hierarchical classification of Landsat 8 OLI images[J]. *ISPRS Journal of Photogrammetry and Remote Sensing* 164: 11–25. doi: 10.1016/j.isprsjprs.2020.03.020.
- Ministry of Housing and Urban-Rural Development. (2012). Code for Classification of Urban Land Use and Planning Standards of Development Land. GB50137-2011.
- NOAA National Centers for Environmental Information. (2020). State of the Climate: Global Climate Report for Annual 2020. <https://www.ncdc.noaa.gov/sotc/global/202013>.
- Odum, H. T. (1996). *Environmental Accounting: Emergy and environmental decision making*[M]. Wiley.
- OECD/European Union/JRC. (2008). Handbook on Constructing Composite Indicators: Methodology and User Guide, OECD Publishing, Paris. doi:10.1787/9789264043466-en.
- Ouyang, Z. Y., Xu, W. H., Xiao, Y. *et al.* (2017). *China's ecosystem pattern, quality, services and evolution*[M]. Beijing: Science Press.
- Pekel, J., Cottam, A., Gorelick, N., *et al.* (2016). High-resolution mapping of global surface water and its long-term changes[J]. *Nature* 540: 418–422. doi: 10.1038/nature20584.
- Peng, D. Zhang, B. Wu, C., *et al.* (2017). Country-level net primary production distribution and response to drought and land cover change[J]. *Science of The Total Environment* 574: 65–77. doi:10.1016/j.scitotenv.2016.09.033.
- Pradhan, P., Costa, L., Rybski, D., *et al.* (2017). A systematic study of sustainable development goal (SDG) interactions[J]. *Earths Future* 5(11): 1169–1179. doi:10.1002/2017ef000632.
- Ren, C. Y., Wang, Z. M., Zhang, Y. Z., *et al.* (2019). Rapid expansion of coastal aquaculture ponds in China from Landsat observations during 1984–2016[J]. *International Journal of Earth Observation and Geoinformation* 82: 101902. doi: 10.1016/j.jag.2019.101902.
- Rodrigues, A. S. L., Pilgrim, J. D., Lamoreux, J. F. *et al.* (2006). The value of the IUCN Red List for conservation[J]. *Trends in Ecology & Evolution* 21(2): 71–76. doi:10.1016/j.tree.2005.10.010.
- Sachs, J., Schmidt-Traub, G., Kroll, C., *et al.* (2019). Sustainable Development Report 2019. New York: Bertelsmann Stiftung and Sustainable Development Solutions Network (SDSN). <http://sustainabledevelopment.report>.
- Sachs, J., Schmidt-Traub, G., Kroll, C., *et al.* (2020). *Sustainable Development Report 2020: The Sustainable Development Goals and COVID-19*[M]. Cambridge: Cambridge University Press.
- Stabile, M. C. C., Guimaraes, A. L., Silva, D. S., *et al.* (2020). Solving Brazil's land use puzzle: Increasing production and slowing Amazon deforestation[J]. *Land Use Policy* 91: 104326. doi: 10.1016/j.landusepol.2019.104362.
- Stephens, D. L. B., Carlson, R. E., Horsburgh, C. A., *et al.* (2015). Regional distribution of Secchi disk transparency in waters of the United States[J]. *Lake and Reservoir Management* 31(1): 55–63. doi: 10.1080/10402381.2014.1001539.
- Sun H. (1994). *Agricultural Natural Resources and Regional Development in China*[M]. Nanjing: Jiangsu Science & Technology Press.
- UN. (2015a). Transforming our world: The 2030 agenda for sustainable development annex A/RES/70/1.<https://sustainabledevelopment.un.org/post2015/transformingourworld>.
- UN. (2015b). Sendai Framework for Disaster Risk Reduction 2015-2030. Geneva: United Nations.
- UN. (2019). The Sustainable Development Goals Report 2019. New York: United Nations. <https://www.un.org/development/desa/publications/sustainable-development-goals-report-2019.html>.
- UN. (2020a). The Sustainable Development Goals Report 2020. New York: United Nations. <https://www.un.org/development/desa/publications/publication/sustainable>

- development-goals-report-2020.
- UN. (2020b). Sustainable Development Goals Progress Chart 2020. <https://unstats.un.org/sdgs/report/2020/progress-chart-2020.pdf>.
- UN. (2021a). The Sustainable Development Goals Report 2021. New York: United Nations.
- UN. (2021b). Goal 6: Ensure access to water and sanitation for all. <https://www.un.org/sustainabledevelopment/water-and-sanitation/>
- UN. (2021c). High-level political forum on sustainable development, convened under the auspices of the Economic and Social Council. Progress towards the Sustainable Development Goals. Report of the Secretary-General. <https://unstats.un.org/sdgs/files/report/2021/secretary-general-sdg-report-2021--EN.pdf>
- UN Office for Disaster Risk Reduction (UNDRR). (2019). Global Assessment Report on Disaster Risk Reduction, Geneva, Switzerland, United Nations Office for Disaster Risk Reduction (UNDRR).
- UNEP. (2020a). Emissions Gap Report 2020. Nairobi. <http://www.unep.org/emissions-gap-report-2020>.
- UNEP. (2020b). Progress on Integrated Water Resources Management. Global Baseline for SDG 6 Indicator 6.5.1: Degree of IWRM Implementation. <https://www.unwater.org/publications/progress-on-integrated-water-resources-management-651/>.
- UNEP. (2021). Measuring Progress: Environment and the SDGs. Retrieved from UNEP-DHI. Monitoring Guide for SDG Indicator 6.5.1. <http://iwrmdataportal.unepdhi.org/aboutsdg651>.
- UN-Water. (2016). Water and Sanitation Interlinkages across the 2030 Agenda for Sustainable Development. 29 August, 2016. Geneva, Switzerland. <https://www.unwater.org/publications/water-sanitation-interlinkages-across-2030-agenda-sustainable-development/>.
- UN-Water. (2018). Progress on Water-related Ecosystems: Piloting the Monitoring Methodology and Initial Findings for SDG Indicator 6.6.1. <https://www.unwater.org/publications/progress-on-water-related-ecosystems-661/>.
- UN-Water. (2020a). The Sustainable Development Goal 6 Global Acceleration Framework. <https://www.unwater.org/publications/the-sdg-6-global-acceleration-framework/>.
- UN-Water. (2020b). Measuring Change in the Extent of Water-related Ecosystems Over Time. <https://sdg.data.gov/6-6-1/>.
- UN-Water. (2021). Summary Progress Update 2021 – SDG 6 – water and sanitation for all. Version: 1 March 2021. Geneva, Switzerland. <https://www.unwater.org/publications/summary-progress-update-2021-sdg-6-water-and-sanitation-for-all/>.
- Wang, J. M., Wang, H. D., Cao, Y. G., *et al.* (2016). Effects of soil and topographic factors on vegetation restoration in opencast coal mine dumps located in a loess area[J]. *Scientific Reports* 6: 22–58. doi: 10.1038/srep22058.
- Wang, S., Li, J., Zhang, B., *et al.* (2020). Changes of water clarity in large lakes and reservoirs across China observed from long-term MODIS[J]. *Remote Sensing of Environment* 247: 111949. doi: 10.1016/j.rse.2020.111949.
- Wang, Y. Q. (2020). Poyang Lake and wintering Siberian cranes[J]. *Frontiers in Ecology and the Environment* 18(2): 100. doi:10.1002/fee.2171.
- Wei, Y. Q., Li, X., Gao, F., *et al.* (2018). The United Nations Sustainable Development Goals (SDG) and the response strategies of China[J]. *Advances in Earth Science* 33(10): 1084–1093. doi: CNKI:SUN:DXJZ.0. 2018-10-011.
- Wei, Y. Q., Zhang, L., Wang, J. N. *et al.* (2021). Chinese caterpillar fungus (*Ophiocordyceps sinensis*) in China: Current distribution, trading, and futures under climate change and overexploitation[J]. *Science of the Total Environment* 755: 142548. doi:10.1016/j.scitotenv.2020.142548.
- Weitz, N., Carlsen, H., Nilsson, M., *et al.* (2018). Towards systemic and contextual priority setting for implementing the 2030 Agenda[J]. *Sustainability Science* 13(2): 531–548. doi:10.1007/s11625-017-0470-0.
- World Meteorological Organization (WMO). (2020). United in Science. https://public.wmo.int/en/resources/united_in_science.
- Wu, B. F., Qian, J. K., Zeng, Y., *et al.* (2017). *Land Cover Atlas of the People's Republic of China*[M]. Beijing: China Cartographic Publishing House.
- Wu, Z., Wu, J., Liu, J., *et al.* (2013). Increasing terrestrial vegetation activity of ecological restoration program in the Beijing-Tianjin sand source region of China[J]. *Ecological Engineering* 52: 37-50. doi:10.1016/j.ecoleng.2012.12.040.
- Xu, Z., Chau, S. N., Chen, X., *et al.* (2020). Assessing progress towards sustainable development over space and time[J]. *Nature* 577: 74–78. doi: 10.1038/s41586-019-1846-3.
- Yan, X. D., Zhao, J. F. (2007). Establishing and validating individual-based carbon budget model FORCCHN of forest ecosystems in China[J]. *Acta Ecologica Sinica* 27: 2684–2694.

doi: 10.1016/S1872-2032(07)60056-0.

Zhang, X., Du, S., Wang, Q. (2017). Hierarchical semantic cognition for urban functional zones with VHR satellite images and POI data[J]. *ISPRS Journal of Photogrammetry and Remote Sensing* 132: 170–184. doi: 10.1016/j.isprsjprs.2017.09.007.

Zhang, X., Du, S., Zheng, Z. (2020). Heuristic sample learning for complex urban scenes: Application to urban functional-zone mapping with VHR images and POI data[J]. *ISPRS Journal of Photogrammetry and Remote Sensing* 161: 1–12. doi: 10.1016/j.isprsjprs.2020.01.005.

Zhao, J. F., Ma, J. Y., Zhu, Y. J. (2019). Evaluating impacts of climate change on net ecosystem productivity (NEP) of global different forest types based on an individual tree-based model FORCCHN and remote sensing[J]. *Global and Planetary Change* 182: 103010. doi: 10.1016/j.gloplacha.2019.103010.

Zhao, J. F., Ma, J. Y., Hou, M. T., *et al.* (2020). Spatial–temporal variations of carbon storage of the global forest ecosystem under future climate change[J]. *Mitigation and Adaptation Strategies for Global Change* 25: 603–624. doi:10.1007/s11027-019-09882-5.

Zheng, C., Jia, L., Hu, G., *et al.* (2019). Earth observations-based evapotranspiration in northeastern Thailand[J]. *Remote*

Sensing 11(2): 138. doi: 10.3390/rs11020138.

Zheng, Y. M., Wang, S. D., Cao, Y., *et al.* (2021). Assessing the ecological vulnerability of protected areas by using Big Earth Data. *International Journal of Digital Earth* doi:10.1080/17538947.2021.1962995.

Zhou, M., Liu, D., Anderson, D., *et al.* (2015). Introduction to the special issue on green tides in the Yellow Sea[J]. *Estuarine, Coastal and Shelf Science* 163: 3–8. doi: 10.1016/j.ecss.2015.06.023.

Zou, L., Hu, B. S., Qi, S. H., *et al.* (2021). Spatiotemporal variation of Siberian Crane habitats and the response to water level in Poyang Lake wetland, China[J]. *Remote Sensing* 13:140. doi:10.3390/rs13010140.

Zuo, L., Zhang, Z., Carlson, K. M., *et al.* (2018). Progress towards sustainable intensification in China challenged by land-use change[J]. *Nature Sustainability* 1(6): 304–313. doi: 10.1038/s41893-018-0076-2.

Zwart, S. J., Bastiaanssen, W. G. M., de Fraiture, C., *et al.* (2010). WATPRO: A remote sensing based model for mapping water productivity of wheat[J]. *Agricultural Water Management* 97(10): 1628–1636. doi: 10.1016/j.agwat.2010.05.017.

Core Team of Authors

Leading author

Guo Huadong International Research Center of Big Data for Sustainable Development Goals

Authors (Alphabetically arranged)

Bai Lubin Peking University
Bian Jinhu Institute of Mountain Hazards and Environment, Chinese Academy of Sciences
Cao Min Nanjing Normal University
Chen Fang International Research Center of Big Data for Sustainable Development Goals
Chen Min Nanjing Normal University
Chen Yu International Research Center of Big Data for Sustainable Development Goals
Chen Jingming University of Toronto
Chen Qiting Aerospace Information Research Institute, Chinese Academy of Sciences
Chen Xidong International Research Center of Big Data for Sustainable Development Goals
Chen Yaxi Aerospace Information Research Institute, Chinese Academy of Sciences
Cheng Yi Institute of Geographic Sciences and Natural Resources Research, Chinese Academy of Sciences
Cheng Zhifeng Institute of Geographic Sciences and Natural Resources Research, Chinese Academy of Sciences
Dong Jinwei Institute of Geographic Sciences and Natural Resources Research, Chinese Academy of Sciences
Dou Yinyin Institute of Geographic Sciences and Natural Resources Research, Chinese Academy of Sciences
Du Dandan Aerospace Information Research Institute, Chinese Academy of Sciences
Du Shihong Peking University
Du Shouhang China University of Mining & Technology, Beijing
Du Xiaoping International Research Center of Big Data for Sustainable Development Goals
Duan Hongtao Nanjing Institute of Geography and Limnology, Chinese Academy of Sciences
Fan Meng Aerospace Information Research Institute, Chinese Academy of Sciences
Fan Xinyue Research Center for Eco-Environmental Sciences, Chinese Academy of Sciences
Fang Shibo Chinese Academy of Meteorological Sciences
Feng Yaya Northwest Institute of Eco-Environment and Resources, Chinese Academy of Sciences
Feng Yuning Peking University
Fu Shujing Beijing Forestry University
Gao Fenglei First Institute of Oceanography, Ministry of Natural Resources
Gu Haifeng Third Institute of Oceanography, Ministry of Natural Resources
Guo Changqing Institute of Geographic Sciences and Natural Resources Research, Chinese Academy of Sciences
Han Mei Research Center for Eco-Environmental Sciences, Chinese Academy of Sciences
Han Qunli Aerospace Information Research Institute, Chinese Academy of Sciences
He Zhiwei Institute of Oceanology, Chinese Academy of Sciences

Hou Yali	Institute of Geographic Sciences and Natural Resources Research, Chinese Academy of Sciences
Hu Bisong	Jiangxi Normal University
Hu Guangcheng	Aerospace Information Research Institute, Chinese Academy of Sciences
Huang Kan	Academy of Inventory and Planning, National Forestry and Grassland Administration
Huang Lei	International Research Center of Big Data for Sustainable Development Goals
Huang Chunlin	Northwest Institute of Eco-Environment and Resources, Chinese Academy of Sciences
Huang Wenjiang	International Research Center of Big Data for Sustainable Development Goals
Jia Li	Aerospace Information Research Institute, Chinese Academy of Sciences
Jia Gensuo	Institute of Atmospheric Physics, Chinese Academy of Sciences
Jia Mingming	Northeast Institute of Geography and Agroecology, Chinese Academy of Sciences
Jia Shaofeng	Institute of Geographic Sciences and Natural Resources Research, Chinese Academy of Sciences
Jia Yuanxin	Academy of Inventory and Planning, National Forestry and Grassland Administration
Jiang Min	Aerospace Information Research Institute, Chinese Academy of Sciences
Jiang Huiping	International Research Center of Big Data for Sustainable Development Goals
Jiang Yunzhong	China Institute of Water Resources and Hydropower Research
Ju Weimin	Nanjing University
Kong Lingqiao	Research Center for Eco-Environmental Sciences, Chinese Academy of Sciences
Kong Xiangji	Academy of Inventory and Planning, National Forestry and Grassland Administration
Kuang Wenhui	Institute of Geographic Sciences and Natural Resources Research, Chinese Academy of Sciences
Li Yang	Institute of Geographic Sciences and Natural Resources Research, Chinese Academy of Sciences
Li Ainong	Institute of Mountain Hazards and Environment, Chinese Academy of Sciences
Li Jingxi	First Institute of Oceanography, Ministry of Natural Resources
Li Junsheng	International Research Center of Big Data for Sustainable Development Goals
Li Mingyang	Aerospace Information Research Institute, Chinese Academy of Sciences
Li Xiaosong	International Research Center of Big Data for Sustainable Development Goals
Li Yifan	Institute of Oceanology, Chinese Academy of Sciences
Liang Dong	International Research Center of Big Data for Sustainable Development Goals
Lin Hui	Jiangxi Normal University
Liu Bo	Peking University
Liu Jie	Aerospace Information Research Institute, Chinese Academy of Sciences
Liu Zhe	National Disaster Reduction Center of China, Ministry of Emergency Management
Liu Haimeng	Institute of Geographic Sciences and Natural Resources Research, Chinese Academy of Sciences
Liu Liangyun	International Research Center of Big Data for Sustainable Development Goals
Liu Nanjiang	National Disaster Reduction Center of China, Ministry of Emergency Management
Lu Jing	Aerospace Information Research Institute, Chinese Academy of Sciences
Lu Shanlong	International Research Center of Big Data for Sustainable Development Goals
Luo Jin	Jiangxi Normal University
Luo Lei	International Research Center of Big Data for Sustainable Development Goals
Ma Zhenzhen	China Institute of Water Resources and Hydropower Research

Mao Dehua	Northeast Institute of Geography and Agroecology, Chinese Academy of Sciences
Mi Xiangcheng	Institute of Botany, Chinese Academy of Sciences
Ouyang Zhu	Institute of Geographic Sciences and Natural Resources Research, Chinese Academy of Sciences
Ouyang Zhiyun	Research Center for Eco-Environmental Sciences, Chinese Academy of Sciences
Pan Tianshi	Aerospace Information Research Institute, Chinese Academy of Sciences
Peng Dailiang	International Research Center of Big Data for Sustainable Development Goals
Qi Shuhua	Jiangxi Normal University
Qin Tian	Fuzhou University
Shangguan Donghui	Northwest Institute of Eco-Environment and Resources, Chinese Academy of Sciences
Su Hua	Fuzhou University
Sun Tao	Academy of Inventory and Planning, National Forestry and Grassland Administration
Sun Chengjun	First Institute of Oceanography, Ministry of Natural Resources
Sun Zhigang	Institute of Geographic Sciences and Natural Resources Research, Chinese Academy of Sciences
Sun Zhongchang	International Research Center of Big Data for Sustainable Development Goals
Tang Hailong	Sun Yat-sen University
Tao Jinhua	Aerospace Information Research Institute, Chinese Academy of Sciences
Tian Yu	China Institute of Water Resources and Hydropower Research
Wang Xiao	Aerospace Information Research Institute, Chinese Academy of Sciences
Wang An	Fuzhou University
Wang Meng	Aerospace Information Research Institute, Chinese Academy of Sciences
Wang Yan	Aerospace Information Research Institute, Chinese Academy of Sciences
Wang Yong	Aerospace Information Research Institute, Chinese Academy of Sciences
Wang Yu	Academy of Inventory and Planning, National Forestry and Grassland Administration
Wang Yue	Aerospace Information Research Institute, Chinese Academy of Sciences
Wang Futao	Aerospace Information Research Institute, Chinese Academy of Sciences
Wang Haoyu	Peking University
Wang Jianghao	Institute of Geographic Sciences and Natural Resources Research, Chinese Academy of Sciences
Wang Juanle	Institute of Geographic Sciences and Natural Resources Research, Chinese Academy of Sciences
Wang Lizhe	China University of Geosciences, Wuhan
Wang Shenglei	International Research Center of Big Data for Sustainable Development Goals
Wang Xinyuan	International Research Center of Big Data for Sustainable Development Goals
Wang Zongming	Northeast Institute of Geography and Agroecology, Chinese Academy of Sciences
Wei Yanqiang	Northwest Institute of Eco-Environment and Resources, Chinese Academy of Sciences
Wu Bingfang	Aerospace Information Research Institute, Chinese Academy of Sciences
Wu Wenbin	Institute of Agricultural Resources and Regional Planning, Chinese Academy of Agricultural Sciences
Xia Jisheng	Yunnan University
Xia Lili	Aerospace Information Research Institute, Chinese Academy of Sciences
Xiao Yi	Research Center for Eco-Environmental Sciences, Chinese Academy of Sciences
Xu Benben	Aerospace Information Research Institute, Chinese Academy of Sciences

Xu Weihua	Research Center for Eco-Environmental Sciences, Chinese Academy of Sciences
Yan Dongmei	International Research Center of Big Data for Sustainable Development Goals
Yang Dezhou	Institute of Oceanology, Chinese Academy of Sciences
Yang Shiqi	Institute of Geographic Sciences and Natural Resources Research, Chinese Academy of Sciences
You Jinjun	China Institute of Water Resources and Hydropower Research
Yu Rencheng	Institute of Oceanology, Chinese Academy of Sciences
Yu Le	Tsinghua University
Zeng Hongwei	Aerospace Information Research Institute, Chinese Academy of Sciences
Zhang Bing	Aerospace Information Research Institute, Chinese Academy of Sciences
Zhang Chi	Jiangsu Ocean University
Zhang Di	First Institute of Oceanography, Ministry of Natural Resources
Zhang Li	International Research Center of Big Data for Sustainable Development Goals
Zhang Miao	Aerospace Information Research Institute, Chinese Academy of Sciences
Zhang Peng	National Disaster Reduction Center of China, Ministry of Emergency Management
Zhang Haojie	Fuzhou University
Zhang Xiuyuan	Peking University
Zhang Zengxiang	Aerospace Information Research Institute, Chinese Academy of Sciences
Zhao Junfang	Chinese Academy of Meteorological Sciences
Zheng Hua	Research Center for Eco-Environmental Sciences, Chinese Academy of Sciences
Zheng Chaolei	Aerospace Information Research Institute, Chinese Academy of Sciences
Zheng Shijun	Aerospace Information Research Institute, Chinese Academy of Sciences
Zheng Yaomin	Beijing Technology and Business University
Zheng Yunqiang	Peking University
Zhi Chao	Fuzhou University
Zuo Lijun	Aerospace Information Research Institute, Chinese Academy of Sciences



Contact us:

Add.: No.9 Dengzhuang South Road, Haidian District

Beijing 100094, China

Tel.: +86 10 82176256

Email: casearth@radi.ac.cn

www.cabs.ac.cn